

AD _____

Award Number: DAMD17-99-1-9264

TITLE: Training Program in Breast Cancer Research at the
University of Texas M.D. Anderson Cancer Center

PRINCIPAL INVESTIGATOR: Mien-Chie Hung, Ph.D.

CONTRACTING ORGANIZATION: The University of Texas M.D. Anderson
Cancer Center
Houston, Texas 77030

REPORT DATE: September 2002

TYPE OF REPORT: Annual Summary

PREPARED FOR: U.S. Army Medical Research and Materiel Command
Fort Detrick, Maryland 21702-5012

DISTRIBUTION STATEMENT: Approved for Public Release;
Distribution Unlimited

The views, opinions and/or findings contained in this report are those of the author(s) and should not be construed as an official Department of the Army position, policy or decision unless so designated by other documentation.

20030211 201

REPORT DOCUMENTATION PAGE			Form Approved OMB No. 074-0188	
Public reporting burden for this collection of information is estimated to average 1 hour per response, including the time for reviewing instructions, searching existing data sources, gathering and maintaining the data needed, and completing and reviewing this collection of information. Send comments regarding this burden estimate or any other aspect of this collection of information, including suggestions for reducing this burden to Washington Headquarters Services, Directorate for Information Operations and Reports, 1215 Jefferson Davis Highway, Suite 1204, Arlington, VA 22202-4302, and to the Office of Management and Budget, Paperwork Reduction Project (0704-0188), Washington, DC 20503				
1. AGENCY USE ONLY (Leave blank)	2. REPORT DATE September 2002	3. REPORT TYPE AND DATES COVERED Annual Summary (1 Sep 01 - 31 Aug 02)		
4. TITLE AND SUBTITLE Training Program in Breast Cancer Research at the University of Texas M.D. Anderson Cancer Center		5. FUNDING NUMBERS DAMD17-99-1-9264		
6. AUTHOR(S) Mien-Chie Hung, Ph.D.				
7. PERFORMING ORGANIZATION NAME(S) AND ADDRESS(ES) The University of Texas M.D. Anderson Cancer Center Houston, Texas 77030 E-Mail: mhung@mdanderson.org		8. PERFORMING ORGANIZATION REPORT NUMBER		
9. SPONSORING / MONITORING AGENCY NAME(S) AND ADDRESS(ES) U.S. Army Medical Research and Materiel Command Fort Detrick, Maryland 21702-5012		10. SPONSORING / MONITORING AGENCY REPORT NUMBER		
11. SUPPLEMENTARY NOTES Report contains color.				
12a. DISTRIBUTION / AVAILABILITY STATEMENT Approved for Public Release; Distribution Unlimited			12b. DISTRIBUTION CODE	
13. ABSTRACT (Maximum 200 Words) With the continuous funding from the US army/DOD, the training program on breast cancer research at MDACC has had a successful third year. The training program has supported four predoctoral and two postdoctoral fellows. Each trainee has made notable progress as evidenced by publications and presentations at national meetings. Significant strides have been made within the scope of the original specific aims in the following research areas: 1) Therapeutic approaches for breast cancer through regulation of oncogene and tumor suppressor gene expression, and control of signal transduction, apoptosis, and DNA repair; 2) Use of animals to understand the biology of breast cancer and to provide models for preclinical therapeutic and preventive studies; 3) Novel preventive strategies for breast cancer; 4) Population-based studies on breast cancer; 5) Molecular diagnostic/prognostic factors for breast cancer; and 6) The basis biology of breast cancer. In addition to laboratory pursuits each trainee has participated in departmental group meetings, journal clubs, and retreats. The goal of the training program is to further the successful training of fellows who will develop research programs of their own which continue to tackle problems of breast cancer.				
14. SUBJECT TERMS breast cancer			15. NUMBER OF PAGES 181	
			16. PRICE CODE	
17. SECURITY CLASSIFICATION OF REPORT Unclassified	18. SECURITY CLASSIFICATION OF THIS PAGE Unclassified	19. SECURITY CLASSIFICATION OF ABSTRACT Unclassified	20. LIMITATION OF ABSTRACT Unlimited	

Table of Contents

Cover	1
SF 298	2
Table of Contents	3
Introduction	4
Body	5
Key Research Accomplishments	9
Reportable Outcomes	11
Conclusions	13
Appendices	14

Introduction

The breast cancer training program at the University of Texas M. D. Anderson Cancer Center is a multidisciplinary research program comprising students and faculty from twenty different departments. The ultimate goal of this training program is to provide support to aid the development of exceptional scientists in the field of breast cancer research. The predoctoral and postdoctoral trainees for the U. S. army/Department of Defense (DOD) training grant are chosen from the laboratories of all faculty involved in the entire Breast Cancer Research Program at MDACC which includes over seventy faculty members and twenty departments. The scope of the research conducted by the trainees includes a variety of topics related to breast cancer research. Some trainees are conducting research aimed at developing novel therapeutic approaches for breast cancer through regulation of oncogenes and tumor suppressor genes and control of signal transduction, apoptosis and DNA repair. Others are using animals to understand the biology of breast cancer and to develop models for pre-clinical therapeutic and preventive studies. Still others are studying molecular diagnostic/prognostic factors for breast cancer and developing novel preventive strategies for this disease. The trainees are involved in many departmental and interdepartmental events including journal clubs, group meetings, retreats, and seminars. These activities outside of the laboratory provide opportunities for the trainees to gain a truly multi-disciplinary perspective on their own research projects by communicating and collaborating with researchers from each department at MDACC involved in breast cancer research. The breast cancer training program at MDACC is well on its way to producing superior investigators who will continue to explore the problems of breast cancer well into the future.

Body

With continual support from the U.S. Army/DOD to develop the Breast Cancer Training Program at the University of Texas M. D. Anderson Cancer Center (UT-MDACC) has led to another successful year in breast cancer research for several predoctoral and postdoctoral fellows. The Breast Cancer Training Program at UT-MDACC was developed to provide support for exceptional young scientist training in laboratories that are part of the Breast Cancer Research Program (BCRP) at UT-MDACC. The program provides comprehensive interdisciplinary research training to each fellow. The program faculty is comprised of members who cover a full spectrum of breast cancer research, including investigators involved in basic, translation, clinical and population-based studies related to breast cancer. The strength of the training programs at UT-MDACC stem from the strong interactions that take place between basic science researchers and clinicians in the exciting environment, which allows for swift transfer of scientific discoveries from the laboratory to the clinic. Pre-doctoral and postdoctoral trainees at MDACC benefit from this unique environment and are able to gain unparalleled experience in multidisciplinary studies. The ultimate goal of this training program is to train pre-doctoral and postdoctoral fellows to become highly qualified breast cancer researchers who will develop programs of merit in breast cancer research.

The achievements of trainees in the first two years are exceptional and include publication in several highly reputable journals such as *Nature Cell Biology*, *Oncogene*, *Cancer Research*, and *Molecular Cell Biology*. In this third year, the trainee are also very productive, they have been co-authors in reputable journals such as *Molecular Cell*, *Cancer Cell*, *Oncogene*, etc. The followings are summaries of the accomplishment of pre- and post-doctoral trainees in the third year:

Postdoctoral trainees:

Yoichi Nagata, M.D., Ph.D.

The PTEN tumor suppressor protein inhibits the activation of PI-3K and its downstream target, Akt. We have investigated whether PTEN deficiency may render breast cancer cells resistant to Herceptin. First, we utilized a PTEN antisense oligonucleotide to demonstrate that inhibition of PTEN expression impairs Herceptin-mediated Akt dephosphorylation in a breast cancer cell line, SKBR3 and does not exhibit any cell toxicity *in vitro*. The breast cancer cells harboring reduced PTEN are more resistant to Herceptin than cells with a normal amount of PTEN. In addition, we showed that breast cancer cells with reduced PTEN are also less sensitive to a combination therapy, i.e. Herceptin with Taxol. Currently, we are exploring the molecular mechanism of PTEN activation by Herceptin.

Seyed M. A. Najafi, Ph.D.

The adenoviral early gene product, E1A functions as a general tumor suppressor protein in human cancer. In this study, we have investigated molecular mechanisms of E1A in

vitro. We have established stable E1A transfectants in two cell lines, MDA-MB-231 (breast) and SKOV3-ip1 (ovary). By using cDNA microarray to compare gene expression between parental and transfectants, we observed that E1A transfectants have higher level (more than 10 fold) of p21^{cip1} (a cyclin-dependent kinase inhibitor) expression. The E1A induced p21^{cip1} are mainly localized to the nuclei where it functions as a CDK inhibitor. To further test whether E1A reduction in cell growth is due to induction of p21^{cip1}, we have treated MDA-MB-231 cells and its E1A stable transfectant cells with a specific antisense oligonucleotide to block p21^{cip1} expression. The results have shown that the antisense oligonucleotide of p21^{cip1} reduces its expression in both parental and E1A transfectant cells and the growth rate increases in parental and E1A transfectant cells by 18% and 53%, respectively. This may suggest that the growth inhibition by E1A is mediated in part through induction of nuclear p21^{cip1}. Therefore, our results support the role of E1A as an anti-cancer drug, which may regulate an essential cell cycle modulator, p21^{cip1}.

Chenyi Zhou, Ph.D.

Germ-line mutations in breast cancer susceptibility gene 1 (BRCA 1) are responsible for approximately half of all cases of hereditary breast cancer and for almost all combined hereditary breast and ovarian cancer cases. BRCA1 has been shown to be involved in DNA repair and maintenance of genomic instability. We have shown that the carboxyl-terminal of BRCA1 is required for BRCA1 foci formation and is needed for assembly of BRCA1 and RAD51 DNA repair complex after the treatment with DNA-damaging reagent cisplatin but not after ionizing irradiation. In addition, our recent data suggest that BRCA1 is also involved in the regulation of the catalytic subunit of human telomerase (hTERT), a gene involved cellular immortalization, whose expression is repressed in normal human cells but is activated in immortal cells and during tumorigenesis. We are currently investigating underlying molecular mechanism of such regulation and to identify whether there is tissue specific regulation involved in breast and ovarian cancer development. Our preliminary data showed that BRCA1 could down-regulate telomerase activity by interacting with c-MYC proto-oncogene, which is up-regulated in breast cancer. In addition, we plan to do a large cohort of clinical patients breast samples to examine whether such regulation can be validated in vivo. Understand such regulation may shed new light into molecular basis how BRCA1 mutation

Jijiang Zhu, Ph.D.

Our work is focus on the role of environmental carcinogen exposure and genetic susceptibility in breast cancer etiology. We have found a significant association between the level of DNA damage induced by a dietary carcinogen PhIP and the risk of breast cancer. We also observed that breast tissues from cancer patients have a significantly higher level of 8-hydroxdeoxyguanosine that of non-cancer controls. We are continuing this line of research by measuring the association of oxidative DNA damage and mitochondrial gene mutations, in addition to examining the association between genetic susceptibility to oxidative stress and cancer risk.

Pre-doctoral trainees:

Chi-Ping Day

The integrin family of adhesion receptors contributes in cell survival, proliferation, tumor growth and metastasis. Integrin has been shown to cooperate with HER2/neu to increased malignancy. It is well known that HER2/neu overexpression correlates with poor survival of breast cancer patients. The integrin linked kinase (ILK) is a transducer molecule which is directly downstream effector of integrin. We have investigated the role of ILK in activation of NF- κ B by HER2/neu. Our results have suggested that HER-2/neu may activate the kinase activity of ILK. Furthermore, activation of ILK kinase activity can be blocked by emodin (a tyrosine kinase inhibitor) and wortmannin (a PI-3K inhibitor) in HER2/neu-overexpressing cells, it implies that a tyrosine kinase (possibly HER2/neu) and PI-3K are required for activation of ILK. ILK-kinase dead transfectants of HER-2/neu overexpressing NIH3T3 cells are more sensitive to TNF- α induced apoptosis and anoikis, and fail to activate transcriptional activity of NF- κ B, which is active in HER2/neu overexpressing cells via PI-3K/Akt pathway.

Keng-Hsueh Lan

Our investigation focuses on the development a penetratin-based targeted delivery system to introduce specific therapeutic peptides into HER2/neu-overexpressing breast cancer cells. We have synthesized a biotin-P3-AHNP peptide. The AHNP is developed based on a recombinant humanized anti-HER2 monoclonal antibody rhuMab4D5 (Herceptin). We have observed that P3-AHNP peptide translocates to cytoplasmic compartment better than P3 alone in both 435.eB and MDA-435 breast cancer cell lines. The P3 conjugated AHNP peptide in HER2/neu-overexpressing breast cancer cell lines, 435.eB and SKBR3, which were pretreated with Herceptin has exhibited lower translocation ability. Therefore, the data suggested that translocation ability of P3-AHNP may be due to the help of AHNP. We also demonstrated that as low as 2nM of P3-AHNP is sufficient to exhibit efficient delivery and specific targeting of HER2/neu-overexpressing breast cancer cells *in vitro*.

Yan Li

The Bik gene is a pro-apoptotic member in the BCL-2 family. Bik forms heterodimers with various anti-apoptotic proteins, including BCL-2 and BCL-X_L, the association of which hinders the function of the anti-apoptotic proteins. We have constructed various Bik mutants (bikT33D, bikS35D and bikT33S35D) to achieve the optimal apoptosis ability *in vitro* and observed anti-tumor effect in mice *ex vivo* and *in vivo*. Thus, bik mutants are potential candidates in a gene therapy setting. Another study involves in examining the role of HIF in metastasis and angiogenesis in HER-2/neuoverexpressing breast cancer cells. We have found that emodin (a tyrosine kinase inhibitor) inhibits HIF-1 α mediated angiogenesis in HER2/neu-overexpressing breast cancer cell lines.

Xiaoyan Wang

We have examined the effect of viral particle replicons (VPR) containing a rat Neu gene (developed by Alpha Vax, Inc.) in pre-immunization protection experiments in two animal tumor models: mammary fat pad and experimental lung metastasis. We have observed that VPR-neu can effectively protect neu-transgenic mice from developing spontaneous mammary tumors that rise at ~100 days of age. The VPR-neu vaccinated transgenic mice were tumors-free at 230 days of age. By tetramer analysis, the VPR-neu vaccinated mice had an increased in the number of neu-specific CD8⁺ spleen T cells containing intracellular IFN- γ . In addition, the vaccination condition, which induces tumor protection corresponds precisely with *in vitro* measurement of T cell immunity (tetramer and INF- γ assays). Therefore, our results indicate that the mechanism of anti-tumor effect of VPR-neu vaccine is through induction of activated CD8⁺ T cells.

Key Research Accomplishments

- Construct PTEN-specific antisense oligonucleotide and optimize the treatment condition to reduce PTEN expression level efficiently in breast cancer cell lines, SKBR3 and BT 474 without significant cell toxicity.
- By using PTEN antisense oligonucleotide, the reduced PTEN expression not only impairs Herceptin-mediated Akt dephosphorlation, but resists to Herceptin-induced cell growth arrest in SKBR3 cells.
- Reduced PTEN expression renders SKBR3 cells resistant to a combination therapy, Herceptin + Taxol treatment, which is clinical standard strategy to treat breast cancer patients.
- E1A induces p21^{cip1} expression, a cyclin-dependent kinase inhibitor, in E1A stable transfectants in breast cancer cell lines, MDA-MB-132 and SKBR3.
- Only larger isoform of E1A, 13S E1A could transactivate p21^{cip1} expression and the induced p21^{cip1} predominantly localizes to the nuclei, where it functions as a Cdk inhibitor.
- Using p21^{cip1} antisense oligonucleotide to treat parental and E1A transfectant cells, both cells have p21^{cip1} reduced expression and increased growth rate.
- E1A anti-cell growth ability may due to induction of a cell cycle modulator, p21^{cip1} *in vitro*.
- C-terminal of BRAC1 is essential for BRAC1 foci formation and is required for assembly BRAC1 with RAD 51, a DNA repair complex after cells treated with cisplatin (a DNA damaging agent) but not with ionizing irradiation.
- BRAC1 regulates the catalytic subunit of human telomerase (hTERT), whose expression is repressed in normal cells but is upregulated in immortal cells and during tumorigenesis.
- BRAC1 downregulates telomerase activity by interacting with c-Myc which is upregulated in breast cancer.
- Discover that a significant association between the level of DNA damage is induced by a dietary carcinogen 2-amino-1-methyl-6-pheylimidazo (4,5-b) pyridine (PhIP) and the risk of breast cancer.
- Breast tissues from breast cancer patients have a higher level of 8-hydroxdeoxyguanosine (causing oxidative DNA damages) than that of non-cancer controls.

- Establish a HER2/neu stable transfectant in NIH3T3 cells (3T3-HER2) and a ILK-kinase dead (ILK-KD) stable transfectant in 3T3-HER2 cells.
- ILK-KD transfectants of 3T3-HER2 are more sensitive to TNF α -induced apoptosis and anoikis.
- TNF α could activate transcriptional activity of NF- κ B in 3T3 and 3T3-HER2 cells but fails to do so in the ILK-KD transfectants of 3T3-HER2 cells.
- Atyrosine kinase inhibitor, emodin and a PI-3K inhibitor, wortmannin could inhibit kinase activity of ILK in 3T3-HER2 cells. It implies that kinase activity of HER2 and PI-3K activity are imperative for activation of ILK.
- Successfully develop biotin-P3-AHNP, a penetratin-based delivery system targeting specifically HER2/neu overexpressing breast cancer cell lines, 435.eB and MDA-MB-435.
- As low as 2nM of P3-AHNP is sufficient to show efficient delivery and is specific targeting of HER2/neu-overexpressing breast cancer cells *in vitro*.
- In both 435.eB and MDA-MB-435 breast cancer cell lines, P3-AHNP translocation to cytoplasmic compartment is hindered with Herceptin pretreatment.
- Bik mutant trasnfectants successfully inhibit cell proliferation and enhances apoptosis in human breast cancer cells *in vitro*.
- Bik mutants inhibit tumor growth in mice *ex vivo* and *in vivo*. The Bik mutants (bikT33D, bikS35D and bik T33S35D) are potential candidates in a gene therapy setting.
- Emodin (a tyrosine kinase inhibitor) inhibits HIF-1 α -mediated angiogenesis in HER2/neu-overexpressing breast cancer cell lines.
- VPR-neu effectively protects neu-transgenic mice from developing spontaneous mammary tumors.
- Mice vaccinated with VPR-neu have increased in CD8⁺ spleen T cells containing intracellular INF- γ .
- Mechanism of anti-tumor effect of the CPR-neu vaccine is possible through induction of activated CD8⁺ T cells.

Reportable Outcomes

Peer-reviewed:

1. **Zhou, C.**, Smith, J.L., and Liu, J.. Molecular Phenotype of an Endometrioid Ovarian Cancer Cell Line Carrying a Defective BRCA1 Gene: A Potential Model To Study Hereditary Ovarian Cancer. *Oncogene* (in revision) 2002
2. **Zhou, C.** and Liu, J.. Regulation of human telomerase expression in ovarian cancer cell line. *Oncogene* (submitted) 2002
3. **Zhu, J. J.**, P. Chang, P., Bondy, M. L., Sahin, A., Singletary, S. E., Takahashi, Shirai, S. T. and Li, D. Detection of 2-Amino-1-methyl-6-phenylimidazo[4,5-b]-pyridine -DNA Adducts in normal Breast Tissues and Risk of Breast Cancer. *Cancer Res.*
4. Li, D., Zhang, W. Q., **Zhu J. J.**, Chang, P., Sahin, A., Singletary, S. E., Bondy, M. Hazra, T., Mitra, S., Lau, S., Shen, J. J. and DiGiovanni, J. Oxidative DNA damage and 8-hydroxyguanosine DNA glycosylase/apurinic lyase (hOGG1) in human breast cancer. *Molecular Carcinogenesis*, 31:214-223, 2001.
5. Kwong, K. Y., Zou, Y., **Day, C.-P.** and Hung, M.-C. The suppression of colon cancer cell growth in nude mice by targeting β -catenin/TCF pathway. *Oncogene* (in press), 2002.
6. Tan, M., Jing, T., **Lan, K.-H.**, Neal, C. L., Li, P., Lee, S., Fang, E., Nagata, Y., Liu, J., Arlinghaus, R., Hung, M.-C. and Yu, D.-H. Phosphorylation on tyrosine-15 of p34^{cdc2} by ErbB2 inhibits p34^{cdc2} activation and is involved in resistance to Taxol-induced apoptosis. *Mole. Cell* 9: 993-1004, 2002.

7. Deng, J., Miller, S. A., Wang, H.-Y., Xia, W., Wen, Y., Zhou, B., Lin, S.-Y., **Li, Yan** and Hung, M.-C. β -Catenin interacts with and inhibits NF- κ B in human colon and breast cancers.. *Cancer Cell (in press)*, 2002.

Abstract:

1. **Zhu J. J.**, Chang P, Bondy ML, Sahin AA, Singletary ES, Takahashi S, Shirai T and Li D. Detection of 2-amino-1-methyl-6-phenylimidazo(4,5-b)pyridine (PhIP)-DNA adducts in normal breast tissues by immunohistochemistry and risk of breast cancer. Proc. Am Assoc.Cancer Res. 43, A5044, 2002.
2. **Zhou, C.**, Huang, P. and Liu, J.. Regulation of brca1 depends on p53 status following treatment with cisplatin. Era of Hope DOD Breast Cancer Research Program Meeting September 25-28, 2002, Orlando Florida
3. **Zhou, C.** and Liu, J.. Inhibition of the catalytic subunit of human telomerase expression by BRCA1 in human ovarian cancer cell lines, The 93nd AACR Annual Meeting, 2002, San Francisco, CA.
4. **Li, Yan** and Hung, M.-C. PI3/Akt Enhance HIF pathway to Activate Vascular Endothelial Growth Factor Expression in Her2/neu overexpressing cells. M.D. Anderson Cancer Center Program Retreat, 2002.
5. **Wang, X.**, Wang, J. and Lachman, L. B. Vaccination Against HER2/*neu* Using Alphavirus-Based Vectors. M. D. Anderson Cancer Center Trainee Recognition Day, 2002.

Conclusion

In conclusion, the U.S. Army/DOD Breast Cancer Research Training Program at the University of Texas M. D. Anderson Cancer Center has had a continuing successful third year. Each U.S. Army/DOD Training Grant recipient has benefited from the multidisciplinary program as evidenced by significant progress in their respective research projects and an outstanding publication record. Additionally, each trainee has gained invaluable knowledge and critical thinking skills as a result of departmental and inter-departmental seminars and group meetings. With continued support from the U.S. Army/DOD Breast Cancer Research Program, UT-MDACC will prosper in training scientists in the field of breast cancer research.

**Molecular Phenotype of an Endometrioid Ovarian Cancer Cell Line Carrying
a Defective BRCA1 Gene: A Potential Model To Study Hereditary
Ovarian Cancer**

Chenyi Zhou, Janice L. Smith* and Jinsong Liu¹

Department of Pathology, Division of Pathology and Laboratory Medicine, The University of Texas M. D. Anderson Cancer Center, 1515 Holcombe Boulevard, Houston, TX 77030-4095; Laboratory for cytogenetic service, 7400 Fannin Suite 1200, Houston, TX 77054*

Running title: Molecular phenotype of an ovarian cancer cell line carrying a defective BRCA1 gene

Key words: ovarian cancer, BRCA1, cell cycle, genetic instability, ionizing radiation

¹To whom correspondence should be addressed: Department of Pathology, Division of Pathology and Laboratory Medicine, Box 85, The University of Texas M. D. Anderson Cancer Center, 1515 Holcombe Boulevard, Houston, TX 77030-4095. Phone: (713) 745-1102; Fax: (713) 792-5529; E-mail: jliu@mdanderson.org.

Abstract

BRCA1, the gene responsible for approximately 50% of all cases of hereditary breast and ovarian cancers, has been implicated in the maintenance of genomic stability through DNA repair. Such function is mediated, at least in part, through two tandem BRCA1 C-terminal (BRCT) repeats. Despite of substantial amount of knowledge generated about this protein since it was cloned in 1994, there is no well-characterized ovarian cell line carrying a defective BRCA1 gene to allow detailed experimental analysis of BRCA1 function in human ovarian cancer. In this report, we examined the molecular phenotype of SNU-251, an endometrioid ovarian cancer cell line derived from a cancer patient carrying a nonsense mutation at amino acid 1815 of BRCA1. Loss of C-terminal 49 amino acids due to this point mutation (from G to A) did not affect the expression of the truncated BRCA1 protein, but it did cause a loss of transcriptional activation of the endogenous p21 gene, prevented G2-M cell-cycle arrest, inhibited BRCA1 subnuclear assembly, and increased sensitivity of the cells to ionizing radiation. Consistent with the role of BRCA1 in maintaining genomic instability, this mutant cell line contained numerous chromosomal abnormalities. Our results suggest that the C-terminal 49 amino acids of BRCA1 results in a loss of full BRCA1 function in this cell line, suggesting that SNU-251 may be a useful model to study the development of hereditary human ovarian cancer.

Germline mutations in *BRCA1* are responsible for approximately 50% of inherited breast and ovarian cancers (Easton et al., 1993). *BRCA1* encodes a 1863-amino-acid nuclear phosphoprotein that is maximally expressed during S phase (Chen et al., 1996b; Scully et al., 1996). Exposure to γ -radiation, UV light, or the DNA-replication inhibitor hydroxyurea causes rapid phosphorylation of BRCA1, indicating that BRCA1 is a target of the DNA damage response pathway (Scully et al., 1997a). In the absence of DNA damage, BRCA1 is localized to discrete nuclear foci during the S and G2 phases of the cell cycle. Exposure to DNA-damaging reagents induces localization of BRCA1 to new loci, some of which are sites of DNA synthesis. BRCA1 interacts with both Rad51, a human homologue of bacterial RecA, a protein involved in homologous chromosome recombination and post irradiation DNA repair (Chen et al., 1999; Chen et al., 1998; Scully et al., 1997b) and with RAD50-Mre11-p95 complex involved in nonhomologous DNA repair (Zhong et al., 1999). BRCA1 can arrest the cell cycle by stimulating transcription of the cyclin-dependent kinase inhibitor p21^{WAF/CIP1} (Somasundaram et al., 1999; Somasundaram et al., 1997). In addition, BRCA1 binds p53 and works cooperatively *in vivo* (Chai et al., 1999; Ouchi et al., 1998; Zhang et al., 1998). While complete BRCA1 knockout mice exhibited lethal phenotype, conditional knockouts in the mammary epithelial cells of female mice cause genetic instability and blunted ductal morphogenesis and breast tumor formation (Xu et al., 1999a; Xu et al., 1999b).

The C-terminal region of BRCA1 contains two tandem BRCA1 C-terminal (BRCT) repeats that are homologous to many proteins involved in DNA repair (Bork et al., 1997; Callebaut and Mornon, 1997). A large number of BRCA1 germline mutations have been detected in the BRCT repeats and throughout the entire coding region of BRCA1 in patients with familial breast and ovarian cancer. Despite many mutations identified in this gene from patient's lymphocytes or tumor samples, very few breast or ovarian cancer cell lines carrying *BRCA1* germline mutations are

available to allow detailed experimental analysis of the function of BRCA1 protein. The breast cancer cell line, HCC1937 (Tomlinson et al., 1998), which carries the BRCA1 5382 insC mutation, has been widely used to analyze the function of BRCA1 (Cortez et al., 1999; Scully et al., 1999; Zhong et al., 1999). Mutation in this cell line causes truncation of BRCA1 proteins and the loss of the entire second BRCT repeat. The only reported ovarian cancer cell is SNU251, an endometrioid ovarian cell line which carries a single-base G-to-A transition in exon 23, resulting in a stop codon at amino acid 1815 of BRCA1 and a predicted loss of the half of second BRCT repeat (Yuan et al., 1997). However, limited characterization about this cell line prevents its widespread use as a model system for hereditary ovarian cancer, since it is unclear whether this cell line has the phenotype attributed by the defective BRCA1 gene. This study was designed to determine the phenotype of SNU-251 cells and compare it to that of a sporadic ovarian cancer cell line carrying wild-type BRCA1 to determine whether SNU-251 can be used as a model system to study hereditary ovarian cancer.

Previous studies have shown that the SNU-251 ovarian cancer cell line carries a single-base G-to-A transition in exon 23 of BRCA1 that creates a stop codon at amino acid 1815 of the protein (Yuan et al., 1997). This mutation is predicted to cause the loss of the C-terminal 49 amino acids of the BRCA1 protein which contained second half of the BRCT repeat. Figure 1A shows a schematic of the major known functional BRCA1 domains. It is unclear whether the G-to-A transition in SNU-251 cells interferes with the expression of the mutant BRCA1 protein. Because no known publication has used SNU-251 cells to study BRCA1 function since the cell line was first described (Yuan et al., 1997), we decided to first confirm the described point mutation in the *BRCA1* gene in this cell line. The DNA fragment in exon 23 that contained the mutation was amplified with PCR, and single strand conformation polymorphism analysis (SSCP) was used to detect the mutation.

Results showed a different band-shift pattern for DNA from SNU-251 cells than for DNA from SK-OV3 ovarian cancer cells which carry wild-type BRCA1 gene (Figure 1B). Sequence analysis showed a single base G-to-A transition at amino acid 1815 in exon 23 of SNU-251 cells as previously described (Figure 1C). Western blot analysis showed a 210-kD protein from SNU-251 cells and a 220-kD protein from SKOV3 cells (Figure 1D). To further demonstrate that the C-terminal 49 amino acids were lost in the truncated 210-kD BRCA1 protein, we examined protein expression using the C20 antibody, which specifically recognizes the C-terminus of BRCA1. As shown in Figure 1E, the C20 antibody did not recognize the BRCA1 protein in SNU-251 cells but did recognize the wild-type BRCA1 protein in SKOV3 cells, demonstrating that the DNA in SNU-251 cells encoded a truncated BRCA1 protein lacking the last 49 amino acids. In addition, we sequenced the p53 gene from SNU-251 and showed a previously described three base TCA deletion in exon 7 of SNU-251 cells (Yuan et al., 1997). Western blot analysis showed a high level of mutant p53 protein expression in SNU-251 cells as compared with that in normal ovarian surface epithelial cells (Figure 1F). It is unclear how the last 49 amino acids of BRCA1 affect protein stability. We examined BRCA1 protein levels in the presence of the proteinase inhibitor ALLN. As shown in Figure 1G, levels of both wild-type and truncated BRCA1 increased in the presence of ALLN, suggesting that the second BRCT repeat did not affect BRCA1 stability. A faint 220 kD protein band was also observed in the presence of ALLN, but its significance was not clear since SNU-251 cells showed homozygous mutation by sequence analysis.

BRCA1 has been shown to bind directly to the p53 protein to activate p53-dependent gene expression, since one of the binding site for p53 is located in the C-terminal BRCT repeats (Chai et al., 1999; Monteiro et al., 1996; Ouchi et al., 1998). It is unclear whether deletion of last 49 amino acids of the second BRCT repeat is sufficient to disrupt the function of the protein or

whether the two repeats are functionally redundant and serve as a protective mechanism against DNA damage. To determine the function of the last 49 amino acids, we constructed three *in vitro* expression vectors, pcDNA3 (wtBRCA1), containing the wild-type BRCA1 gene; pcDNA3 (BRCA1 Δ 1815-1863)]; identical to endogenous BRCA1 in SNU-251 cells, and the pcDNA3 (BRCA1 Δ 1158-1863) containing neither BRCT repeat. Each plasmid was transfected into HeLa cells, and the expression of endogenous p21 was analyzed by semi-quantitative reverse transcription-PCR. As indicated in Figure 2A, the wild-type BRCA1 expression vector (lane 2) strongly stimulated endogenous p21 expression when compared with a control vector without the BRCA1 gene (lane 1), while the BRCA1 expression vector without the last 49 amino acids of the second BRCT repeat (lane 3) or and the one with neither BRCT repeat did not induce transcription of p21 (lane 4). Under normal physiologic conditions, two major cell-cycle checkpoints are G₁-S and G₂-M. The G₁-S checkpoint arrests cells in G₁, thereby preventing damaged DNA from being duplicated, and the G₂-M checkpoint prevents damaged chromosomes from segregating the cells that harbor them from entering mitosis. It is unclear whether the last 49 amino acids of BRCA1 are sufficient to disrupt its function of arresting cells in G₁-S or G₂-M. As shown in Figure 2B, consistent with the absence of functional p53 in SNU-251 and SK-OV3 cells, neither cells arrested in G₁-cells after 10 Gy γ -irradiation. Although SNU-251 cells and SKOV3 cells both arrested at G₂-M after 15 (71.2% versus 72.6%) and 24 h (76.6% versus 79.3%) after ionizing radiation, SNU-251 cells lost this G₂-M checkpoint arrest compared to SKOV3 after 48 h (29.6% versus 70.1%, Figure 2B; Table 1). This result implied that mutant BRCA1 was not sufficient to arrest SNU-251 cells at the G₂-M checkpoint.

Loss of the entire second BRCT repeat has been reported to confer sensitivity of HCC1937 breast cancer cells to ionizing radiation and unchecked cell-cycle progression,

however, it is unclear whether loss of a portion of the second BRCT repeat causes a similar phenotype. To examine the sensitivity of SNU-251 cells to ionizing radiation, we performed a clonogenic survival assay. Upon treatment with different doses of ionizing radiation, SNU-251 cells showed more sensitivity to the ionizing radiation than did SKOV3 ovarian cancer cells (Figure 3A). This finding implied that partial deletion of the second BRCT domain caused increased sensitivity to ionizing radiation, suggesting that both BRCT repeats were required to provide resistance to ionizing radiation.

Upon ionizing irradiation, BRCA1 forms discrete subnuclear foci with other DNA repair proteins, such as RAD51. To examine whether BRCA1 subnuclear assembly was affected by loss of the last 49 amino acids, SNU-251 and SKOV3 cells were exposed to ionizing radiation and were then stained with an anti-BRCA1 antibody after 8 h. (Figure 3B). After ionizing radiation, 70% of SKOV3 cells and only 8% of SNU-251 cells were positive for nuclear foci. In addition, approximately 70% of SKOV3 cells and less than 1% of SNU-251 cells had more than 50 visible nuclear foci (Figure 3C). These results implied that the last 49 amino acids of BRCA1 were required for BRCA1 subnuclear assembly after ionizing radiation.

BRCA1-associated breast and ovarian carcinomas have been reported to be associated with high genomic instability, negative estrogen-receptor status, and a high frequency of p53 mutation. In this context, we performed karyotypic analysis of SNU-251 cells, which showed aneuploidy and structural abnormalities, a phenotype commonly associated with ovarian epithelial carcinoma. In four dividing cells analyzed, the chromosome number per cell ranged from 69 to 73, each cell had multiple random abnormalities found only in that cell, but there were some abnormalities which were consistent among the cells. Numerical clonal abnormalities included loss of two copies of the X, 2, 14, and 17 and loss of one copy of 10, 12,

15, 16, 18, 21 and 22 (Figure 4A). When telomerase activity was examined in SNU-251 and SKOV3 cells using TRAP assay, both cell lines showed high levels of telomerase expression (Figure 4B), suggesting that activation of telomerase is an important step for ovarian tumor formation.

Because no known ovarian cancer cell line as a model system to study hereditary human ovarian cancer, we examined the phenotype of SNU-251, a natural occurring endometrioid ovarian cancer cell line carrying a defective BRCA1 gene. We compared the phenotype of this cell with a sporadic ovarian cancer cell line containing wild type BRCA1 to study the role of BRCA1 in ovarian cancer development. We examined the role of the C-terminal 49 amino acids of BRCA1 in transcriptional activation of p21, and G₂-M cell cycle progression, sensitivity to ionizing radiation, subnuclear assembly, chromosomal abnormalities, mutant p53 protein expression, and activation of telomerase expression. Our results indicated that loss of the last 49 amino acids was sufficient to inhibit the transcriptional activation of p21, and prevent the arrest of cells in the G₂-M phase, increase the sensitivity of cells to ionizing radiation, and prevent BRCA1 subnuclear assembly. However, it is important to point out that SNU251 also carries a mutation in hMLH1 gene, which has been reported to affect G₂-M cell cycle arrest (Yan et al., 2001). Therefore, SNU-251 G₂-M cell cycle arrest is also partially contributed by mutation in hMLH1. However, mutation in hMLH1 did not affect the survival of cells after high-dose-rate ionizing irradiation (Yan et al., 2001), therefore, the sensitivity of cell survival to ionizing irradiation in SNU-251 can be attributed specifically by a defective BRCA1 gene. In addition, these cells exhibit marked chromosomal instability and high level of telomerase expression. Our data are consistent with known function of BRCA1 derived from the study of HCC1937 cell, a breast cancer cell line defective BRCA1. Therefore, the development of hereditary ovarian

might involve a similar pathway as these described in hereditary breast cancer. With above well-characterized features about this ovarian cancer cell line, SNU-251 could provide a useful model to test sensitivity to radiation or other chemotherapy drugs used in the treatment of human ovarian cancer carrying BRCA1 mutation.

References

- Blagosklonny MV, An WG, Melillo G, Nguyen P, Trepel JB and Neckers LM. (1999). *Oncogene*, **18**, 6460-6468.
- Bork P, Hofmann K, Bucher P, Neuwald AF, Altschul SF and Koonin EV. (1997). *FASEB J.*, **11**, 68-76.
- Callebaut I and Mornon JP. (1997). *FEBS Lett.*, **400**, 25-30.
- Chai YL, Cui J, Shao N, Shyam E, Reddy P and Rao VN. (1999). *Oncogene*, **18**, 263-268.
- Chen CF, Li S, Chen Y, Chen PL, Sharp ZD and Lee WH. (1996a). *J. Biol. Chem.*, **271**, 32863-32868.
- Chen JJ, Silver D, Cantor S, Livingston DM and Scully R. (1999). *Cancer Res.*, **59**, 1752s-1756s.
- Chen PL, Chen CF, Chen Y, Xiao J, Sharp ZD and Lee WH. (1998). *Proc. Natl. Acad. Sci. USA*, **95**, 5287-5292.
- Chen Y, Farmer AA, Chen CF, Jones DC, Chen PL and Lee WH. (1996b). *Cancer Res.*, **56**, 3168-3172.
- Cortez D, Wang Y, Qin J and Elledge SJ. (1999). *Science*, **286**, 1162-1166.
- Easton DF, Bishop DT, Ford D and Crockford GP. (1993). *Am. J. Hum. Genet.*, **52**, 678-701.
- Kim NW and Wu F. (1997). *Nucleic Acids Res.*, **25**, 2595-2597.
- Liu J, Prolla G, Rostagno A, Chiarle R, Feiner H and Inghirami G. (2000). *Oncogene*, **19**, 2767-2773.
- Monteiro AN, August A and Hanafusa H. (1996). *Proc. Natl. Acad. Sci. USA*, **93**, 13595-13599.

- Ouchi T, Monteiro AN, August A, Aaronson SA and Hanafusa H. (1998). *Proc. Natl. Acad. Sci. USA*, **95**, 2302-2306.
- Scully R, Chen J, Ochs RL, Keegan K, Hoekstra M, Feunteun J and Livingston DM. (1997a). *Cell*, **90**, 425-435.
- Scully R, Chen J, Plug A, Xiao Y, Weaver D, Feunteun J, Ashley T and Livingston DM. (1997b). *Cell*, **88**, 265-275.
- Scully R, Ganesan S, Brown M, De Caprio JA, Cannistra SA, Feunteun J, Schnitt S and Livingston DM. (1996). *Science*, **272**, 123-126.
- Scully R, Ganesan S, Vlasakova K, Chen J, Socolovsky M and Livingston DM. (1999). *Mol. Cell*, **4**, 1093-1099.
- Somasundaram K, MacLachlan TK, Burns TF, Sgagias M, Cowan KH, Weber BL and el-Deiry WS. (1999). *Oncogene*, **18**, 6605-6614.
- Somasundaram K, Zhang H, Zeng YX, Houvras Y, Peng Y, Wu GS, Licht JD, Weber BL and El-Deiry WS. (1997). *Nature*, **389**, 187-190.
- To MD, Done SJ, Redston M and Andrulis IL. (1998). *Am. J. Pathol.*, **153**, 47-51.
- Tomlinson GE, Chen TT, Stastny VA, Virmani AK, Spillman MA, Tonk V, Blum JL, Schneider NR, Wistuba, II, Shay JW, Minna JD and Gazdar AF. (1998). *Cancer Res.*, **58**, 3237-3242.
- Xu X, Wagner KU, Larson D, Weaver Z, Li C, Ried T, Hennighausen L, Wynshaw-Boris A and Deng CX. (1999a). *Nature. Genet.*, **22**, 37-43.
- Xu X, Weaver Z, Linke SP, Li C, Gotay J, Wang XW, Harris CC, Ried T and Deng CX. (1999b). *Mol. Cell*, **3**, 389-395.

- Yan T, Schupp JE, Hwang HS, Wagner MW, Berry SE, Strickfaden S, Veigl ML, Sedwick WD, Boothman DA and Kinsella TJ. (2001). *Cancer Res.*, **61**, 8290-8297.
- Yuan Y, Kim WH, Han HS, Lee JH, Park HS, Chung JK, Kang SB and Park JG. (1997). *Gynecol. Oncol.*, **66**, 378-387.
- Zhang H, Somasundaram K, Peng Y, Tian H, Bi D, Weber BL and El-Deiry WS. (1998). *Oncogene*, **16**, 1713-1721.
- Zhong Q, Chen CF, Li S, Chen Y, Wang CC, Xiao J, Chen PL, Sharp ZD and Lee WH. (1999). *Science*, **285**, 747-750.

Acknowledgements

This work was supported in part by institutional start-up funds, an institutional research grant, and career development award from M. D. Anderson Cancer Center Specialized Program of Research Excellence (*SPORE*) in Ovarian Cancer (to J.L.). C. Z. is the recipient of a post-doctoral fellowship from U.S. Army Breast Cancer Research Program, department of defense, Grant No. DAMD17-99-1-9264 and the M. D. Anderson Cancer Center *SPORE* in Ovarian Cancer. The authors want to thank Dr. Arnout C Ruifrok for help in imaging analysis.

Figure Legends

Figure 1. (A) Schematics of the wild-type and truncated BRCA1 protein. Major known functional domains are indicated. Ring-finger, ring-finger DNA-binding domain; NLS, nuclear localization sequence; BRCT1 and BRCT2, BRCA1 C-terminal domain 1 and domain 2; wt, wild-type BRCA1. (B) Single-strand DNA conformation polymorphism analysis of exon 23 of the BRCA1 gene from SKOV3 and SNU-251 ovarian cancer cells. The SNU-251 endometrioid ovarian cancer cell line was a generous gift of Dr. Jae-Gahb Park (Korea Cell Line Bank, Seoul National University, Korea) (Yuan et al., 1997). PCR was used to amplify exon 23 of the *BRCA1* gene. Primers used to detect mutations in exon 23 of *BRCA1* were *BRCA1* forward primer (nt 4303-4320): 5'-agcagagggataccatgc and reverse primer (nt 4741-4758) 5'-caatcgtgtggcccagact. PCR was performed as previously described (Yuan et al., 1997). The resulting DNAs were analyzed in a nondenaturing 4% polyacrylamide gel, and the bands with an altered migration pattern were purified and analyzed by dideoxy sequencing. An arrow indicates the shifted DNA band. (C) DNA sequence analysis of exon 23 of the *BRCA1* gene. A single-base G-to-A transition creates a stop codon, resulting in a BRCA1 protein truncated at amino acid 1815 in SNU-251 cells but not in SKOV3 cells. DNA alignment indicates this G-to-A mismatch. (D) Western blot analysis of the BRCA1 protein in SKOV3 and SNU-251 cells. Wild-type BRCA1 (220 kD) in SKOV3 cells and a truncated form of BRCA1 (210 kD) in SNU-251 cells were indicated by a small and big arrow respectively. Immunoblotting was performed as previously described (Liu et al., 2000; Scully et al., 1997a). (E) Loss of immunoreactivity of truncated BRCA1 protein to anti-BRCA1 C-terminal antibody C20. The membrane from (D) was stripped and reprobed with anti-BRCA1 antibody C-20 (Santa Cruz Biotechnology Inc., Santa Cruz). (F) Mutant p53 protein expression in SNU-251 and normal ovarian surface epithelial cells (NOE).

The method using for detecting P53 is the same as (D) except p53 primary antibody. (G) Stability of truncated BRCA1 after exposure to the proteinase inhibitor N-acetyl-leu-leu-norleucinal (ALLN). SKOV3 and SNU-251 cell lines were cultured in RPMI 1640 medium supplemented with 10 ng/ml of epithelial growth factor and 10% fetal bovine serum in the presence of antibiotics for 24 h and then exposed to culture media with (+) or without (-) 100 μ M ALLN for 6 h. BRCA1 protein expression levels were analyzed using Western blotting using a previously described protocol (Blagosklonny et al., 1999)

Figure 2. (A) Semi-quantitative reverse transcription (RT)-PCR showing endogenous p21^{WAF1/CIP1} expression affected by BRCA1. HeLa cells (1×10^5) were transiently transfected with 2 μ g of BRCA1-expressing plasmids using Fugen 6 reagent according to the manufacturer's protocol. Forty-eight hours after transfection, RNAs were isolated using the Trizol RNA isolation kit and subjected to RT-PCR. For cDNA synthesis, 2 μ g of total RNA and random hexamers were added to the reaction mixture following the vender's instructions (Qiagen, Valencia, CA). A 5- μ l aliquot of synthesized cDNA was used as a template for amplification of p21 or glyceraldehyde-3-phosphate dehydrogenase (GAPDH) respectively as previously described (To et al., 1998). PCR products were run on a 10% polyacrylamide gel and stained with SYBR Green I (FMC BioProducts, Rookland, ME). GAPDH was used as an internal control. Lane 1, pcDNA3 vector only; lane 2, pcDNA3 (wtBRCA1); lane 3, pcDNA3 (BRCA1 Δ 1815-1863); lane 4, pcDNA3 (BRCA1 Δ 1158-1863). Plasmids were constructed as follows: wild-type BRCA1 cDNA was cut by *Hind*III and *Eco*RV from the vector pUHD10.3 (gift from Dr. Deniel Haber, Harvard University) and subcloned into the pcDNA3 expression vector to generate plasmid pcDNA3 (wtBRCA1). Mutant BRCA1 expression vector, pcDNA

(BRCA1 Δ 1815-1863), which contains a truncated BRCA1 protein without its C-terminal 49 amino acids, was constructed in two steps. First, a DNA fragment containing nucleotides (nt) 4790-5071 of BRCA1 was synthesized by polymerase chain reaction (PCR) using two primers: forward primer (nt) 4790-4814 5'-gatctagagggaaccccttacctggaa and reverse primer (nt 5548-5563) 5'-cctctagatcaggcatctggctgca. An *Xba*I site (underlined) and a stop codon in the reverse orientation (bold) were included in the 3' primer. Second, the PCR products were purified and cut by *Xba*I, and the DNA fragment between the *Xba*I site of the BRCA1 cDNA (at nt 4790) and the *Xba*I site of the polylinker in pcDNA3 (wtBRCA1) was removed and replaced with the PCR fragment. A mutant BRCA1 expression vector with a deletion of the C-terminal 305 amino acids of BRCA1 pcDNA (BRCA1 Δ 1558-1863) was constructed by removing the same fragment from the pcDNA3 (wtBRCA1) vector and religating the remaining backbone.

(B) Cell-cycle analysis of SK-OV3 and SNU-251 cells. Cells were plated and harvested in log phase after 15, 24 or 48 h with or without 10 Gy of ionizing radiation. Cells were fixed, stained with 0.04 mg/ml propidium iodine containing 5 μ g/ml RNase. Flow cytometry was performed with a Coulter XL analytical cytometer. The data were analyzed with MultiCycle for Windows .

Figure 3. (A) Clonagenic survival assay. SNU-251 and SKOV3 cells were plated and then exposed to 1, 2, or 4 Gy of ionizing radiation or were mock-exposed (0 Gy). Cells were cultured for 8 to 10 days, and colonies were stained with crystal violet and counted. Each experiment was repeated three times. The number of surviving colonies was normalized to total number of mock-exposed colonies. Standard error bars were shown on the graph. Where error bars are not seen, standard errors are too small to show on the graph. (B) The C-terminal 49 amino acids of BRCA1 are required for foci formation after ionizing radiation. Cells were irradiated with 12 Gy

or not irradiated and stained with mouse anti-BRCA1 monoclonal antibody Ab-1 followed by a Texas Red-conjugated anti-mouse antibody. Nuclei were stained with 4' 6'-diamidino-2-phenylindole (DAPI). NT, no treatment. (C) Percentage of foci positive in SKOV3 and SNU-251 cells. Cells containing more than 10 nuclear foci were considered "positive". About 200 cells were counted for each cell line. Microscopic images were acquired using confocal microscopy (Leica) and were processed using Adobe Photoshop software.

Figure 4. (A) Chromosomal abnormalities in SNU-251 cells were determined by routine cytogenetic techniques. (B) Telomerase activity was measured using the telomerase repeat amplification protocol (TRAP)-eze telomerase detection kit (Oncor Inc., Gaithersburg, MD) in extracts derived from SNU-251, SKOV3, normal ovarian surface epithelial cells (NOE), and controls with (+) or without (-) 85°C heat inactivation. Our methodology was based on that originally described by Kim and Wu (Kim & Wu, 1997). L, PCR positive control; N, negative cell extract; and P, positive cell extract.

Table 1 Summary of percentage of cells in different phases of cell cycle

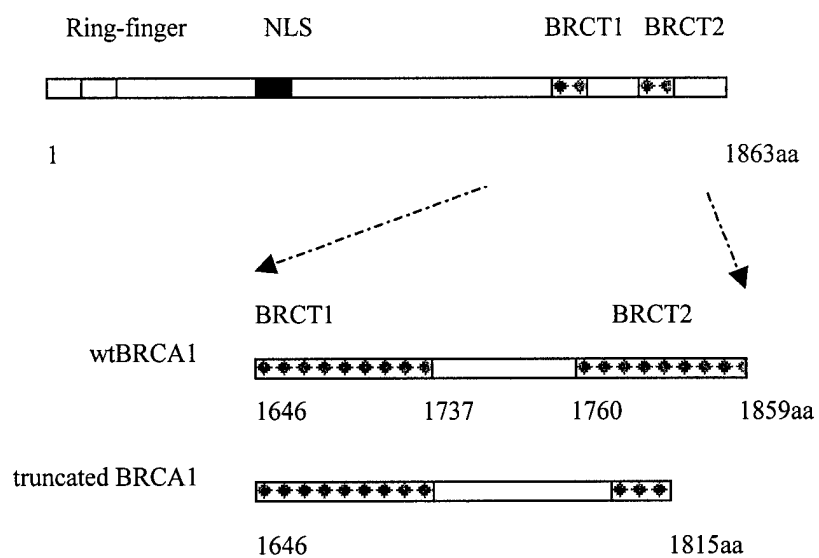
Time	Cell-cycle phases	SKOV3		SNU-251	
		Control	irradiation	Control	irradiation
0 h	G1	41	41	58	58
	S	50	50	20	20
	G2/M	8	8	20	20
15 h	G1	58	2	45	10
	S	31	10	26	38
	G2/M	10	87	28	51
24 h	G1	58	10	49	11
	S	29	4	25	33
	G2/M	11	85	24	55
48 h	G1	75	35	62	57
	S	15	9	19	18
	G2/M	9	54	18	24

Table 2.

Cell Line	Mutation	Exon/IVS
SNU251	IVS delC (83556)	IVS3
	IVS4 A →G (89068)	IVS4
	IVS8 G →T (119118)	IVS8
	Del T(118993)	Exon8

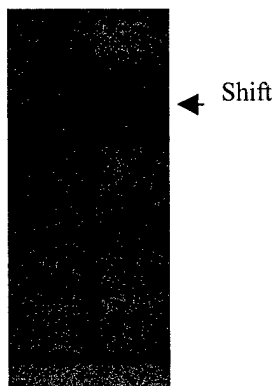
Figure 1

A

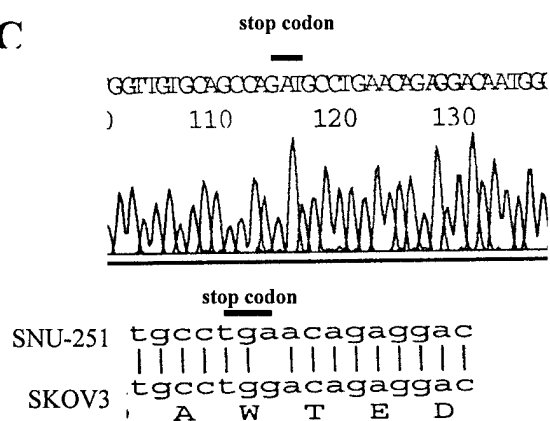


B

SKOV3 SNU-251

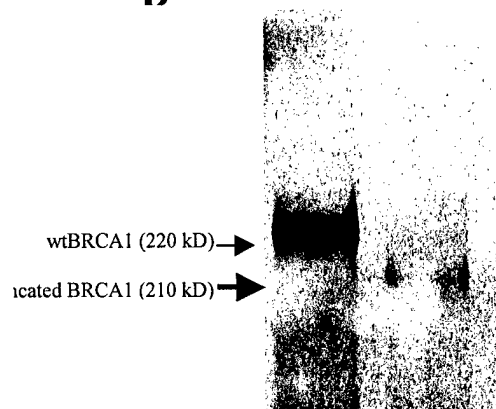


C



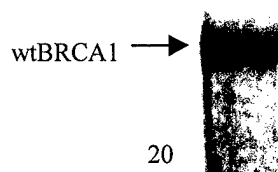
D

SKOV3 SNU-251



E

SKOV3 SNU-251



F

SNU-251 NOE



G

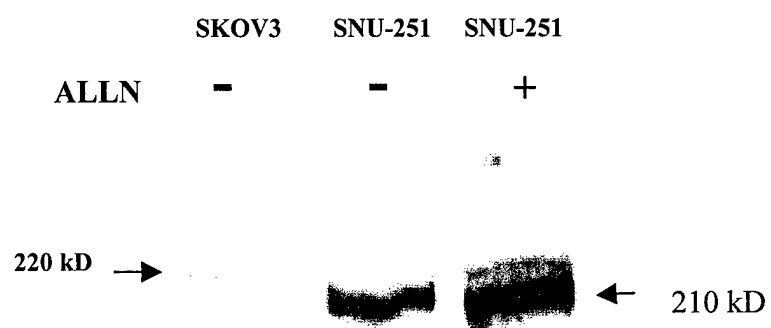
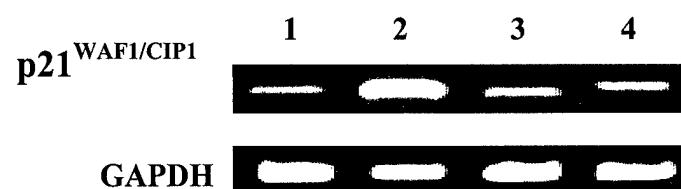


Figure 2

A



B

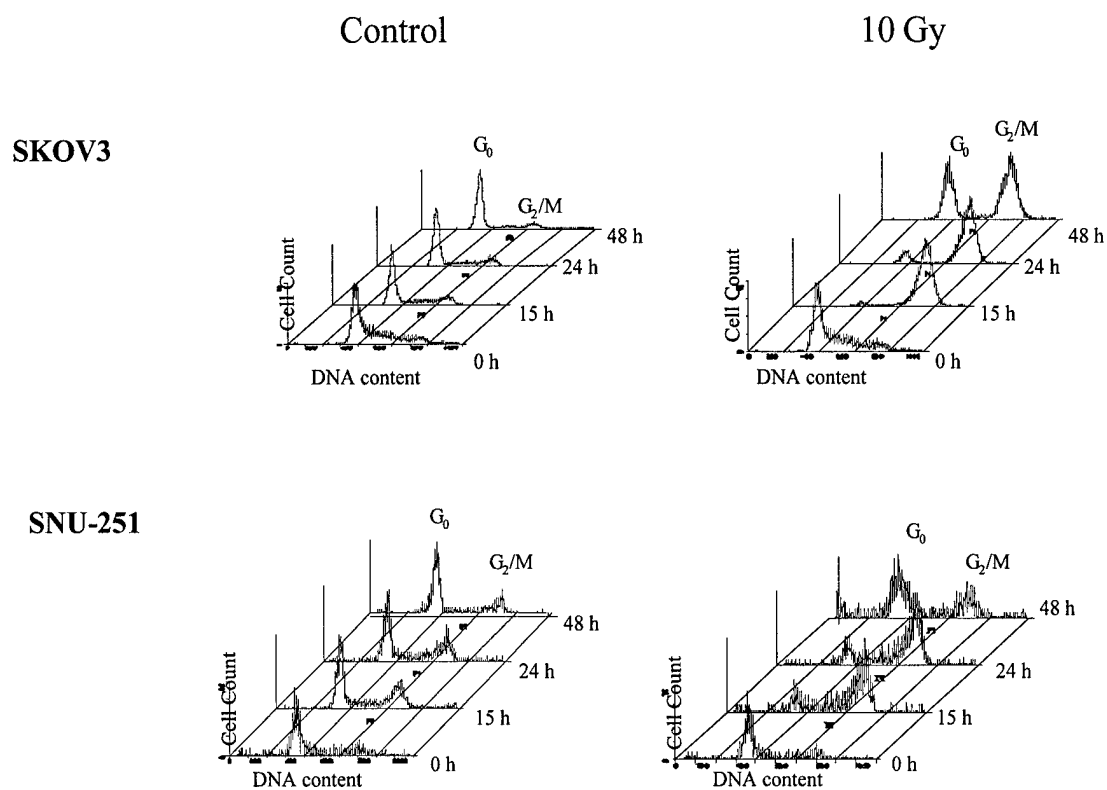
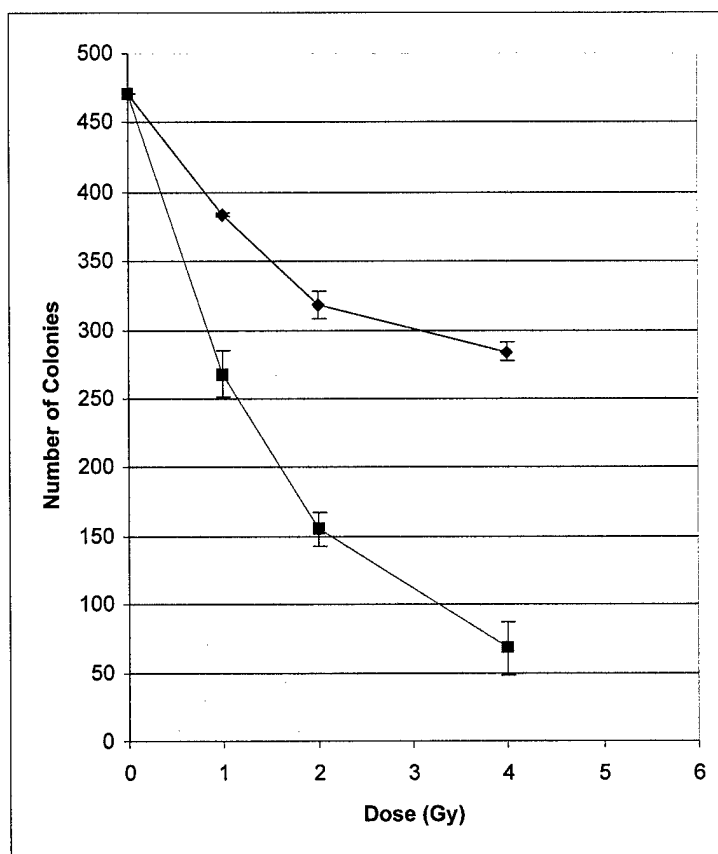
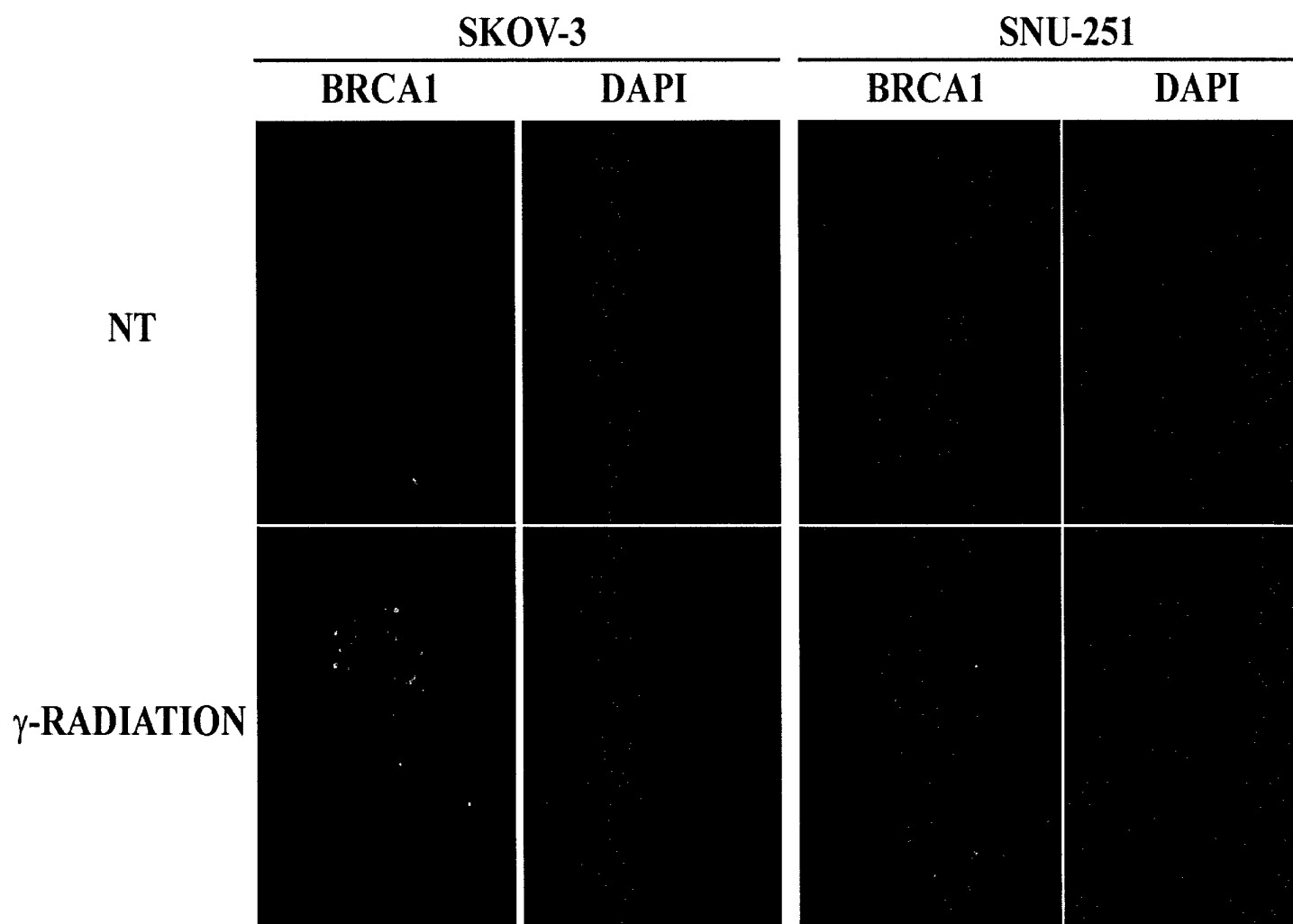


Figure 3

A



B



C

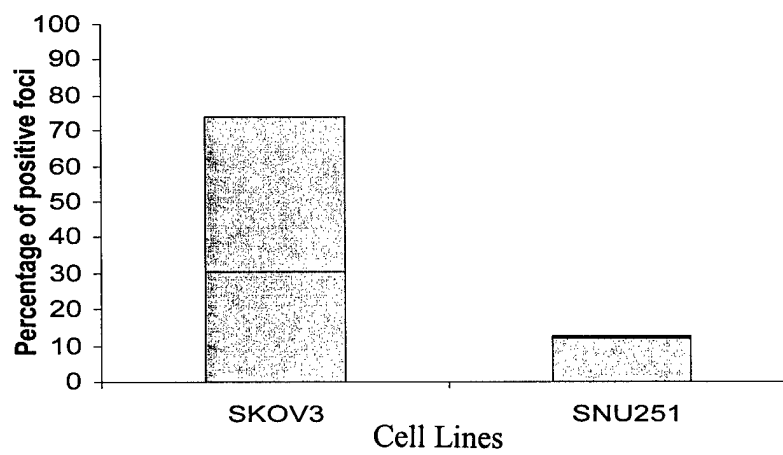
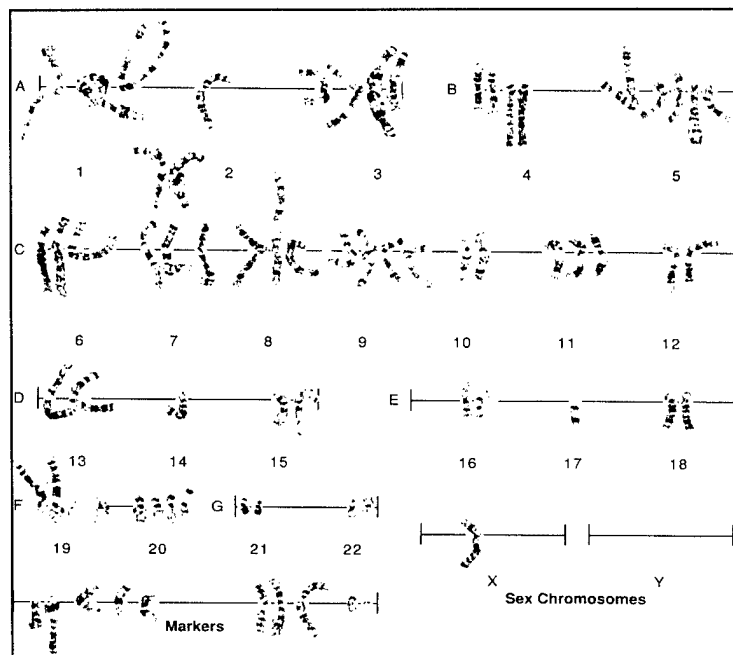


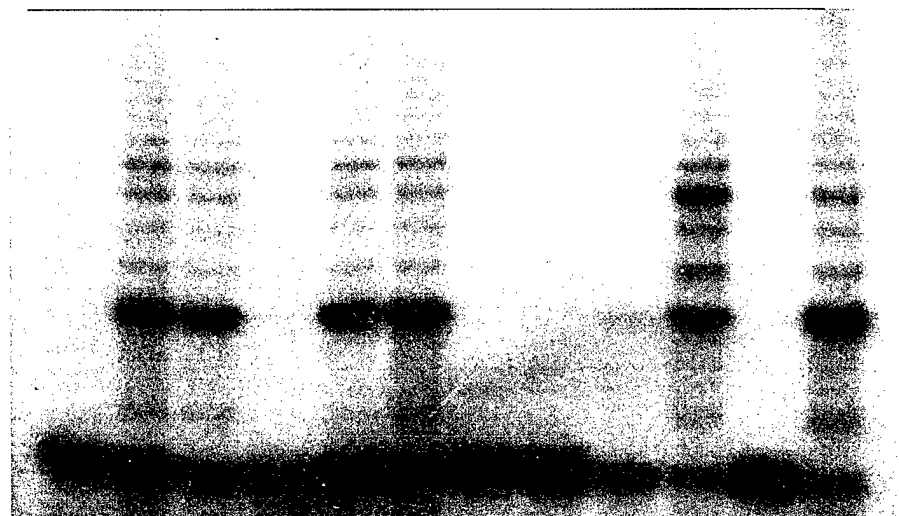
Figure 4

A



B

	SNU-251			SKOV3			NOE			Controls		
μ g of cell extracts	0.8	0.4	0.8	0.8	0.4	0.8	0.8	0.4	0.8	L	N	P
Heat	+	-	-	+	-	-	+	-	-	-	-	-



Inhibition of the Catalytic Subunit of Human Telomerase Expression by BRCA1 in Human Ovarian Cancer Cells

Chenyi Zhou and Jinsong Liu*

Department of Pathology, Division of Pathology and Laboratory Medicine, The University of Texas M. D. Anderson Cancer Center, 1515 Holcombe Boulevard, Houston, TX 77030-4095

Running Title: Regulation of Telomerase by BRCA1

Key Words: BRCA1; hTERT; Myc; ovarian cancer

*To whom correspondence should be addressed: Department of Pathology, Division of Pathology and Laboratory Medicine, Box 85, The University of Texas M. D. Anderson Cancer Center, 1515 Holcombe Boulevard, Houston, TX 77030-4095. Phone: (713) 745-1102; Fax: (713) 792- 5529; E-mail: jliu@mdanderson.org.

Abstract

The catalytic subunit of human telomerase (hTERT) is responsible for the synthesis and maintenance of the telomeric repeats at the distal ends of human chromosomes. Multiple studies have demonstrated that telomerase expression is repressed in normal human cells but is activated in immortal cells and during tumorigenesis. The mechanism by which telomerase expression is regulated is not fully understood. Previous studies have shown that Myc and estrogen receptors can stimulate hTERT transcription through the binding sites located on the hTERT promoter. In this report, we provide evidence that *BRCA1*, a tumor suppressor gene responsible for approximately half of all cases of hereditary breast cancer and almost all cases of combined breast and ovarian cancers, can inhibit the transcription of hTERT through its direct interaction with Myc and partially through the estrogen receptors. We found that in ovarian cancer cells, Myc activated hTERT expression by 3-fold, and BRCA1 completely abrogated this activation. A mutation in the Myc binding site (E-box) of hTERT promoter resulted in the loss of Myc activation and in inhibition by BRCA1. We also found that deletion of the Myc-binding domain in BRCA1 resulted in the loss of its inhibition to the transcription of the hTERT promoter. BRCA1 can also inhibit the transcriptional activation by estrogen receptors when the hTERT promoter containing estrogen receptor binding sites is used in such an assay. Taken together, our data indicate that BRCA1 is involved in regulating cellular immortalization through the modulation of Myc and estrogen receptors on hTERT promoter. Such regulation may provide a molecular-mechanic explanation for why a BRCA1 mutation results in cancer development only in tissues with a high level of estrogen, such as breast and ovary.

The ends of human chromosomes composed of repetitive, non-coding DNA sequences (5'-TTAGG-3'), ranging in size of approximately 5-20 kb. These highly conserved and specialized structures provide protective mechanisms for stabilizing chromosomes and prevent them from being recognized as double-strand breaks and other chromosome destabilizing agents (Blackburn, 1991; Moyzis et al., 1988). Telomerase is responsible for the synthesis and maintenance of the telomeric repeats (Greider and Blackburn, 1985). Telomerase comprises several subunits, including an RNA subunit and the catalytic subunit. The RNA subunit provides the template for the synthesis of telomeres (Feng et al., 1995). The catalytic subunit functions as reverse transcriptase and is responsible for the synthesis of telomeres using the RNA template (Meyerson et al., 1997; Nakamura et al., 1997). With each cell division, the telomeres get shorter, and after dozens of these cell divisions, the telomeres decrease to certain critical number and the cell eventually dies (Counter et al., 1992; Harley et al., 1990). By stable enforced expression of hTERT, cells are able to bypass senescence and extend their lives (Bodnar et al., 1998). Multiple studies have shown that telomerase activity is repressed in normal cells but activated in immortal cells and during tumorigenesis of breast and ovarian cancers (Counter et al., 1994; Kim et al., 1994; Shay and Bacchetti, 1997). These findings suggest that telomerase activation may play an important role in cellular immortalization and in early stages of tumor progression.

Several studies have shown that the Myc oncoprotein can activate hTERT transcription through its direct binding to the E-box in the hTERT promoter and that it synchronistically interacts with nearby Sp1 (Greenberg et al., 1999; Kyo et al., 2000; Takakura et al., 1999; Wu et al., 1999). In addition, two estrogen receptor-binding sites located on upstream of the hTERT promoter have been shown to be important in mediating the hTERT response to estrogen

stimulation (Kyo et al., 1999). Interestingly, BRCA1, a gene responsible for approximately half of all cases of hereditary breast cancer and for almost all case of combined hereditary breast and ovarian cancers (Gayther et al., 1998), has been shown to interact with Myc (Wang et al., 1998). It encodes an 1863 amino acid, 220-kDa nuclear phosphoprotein, and acts in concert with DNA-repair enzymes to maintain the integrity of the genome. BRCA1 also interacts with hRad51, a human homologue of bacterial RecA, a protein involved in homologous chromosome recombination and postradiation DNA repairs (Scully et al., 1997). A mutation in p53 can accelerate breast cancer development in both homozygous *BRCA1* knockout mice, and mice heterozygous for both *BRCA1* and p53 mutation (*BRCA1*^{+/-} / p53^{+/-}) developed mammary gland tumors after being radiated with a low frequency of γ -radiation (Cressman et al., 1999; Xu et al., 1999a). BRCA-deficient cells display spontaneous chromosomal abnormalities, defective G₂/M repair, and centrosome amplification (Xu et al., 1999b). Because Myc is amplified in many different types of human cancer, it is possible that BRCA1 may form a complex with Myc to regulate cellular growth, proliferation, and oncogenesis in different organs. However, it is unclear why BRCA1 involved in multiple functions of multiple cell types leads to development of breast and ovarian cancer only when it is mutated. Recent studies have shown that BRCA1 can bind to estrogen receptors and suppress estrogen response (Fan et al., 2001; Fan et al., 1999). Thus, BRCA1 may suppress the weak oncogenetic effect associated with high levels of estrogen. However, the specific target gene for the BRCA1-Myc complex and the BRCA1-estrogen receptor has not been identified. Because the hTERT promoter contains both estrogen receptors and Myc binding sites, we speculate that it may be a potential target for BRCA1. Understanding how telomerase is regulated at the molecular level may shed new light on the role of BRCA1 in the tissue-specific development of human breast and ovarian cancers.

We undertook a series of experiments using various hTERT-luciferase constructs, BRCA1 expression constructs, and ovarian cancer cell lines with known BRCA1 status. To examine the effect of BRCA1 on the transcriptional activity of the hTERT promoter, we ligated the hTERT promoter into a vector containing the luciferase (LUC) reporter gene. The schematic of hTERT-luciferase chimeric constructs is shown in Figure 1A. The plasmid pHTERT (-169 ~ +58 nt) was transfected into either a wild type BRCA1 ovarian cancer cell line, SKOV3, or a BRCA1-deficient ovarian cancer cell line, SNU-251, which is an endometrioid ovarian cell line that carries a single-base G-to-A transition in exon 23, resulting in a stop codon at amino acid 1815 of BRCA1 and a predicted loss of half of the second BRCA1 c-terminal (BRCT) repeat (Yuan et al., 1997). An approximate 3-fold increase in the level of hTERT transcription as indicated by the luciferase activity was observed when a plasmid pHTERT (-169 ~ +58 nt) was cotransfected with the Myc expression plasmid (Figure 1B, lane 2), compared with those without the Myc expression plasmid (Figure 1B, lane 1) in both SNU-251 and SKOV3 cells. The activation was inhibited almost to the basal level in SNU-251, and a slight weak inhibition occurred in SKOV3 following cotransfection with the wild type BRCA1 expression plasmid (Figure 1B, lane 4); this repression was dose dependent (Figure 1B, lane 3 and lane 4).

To examine the effect of BRCA1 on the transcriptional regulation of hTERT promoter through the Myc DNA binding site, we performed luciferase assays using a hTERT-luciferase chimeric construct containing a mutation in the Myc binding site of the hTERT promoter, pHTERT (Δ Myc1, -169 ~ +58 nt), together with its wild type counterpart, pHTERT (-169 ~ +58 nt) after they were transfected into SNU-251 cells. As shown in Figure 1C, an approximate 3-fold stimulation of transcriptional activity from pHTERT (-169 ~ +58 nt) was observed when it was cotransfected with the Myc expression plasmid (lane 2, indicated by the solid bar),

compared with those without the Myc expression plasmid (lane 1). Mutation in the Myc binding site in plasmid pH_{hTERT} (Δ Myc1, -169 ~ +58 nt) resulted in a loss of transactivation by Myc (Figure 1C, lane 2, indicated by the dash bar). BRCA1 did not further decrease the basal level of transcription from the hTERT-luciferase constructs (Figure 1C, lane 3), suggesting that BRCA1 inhibits the level of transcription through this Myc binding site on the hTERT promoter. While a similar transfection was carried out in 293T cells, Myc stimulated the transcription from the hTERT promoter as in SNU-251 and SKOV3 cells (Figure 1D, lane 2). However, cotransfection with BRCA1 mildly stimulated the transcriptional activity of the hTERT promoter instead of repression, as above described (Figure 1D, lane 3). Based on these results, we concluded that repression of transcriptional activity of the catalytic subunit of hTERT by BRCA1 is ovarian cancer-cell specific. Such repression is more dramatic in ovarian cancer cell lines carrying the homozygous BRCA1 mutation, SNU-251.

An earlier study (Wang et al., 1998) showed that BRCA1 also interacted with Myc through a specific binding domain in the BRCA1 protein. Whether this specific binding domain plays an important role in inhibiting the Myc-mediated transactivation of the hTERT promoter is not known. To examine the role of the Myc-binding domain in regulating the hTERT promoter, we constructed a mutant BRCA1 expression plasmid, pcDNA3 (Δ Myc, BRCA1), which contained the mutant BRCA1 without Myc-binding domain (Figure 2A). Luciferase assays were performed using these mutant BRCA1 and wild-type BRCA1 expression plasmids after they were transfected into SNU-251. We found no repression of luciferase activity from the hTERT core promoter (-169 ~ +58 nt) (Figure 2B, lane 4, indicated by the solid bar) and only a mild inhibition when the hTERT whole promoter (-3330 ~ +58 nt) was cotransfected with the mutant BRCA1 expression plasmid and the Myc expression plasmid (Figure 2B, lane 4,

indicated by the dashed bar), compared with the wild type BRCA1 plasmid (Figure 2B, lane 3). These results demonstrated that the specific Myc binding domain in BRCA1 is required to inhibit the transcription activation of the hTERT promoter.

To further examine whether BRCA1 can interact with Myc on the hTERT promoter *in vivo*, we examined BRCA1 and Myc interaction using a gel mobility shift assay (GMSA). The oligonucleotides containing a Myc binding site derived from hTERT promoter were labeled with [γ - 32 P] and were incubated with nuclear extracts. The resulting DNA-protein complexes were detected in non-denaturing polyacrylamide gels. As shown in Figure 3A, incubation of the oligonucleotides containing a Myc binding site derived from the hTERT promoter yielded two bands (lane 2). The top band could be competed away by an oligonucleotide containing a wild-type Myc binding site (lane 3) but not by an oligonucleotide containing mutations in this binding site (lane 4). In contrast, the lower band was competed away either by an oligonucleotide containing a wild-type or by a mutant Myc binding site, suggesting that the top band represents the specific DNA-Myc complex and the lower band represents the nonspecific one (lane 3 and lane 4). The specific DNA-Myc complex was further demonstrated (Figure 3B) when incubation of an increased concentration of the anti-Myc antibody decreased the binding activity of the top band but not the low band (lane 7-9), similarly to what was previously reported (Kyo S et al., 2000). The DNA-binding activity of Myc was diminished when these DNA-Myc binding complexes were incubated in the presence of the anti-BRCA1 antibody (Figure 3C, lane 13-15) but not in the presence of normal serum IgG, as shown in Figure 3C, lane 12. The top band decreased markedly compared with the lower band, suggesting that the anti-BRCA1 antibody binds to the Myc-BRCA1 complex and decreases its binding to the Myc binding sites. These

results suggest that BRCA1 inhibits the transcriptional activity of hTERT through direct interaction with Myc in the core promoter of hTERT.

BRCA1 is known to interact with estrogen receptors and inhibit the transcriptional activity of the estrogen receptor (ER) (Fan et al., 2001; Fan et al., 1999). Because two estrogen receptor-responsive elements (ERE) have been found upstream of the hTERT promoter (Takakura et al., 1999), these binding sites may also be the potential targets for BRCA1-mediated inhibition of hTERT. To test whether BRCA1 inhibited transcriptional activity through the estrogen response elements in the hTERT promoter, we used a full-length hTERT promoter (-3328 ~ +58 nt) luciferase chimeric construct that included two estrogen-receptor binding sites and cotransfected it with the expression plasmid containing ER in the absence or presence of estradiol. We found only a minimal increase in the level of luciferase activity when estradiol or the estrogen receptor was introduced alone (Figure 4, lane 2 and lane 3, indicated by the solid bar). However, an approximate 2-fold increase occurred in the levels of luciferase activity when estradiol and the estrogen receptor expression plasmid were introduced together (Figure 4, lane 4, indicated by the solid bar). Transfection with the BRCA1 expression plasmid abolished the transcription activation by the estrogen receptor-estradiol complex but did not abolish the basal level of hTERT transcription, as indicated by the luciferase activity (Figure 4, lane 5). In contrast, with the core hTERT promoter, the basal level of transcription was approximately 2-fold higher than that of the whole hTERT promoter (Figure 4, lane 1-3, indicated by the dashed bar). Co-transfection of the estrogen receptor expression plasmid in the presence or absence of estradiol with or without the BRCA1 expression plasmid had no effect on the level of transcription of the core hTERT promoter (Figure 4, lane 2-5, indicated by the dashed bar). These results demonstrated that upstream sequence of the hTERT core promoter

contains inhibitory elements to the basal level of hTERT transcription, as well as estrogen-responsive elements, as previously reported (Braunstein et al., 2001; Kyo et al., 1999; Misiti et al., 2000).

The results presented demonstrate that the transcription of hTERT promoter is negatively regulated by BRCA1. Although the function of BRCA1 has been studied extensively since its cloning in 1994 (Miki et al., 1994), our studies have demonstrated the first direct link between BRCA1 and hTERT and suggest that BRCA1 may regulate cellular immortalization through hTERT, a critical early step in carcinogenesis. Based on these findings, we proposed that the negative regulation of hTERT by BRCA1 might be involved in the suppression of breast and ovarian cancer development in women carrying the heterozygous BRCA1 mutation. This model is shown in Figure 5. In non-breast and non-ovarian tissues, estrogen levels are low; therefore, the estrogen receptor stays inactive. A constitutive high level of the BRCA1 protein binds to the Myc protein, turns off transcription of hTERT, and prevents incidental cellular immortalization. Conversely, in breast and ovarian tissues from women without the BRCA1 mutation, high levels of estrogen are present, and estrogen binds to the estrogen receptor and synergistically interacts with Myc to stimulate the transcription of hTERT. However, high levels of the BRCA1 protein can counteract the stimulation of the hTERT promoter by estrogen and Myc when both alleles of BRCA1 are functional. In women with the heterozygous BRCA1 mutation or homozygous mutation after it loses its wild type allele of BRCA1, such an inhibitory effort by BRCA1 is attenuated or lost as a result of a decreased level or absence of the functional BRCA1 protein, which leads a sustained high level of hTERT mRNA transcription and increased frequency of cellular immortalization. These immortalized cells are susceptible to additional genetic mutations and eventually grow into clinically detectable tumors only in breast and ovary tissues.

Elledge and Amon recently proposed a hypothesis to explain this tissue-specific development in BRCA1 patients (Elledge SJ and Amon A, 2002). These authors suggested that there is selective pressure for the continued growth of breast and ovarian epithelia without the functional BRCA1 allele, while such breast and ovarian cells are susceptible to cell death in non-breast and non-ovarian tissue. However, the specific pathway or genes responsible for such a selection were not known. Li et al. recently presented evidence that BRCA1 inhibits hTERT expression in breast cancer cells (Li et al., 2002). In their study, BRCA1 alone appeared insufficient to inhibit the transcriptional activity of hTERT but required a novel cofactor called Nmi. However, in our study, this additional factor was not required in ovarian cancer cells. The difference could be due to the different pathways involved in the development of breast and ovarian cancers or in the different cell lines used. Nevertheless, the results presented here, together with those reported previously by Li et al., suggest that BRCA1 inhibits tumor growth at least in part through the inhibition of cellular immortalization. Our demonstration that BRCA1 negatively regulate hTERT, a gene involved in cellular immortalization, provides a mechanistic support for Elledge and Amon's hypothesis. In addition, our results demonstrate that hTERT promoter is a target gene for BRCA1 inhibition and that loss of such inhibition may lead to tissue-specific immortalization and to subsequent tissue-specific development of breast and ovarian cancers.

REFERENCES

- Blackburn EH. (1991). *Nature*, **350**, 569-573.
- Bodnar AG, Ouellette M, Frolkis M, Holt SE, Chiu C-P, Morin GB, Harley CB, Shay JW, Lichtsteiner S and Wright WE. (1998). *Science*, **279**, 349-352.
- Braunstein I, Cohen-Barak O, Shachaf C, Ravel Y, Yalon-Hacohen M, Mills GB, Tzukerman M and Skorecki KL. (2001). *Cancer Res.*, **61**, 5529-5536.
- Counter CM, Avilion AA, LeFeuvre CE, Stewart NG, Greider CW, Harley CB and Bacchetti S. (1992). *Embo J.*, **11**, 1921-1929.
- Counter CM, Hirte HW, Bacchetti S and Harley CB. (1994). *Proc. Natl. Acad. Sci. USA*, **91**, 2900-2904.
- Cressman VL, Backlund DC, Hicks EM, Gowen LC, Godfrey V and Koller BH. (1999). *Cell Growth Differ.*, **10**, 1-10.
- Elledge SJ and Amon A. (2002). *Cancer Cell*, **1**, 129-132.
- Fan S, Ma YX, Wang C, Yuan RQ, Meng Q, Wang JA, Erdos M, Goldberg ID, Webb P, Kushner PJ, Pestell RG and Rosen EM. (2001). *Oncogene*, **20**, 77-87.
- Fan S, Wang J-A, Yuan R, Ma Y, Meng Q, Erdos MR, Pestell RG, Yuan F, Auborn KJ, Goldberg ID and Rosen EM. (1999). *Science*, **284**, 1354-1356.
- Feng J, Funk WD, Wang SS, Weinrich SL, Avilion AA, Chiu CP, Adams RR, Chang E, Allsopp RC and Yu J. (1995). *Science*, **269**, 1236-1241.
- Gayther SA, Pharoah PD and Ponder BA. (1998). *J. Mammary Gland Biol. Neoplasia*, **3**, 365-376.

- Greenberg RA, O'Hagan RC, Deng H, Xiao Q, Hann SR, Adams RR, Lichtsteiner S, Chin L, Morin GB and DePinho RA. (1999). *Oncogene*, **18**, 1219-1226.
- Greider CW and Blackburn EH. (1985). *Cell*, **43**, 405-413.
- Harley CB, Futcher AB and Greider CW. (1990). *Nature*, **345**, 458-460.
- Kim NW, Piatyszek MA, Prowse KR, Harley CB, West MD, Ho PL, Coviello GM, Wright WE, Weinrich SL and Shay JW. (1994). *Science*, **266**, 2011-2015.
- Kyo S, Takakura M, Kanaya T, Zhuo W, Fujimoto K, Nishio Y, Orimo A and Inoue M. (1999). *Cancer Res.*, **59**, 5917-5921.
- Kyo S, Takakura M, Taira T, Kanaya T, Itoh H, Yutsudo M, Ariga H and Inoue M. (2000). *Nucleic Acids Res.*, **28**, 669-677.
- Li H, Lee T-H and Avraham H. (2002). *J. Biol. Chem.*, (in Press).
- Meyerson M, Counter CM, Eaton EN, Ellisen LW, Steiner P, Caddle SD, Ziaugra L, Beijersbergen RL, Davidoff MJ, Liu Q, Bacchetti S, Haber DA and Weinberg RA. (1997). *Cell*, **90**, 785-795.
- Miki Y, Swensen J, Shattuck-Eidens D, Futreal PA, Harshman K, Tavtigian S, Liu Q, Cochran C, Bennett LM, Ding W, Bell R, Rosenthal J, Hussey C, Tran T, McClure M, Frye C, Hattier T, Phelps R, Haugen-Strano A, Katcher H, Yakumo K, Gholami Z, Shaffer D, Stone S, Bayer S, Wray C, Bogden R, Dayananth P, Ward J, Tonin P, Narod S, Bristow PK, Norris FH, Helvering L, Morrison P, Rosteck P, Lai M, Barrett JC, Lewis C, Neuhausen S, Cannon-Albright L, Goldgar D, Wiseman R, Kamb A and Skolnick MH (1994). *Science*, **266**, 66-71.

- Misiti S, Nanni S, Fontemaggi G, Cong YS, Wen J, Hirte HW, Piaggio G, Sacchi A, Pontecorvi A, Bacchetti S and Farsetti A. (2000). *Mol. Cell. Biol.*, **20**, 3764-3771.
- Moyzis RK, Buckingham JM, Cram LS, Dani M, Deaven LL, Jones MD, Meyne J, Ratliff RL and Wu JR. (1988). *Proc. Natl. Acad. Sci., USA*, **85**, 6622-6626.
- Nakamura TM, Morin GB, Chapman KB, Weinrich SL, Andrews WH, Lingner J, Harley CB and Cech TR. (1997). *Science*, **277**, 955-959.
- Scully R, Chen J, Plug A, Xiao Y, Weaver D, Feunteun J, Ashley T and Livingston DM. (1997). *Cell*, **88**, 265-275.
- Shay JW and Bacchetti S. (1997). *Eur. J. Cancer*, **33**, 787-791.
- Takakura M, Kyo S, Kanaya T, Hirano H, Takeda J, Yutsudo M and Inoue M. (1999). *Cancer Res.*, **59**, 551-557.
- Wang Q, Zhang H, Kajino K and Greene MI. (1998). *Oncogene*, **17**, 1939-1948.
- Wu KJ, Grandori C, Amacker M, Simon-Vermot N, Polack A, Lingner J and Dalla-Favera R. (1999). *Nat. Genet.*, **21**, 220-224.
- Xu X, Wagner KU, Larson D, Weaver Z, Li C, Ried T, Hennighausen L, Wynshaw-Boris A and Deng CX. (1999a). *Nat. Genet.*, **22**, 37-43.
- Xu X, Weaver Z, Linke SP, Li C, Gotay J, Wang XW, Harris CC, Ried T and Deng CX. (1999b). *Mol. Cell*, **3**, 389-395.
- Yuan Y, Kim WH, Han HS, Lee JH, Park HS, Chung JK, Kang SB and Park JG. (1997). *Gynecol. Oncol.*, **66**, 378-387.

Acknowledgments

This work was supported in part by institutional start-up funds, an institutional research grant, and a career development award from the M. D. Anderson Cancer Center Specialized Program Of Research Excellence (*SPORE*) in Ovarian Cancer (to J. L.). C. Z. is the recipient of a postdoctoral fellowship from the U.S. Army Breast Cancer Research Program, Department of Defense, Grant No. DAMD17-99-1-9264 and the M. D. Anderson Cancer Center *SPORE* in Ovarian Cancer.

We would like to thank Dr. Danial Haber for providing the BRCA1 cDNA, Dr. Satoru Kyo for the hTERT promoter, Dr. Robert Eisenman for the Myc-expression plasmid and Ming-Jer Tsai for estrogen receptor expression plasmid. We thank Gayle Nesom for her editorial help.

Figure Legends

Figure 1 (A) Schematic of hTERT-luciferase chimeric constructs. Plasmid pH_{TERT} (-3328~+77 nt) containing the whole hTERT promoter (~3.3 kb) was a gift by Dr. Satoru Kyo, Kanazawa University, Japan. The core promoter region (from -169 to +58 nt) of hTERT was obtained by polymerase chain reaction (PCR) amplification using the pH_{TERT} (~3.3 kb) plasmid as a template. A pair of primers containing restriction enzyme *Mlu*I and *Bgl*III sites (bolded) at the 5' end were synthesized according to the nucleotides sequence from -169 ~ -148 together with a *Mlu*I restriction site and two extra GA nucleotides at its 5' end, (5'-GA**ACGCGT**TCCCCACGTGGCGGAGGGAC-3'), the 3' primer was synthesized according to the sequence from +37 ~ +58, together with a *Bgl*III restriction site and two extra GC nucleotides at its 5' end (5'-GCAGAT**CTAGGGCT**TCCCACGTGCGCAGC-3'). The resulting PCR product was cut by *Mlu*I and *Bgl*III and subcloned into a pGL3 basic vector to create the pH_{TERT} (-169 ~ +58 nt) plasmid. The plasmid pH_{TERT} (Δ Myc1, -169 ~ +58 nt), with a three-base-pair substitution (CAC→TTT) in the E box of core promoter, was generated using a 5' primer (-169 ~ -148) similar to the 5' primer used above, except for the three-base-pair mutation (underlined): 5'-GAACGCGTTC**CCCTTT**GTGGCGGAGGGAC-3', paired with the same 3' primer used above to generate a wild type core promoter. Two estrogen-receptor binding sites in the hTERT region are also illustrated. ERE, estrogen receptor element; Sp1, Sp1 binding site; Myc, Myc-DNA binding site; Max, Max binding site; LUC, luciferase. (B) The effect of Myc and BRCA1 on the level of hTERT transcription. The SKOV3 cells were purchased from American Type Culture

Collection (ATCC, Manassas, VA). The ovarian cancer cell line, SNU251, was a gift from Dr. Jae-Gahb Park (Korea Cell Line Bank, Seoul National University, South Korea). Both cell lines were maintained in RPMI 1640 cell culture medium with 10% fetal bovine serum in the presence of appropriate antibiotics. All cells were cultured at 37°C in a 5% CO₂ incubator. Plasmid pH₂TERT (-169 ~ +58 nt) was cotransfected with the Myc expression plasmid in the presence or absence of the wild type BRCA1 expression plasmid into SNU251 or SKOV3 cells. Luciferase activity was measured 48 hours after transfection. Activity was normalized using β -galactosidase activity. Luciferase activity was assayed using the luciferase reporter assay system (Promega, Madison, WI) and normalized as 100% in the presence of the Myc expression plasmid. Luciferase activity in SNU-251 cells is indicated by (□), and in SKOV3 cells by (■). A total of 4 μ g of plasmid was used in each transfection. The error bar represents the standard deviation. Each experiment was performed three times. The Myc expression plasmid was a gift from Dr Robert Eisenman, Fred Hutchinson Cancer Center, University of Washington. (C) The effect of the Myc binding site in the hTERT promoter on the BRCA1-mediated inhibition in SNU251 ovarian cancer cells. The wild type hTERT core promoter is indicated by (□), and the mutant core promoter without a Myc binding site by (□). The presence or absence of each plasmid used in each transfection is indicated by + or -. The name of each plasmid was indicated on the left lower position of the figure. (D) The effect of Myc and BRCA1 on the hTERT promoter in 293T cells. The presence or absence of each plasmid is indicated by + or -. A total of 4 μ g of plasmid was used in each transfection. The name of each plasmid was indicated below the figure.



Figure 2 (A) Schematic of mutant and wild type BRCA1 constructs. Plasmid pcDNA3 (wtBRCA1) was constructed by ligating BRCA1 cDNA, which was excised out using *HindIII* and *EcoRV* from plasmid provided by Dr. Danial A. Haber, Harvard Medical School, into pcDNA3 (Invitrogen, Carlsbad, CA). The mutant BRCA1 expression plasmid pcDNA3 (Δ MycBRCA1), without a Myc binding domain in BRCA1, was generated by replacing the cDNA BRCA1 fragment between *AttII* and *KpnI* sites in pcDNA3 (wtBRCA1) with a DNA fragment flanked by *AttII* and *KpnI* (underlined); This fragment was obtained using the pcDNA3 (wtBRCA1) plasmid as the template with a pair of primers: BRCA1 (R): 5'-ACCAGGGTACCAATGAAATACTGCT-3' (nt 2418-2441) and BRCA1 (F): 5'-AGACGTCTCAGGGAACCTAACCAAACGGAGCAGAATG GTC-3' (nt 1719-1749). (B) The effect of the Myc-binding domain in BRCA1 on the level of transcriptional activity of hTERT promoter. Core () or whole promoters of hTERT () were used in each experiment. A total of 4 μ g of DNA was used in each transfection. Each experiment was done three times; the difference between each transfection experiment is indicated by the error bars.

Figure 3 (A) Detection of the Myc-BRCA1-DNA complex. A gel mobility shift assay was used to show that the Myc protein was able to form a specific DNA-Myc complex with the hTERT promoter. wt: wild type Myc binding site; m: mutant Myc binding site. The specific Myc-DNA complex is indicated by the big arrow, and the non-specific binding by small arrow. All lanes contained a [γ - 32 P]-labeled oligonucleotide with a wild type Myc binding site. Lane 1, without nuclear extract; lane 2, with nuclear extract;

lane 3, with nuclear extract and unlabeled wild-type oligonucleotides containing the Myc binding site; lane 4, with nuclear extract and an unlabeled oligonucleotide with a mutated Myc binding site. (B) Inhibition of the binding of the Myc protein to DNA by anti-Myc antibody. An increased concentration of the anti-Myc antibody progressively decreased the binding of Myc to the hTERT promoter. (C) Inhibition of the binding of Myc to DNA by an increased concentration of anti-BRCA1 antibody. Method: Nuclear cell extracts from SKOV3 cells (10 μ g) were incubated with a DNA binding buffer (50 mM HEPES (pH 7.9), 100 mM KCl, 2 mM EDTA, 2 mM DTT), 4% BSA, 6% glycerol and 50 μ g/mL of poly (dC-dG) in the presence or absence of an unlabeled competitor oligonucleotide (20 fold excess) or antibody (from 0.1 μ g to 1 μ g) on ice for 20 minutes. A 5,000-cpm-labeled probe containing a wild type Myc binding site in hTERT promoter, 5'-GCGCTCCCCACGTGGCGGAGGG-3', (hTERT nt: -172 ~ -150) was added to the nuclear extract and incubated for 20 minutes. The oligonucleotide containing the mutant Myc binding site is identical to the wild type sequence probe except for the two base pair changes underlined, 5'-GCGCTCCCCACGGAGCGGAGGG-3', (hTERT nt: -172 ~ -150). The anti-Myc antibody (N262) and normal serum IgG were obtained from Santa Cruz Biotechnology Inc., Santa Cruz, CA, and the anti-BRCA1 antibody (Ab-1) from Oncogene Research, Cambridge, MA. Reaction mixtures were loaded on a 4% nondenatured polyacrylamide gel and then dried prior to the autoradiography. wt, wild type oligonucleotide; m, mutant oligonucleotide.

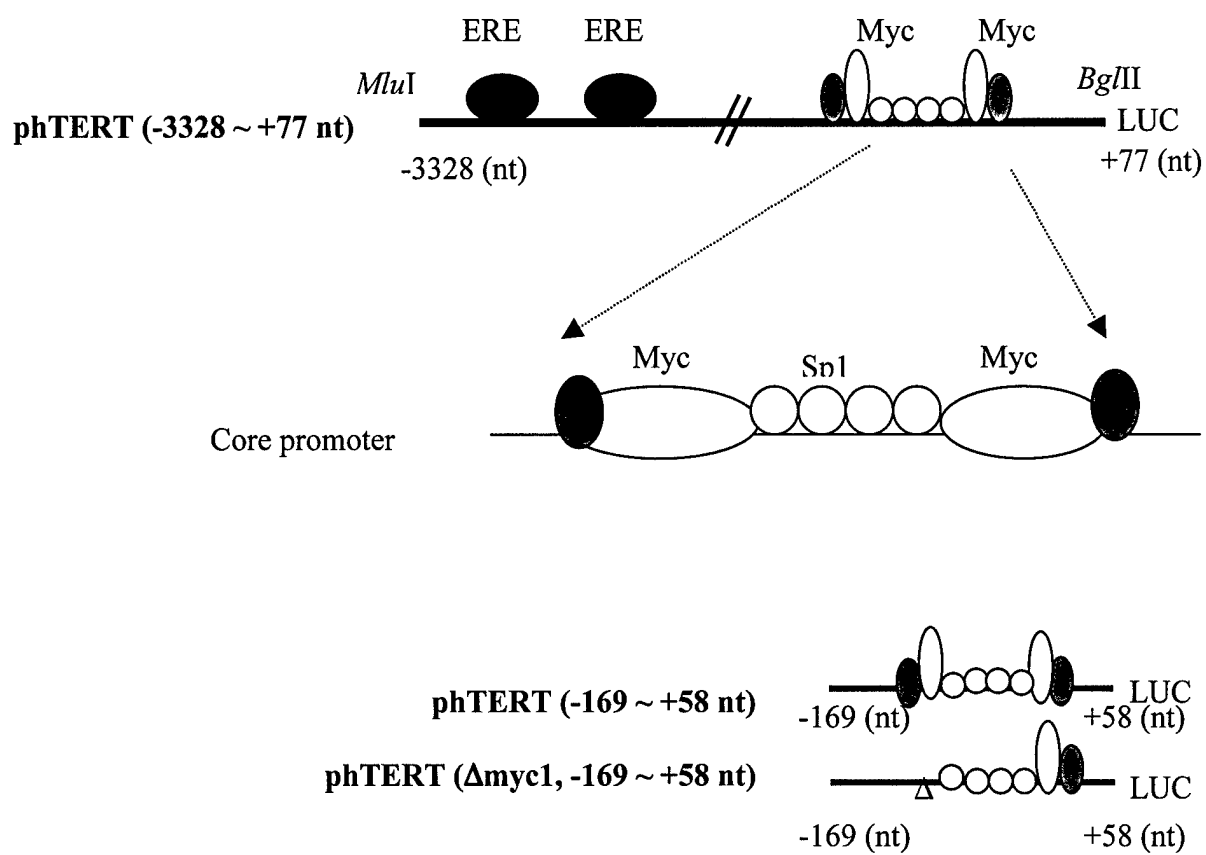
Figure 4 BRCA1 negatively regulated hTERT transcription through the estrogen receptors in SNU-251. Plasmid pHERT (-169 ~ +58 nt) or pHERT (-3328 ~ +77 nt)

was cotransferred with the estrogen receptor expression plasmid into SNU-251 cells in the presence or absence of estradiol. Luciferase activity was measured as described above (see Figure 1 legend). Luciferase activity was normalized as 100% in the presence of the estrogen receptor and estradiol. Either whole (\square) or core promoters of hTERT (\boxminus) were used in each experiment. The presence or absence of each plasmid or estradiol (E2) used in each transfection is indicated by + or -.

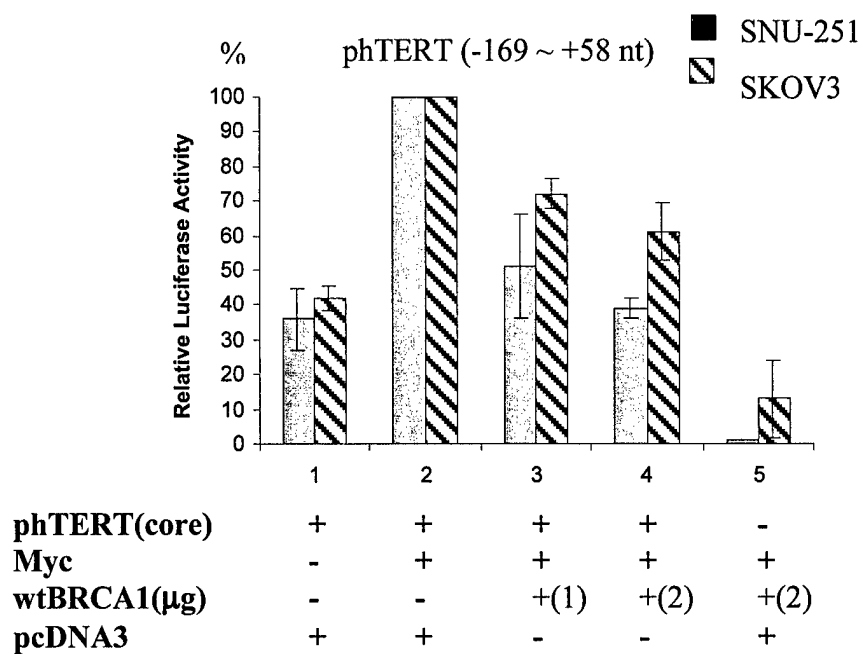
Figure 5 A model for the tissue-specific development of breast and ovarian cancers in women with the heterozygous BRCA1 mutation. The level of expression of the hTERT promoter is indicated by a small, thin, or big, thick arrow. ERE (\square), estrogen responsive element; Myc (\blacksquare), Myc binding site; Sp1 (\bigcirc), Sp1 binding site; ER (\bullet), estrogen receptor; E2, estradiol.

Figure 1

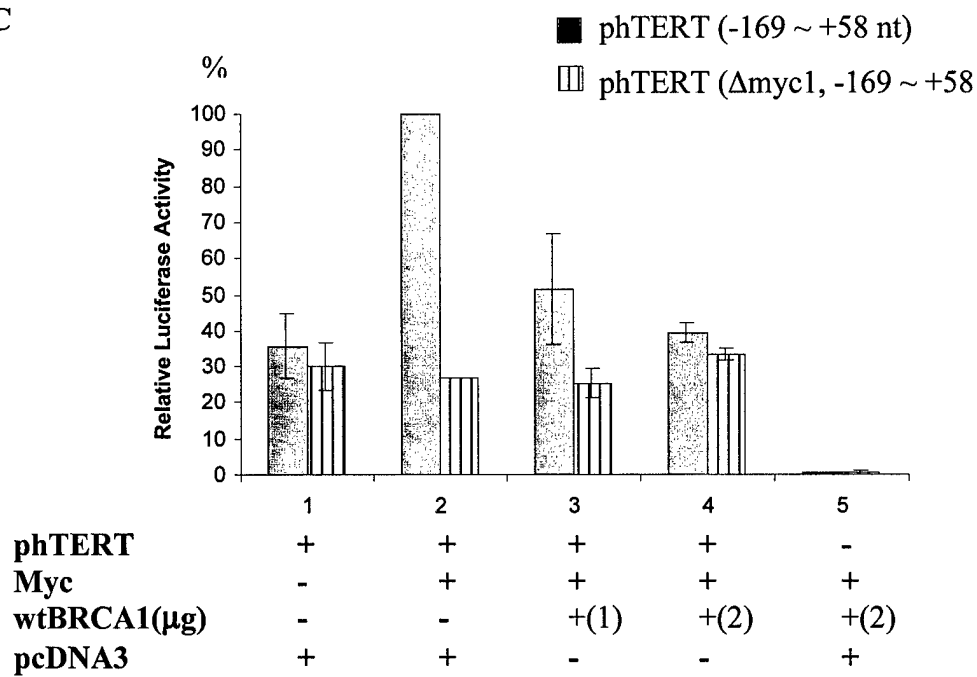
A



B



C



D

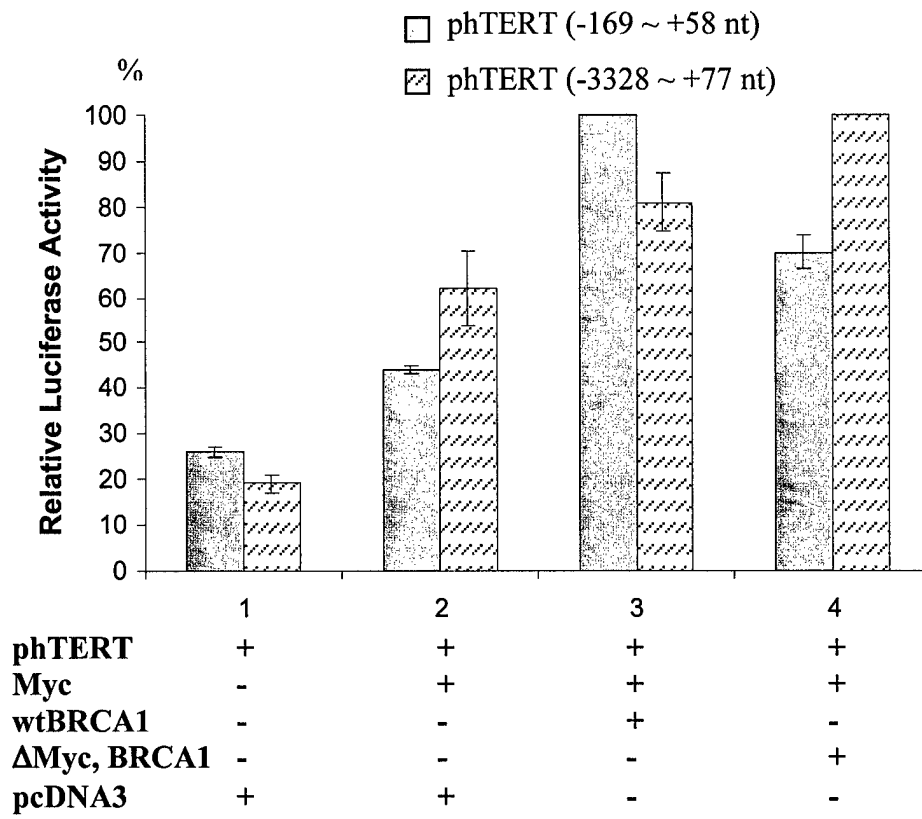
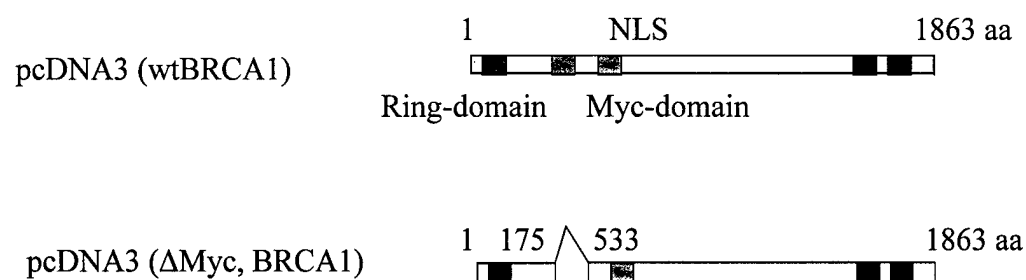


Figure2

A



B

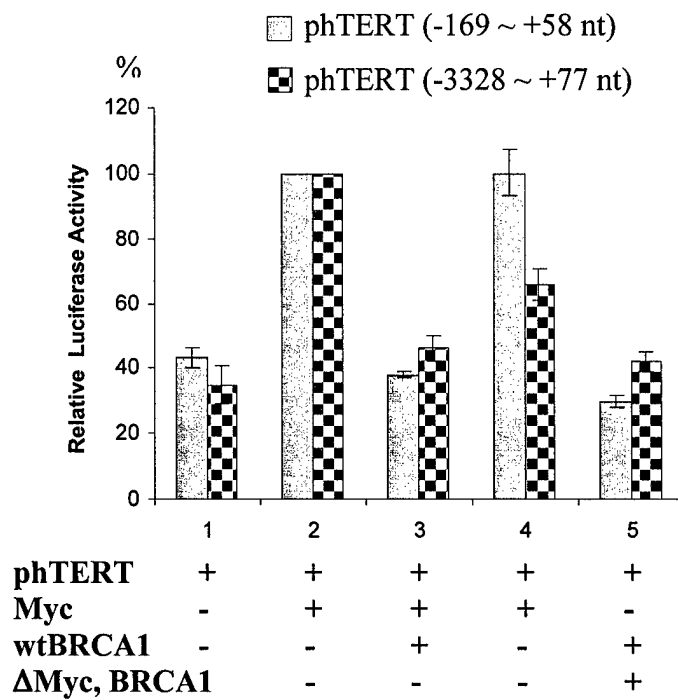


Figure 3

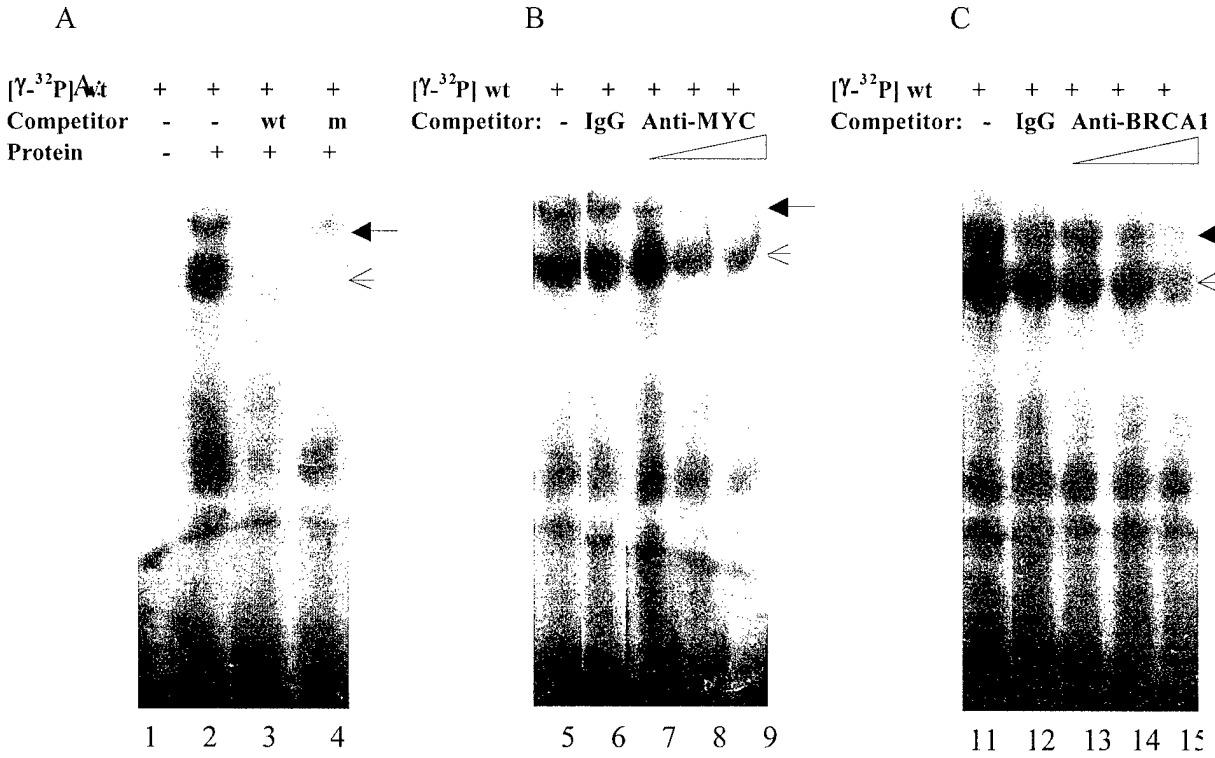


Figure 4

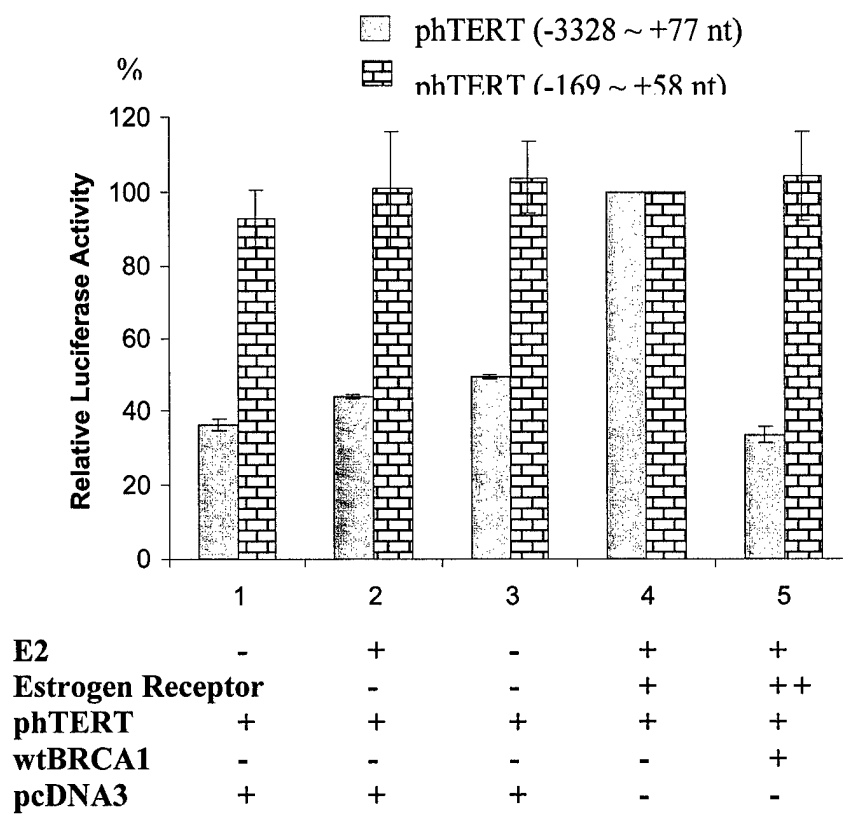
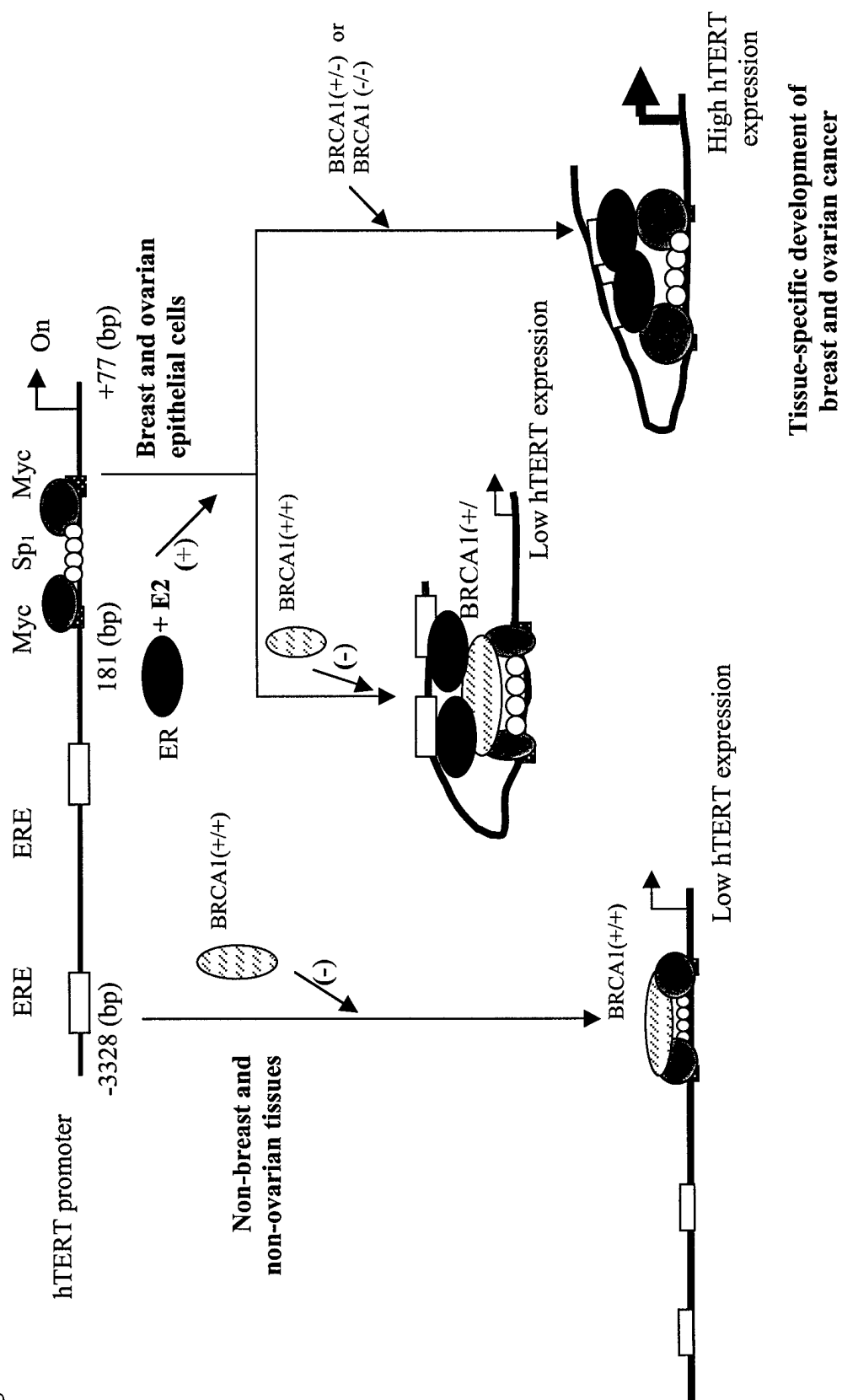


Figure 5



Oxidative DNA Damage and 8-Hydroxy-2-Deoxyguanosine DNA Glycosylase/Apurinic Lyase in Human Breast Cancer

Donghui Li,^{1*} Weiqing Zhang,¹ Jijiang Zhu,¹ Ping Chang,¹ Aysegul Sahin,² Eva Singletary,³ Melissa Bondy,⁴ Tapas Hazra,⁵ Sankar Mitra,⁵ Serrine S. Lau,⁶ Jianjun Shen,⁷ and John DiGiovanni⁷

¹Department of Gastrointestinal Medical Oncology, The University of Texas M. D. Anderson Cancer Center, Houston, Texas

²Department of Pathology, The University of Texas M. D. Anderson Cancer Center, Houston, Texas

³Department of Surgical Oncology, The University of Texas M. D. Anderson Cancer Center, Houston, Texas

⁴Department of Epidemiology, The University of Texas M. D. Anderson Cancer Center, Houston, Texas

⁵Sealy Center for Molecular Science, The University of Texas Medical Branch at Galveston, Galveston, Texas

⁶Division of Pharmacology and Toxicology, The University of Texas at Austin, Austin, Texas

⁷Department of Carcinogenesis, The University of Texas M. D. Anderson Cancer Center, Science Park–Research Division, Smithville, Texas

To test the hypothesis that oxidative stress is involved in breast cancer, we compared the levels of 8-hydroxy-2-deoxyguanosine (8-oxo-dG), an oxidized DNA base common in cells undergoing oxidative stress, in normal breast tissues from women with or without breast cancer. We found that breast cancer patients (N = 76) had a significantly higher level of 8-oxo-dG than control subjects (N = 49). The mean (\pm SD) values of 8-oxo-dG/ 10^5 dG, as measured by high-performance liquid chromatography electrochemical detection, were 10.7 ± 15.5 and 6.3 ± 6.8 for cases and controls, respectively ($P = 0.035$). This difference also was found by immunohistochemistry with double-fluorescence labeling and laser-scanning cytometry. The average ratios ($\times 10^6$) of the signal intensity of antibody staining to that of DNA content were 3.9 ± 7.2 and 1.1 ± 1.4 for cases (N = 57) and controls (N = 34), respectively ($P = 0.008$). There was no correlation between the ages of the study subjects and the levels of 8-oxo-dG. Cases also had a significantly higher level of 8-hydroxy-2-deoxyguanosine DNA glycosylase/apurinic lyase (hOGG1) protein expression in normal breast tissues than controls ($P = 0.008$). There was no significant correlation between hOGG1 expression and 8-oxo-dG. Polymorphism of the *hOGG1* gene was very rare in this study population. The previously reported exon 1 polymorphism and two novel mutations of the *hOGG1* gene were found in three of 168 cases and two of 55 controls. In conclusion, normal breast tissues from cancer patients had a significantly higher level of oxidative DNA damage. The elevated level of 8-oxo-dG in cancer patients was not related to age or to deficiency of the *hOGG1* repair gene.

© 2001 Wiley-Liss, Inc.

Key words: 8-hydroxy-2-deoxyguanosine; 8-hydroxy-2-deoxyguanosine DNA glycosylase/apurinic lyase; breast tissue

INTRODUCTION

Epidemiological studies showed that predominantly vegetarian populations, which presumably consume large quantities of antioxidants, have lower incidence rates of breast cancer than other populations, suggesting that free radicals have a role in mammary carcinogenesis [1]. In animal models of chemical-induced mammary tumorigenesis, high-fat diets are associated with increased tumor incidence, and this effect is diminished by antioxidants [2], further supporting the hypothesis that free radical mechanisms of action are involved in mammary carcinogenesis. Free radicals can be generated by ionizing radiation, chemical carcinogens, and endogenous processes, such as cellular respiration, lipid peroxidation, the action of cellular oxidases, and autooxidation of cellular molecules [3]. Previous studies have shown that metabolites of chemical carcinogens, such as polycyclic aromatic

hydrocarbon compounds and estrogen, can undergo redox cycling, a process that generates free radicals and oxidative stress [4–6]. Animal experiments have shown that exposure to pesticides significantly increases the level of 8-hydroxy-2-deoxyguanosine (8-oxo-dG), which reflects oxidative DNA damage [7–9].

*Correspondence to: Department of Gastrointestinal Medical Oncology, The University of Texas M. D. Anderson Cancer Center, Box 426, 1515 Holcombe Blvd., Houston, TX 77030.

Received 12 January 2001; Revised 7 May 2001; Accepted 22 May 2001

Abbreviations: 8-oxo-dG, 8-hydroxy-2-deoxyguanosine; hOGG1, 8-hydroxy-2-deoxyguanosine DNA glycosylase/apurinic lyase; HPLC, high-performance liquid chromatography; EC, electrochemical detection; FITC, fluorescein isothiocyanate; PI, propidium iodide; PCR, polymerase chain reaction; SSCP, single-strand conformation polymorphism

Published online 15 August 2001; DOI 10.1002/mc.1056

**This Page Intentionally
Left Blank**

Several lines of evidence from human studies also support the role of oxidative stress and lipid peroxidation in breast cancer. For example, elevated levels of mutagenic cholesterol peroxides [10], malondialdehyde [11–13], 5-hydroxymethyl-2'-deoxyuridine [14], and 8-oxo-dG [15] have been detected in breast cancer patients and in women with an increased risk of breast cancer. Tamoxifen, the antiestrogen most widely used in the treatment and chemoprevention of breast cancer, has been found to inhibit lipid peroxidation [16] by reducing serum levels of malondialdehyde in cancer patients [17]. In addition, a high dietary intake of fat has been shown to increase oxidative DNA damage and lipid peroxidation-induced DNA damage in lymphocytes of women with an increased risk of breast cancer [18–20]. Most important, one study found that the breast cancer susceptibility gene *BRCA1* is required for transcription-coupled repair of oxidative DNA damage but is not required for the repair of other types of DNA damage [21]. Although few mutations of the *BRCA1* gene have been found in sporadic cases of breast cancer, reduced expression of *BRCA1* has been found in these tumors [22]. These findings provide strong evidence of the importance of oxidative DNA damage in breast cancer and suggest that oxidative DNA damage could be the common mechanism of action by which estrogen, dietary fat, and carcinogen exposure affect breast cancer development.

Among the numerous oxidized DNA bases, 8-oxo-dG has received considerable attention because of its demonstrated mutagenic potential [23]. This stable premutagenic oxidative lesion also has been recognized as a potential marker of target organ damage from reactive oxygen species [24], and its level correlates well with the incidence of cancer [25,26]. Elevated levels of 8-oxo-dG have been reported in breast tumors compared with tissue samples from noncancer controls [15]. But the levels of oxidative DNA damage in normal breast tissues from women with and without breast cancer have never been compared.

The repair of 8-oxo-dG-related DNA damage involves several newly identified enzymes, including the mutM homologue/8-oxo-dG DNA glycosylase/apurinic lyase (*hOGG1*) gene [27]. *hOGG1* is a human homologue of the yeast 8-oxo-dG glycosylase/apurinic lyase, which is an 8-oxo-dG glycosylase/apurinic lyase. A polymorphism of *hOGG1* exon 1 has been associated with an increased risk of lung cancer in Japanese [28,29]. The frequency and biological significance of this polymorphism have not been tested in other ethnic groups or other cancers. In this study we investigated the expression level and polymorphism of the *hOGG1* gene in relation to the levels of 8-oxo-dG in normal breast tissues from breast cancer patients and from healthy women undergoing reduction mammoplasty.

MATERIALS AND METHODS

Study Subjects and Tissue Samples

The study subjects included 101 women with newly diagnosed breast cancer who were undergoing surgery without previous radiotherapy or chemotherapy at The University of Texas M. D. Anderson Cancer Center (Houston, TX) between 1997 and 1999. The histopathologic characteristics of the tumors are given in Table 1. Most cases were very early stage tumors. The controls included 51

Table 1. Histopathologic Characteristics*

Characteristic	Number
Tumor type	
DCIS	33
IDC	59
Other [†]	9
Tumor stage [‡]	
Tis	33
T1	40
T2	24
T3	1
Nuclear grade [§]	
1	7
2	46
3	42
Ki-67	
<17%	24
17–34%	3
>34%	15
Nodes	
N0	81
N1	19
N3	1
ER	
+	48
–	15
±	4
PR	
+	40
–	22
±	5
Her2	
+	15
–	24
±	3

*DCIS, ductal carcinoma in situ; IDC, invasive ductal carcinoma; ER, estrogen receptor; PR, progesterone receptor; Her2, Her2 protein expression.

[†]"Other" represents two medullary carcinomas, two infiltrating lobular carcinomas, two noninfiltrating lobular carcinomas in situ, one tubular carcinoma, and one mucinous carcinoma.

[‡]Tis, DCIS; Ki67, a cell proliferation marker; T1, tumor less than 2 cm in greatest diameter; T2, tumor greater than 2 cm but less than 5 cm; T3, tumor greater than 5 cm.

[§]1, well differentiated; 2, moderately differentiated; 3, poorly differentiated.

^{||}N0, no regional lymph node involvement; N1, metastasis to ipsilateral axillary lymph nodes; N3, metastasis to ipsilateral internal mammary lymph nodes.

women with no cancer history who were undergoing reduction mammoplasty at a local plastic surgery clinic. The age and ethnicity characteristics of both groups are listed in Table 2. Young black women were overrepresented among the noncancer controls. Fresh tissue samples were obtained within 6 h after surgery. Tissue samples were first examined by a pathologist and then kept on ice or in a refrigerator until processed by the research laboratory. Tissues from cases and controls were handled in the same manner during the procurement process. Peripheral blood samples were obtained from 168 cases and 55 controls. The use of human tissues in this study was approved by M. D. Anderson Cancer Center's Institutional Review Board.

Measurement of 8-oxo-dG by High-Performance Liquid Chromatography and Electrochemical Detection

Tissue samples were kept in a -80°C freezer until DNA was isolated. DNA was isolated from tissue samples of 76 cases and 49 controls by a phenol/chloroform procedure, after the fat tissues were carefully dissected. 8-oxo-dG was analyzed by high-performance liquid chromatography (HPLC) (Shimadzu LC-10AS, Columbia, MD) on a column coupled to an ultraviolet photodiode array (Shimadzu SPD M10A) and electrochemical detectors (ESA CoulArray, New York, NY). For electrochemical detection (EC), the channels, numbered 1 through 4, were set to 200, 290, 380, and 430 mV, respectively. The method used for analyzing the 8-oxo-dG levels in the DNA samples was a previously described method [30], with modifications. Briefly, an aliquot of DNA (5–10 μg) was dried in an Eppendorf tube and reconstituted in 10 μL of water. Then 66 μL of 2 mM sodium acetate buffer at pH 4.5 and 10 μL of 0.1 mM zinc chloride were added, and the mixture was hydrolyzed with 4 μL of nuclease P1 (0.5 $\mu\text{g}/\mu\text{L}$ in 30 mM NaOAc at pH 5.3) at 37°C for 2 h in a water bath. The DNA digest was incubated for another 1 h after adding 8 μL of 80 mM Tris base and 4 μL of alkaline phosphatase (0.1 U/ μL).

Aliquots (75 μL) of the DNA hydrolysate were injected onto a Partisil 5 μM ODS-3 reverse-phase analytical column (25 cm \times 4.6 mm inner diameter;

Whatman, Clifton, NJ) that was maintained at 25°C . The mobile phase contained 4 mM citric acid, 8 mM ammonium acetate at pH 4.0, 5% methanol, and 20 mg of EDTA saturated with helium (ultrapure grade). The flow rate was 1 mL/min. 8-oxo-dG was eluted with a retention time of 21 min and was quantified by analysis of EC channel 2 (290 mV). deoxycytidine, thymidine, deoxyguanosine, and deoxyadenosine, which usually elute with retention times of 9.6, 18.0, 19.9, and 30.5 min, respectively, were quantified by ultraviolet absorption at 254 nm. A standard curve was generated with different concentrations of an 8-oxo-dG standard (Sigma Chemical Co., St. Louis, MO) for quantification. The 8-oxo-dG standard was run between samples to confirm that the chromatography process was working properly. The levels of oxidative DNA damage were expressed as 8-oxo-dG/ 10^5 dG. Analysis of 8-oxo-dG was carried out by a person who had no knowledge of the sample coding.

Immunohistochemical Detection and Laser Scanning Cytometry

8-oxo-dG was measured in paraffin sections of normal breast tissues from 57 cases and 34 controls. The antibody against 8-oxo-dG was purchased from PharMingen (San Diego, CA), and 8-oxo-dG was purchased from Calbiochem (La Jolla, CA). The double-fluorescent labeling method was performed as previously reported [31,32], with some modifications. Briefly, tissue sections were deparaffinized with xylene and rehydrated with serial ethanol. The tissue sections were then boiled in a microwave oven for 3 min for antigen retrieval and digested with RNase and pepsin. After washing with phosphate-buffered saline, nonspecific binding sites were blocked with normal horse serum. The primary antibody was applied at a dilution of 1:2500, and the tissue sections were then incubated at 4°C overnight. After washing with phosphate-buffered saline, the sections were reacted with goat anti-mouse immunoglobulin G (1:200) and conjugated with fluorescein isothiocyanate (FITC) at 37°C for 30 min. The slides were finally covered with the antifade Vectashield mounting medium with propidium iodide (PI) (Vector Laboratories Inc., Burlingame, CA).

In this assay, DNA was labeled with PI, and 8-oxo-dG was identified by the primary antibody and FITC-conjugated secondary antibody. The staining intensity of 8-oxo-dG (FITC signals) and nuclear DNA content (PI signals) in epithelial cells were quantified by laser scanning cytometry [33] (Compucyte Corporation, Cambridge, MA). Data were expressed as ratios of FITC signals to PI signals. An average of 3000 cells was scanned on each section. To show staining specificity, the following control experiments were performed: cells or tissues were reacted with primary antibodies that had been

Table 2. Demographic Characteristics

Characteristics	Cases (N = 101)	Controls (N = 51)
Age (yr)*	42.7 \pm 5.8	32.9 \pm 8.6
Ethnicity		
White (non-Hispanic)	73 (72%)	23 (45%)
Hispanic	11 (11%)	2 (4%)
Black	14 (14%)	25 (49%)
Other	3 (3%)	1 (2%)

*Mean \pm SD.

pre-absorbed with the antigen 8-oxo-dG, sections were stained without primary antibody, and cells or tissues were treated with DNase before staining. Background staining on each slide was subtracted. Experimental variations between different batches were corrected by including a control slide in each batch of samples processed.

Expression of hOGG1 in Breast Tissues

Expression of the hOGG1 protein was evaluated in 59 normal adjacent tissues and 33 tumors of breast cancer patients as well as 41 normal breast tissues from noncancer controls. The antibody against the hOGG1 protein was generated in Dr. S. Mitra's laboratory [34]. The secondary antibody was biotin-conjugated goat anti-mouse immunoglobulin G. The avidin-biotin-horseradish peroxidase complex was added after the second antibody. To localize peroxidase, sections were treated with a freshly prepared diaminobenzidine solution for 2–5 min. The stained sections were evaluated by a pathologist who was blind to disease status and the 8-oxo-dG levels of the samples. The expression of hOGG1 was scored by the intensity of the nuclear staining and the percentage of cells with positive staining. The staining intensity was expressed as 0 = negative, 1 = borderline positive, 2 = weak positive, and 4 = strong positive. The proportion of cells with staining was expressed as follows: 1 = $\leq 50\%$ of the cells were positive, and 2 = $> 50\%$ of the cells were positive. A final score was obtained by multiplying the number of the staining intensity with the number of the proportion of cells with staining.

Polymorphism in the *hOGG1* Gene

DNA was isolated from peripheral lymphocytes by the phenol/chloroform procedure. Genetic polymorphism of *hOGG1* was detected by polymerase chain reaction (PCR) coupled with the single-strand conformation polymorphism (SSCP) method described by Ishida et al. [28]. Briefly, radiolabeled primers for exon 1 (5'-ACGAGGCCTGGTCTGGG-TAG-3' and 5'-TTTGTACCCCATGCCAGGCAG-3') were used for amplification. The PCR fragments were labeled by addition of 0.25 μ L of [α - 32 P]dCTP into each 25- μ L PCR. The PCR conditions were 92°C for 2 min for one cycle, followed by 35 cycles at 94°C for 30 s for denaturation and 72°C for 40 s for both annealing and extension. The PCR product was first diluted 1:5 in an SSCP loading buffer, heat-denatured, and then separated on a nondenaturing 0.5 \times mutation detection enhancement gel with 5% glycerol at ambient temperature. Samples with unique SSCP patterns were sequenced to identify mutation/polymorphism. Positive DNA controls for alleles 1, 2, and 3 of the exon 1 polymorphism of *hOGG1* were kindly provided by Drs. Toshimitsu Ishida and Hiroyuki Aburatani (Genome Science

Division, Research Center for Advanced Science and Technology, University of Tokyo, Tokyo, Japan).

Statistical Analysis

The levels of 8-oxo-dG were expressed as means \pm SD. The means of case and control groups were compared by using Student's *t* test. The correlations between levels of 8-oxo-dG and age, ethnicity, tumor characteristics, and hOGG1 expression were analyzed by multiple linear regression.

RESULTS

To determine whether breast cancer cases have a higher level of oxidative stress than controls, 8-oxo-dG was measured by HPLC-EC in DNA samples from normal breast tissues. The level of 8-oxo-dG was significantly higher in women with breast cancer than in the noncancer controls (Table 3). The mean levels of 8-oxo-dG/ 10^5 dG were 6.3 ± 6.8 and 10.7 ± 15.5 for controls (N = 49) and cases (N = 76), respectively ($P = 0.035$). To confirm this observation, 8-oxo-dG also was measured in normal tissue sections by immunohistochemistry with double-fluorescent labeling. Typical staining patterns for the 8-oxo-dG antibody (green signal) and for the DNA content (red signal) in epithelial cells of breast tissues are shown in Figure 1. Positive staining of 8-oxo-dG also was seen in the nuclei of adipocytes (data not shown). The staining intensities for the epithelial cells were quantified by laser scanning cytometry and expressed as the ratio of the antibody signal (green) to the DNA signal (red). The case cells had a significantly higher intensity of 8-oxo-dG staining than the control cells. The mean ratios ($\times 10^6$) of the green signal to the red signal were 3.9 ± 7.2 and 1.1 ± 1.4 for cases (N = 57) and controls (N = 34), respectively ($P = 0.008$).

Because young black women were overrepresented among the controls, compared with cases, the effect of age and ethnicity on the level of 8-oxo-dG was determined by multiple regression analysis. A very weak age-dependent increase of 8-oxo-dG was seen among controls (Figure 2), but a negative correlation between age and level of 8-oxo-dG was

Table 3. Levels of 8-oxo-dG in Breast Tissues*

	Mean	SD	N	P (t test)
HPLC [†]				
Control	6.3	6.8	49	0.035
Case	10.7	15.5	76	
IHC [‡]				
Control	1.1	1.4	34	0.008
Case	3.9	7.2	57	

*HPLC, high-performance liquid chromatography; IHC, immunohistochemistry.

[†]Number of 8-oxo-dG in 10^5 guanine nucleotides.

[‡]Ratio of antibody signal to DNA signal.

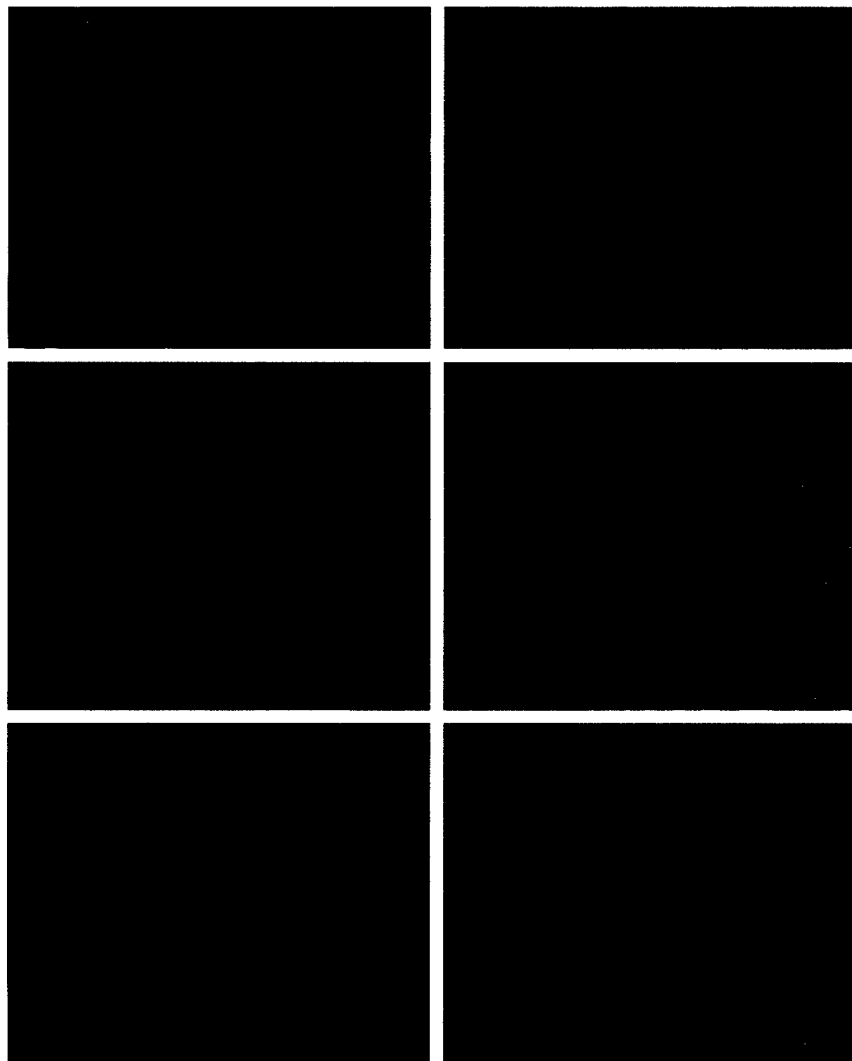


Figure 1. 8-Oxo-dG in epithelial cells of human breast tissues detected by immunohistochemistry with double-fluorescent labeling. Red signal, DNA labeled with PI; green signal, 8-oxo-dG detected with a FITC-conjugated antibody. Top panels, a sample with strong intensity of antibody staining; middle panels, a sample with relatively weak staining intensity; lower panels, a sample with negative staining in some areas and very weak staining in other areas of the tissue.

seen among cases (Table 4). When cases and controls were pooled, no significant correlation was detected between age or ethnicity and the level of 8-oxo-dG (Table 4). Regression analysis also failed to detect any significant correlation between the level of 8-oxo-dG and any of the clinical characteristics of the tumors (Table 4).

To determine whether the level of 8-oxo-dG was related to the expression of hOGG1, a repair enzyme for oxidative DNA damage, hOGG1 protein was detected by immunohistochemistry in both tumor and normal tissue sections. hOGG1 protein was present in the nuclei and cytoplasm of epithelial cells, adipocytes, and stromal cells of both normal and tumor tissues (Figure 3). The expression levels of hOGG1 in epithelial cells of normal tissues

were scored significantly higher in cancer cases (3.34 ± 1.95 ; $N = 59$) than in noncancer controls (2.27 ± 1.96 ; $N = 41$) ($P = 0.008$). On the other hand, the staining intensities of hOGG1 in paired tumor and normal adjacent tissues were quite similar ($N = 33$, $P = 0.67$; data not shown). When the relationship between the levels of 8-oxo-dG and the expression of hOGG1 was examined in the 91 pairs of tissue from 57 cases and 34 controls (Table 5), no significant correlation was found ($r = 0.11$; $P = 0.3$). Because we did not have enough tissue sections, 8-oxo-dG was not measured in tumors.

Variations of *hOGG1* exon 1 in human breast tissues were analyzed by SSCP and sequencing. In addition to the previously reported three polymorphisms [28,29], two new mutations/poly-

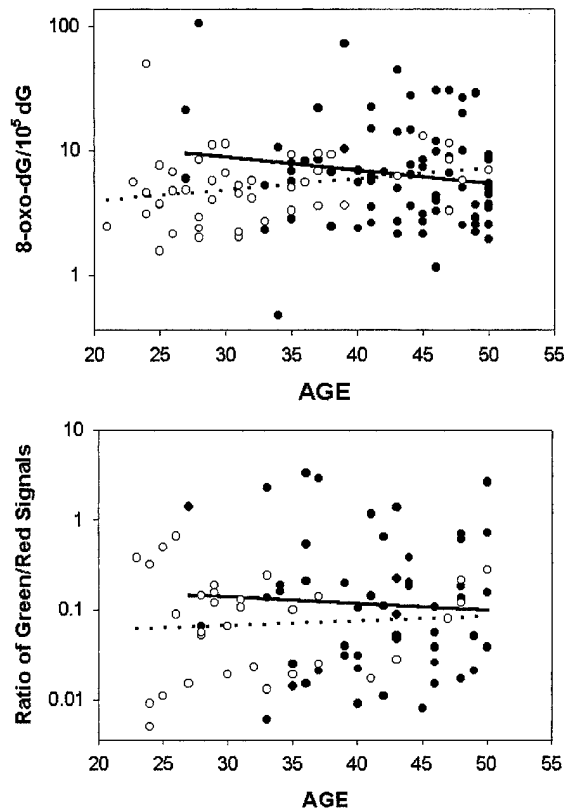


Figure 2 Correlation between age and the level of 8-oxo-dG in normal breast tissues of cancer patients (filled circles) and noncancer controls (open circles). Upper panel, 8-oxo-dG measured by HPLC-EC; lower panel, 8-hydroxyguanine measured by immunohistochemistry. The dotted and solid regression lines are for controls and cases, respectively. None of the regression values were statistically significant.

morphisms were identified by SSCP analysis, as shown in Figure 4A. DNA sequencing showed a G-to-A transition at the intron/exon junction in one cancer case (Figure 4B). The other new polymorphism was a G-to-A transition at position +22 of intron 1 (Figure 4C). This polymorphism was detected in one case and one control subject. The previously reported G-to-T allele 3 of the *hOGG1* polymorphism [28,29] also was detected in one case and one control subject (Figure 4D).

DISCUSSION

A large proportion of human breast cancer cases cannot be explained by known risk factors. Accumulating evidence suggests that oxidative stress may be a common link in many suspected risk factors for breast cancer. This study, using both biochemical and immunohistochemical methods, showed a significantly higher level of 8-oxo-dG, and thus oxidative DNA damage, in normal breast tissues of breast cancer cases than noncancer controls. This observation is in accordance with previous reports of a substantial increase in oxida-

Table 4. Multiple Regression of 8-oxo-dG (by HPLC) on Select Variables*

Variable	Coefficient	P value
Age	-0.265	0.102
Ethnicity	0.570	0.613
Case-control status	-6.822	0.011
Control alone		
Age	0.010	0.932
Ethnicity	-1.375	0.152
Case alone		
Age	-0.663	0.031
Ethnicity	2.125	0.240
Tumor stage	4.657	0.835
Nodes	-5.874	0.769
Nuclear grade	-1.668	0.218
ER	0.340	0.918
PR	0.169	0.960
Ki-67	1.124	0.159
Her2	0.625	0.403

*ER, estrogen receptor; PR, progesterone receptor; Her2, Her2 protein; Ki67, a cell proliferation member.

tive base lesions in the DNA of invasive ductal carcinoma [35,36]. One can always argue that the elevated level of 8-oxo-dG in tumor tissues is a consequence of tumor formation. Because most of the tumors in our study were at a very early stage, the relationship between the level of oxidative DNA damage and the stage of tumor cannot be evaluated properly. Nonetheless, the substantially higher level of 8-oxo-dG in normal breast tissues without tumor cells and the fact that women at increased risk for breast cancer have significantly higher levels of lipid peroxidation [11-14] support the hypothesis that oxidative DNA damage may play a causative role in the development of breast cancer.

The average value of 8-oxo-dG/ 10^5 dG (10.7 ± 15.5 in normal breast tissues of cancer patients) was relatively higher in the current study than previously reported values (3.6 ± 0.4 and 5.1 ± 0.7 in breast tumor and normal adjacent tissues, respectively), as measured by HPLC-EC [37]. This difference can be explained in part by the method used for DNA isolation. The DNA samples in our study were not prepared with a phenol-free procedure for the purpose of measuring oxidative DNA damage. Because samples from all study subjects were prepared and processed in the same manner, however, it is unlikely that the significant difference between cases and controls was an artifact. Moreover, the higher values in cases than controls, as detected by HPLC-EC, was confirmed by the immunohistochemical method.

Our study used a newly developed method, double-fluorescent labeling and laser-scanning cytometry, to measurement DNA damage. This method has several advantages over other available

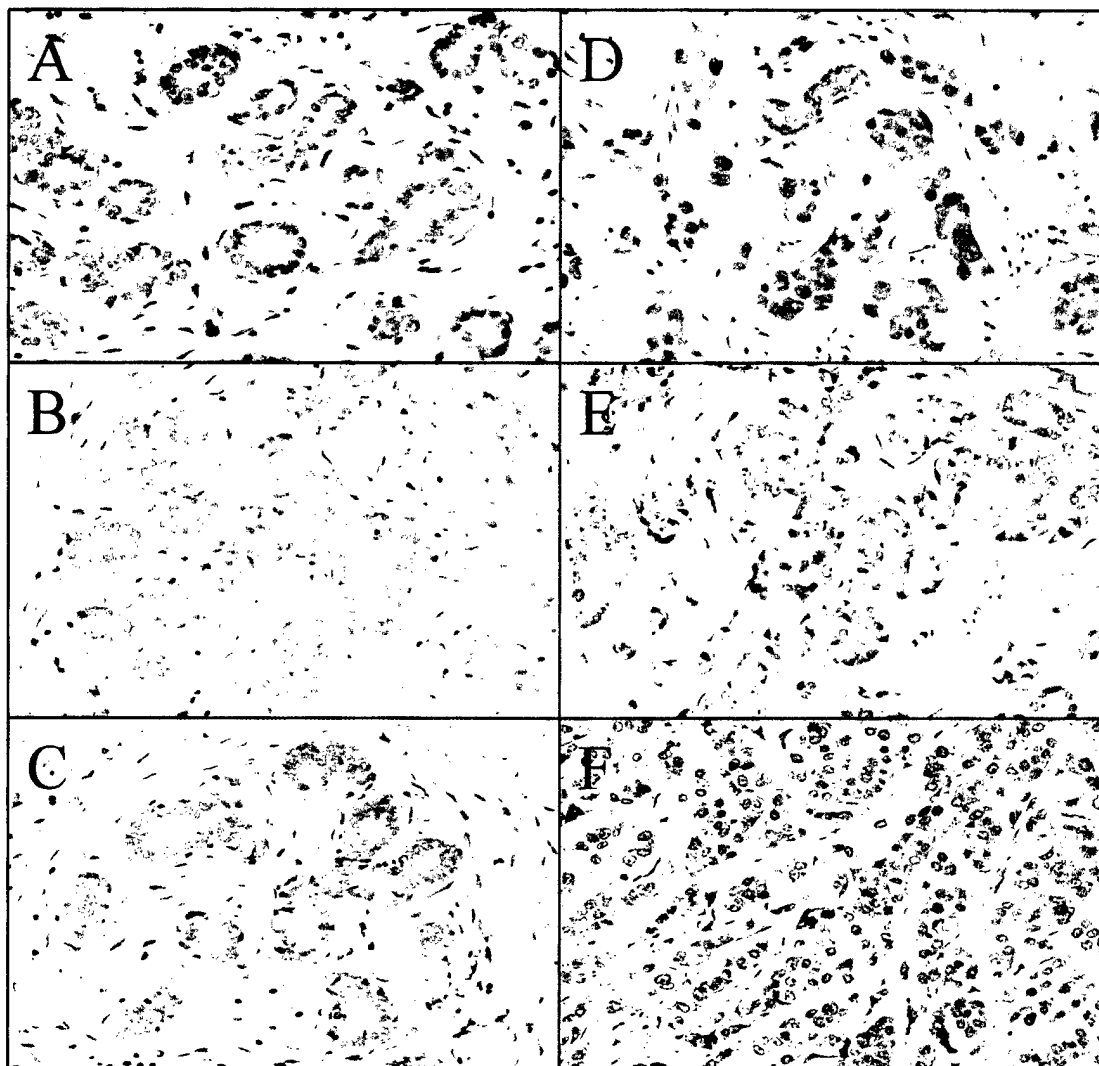


Figure 3. Typical expression patterns of the hOGG1 protein in human breast tissues (200 \times). (A–C) Normal breast tumor tissues. (D–F) Breast tumors. Top panels, negative controls; middle panels, relatively weak staining; lower panels, high level of hOGG1 expression.

methods. First, it can be applied to tissue sections with a small number of cells. Second, the measurement of adduct level is adjusted by the amount of DNA in each cell. Third, quantification and localization of DNA adducts by laser-scanning cytometry allow for adduct measurements in a large number of cells and in specific cell types on each section. We have validated this method [32] and describe it in detail elsewhere (Li et al., manuscript in preparation).

Using reduction mammoplasty samples as control is not an ideal study design. Women undergoing reduction mammoplasty may have endocrine or metabolism disorders that can affect the level of oxidative stress in their breasts. In addition, young black women were overrepresented in this control group. Moreover, the age and ethnicity differences

between our controls and cases did not explain the higher level of 8-oxo-dG in cancer cases. In fact, cases showed an inverse relationship between 8-oxo-dG level and age. The level of oxidative stress in the body could be affected by environmental factors, such as diet and carcinogen exposure. It also could be determined by intrinsic factors, such as the functions of many genes involved in the defense mechanism. Several of these aspects are under investigation in our ongoing studies. Here we focused on the association between 8-oxo-dG and the DNA repair enzyme hOGG1.

As previously reported in a mouse model, inactivation of the DNA repair gene 8-oxo-dG glycosylase results in the accumulation of 8-oxo-dG in tissue [38]. Mutation in the *hOGG1* gene has been associated with an increased risk of lung cancer

Table 5. Level of 8-Oxo-dG and hOGG1 Expression in Breast Tissues*

Case	LSC†	hOGG1 (normal)	hOGG1 (tumor)	Control	LSC	hOGG1
BC002	26.14	6		BC077		1
BC004	13.93	8		BC065	0.66	1
BC014	22.41	6		BC068	2.82	1
BC016	6.49	0		BC069	1.47	2
BC019	1.09	0		BC072	1.00	1
BC023	5.33	6		BC075	1.58	1
BC025	7.10	1	1	BC079	0.18	1
BC036	1.98	0	3	BC080	0.23	3
BC039	1.87	1		BC081	0.09	4
BC053	0.39	2		BC082	0.11	4
BC054	1.89	4		BC083	0.05	4
BC055	0.48	3	1	BC088	0.17	1
BC056	2.09	1		BC089	0.19	2
BC057	0.52	6		BC090	0.25	2
BC060	1.84	4	1	BC095	0.28	6
BC062	3.80	3	2	BC107	0.09	1
BC063	0.67	6		BC112	0.15	6
BC064	0.57	4		BC114	0.13	8
BC067	1.57	6		BC117	3.20	6
BC071	1.43	6	2	BC119	1.89	2
BC073	1.06	4	4	BC134	3.77	2
BC074	0.39	8		BC141	1.42	0
BC084	0.09	6		BC147	4.97	4
BC087	0.25	3		BC149		0
BC091	0.31	6	6	BC156	6.55	2
BC092	0.06	4		BC164	1.31	2
BC093	0.22	4	6	BC166	1.08	0
BC098	0.11	2		BC167	1.21	2
BC101	0.15	2	4	BC172	0.53	2
BC102	0.14	0	2	BC174		0
BC104	0.26	6		BC177		0
BC105	0.31	6		BC178	0.90	4
BC106	0.15	3		BC185		0
BC108	0.40	2		BC191	2.43	4
BC111	0.08	4	1	BC194		2
BC121	6.98	2		BC201	0.19	4
BC123	0.90	2	3	BC207	0.81	0
BC124	2.24	4	4	BC220		0
BC125	28.76	3	4	BC221	2.17	4
BC128	0.53	2	4	BC230	1.22	2
BC133	32.32	3	2	BC231	0.57	2
BC136	1.47	2	1			
BC137	1.36	4	1			
BC140	1.99	2	2			
BC146	11.6	2	4			
BC154	0.17	2	1			
BC158	1.61	2	2			
BC160	0.53	2	2			
BC173	13.87	2	4			
BC175	6.09	2	1			
BC180	1.13	2	4			
BC188	2.02	4	4			
BC190	1.58	4	3			
BC197	5.32	2	4			
BC206	0.21	2	1			
BC209	0.21	4	6			
BC210	1.38	3	1			
BC159		3				
BC202		4				

*LSC, laser-scanning cytometry.

†Ratio of green/red signals $\times 10^6$, as measured by laser-scanning cytometry.

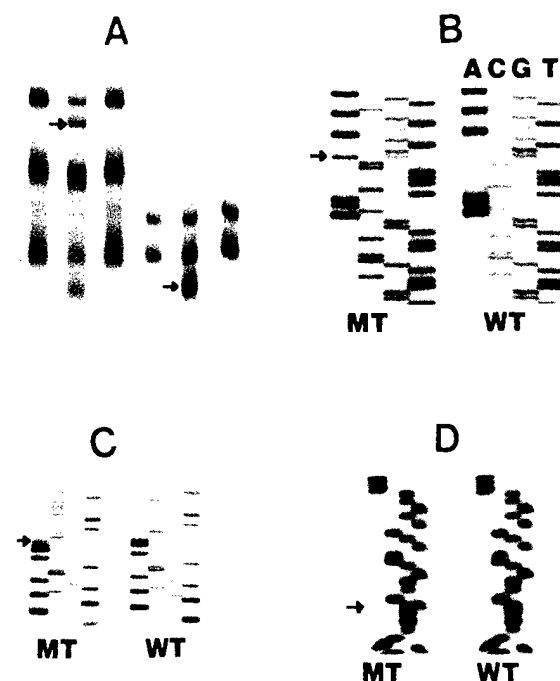


Figure 4. Mutations/polymorphisms of the *hOGG1* gene, as detected by SSCP and DNA sequencing. (A) Examples of shifted bands detected by SSCP analysis. (B) G-to-A transition at the intron/exon junction. (C) G-to-T transition at position +22 of intron 1. (D) A previously reported G-to-T allele 3 polymorphism of exon 1. WT, wild type; MT, mutant. Arrows indicate shifted band or mutant sequence.

[28,29]. Our present study explored whether the higher level of 8-oxo-dG in cancer cases was related to a lack of expression of the *hOGG1* gene. We found that the expression level of the *hOGG1* protein in breast tissues was actually higher in cases than in controls. Therefore, the increased level of oxidative DNA damage in breast cancer cases was not due to decreased expression of the *hOGG1* protein. As reported by Shinmura et al. [39], *hOGG1* protein is constitutively expressed in cancerous and noncancerous human cells. The expression of the 8-oxo-dG glycosylase gene in rats can be induced by exposure to diesel exhaust particles [40]. Therefore, the higher level of *hOGG1* protein expression in cancer cases may be a mechanism of compensation for a high level of oxidative stress.

Mutation of the *hOGG1* gene has been reported in tumors of the lung, kidney, and stomach in two studies, but the frequency is fairly low [41,42]. The exon 1 *hOGG1* polymorphism has been associated with increased susceptibility to lung cancer in the Japanese [28,29], but the frequency of this polymorphism was found to be much lower in the current study population than in the Japanese. The biological significance of the two new polymorphisms of the *hOGG1* gene in breast cancer needs further investigation. Because one of the polymorphic sequences was in an exon/intron junction, it may lead to a splicing variant of the gene.

Whether any of the polymorphisms of the *hOGG1* gene affects the function of the enzyme is not shown. Our data did not indicate that *hOGG1* has a significant role in human breast cancer, but it is likely that no single polymorphism of a low-penetrant gene could sufficiently predict cancer risk, and a panel of susceptibility markers is needed to define the high-risk group.

ACKNOWLEDGMENTS

We thank Regina R. Sherrod and Noelle Heinze for editorial assistance. This work was supported by NCI grants CA 70264 and CA 81063 and NIEHS Center Grant P30 CA ES07784.

REFERENCES

- Carroll KK. Dietary fat and breast cancer. *Lipids* 1992;27:793-797.
- Welsh CW. Review of the effects of dietary fat on experimental mammary gland tumorigenesis: Role of lipid peroxidation. *Free Radic Biol Med* 1995;18:757-773.
- Frenkel K. Carcinogen-mediated oxidant formation and oxidative DNA damage. *Pharmacol Ther* 1992;53:127-166.
- Guyton KZ, Kensler TW. Oxidative mechanisms in carcinogenesis. *Br Med Bull* 1993;49:523-544.
- Sipe HJ, Jordan SJ, Hanna PM, Mason RP. The metabolism of 17 β -estradiol by lactoperoxidase: A possible source of oxidative stress in breast cancer. *Carcinogenesis* 1994;15:2637-2643.
- Roy D, Liehr JG. Elevated 8-hydroxy-deoxyguanosine levels in DNA of diethylstilbestrol-treated Syrian hamsters: Covalent DNA damage by free radicals generated by redox cycling of diethylstilbestrol. *Cancer Res* 1991;51:3882-3885.
- Lodovici M, Aioli S, Monserrat C, Dolara P, Medica A, Di Simplicio P. Effects of a mixture of 15 commonly used pesticides on DNA levels of 8-hydroxy-2-deoxyguanosine and xenobiotic metabolizing enzymes in rat liver. *J Environ Pathol Toxicol Oncol* 1994;13:163-168.
- Lodovici M, Casalini C, Briani C, Dolara P. Oxidative liver DNA damage in rats treated with pesticide mixtures. *Toxicology* 1997;117:55-60.
- Oakley GG, Devanaboyina U, Robertson LW, Gupta RC. Oxidative DNA damage induced by activation of polychlorinated biphenyls (PCBs): Implications for PCB-induced oxidative stress in breast cancer. *Chem Res Toxicol* 1996;9:1285-1292.
- Petrakis NL, Gruenke LD, Craig JC. Cholesterol and cholesterol epoxides in nipple aspirate of human breast fluid. *Cancer Res* 1981;41:2563-2565.
- Boyd NF, McGuire V. The possible role of lipid peroxidation in breast cancer risk. *Free Radic Biol Med* 1991;10:185-190.
- Boyd NF, McGuire V. Evidence of lipid peroxidation in premenopausal women with mammographic dysplasia. *Cancer Lett* 1990;50:31-37.
- Vaca CE, Fang JL, Mutanen M, Valsta L. ³²P-postlabeling determination of DNA adducts of malondialdehyde in humans: Total white blood cells and breast tissue. *Carcinogenesis* 1995;16:1847-1851.
- Frenkel K, Karkoszka J, Glassman T, et al. Serum autoantibodies recognizing 5-hydroxymethyl-2'-deoxyuridine, an oxidative DNA base, as biomarkers of cancer risk in women. *Cancer Epidemiol Biomarkers Prev* 1998;7:49-57.
- Musarrat J, Arezina-Wilson J, Wani AA. Prognostic and aetiological relevance of 8-hydroxyguanosine in human breast carcinogenesis. *Eur J Cancer* 1994;32A:1209-1214.
- Thangaraju M, Vijayalakshmi T, Phil M, Sachdanandam P. Effect of tamoxifen on lipid peroxide and antioxidative

- system in postmenopausal women with breast cancer. *Cancer* 1994;74:78–82.
17. Custodio JBA, Dinis TCP, Almeida LM, Madeira VMC. Tamoxifen and hydroxytamoxifen as intramembraneous inhibitors of lipid peroxidation: Evidence for peroxyl radical scavenging activity. *Biochem Pharmacol* 1994;47:1989–1998.
 18. Djuric Z, Heilbrun LK, Reading BA, Boomer A, Valeriote FA, Matino S. Effects of a low-fat diet on levels of oxidative damage to DNA in human peripheral nucleated blood cells. *J Natl Cancer Inst* 1991;83:766–769.
 19. Djuric Z, Heilbrun LK, Simon MS, et al. Levels of 5-hydroxymethyl-2'-deoxyuridine in DNA from blood as a marker of breast cancer. *Cancer* 1996;77:691–696.
 20. Nair J, Vaca CE, Velic I, Mutanen M, Valsta LM, Bartsch H. High dietary ω -6 polyunsaturated fatty acids drastically increase the formation of etheno-DNA base adducts in white blood cells of female subjects. *Cancer Epidemiol Biomarkers Prev* 1997;6:597–602.
 21. Gowen LC, Avrutskaia AV, Latour AM, Koller BH, Leadon SA. BRCA1 required for transcription-coupled repair of oxidative DNA damage. *Science* 1998;281:1009–1013.
 22. Sourvinos G, Spandidos DA. Decreased BRCA1 expression levels may arrest the cell cycle through activation of p53 checkpoint in human sporadic breast tumors. *Biochem Biophys Res Commun* 1998;245(1):75–80.
 23. Shibutani S, Takeshita M, Grollman AP. Insertion of specific bases during DNA synthesis past the oxidation damaged base 8-hydroxyguanine. *Nature* 1991;349:431–434.
 24. Wood ML, Dizdaroglu M, Gajewski E, Essigmann JM. Mechanistic studies of ionizing radiation and oxidative mutagenesis: Genetic effects of a single 8-hydroxyguanine (7-hydro-8-oxoguanine) residue inserted at a unique site in a viral genome. *Biochemistry* 1990;29:7024–7032.
 25. Kasai H, Nishimura S, Kurokawa Y, Hayashi Y. Oral administration of the renal carcinogen, potassium bromate, specifically produces 8-hydroxyguanosine in rats target organ DNA. *Carcinogenesis* 1987;8:1959–1961.
 26. Umemura T, Sai K, Takagi A, Hasegawa R, Kurokawa Y. Formation of 8-hydroxyguanosine (8-OHdG) in rat kidney DNA after intraperitoneal administration of ferric nitrilo-triacetate (Fe-NTA). *Carcinogenesis* 1990;11:345–347.
 27. Dherin C, Radicella JP, Dizdaroglu M, Boiteux S. Excision of oxidatively damaged DNA bases by the human α -hOgg1 protein and the polymorphic α -hOgg1 (Ser326Cys) protein, which is frequently found in human populations. *Nucleic Acids Res* 1999;27(20):4001–4007.
 28. Ishida T, Takashima R, Fukayama M, et al. New DNA polymorphisms of human MMH/OGG1 gene: Prevalence of one polymorphism among lung-adenocarcinoma patients in Japanese. *Int J Cancer* 1999;80(1):18–21.
 29. Sugimura H, Kohno T, Wakai K, et al. *hOGG1* Ser326Cys polymorphism and lung cancer susceptibility. *Cancer Epidemiol Biomarkers Prev* 1999;8(8):669–674.
 30. Lau SS, Peters MMCG, Kleiner HE, Canales PL, Monks TJ. Linking the metabolism of hydroquinone to its nephrotoxicity and nephrocarcinogenicity. *Adv Exp Med Biol* 1996;387:267–273.
 31. Seiler F, Kirstein U, Eberle G, Hochleitner K, Rajewsky MF. Quantification of specific DNA O-alkylation products in individual cells by monoclonal antibodies and digital imaging of intensified nuclear fluorescence. *Carcinogenesis* 1993;14:1907–1913.
 32. Li D, Zhang W, Chang P, Thomale J, Rajewsky MF, Hittelman WN. DNA adduct measurement by dual fluorescence labeling, laser scanning cytometry and tyramide signal amplification. Abstract Proceedings of the American Association for Cancer Research 2000;41:A3596.
 33. Clatch RJ, Walloch JL, Foreman JR, Kamensky LA. Multi-parameter analysis of DNA content and cytokeratin expression in breast carcinoma by laser scanning cytometry. *Arch Pathol Lab Med* 1997;121:585–592.
 34. Hazra TK, Izumi T, Maiti L, Floyd RA, Mitra S. The presence of two distinct 8-oxoguanine repair enzymes in human cells: Their potential complementary roles in preventing mutation. *Nucleic Acids Res* 1998;26(22):5116–5122.
 35. Malins DC, Polissar NL, Gunselman SJ. Progression of human breast cancers to the metastatic state is linked to hydroxyl radical-induced DNA damage. *Proc Natl Acad Sci U S A* 1996;93:2557–2563.
 36. Malins DC, Holmes EH, Polissar NL, Gunselman SJ. The etiology of breast cancer: Characteristic alteration in hydroxyl radical-induced DNA lesions during oncogenesis with potential for evaluating incidence risk. *Cancer* 1993;71:3036–3043.
 37. Nagashima M, Tsuda H, Takenoshita S, et al. 8-Hydroxydeoxyguanosine levels in DNA of human breast cancers are not significantly different from those of non-cancerous breast tissues by the HPLC-ECD method. *Cancer Lett* 1995;90:157–162.
 38. Minowa O, Arai T, Hirano M, et al. Mmh/Ogg1 gene inactivation results in accumulation of 8-hydroxyguanine in mice. *Proc Natl Acad Sci U S A* 2000;97(8):4156–4161.
 39. Shinmura K, Kohno T, Takeuchi-Sasaki M, et al. Expression of the OGG1-type 1a (nuclear form) protein in cancerous and non-cancerous human cells. *Int J Oncol* 2000;16(4):701–707.
 40. Tsurudome Y, Hirano T, Yamato H, et al. Changes in levels of 8-hydroxyguanine in DNA, its repair and OGG1 mRNA in rat lungs after intratracheal administration of diesel exhaust particles. *Carcinogenesis* 1999;20(8):1573–1576.
 41. Shinmura K, Kohno T, Kasai H, Koda K, Sugimura H, Yokota J. Infrequent mutations of the *hOGG1* gene, that is involved in the excision of 8-hydroxyguanine in damaged DNA, in human gastric cancer. *Jpn Cancer Res* 1998;89(8):825–828.
 42. Chevillard S, Radicella JP, Levalois C, et al. Mutations in OGG1, a gene involved in the repair of oxidative DNA damage, are found in human lung and kidney tumours. *Oncogene* 1998;16(23):3083–3086.

Detection of 2-Amino-1-methyl-6-phenylimidazo[4,5-b]-pyridine -DNA Adducts in Normal Breast Tissues and Risk of Breast Cancer¹

Jijiang Zhu, Ping Chang, Melissa L. Bondy, Aysegul A. Sahin, S. Eva Singletary, Satoru Takahashi, Tomoyuki Shirai, Donghui Li²

Department of Gastrointestinal Medical Oncology (J.Z., P.C., D.L.), Department of Epidemiology(M.L.B.), Department of Pathology (A.A.S.), Department of Surgical Oncology(S.E.S.), The University of Texas M. D. Anderson Cancer Center, Houston, Texas 77030; Nagoya City University Medical School, Nagoya, Japan (S.T., T.S).

Running Title: PhIP-DNA adduct and Breast Cancer

Key words: DNA damage, PhIP, genetic susceptibility, breast cancer.

¹Supported by National Institutes of Health NIH grant CA 70264, National Institute of Environmental Health Sciences center grant P30 ES07784, NIH cancer center core grant CA 16672, and a research grant from CREST (Core Research for Evolutional Science and Technology), Japan.

²To whom requests for reprints should be addressed,
at the Department of Gastrointestinal Medical Oncology, Box 426,
The University of Texas, M. D. Anderson Cancer Center
1400 Holcombe Boulevard,
Houston, TX. 77030.
Phone (713) 792-2012; Fax: (713) 745-1163;
E-mail:dli@mdanderson.org

³The abbreviations used are: CYP, cytochrome P450; GSTM1, glutathione S-transferase M1; IHC, immunohistochemistry; NAT, N-acetyltransferase; PhIP, 2-Amino-1-methyl-6-phenylimidazo[4,5-b]-pyridine; RAL, relative adduct labeling.

ABSTRACT

2-Amino-1-methyl-6-phenylimidazo[4,5-b]-pyridine (PhIP), the most abundant heterocyclic amine (HCA) in cooked food, is a mammary carcinogen in female rats. In humans, consumption of well-done meat and PhIP intake have been associated with an increased risk of breast cancer, but PhIP-DNA adducts have not been analyzed in breast tissues from women having unknown exposure to HCAs. Using an immunohistochemistry (IHC) method, we measured PhIP-DNA adducts in normal breast tissues of 105 women having newly diagnosed breast cancer in comparison with those of 49 women undergoing reduction mammoplasty. The IHC method was first validated in MCF-7 cells treated with different doses of *N*-hydroxy-PhIP. We detected significant dose-response relationship and correlation ($r = 0.94$) between the levels of PhIP-DNA adducts detected by ^{32}P -postlabeling and IHC. Using IHC, PhIP-DNA adducts were detected in 83% and 70% of the normal breast tissue sections from the cancer and control patients respectively. The mean \pm standard error absorbency was 0.30 ± 0.016 and 0.21 ± 0.022 in the cancer and control patients, respectively ($P = 0.003$). Using the median value in the controls as a cut-off point, 71% of the cancer patients and 47% of the controls were distributed in the higher range ($\chi^2 = 8.66$; $P < 0.003$). Logistic regression analysis demonstrated an odds ratio of 6.16 (95% confidence interval 2.07 to 18.36) after adjusting for age and ethnicity ($P = 0.001$). A significant interactive effect of well-done meat consumption and genotypes of *NAT2* and *CYP1A1* on the level of PhIP-DNA adducts was observed. This is the first report of detection of PhIP-DNA adducts in breast tissue samples obtained from women having unknown exposure to HCAs. These data strongly support the hypothesis that HCA exposure contributes to human breast cancer among genetically susceptible individuals.

INTRODUCTION

Breast cancer is the second leading cause of cancer deaths in American women (1). Environmental factors have long been suspected to contribute to human breast cancers, but no specific agents other than radiation have been definitely implicated (2). Urban residency, dietary fat intake, cigarette smoking, alcohol consumption, and exposure to organochlorine compounds have been suspected to play a role, but the associations are either weak or inconclusive. Several lines of experimental evidence support the hypothesis that exposure to environmental carcinogens is involved in human breast cancer. First, a number of compounds present in the environment are potent mammary carcinogens (3). Second, the anatomical features of the breast make it a susceptible target for chemical carcinogens. For example, lipophilic polycyclic aromatic compounds can be stored and concentrated in the human breast fat pad (4). Human mammary epithelial cells have a high capacity for metabolizing these compounds into DNA-binding species and thus can become target cells for carcinogenesis. Third, the spectrum of p53 gene mutations in human breast tumors suggests the involvement of exogenous agents in inducing these mutations in a significant portion of the cases (5). Fourth, mutagenicity and genotoxicity have been detected in nipple aspirates (6), breast cyst fluid samples (7), extracts of mammary lipids from women undergoing reduction mammoplasty (8,9), and human breast milk samples (10). The critical question needs to be answered is what carcinogens are involved in the etiology of human breast cancer.

Heterocyclic amines (HCAs) are pyrolysis products of amino acids and proteins (11) that are formed in a variety of muscle meats when they are cooked and have been shown to induce tumors in experimental animals. Metabolic activation of HCAs into DNA-binding species causing DNA adduct formation is believed to be a key event in HCA-induced carcinogenesis

(12). 2-Amino-1-methyl-6-phenylimidazo-pyridine (PhIP), which is the most abundant HCA in the human diet, has been shown to have the highest carcinogenic potency (13). In addition, animal experiments have shown that long-term exposure to PhIP can induce tumors in the mammary gland in female rats and colon in male rats, which are the two most common sites of carcinogenesis in Western countries (14-16). PhIP and its metabolites also have been detected in human urine (17-19) and milk (20). Furthermore, PhIP-DNA adducts have been detected in human breast tissue samples obtained from individuals given dietary equivalent levels of ^{14}C -labeled PhIP using accelerated mass spectrometry (21). PhIP-DNA adducts have not been analyzed in breast tissue samples obtained from women without the use of preplanned exposure. Nevertheless, recent epidemiological studies have suggested an association between the consumption of well-done meat and an increased risk of breast cancer (22). PhIP is the carcinogen suspected to be present in well-done meat, which is responsible for this increased risk (23). Based on these data, we hypothesize that PhIP exposure plays an important role in human breast carcinogenesis. Were this hypothesis found to be true, we would expect to detect PhIP-DNA adducts in human breast tissues as a marker of exposure and expect an association between the level of PhIP-DNA adducts and risk of cancer. Therefore, in the present study, we examined PhIP-DNA adducts in normal breast tissues of women having or not having breast cancer using an immunohistochemistry (IHC) method. We also explored the possible effect of several environmental factors, i.e. smoking and well-done meat consumption as well as some genetic factors, i.e. polymorphisms of three metabolic genes on the level of PhIP-DNA adducts in human breast tissues.

MATERIALS AND METHODS

Study Subjects and Tissue Samples

A total of 105 normal breast tissue sections were obtained from women having newly diagnosed breast cancer undergoing mastectomy at The University of Texas M.D. Anderson Cancer Center and forty nine normal breast tissue sections were obtained from patients not having cancer undergoing reduction mammoplasty at a different local hospital and used as a control. The use of human tissue sections was approved by the M. D. Anderson Cancer Center Institutional Review Board. The age range of the study participants was 20-50 years. The mean age of the cancer patients (43 ± 6 years) was significantly higher than that of the control patients (32 ± 8 years). Seventy-eight percent of the cancer patients and 43% of the control patients were non-Hispanic whites, while 11% of the former and 51% of the latter were African-Americans. A questionnaire was administered to collect information on cigarette smoking, alcohol use, reproduction and hormonal history, family history of cancer, dietary habits and other risk factors. A blood sample was collected from each study participants. Fresh breast tissue samples were fixed in 10% buffered formalin within 5 hours after surgery and embedded in paraffin. The paraffin blocks were then cut into 5- μ M sections and mounted on aminoalkylsilane-coated slides (Sigma Diagnostics, St. Louis, MO).

In Vitro *N*-hydroxy-PhIP Treatment

MCF-7 cells were treated using *N*-hydroxy-PhIP (NCI Chemical Carcinogen Repository, Kansas City, MO) at a concentration of 0, 0.29, 0.58, 1.17, 2.31, 4.62, 9.37, 18.75, 37.5, 75, 100, 150, or 300 μ M for 2 hours at 37°C. Upon harvesting, cells were divided into two portions for IHC and 32 P-postlabeling, respectively. For IHC, cells were cytospun onto the slides at a concentration of 1×10^5 cells per slide and then fixed in methanol for 10 minutes at room

temperature and stored at -80°C . Also, before being subjected to IHC, the slides were fixed in methanol at -20°C overnight. For ^{32}P -postlabeling, cells were lysed, and DNA was extracted from them using the phenol/chloroform procedure. PhIP-DNA adducts were analyzed using the intensification procedure of the ^{32}P -postlabeling assay (24). Additionally, the intensification factor was determined via duplicate analysis of DNA samples using the standard procedure of the ^{32}P -postlabeling assay.

IHC

PhIP-DNA adduct detection using IHC was performed as described previously (25). Briefly, the paraffin-embedded sections were baked at 65°C overnight, deparaffinized in xylene, and rehydrated in serial alcohol. In addition, endogenous peroxidase activity was blocked using 1% H_2O_2 in methanol for 20 minutes. After treatment using RNase and pepsin, the sections were blocked using 3% bovine serum albumin and normal goat serum. Next, the primary anti PhIP-DNA adduct polyclonal antibody was incubated with the sections at 4°C overnight in a humid chamber at a dilution of 1: 3000. Also, the biotinylated secondary antibody was incubated with the sections at 37°C for 30 minutes, at a dilution of 1: 200. The antibody complex was detected using an avidin-biotin-peroxidase complex solution and visualized using 3,3'-diaminobenzidine (Zymed Laboratories, Inc., San Francisco, CA). A negative control was included in each experiment by omitting the primary antibody. The staining specificity was confirmed using the primary antibody that had been preabsorbed with 2 or 20 $\mu\text{g/mL}$ DNA extract from MCF-7 cells treated with 150 μM *N*-hydroxy-PhIP.

Image Analysis

Tissue sections having an epithelial cell content of 10% or more showed nuclear staining were considered to be positive. The staining intensity was semiquantified via image analysis.

The stained nuclei of mammary epithelial cells were captured as grayscale images from three randomly selected low power fields (100×). Additionally, the nuclear staining intensity was expressed as absorbency. To reduce analytical bias, each batch of samples included samples obtained from both cancer and control patients and the case-control status was blinded to the person who performed the assays.

Genetic polymorphisms

DNA was isolated from peripheral lymphocytes using the phenol/chloroform procedure. Polymorphisms of the *CYP1A1*, *GSTM1*, and *NAT2* genes were determined by PCR and restriction fragment length polymorphism as reported previously (26). An internal control gene was amplified along with *GSTM1* gene. When both *GSTM1* and the internal standard were not amplified, the sample was considered as non-informative. At least 10% of the samples were analyzed in repeats to ensure quality control.

Statistical Analysis

The correlation between the absorbency of PhIP-DNA adducts as measured by IHC and the RAL values measured by ³²P-postlabeling was determined by linear regression analysis. The mean values (\pm SE) of the PhIP-DNA adduct absorbency were compared between cases and controls, smokers and non-smokers and between different subgroups using student's *t*-test. Two-tailed *P* values were calculated for the determination of statistical significance; the significance value was $P < 0.05$. Logistic regression was applied to calculate the odds ratio (OR) and 95% confidence interval (CI) for the association between PhIP-DNA adducts and breast cancer risk after adjusting for age and ethnicity.

RESULTS

Because the antibody against PhIP-DNA adducts had not been previously tested in human tissue, we first verified the specificity and sensitivity of this antibody in MCF-7 cells exposed to a PhIP derivative, *N*-hydroxy-PhIP. A clear dose-dependent increase in nuclear staining intensity (Upper panel, Fig. 1) was detected in the cells exposed to 0.58 to 75 μ M *N*-hydroxy-PhIP (Fig. 2). The staining intensity of cells exposed to the lowest level of *N*-hydroxy-PhIP (0.29 μ M) was not different from that of unexposed cells. The staining intensity leveled off at higher doses (100 to 300 μ M). On average 458 ± 59 cells were analyzed on each slide. Omitting the primary antibody or using a primary antibody preabsorbed with the antigen resulted in an absence or significantly reduced intensity of staining (Fig. 3). When DNA samples obtained from the same cell population were analyzed using 32 P-postlabeling, DNA adducts were not detectable in cells received 0.29 μ M *N*-hydroxy-PhIP. At the doses between 0.58 μ M to 18.75 μ M, two major PhIP-DNA adducts were detected, while four additional adducts appeared in cells that received higher doses of *N*-hydroxy-PhIP (Lower panel, Fig. 1). A significant dose-response relationship was demonstrated within the range of 0.58 to 100 μ M while adducts leveled off at doses greater than 150 μ M (lower panel, Fig. 2). The intensification factor was found 120 for the total adducts and 20 - 200 for each individual spot (data not shown). There was a significant correlation between the staining intensities and relative adduct labeling values in the 32 P-postlabeling analysis ($r = 0.94$) (Fig. 2). Since the detectable level of adducts in cells treated using the lowest dose of *N*-hydroxy-PhIP (0.58 μ M) was 0.78 adducts/ 10^7 nucleotides after correction using the intensification factor, the detection limit of the IHC assay is probably around $1/10^7$ for PhIP-DNA adducts.

We then measured the level of PhIP-DNA adducts in normal breast tissue sections obtained from the 105 cancer and 49 control patients using IHC and the image analysis method. Nuclear staining of PhIP-DNA adducts was clearly visible in the mammary epithelial cells (Fig. 3). On average, 801 ± 252 mammary epithelial cells were analyzed in each tissue section. Positive staining was recorded in 83% (87/105) of the cancer patients and 71% (35/49) of the control patients. Image analysis showed that the mean \pm standard error (SE) absorbency of the positively stained samples was 0.30 ± 0.016 and 0.21 ± 0.022 for the cancer and control patients, respectively ($P = 0.003$). Using the median value (0.24) of staining intensity in the control patients as a cutoff point, we found that 71.4% of the cancer and 46.9% of the control patients were distributed in the higher range ($\chi^2 = 8.66$; $P = 0.003$, Table 1). Logistic regression analysis demonstrated an odds ratio of 6.16 (95% confidence interval 2.07 to 18.36) after adjusting for age and ethnicity ($P = 0.001$).

Using stratified analysis we have explored the possible effect of several factors on the level of PhIP-DNA adducts in breast tissues. As shown in Table 2, we did not find any significant effect of age, ethnicity, smoking, well-done meat consumption and polymorphisms of *CYP1A1*, *GSTM1* and *NAT2* genes on the level of PhIP-DNA adducts in the breast (Table 2). Moreover, when cancer and control patients were pair-matched by race and age, the staining intensity was still significantly higher in the former than in the latter in 17 pairs of samples (data not shown). Using linear regression analysis, we found that the case-control status, not age or ethnicity, was the only significant predictor of the level of PhIP-DNA adducts in breast tissue (data not shown).

Finally we explored the possible gene-environmental interaction on the level of PhIP-DNA adducts in the breast tissues. We did not see any significant interaction between smoking

and genetic polymorphisms on the level of PhIP-DNA adducts. However, we found that individuals consuming well-done meat and having either mutant *CYP1A1* or rapid *NAT2* genotypes had significantly higher level of PhIP-DNA adducts in the breast tissues compared with those who do not consume well-done meat and having the same genotypes (Table 3).

DISCUSSION

We report here the detection of PhIP-DNA adducts in normal breast tissues of women having or not having breast cancer and a significant association between the levels of PhIP-DNA adducts in such tissue and risk of breast cancer. We observed a significant interaction between consumption of well-done meat and polymorphisms of carcinogen-metabolizing genes. To our knowledge, this is the first study to demonstrate the presence of PhIP-DNA adducts in breast tissues from women without preplanned exposure to PhIP. Our data provides a strong evidence supporting the hypothesis that exposure to HCAs in genetically susceptible individuals may contribute to the etiology of human breast cancer.

Several laboratories have attempted to measure HCA-induced DNA adducts in human tissues or lymphocytes. One study (27) reported the detection of PhIP-DNA adducts in only two surgical samples of human colon mucosa ($n = 6$) but no samples of the pancreas ($n = 12$) or bladder epithelium ($n = 6$) using gas chromatography-mass spectrometry (GC/MS) and ^{32}P -postlabeling. Another study (28) reported the detection of HCA-induced DNA adducts in 3 of 38 human tissue samples using ^{32}P -postlabeling. However, in humans who consume meals including well-done meat, HCA-DNA adducts are undetectable in white blood cells using the ^{32}P -postlabeling method (12). Additionally, studies in rats receiving a daily dose of PhIP approximating the human daily intake ($0.1 \mu\text{g/kg}$) have shown that at this dose or even doses that

are 10- to 100-fold higher, PhIP-DNA adducts are also undetectable in tissues and white blood cells when analyzed using GC/MS and ^{32}P -postlabeling (29). Therefore, for the purpose of evaluating potentially genotoxic doses of HCA in humans, the likelihood of detecting HCA-induced DNA adducts in human tissues and white blood cells using the established methods are low. On the other hand, PhIP-DNA adducts have been detected using accelerated mass spectrometry in the breast tissues of humans given dietary equivalent levels of PhIP labeled with ^{14}C before surgery (21). This observation indicates that at doses derived from the human diet, HCAs can induce DNA-adduct formation in the breast tissues. However, this method is limited to adduct detection in samples previously exposed to ^{14}C -labeled HCAs. Therefore, it cannot be applied to epidemiological studies in naturally HCA unexposed human populations.

The availability of the antibody against PhIP-DNA adducts has provided a novel alternate method for detecting of PhIP-DNA adducts in human tissues. Using this antibody, PhIP-DNA adducts have been detected via IHC in tissue sections obtained from rats exposed to PhIP (25), and in normal human prostate tissues transplanted into subcutis of athymic nude mice (30). As this antibody had not been previously applied in other human tissues, however, we first confirmed the specificity and sensitivity of the IHC method in a human mammary epithelial cell system. We observed that staining was specific to PhIP-exposed samples and that there was a clear dose-response relationship in nuclear staining. These results were confirmed via ^{32}P -postlabeling of the same cell samples. Even though the staining intensity leveled off at doses higher than 150 μM , this does not affect the application of this method in human studies, because humans are very rarely exposed to such a high dose of PhIP. The detection limit of the IHC method is about 1 adduct/ 10^7 nucleotides, which is reasonable for human studies.

When the IHC method was applied in this study, we detected PhIP-DNA adducts in a high percentage of normal breast tissue sections obtained from both cancer (83%) and control patients (71%). This is not surprising, because human exposure to PhIP is quite common. Specifically, PhIP has been detected not only in cooked fish and meat but also in cigarette smoke (31), beer and wine (32) and in urban air and diesel engine exhaust particulate (33). Detection of PhIP-DNA adducts in the breast provides supporting evidence that human breast tissues are susceptible to PhIP-induced DNA damage.

In addition, using quantitative analysis we found a significantly higher level of PhIP-DNA adducts in the cancer patients than in the control patients. More importantly, we observed a significant association between the levels of PhIP-DNA adducts in breast tissues and risk of breast cancer. This observation strongly supports the hypothesis that PhIP exposure contributes to human breast cancer. Due to difficulties in obtaining normal breast tissue samples from the control patients, our study was limited in that the cancer and control patients were not well matched by age or race. However, using stratified and regression analysis we did not find a significant effect of age or race on the level of PhIP-DNA adducts. The differences in adduct levels between cancer and control remained significant in paired samples matched by age and race. If confirmed in a larger scale study using well-matched samples, it could put PhIP on top of the list of human breast carcinogens.

Another interesting observation made in this study was the interaction of environmental and genetic factors that determine the level of PhIP-DNA adducts in the breast. Individuals having a mutant *CYP1A1* or rapid *NAT2* genotype and consuming well-done meat showed a significantly higher level of PhIP-DNA adducts in the breast tissues than those with the same genotypes but did not consume well-done meat. Our observation is consistent with the finding of

a previous study that showed a significant relationship between breast cancer risk and consumption of well-done meat among women with the rapid/intermediate *NAT2* genotype (34). These observations further support the hypothesis that well-done meat consumption could increase the risk of breast cancer by inducing DNA damage in the target tissues and women who are genetically susceptible to such exposures may have a higher risk of breast cancer.

REFERENCES

1. American Cancer Society. Cancer facts and figures 2001. Atlanta (GA): American Cancer Society; 2001.
2. John, E.M, Kelsey, J.L. Radiation and other environmental exposures and breast cancer. *Epidemiol Rev.*, 15: 157-162, 1993.
3. El-Bayoumy, K. Environmental carcinogens that may be involved in human breast cancer etiology. *Chem. Res. Toxicol.*, 5: 585-590, 1992.
4. Obana, H., Hori, S., Kashimoto, T., Kunita, N. Polycyclic aromatic hydrocarbons in human fat and liver. *Bull. Environ. Contam. Toxicol.*, 27: 23-27, 1981.
5. Biggs, P.J., Warren, W., Venitt, S., Stratton, M.R. Does a genotoxic carcinogen contribute to human breast cancer? The value of mutational spectra in unraveling the aetiology of cancer. *Mutagenesis*, 8: 275-283, 1993.
6. Petrakis, N.L., Maack, C.A., Lee, R.E., Lyon, M. Mutagenic activity in nipple aspirates of human breast fluid. *Cancer Res.*, 40: 188-189, 1980.
7. Scott, W.N., Miller, W.R. Mutagens in human breast cyst fluid. *J. Cancer Res. Clin. Oncol.*, 117: 254-258, 1991.
8. Martin, F.L., Carmichael, P.L., Crofton-Sleigh, C., Venitt, S., Phillips, D.H., Grover, P.L. Genotoxicity of human mammary lipid. *Cancer Res.*, 56: 5342-5346, 1996.
9. Martin, F.L., Venitt, S., Carmichael, P.L., Crofton-Sleigh, C., Stone, E.M., Cole, K.J., Gusterson, B.A., Grover, P.L., Phillips, D.H. DNA damage in breast epithelial cells: detection by the single-cell gel (comet) assay and induction by human mammary lipid extracts. *Carcinogenesis*, 18: 2299-2305, 1997.

10. Martin, F.L., Cole, K.J., Weaver, G., Williams, J.A., Millar, B.C., Grover, P.L., Phillips, D.H. Genotoxicity of human milk extracts and detection of DNA damage in exfoliated cells recovered from breast milk. *Biochem. Biophys. Res. Commun.*, 59: 319-326, 1999.
11. Wakabayashi, K., Nagao, M., Esumi, H., Sugimura, T. Food-derived mutagens and carcinogens. *Cancer Res.*, 52: 2092-2098, 1992.
12. Schut, H.A.J., Snyderwine, E.G. DNA adducts of heterocyclic amine food mutagens: implications for mutagenesis and carcinogenesis. *Carcinogenesis*, 20: 353-68, 1999.
13. Layton, D.W., Bogen, K.T., Knize, M.G., Hatch, F.T., Johnson, V.M., Felton, J.S. Cancer risk of heterocyclic amines in cooked foods: an analysis and implications for research. *Carcinogenesis*, 16: 39-52, 1995.
14. Ito, N., Hasegawa, R., Sano, M., Tamano, S., Esumi, H., Takayama, S., Sugimura T. A new colon and mammary carcinogen in cooked food, 2-amino-1-methyl-6-phenylimidazo[4,5-b]pyridine (PhIP). *Carcinogenesis*, 12: 1503-1506, 1991.
15. Ghoshal, A., Preisegger, K.H., Takayama, S., Thorgeirsson, S.S., Snyderwine, E.G. Induction of mammary tumors in female Sprague-Dawley rats by the food-derived carcinogen 2-amino-1-methyl-6-phenylimidazo[4,5-b]pyridine and effect of dietary fat. *Carcinogenesis*, 15: 2429-2433, 1994.
16. Imaida, K., Hagiwara, A., Yada, H., Masui, T., Hasegawa, R., Hirose, M., Sugimura, T., Ito, N., Shirai, T. Dose-dependent induction of mammary carcinomas in female Sprague-Dawley rats with 2-amino-1-methyl-6-phenylimidazo[4,5-b]pyridine. *Jpn. J. Cancer. Res.* 87: 1116-1120, 1996.

17. Ushiyama, H., Wakabayashi, K., Hirose, M., Itoh, H., Sugimura, T., Nagao, M. Presence of carcinogenic heterocyclic amines in urine of healthy volunteers eating normal diet, but not of inpatients receiving parenteral alimentation. *Carcinogenesis*, 12:1417-1422, 1991.
18. Kidd, L.C.R., Stillwell, W.G., Yu, M.C., Wishnok, J.S., Skipper, P.L., Ross, R.K., Henderson, B.E., Tannenbaum, S.R. Urinary excretion of 2-amino-1-methyl-6-phenylimidazo[4,5-b]pyridine (PhIP) in white, African-American, and Asian-American men in Los Angeles County. *Cancer Epidemiol. Biomarkers Prev.* 8: 439-445, 1999.
19. Kulp, K.S., Knize, M.G., Malfatti, M.A., Salmon, C.P., Felton, J.S. Identification of urine metabolites of 2-amino-1-methyl-6-phenylimidazo[4,5-b]pyridine following consumption of a single cooked chicken meal in humans. *Carcinogenesis*, 21: 2065-2072, 2000.
20. DeBruin, L.S., Martos, P.A., and Josephy, P D. Detection of PhIP (2-amino-1-methyl-6-phenylimidazo[4,5-b]pyridine) in the milk of healthy women. *Chem. Res. Toxicol.* 14: 1523-1528, 2001.
21. Lightfoot, T.J., Coxhead, J.M., Cupid, B.C., Nicholson, S., Garner, R.C. Analysis of DNA adducts by accelerator mass spectrometry in human breast tissue after administration of 2-amino-1-methyl-6-phenylimidazo[4,5-b]pyridine and benzo[a]pyrene. *Mutat. Res.* 472: 119-127, 2000.
22. Zheng, W., Gustafson, D.R., Sinha, R., Cerhan, J.R., Moore, D., Hong, C.P., Anderson, K.E., Kushi, L.H., Sellers, T.A., Folsom, A.R. Well-done meat intake and the risk of breast cancer. *J. Natl. Cancer Inst.* 90: 1724-1729, 1998.
23. Sinha, R., Gustafson, D.R., Kulldorff, M., Wen, W.Q., Cerhan, JR., Zheng, W. 2-amino-1-methyl-6-phenylimidazo[4,5-b]pyridine, a carcinogen in high-temperature-cooked meat, and breast cancer risk. *J. Natl. Cancer Inst.* 92: 1352-1354, 2000.

24. Snyderwine, E.G., Davis, C.D., Nouse, K., Roller, P.P., Schut, H.A. ³²P-postlabeling analysis of IQ, MeIQx and PhIP adducts formed in vitro in DNA and polynucleotides and found in vivo in hepatic DNA from IQ-, MeIQx- and PhIP-treated monkeys. *Carcinogenesis*, 14:1389-1395, 1993.
25. Takahashi, S., Tamano, S., Hirose, M., Kimoto, N., Ikeda, Y., Sakakibara, M., Tada, M., Kadlubar, F.F., Ito, N., Shirai, T. Immunohistochemical demonstration of carcinogen-DNA adducts in tissues of rats given 2-amino-1-methyl-6-phenylimidazo[4,5-b]pyridine (PhIP): detection in paraffin-embedded sections and tissue distribution. *Cancer Res.*, 58: 4307-4313, 1998.
26. Firozi, P.F., Bondy, M.L., Sahin, A.A., Chang, P., Lukmanji, F., Singletary, E.S., Hassan, M.M, and Li, D. Aromatic DNA Adducts and Polymorphisms of CYP1A1, NAT2, and GSTM1 in Breast Cancer. *Carcinogenesis*, 23: 301-306, 2002.
27. Friesen, M.D., Kaderlik, K., Lin, D., Garren, L., Bartsch, H., Lang, N.P., Kadlubar, F.F. Analysis of DNA adducts of 2-amino-1-methyl-6-phenylimidazo[4,5-b]pyridine in rat and human tissues by alkaline hydrolysis and gas chromatography/electron capture mass spectrometry: validation by comparison with ³²P-postlabeling. *Chem. Res. Toxicol.* 7: 733-739, 1994.
28. Totsuka, Y., Fukutome, K., Takahashi, M., Takahashi, S., Tada, A., Sugimura, T., Wakabayashi, K. Presence of N2-(deoxyguanosin-8-yl)-2-amino-3,8-dimethylimidazo[4,5-f]quinoxaline (dG-C8-MeIQx) in human tissues. *Carcinogenesis*, 17: 1029-1034, 1996.
29. Friesen, M.D., Cummings, D.A., Garren, L., Butler, R., Bartsch, H., Schut, H.A.J. Validation in rats of two biomarkers of exposure to the food-borne carcinogen 2-amino-1-

methyl-6-phenylimidazo[4,5-b]pyridine (PhIP): PhIP-DNA adducts and urinary PhIP.

Carcinogenesis, 17: 67-72, 1996.

30. Cui, L., Takahashi, S., Tada, M., Kato, K., Yamada, Y., Kohri, K., Shirai, T.

Immunohistochemical detection of carcinogen-DNA adducts in normal human prostate

tissues transplanted into the subcutis of athymic nude mice: results with 2-amino-1-methyl-

6-phenylimidazo[4,5-b]pyridine (PhIP) and 3,2'-dimethyl-4-aminobiphenyl (DMAB) and

relation to cytochrome P450s and N-acetyltransferase activity. *Jpn. J. Cancer. Res.* 91(1): 52-

58, 2000.

31. Manabe, S., Tohyama, K., Wada, O., Aramaki, T. Detection of carcinogen 2-amino-1-

methyl-6-phenylimidazole[4,5-b]pyridine (PhIP) in cigarette smoke condensate.

Carcinogenesis, 12: 1945-1947, 1991.

32. Manabe, S., Suzuki, H., Wada, O., Ueki, A. Detection of carcinogen 2-amino-1-methyl-6-

phenylimidazole[4,5-b]pyridine (PhIP) in beer and wine. *Carcinogenesis*, 14: 899-901, 1993.

33. Felton, J.S., Knize, M.G. Heterocyclic-amine mutagens/carcinogens in foods. In Cooper,

C.S., Grover, P. L, editors. *Handbook of experimental pharmacology*. Vol 94. Heidelberg:

Springer-Verlag, Berlin; 1990; p 471-502.

34. Deitz, A.C., Zheng W., Leff, M.A., Gross, M., Wen, W.-Q., Doll, M.A., Xiao, G.H., Folsom,

A.R., Hein, D.W. N-Acetyltransferase-2 Genetic Polymorphism, Well-done Meat Intake,

and Breast Cancer Risk among Postmenopausal Women. *Cancer Epidem Biomarkers Prev.*,

9: 905-910, 2000.

Table 1. Logistic regression analysis of adjusted ORs and CIs for PhIP-DNA adducts in breast tissues associated risk of cancer

Adducts* (Absorbency)	No. (%)		Crude OR (95% CI)	<i>P</i>	Adjusted OR (95% CI)	<i>P</i>
	Cases	Controls				
≤ 0.24	30 (28.6)	26 (53.1)	1.00		1.00	
> 0.24	75 (71.4)	23 (46.9)	2.83 (1.32 –6.07)	0.003	6.16 (2.07 –18.36)	0.001

* The median value of the control group was used as the cut off point.

* Adjusted for age and ethnicity.

Table 2. Stratified analysis of PhIP-DNA adducts in breast tissues

Variable		PhIP Adducts		P value
		N	Mean \pm SD	
Age ^a	≤ 32	35	0.26 \pm 0.019	0.523
	>32	119	0.28 \pm 0.018	
Non-Hispanic Whites		99	0.27 \pm 0.018	0.936
Other Races		55	0.27 \pm 0.020	
Ever Smoker ^b		44	0.27 \pm 0.025	0.837
Never Smoker		87	0.27 \pm 0.017	
Well-done Meat	Yes	52	0.31 \pm 0.021	0.171
	No	40	0.26 \pm 0.028	
<i>CYP1A1</i>	wt/wt	105	0.27 \pm 0.017	1.0
	wt/mt or mt/mt	40	0.27 \pm 0.025	
<i>GSTM1</i>	Null	95	0.28 \pm 0.017	0.684
	Wild type	52	0.27 \pm 0.022	
<i>NAT2</i>	Rapid	55	0.27 \pm 0.022	0.761
	Slow	67	0.26 \pm 0.021	

^aMean age of controls as the cut off point.

^bIndividuals who smoked more than 100 cigarettes in her lifetime.

Table 3. Gene-environmental interaction on the level of PhIP-DNA adducts in breast tissues

Gene	Smoker		Non Smoker		P	Well-done meat Yes		Well-done meat No		P
	N	Mean \pm SE	N	Mean \pm SE		N	Mean \pm SE	N	Mean \pm SE	
<i>CYP1A1</i> wt/wt wt/mt or mt/mt	35	0.27 \pm 0.030	55	0.27 \pm 0.023	0.92	38	0.30 \pm 0.026	32	0.28 \pm 0.032	0.56
	7	0.27 \pm 0.057	28	0.28 \pm 0.023	0.75	12	0.34 \pm 0.033	7	0.20 \pm 0.057	0.05
<i>GSTM1</i> Null WT	13	0.33 \pm 0.045	33	0.27 \pm 0.028	0.15	18	0.33 \pm 0.035	19	0.25 \pm 0.043	0.16
	29	0.25 \pm 0.032	52	0.22 \pm 0.021	0.96	33	0.29 \pm 0.027	21	0.26 \pm 0.039	0.59
<i>NAT2</i> Rapid Slow	16	0.28 \pm 0.047	38	0.28 \pm 0.025	0.85	23	0.35 \pm 0.029	17	0.24 \pm 0.045	0.04
	25	0.27 \pm 0.033	38	0.25 \pm 0.027	0.45	38	0.30 \pm 0.026	32	0.28 \pm 0.032	0.56

FIGURE LEGENDS

Fig. 1. Patterns of PhIP-DNA adducts detected using IHC (Upper panels) and ^{32}P -postlabeling (lower panels) in MCF-7 cells exposed to 0, 18.5, 37.0, 50.0, or 100.0 μM of *N*-hydroxy-PhIP. The patterns indicate a dose-dependent increase in staining intensity and radioactivity.

Fig. 2. Dose-response curve of PhIP-DNA adduct levels in MCF-7 cells treated using *N*-hydroxy-PhIP and correlation between IHC (upper panel) and ^{32}P -postlabeling (lower panel) findings. The bars represent the SDs of staining intensity in numerous cells on each section or relative adduct labeling (RAL) values from triplicate analyses by the ^{32}P -postlabeling assay.

Fig. 3. Detection of PhIP-DNA adducts in normal breast tissues. Panel A: Negative staining. Panel B: Weak positive staining. Panel C: Moderate positive staining. Panel D: Strong positive staining. Panels E and F: the same tissue sections probed with the primary antibody (E) and the antigen pre-absorbed antibody (F). Note greatly reduced staining intensity in panel F compared to panel E. Original amplification, 400 \times .

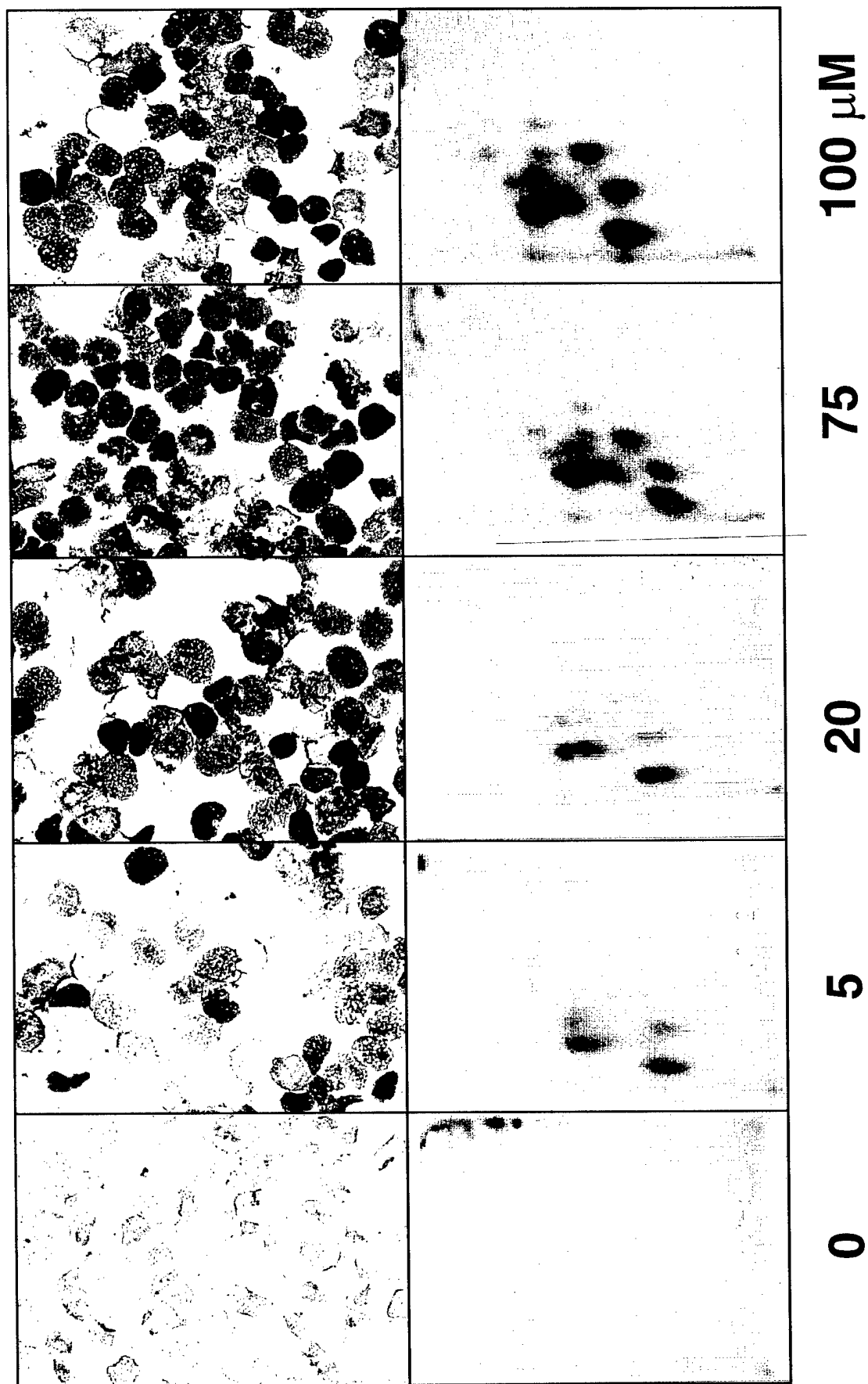


Fig. 1

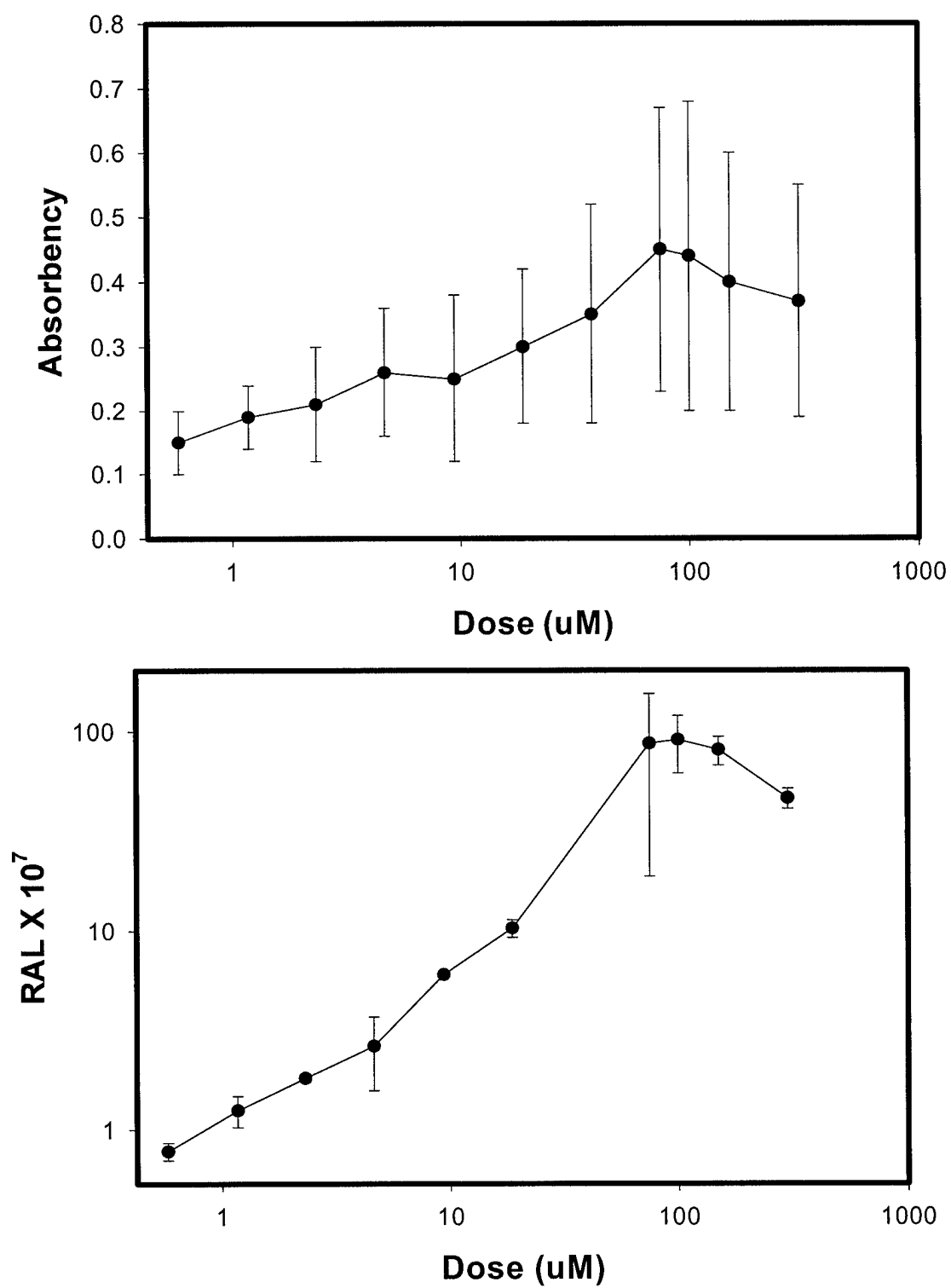


Figure 2

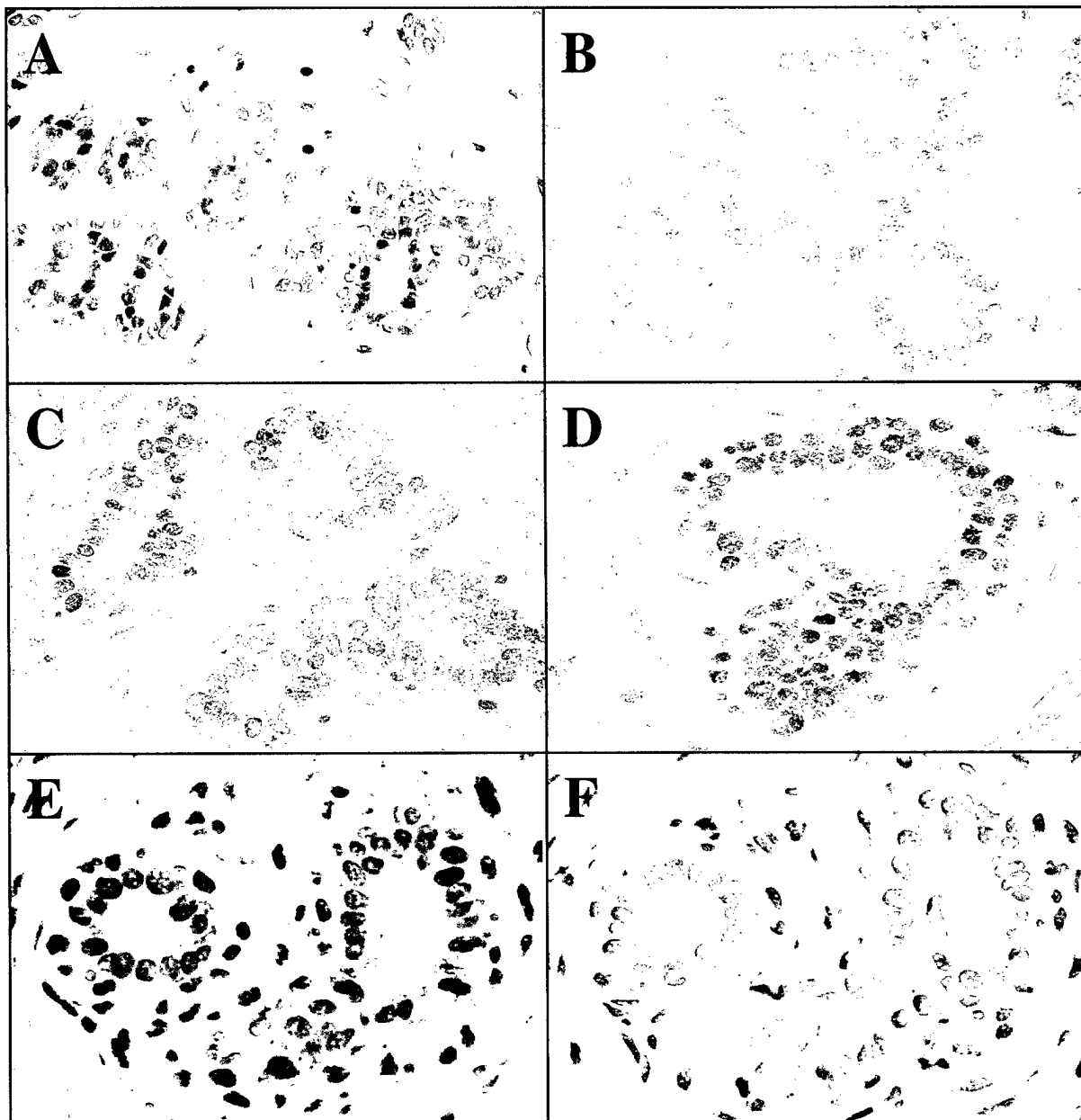


Fig. 3

The suppression of colon cancer cell growth in nude mice by targeting β -catenin/TCF pathway

Ka Yin Kwong^{1,2}, Yiyu Zou¹, Chi-Ping Day^{1,3} and Mien-Chie Hung^{1,*}

¹Department of Molecular and Cellular Oncology, The University of Texas M. D. Anderson Cancer Center, Houston, Texas 77030

²Partial fulfillment of Ph.D. requirement for the Graduate School of Biomedical Sciences, The University of Texas Health Science Center at Houston.

³Predoctoral fellow of the DOD/US Army Breast Cancer Training Grant No. DAMD17-99-9264.

*Correspondence: M-C Hung, Department of Molecular and Cellular Oncology, The University of Texas M.D. Anderson Cancer Center, 1515 Holcombe Boulevard, Houston, Texas 77030. Email: mhung@mail.mdanderson.org

Abstract

The adenomatous polyposis coli (APC) or β -catenin genes are frequently mutated in colorectal cancers, leading to activation of downstream genes with β -catenin/T-cell factor (Tcf)-responsive promoters. We have developed a gene therapy approach selectively targeting colorectal cancer cells in which β -catenin/Tcf4 pathway is activated by using a recombinant adenovirus AdTOP-CMV-TK, which carries a herpes simplex virus thymidine kinase gene (HSV TK) under the control of a β -catenin/Tcf-responsive promoter linking to a minimum CMV promoter. AdTOP-CMV-TK and ganciclovir (GCV) treatment significantly suppressed the growth of human DLD-1 colon cancer cells in nude mice. Furthermore, no significant tumor suppression effect was observed in human hepatoma cell line SK-HEP-1, in which the β -catenin/Tcf pathway is not activated, as a control experiment. In summary, we demonstrated the selective targeting of colorectal cancers with activated β -catenin by AdTOP-CMV-TK and GCV treatment in animal models, as well as its therapeutic potential for colon cancer metastasized to liver.

Mutation in the adenomatous polyposis coli gene (APC) or other components of the Wnt/ β -catenin signaling pathway is believed to be a critical step in colon tumorigenesis. Loss of functional APC protein or constitutively stable β -catenin mutants in cancer cells prevents degradation of the β -catenin protein through the ubiquitin/proteasome pathway. As a result, β -catenin protein is accumulated in the cytoplasm and nucleus of the cancer cells, leading to hyperactivation of downstream target promoters of the Wnt/ β -catenin signaling pathway. The β -catenin protein does not bind DNA by itself; rather, it forms a bipartite complex with the T-cell factor family transcription factors and activates β -catenin /TCF-responsive promoters. Many transcription targets of the Wnt/ β -catenin signaling pathway have been identified, including genes that are involved in tumorigenesis, such as CyclinD-1 (Tetsu and McCormick, 1999; Shtutman, *et al.*, 1999; Lin SY, *et al.*, 2000), c-myc (He *et al.*, 1998a), and metalloprotease (Crawford *et al.*, 1999).

Unlike other common types of human cancers that harbor mutations in diverse pathways, mutations in the APC or β -catenin gene have been identified in most of the colon cancers (70–80%) studied so far (Goss and Groden, 2000; Polakis, 2000.). On the other hand, APC/ β -catenin pathway is usually not activated in most normal tissues. Therefore, a therapeutic strategy targets this pathway could be applied to most patients with primary or metastatic colon cancer. Here we proposed a gene therapy approach that would selectively express a therapeutic gene in colon cancer cells but not liver by targeting Wnt/ β -catenin pathway. During the period of this study, Chen and McCormick reported a similar strategy to target colon cancer cells by a β -catenin/Tcf-responsive promoter in tissue culture. (Chen and McCormick, 2001). In this article, we addressed a similar question and further extend our observation to animal model while improved the expression efficiency of tumor-specific promoter.

As a part of this study, we have developed an adenoviral vector in which expression of the herpes simplex virus thymidine kinase (HSV-TK) gene is driven by a novel β -catenin /TCF-responsive promoter. HSV-TK converts the purine nucleotide analogs ganciclovir

(9-[2-hydroxy-1(hydroxyethoxy)ethoxy]methylguanine, GCV) into monophosphorylated compound. Mammalian kinases can further convert this compound into nucleotide triphosphates that inhibit DNA replication and act as a chain terminator for DNA synthesis. However, the GCV is only poor substrates for mammalian nucleotide monophosphate kinase (Knox, 1999). In the absence of HSV-TK, GCV cannot be converted into monophosphorylated compound and therefore will not be able to inhibit DNA synthesis. Thus, GCV has been used as a pro-drug to kill cancer cells in the gene therapy setting when the HSV-TK gene is used as a therapeutic gene. In colon cancer, the activated β -catenin/TCF-responsive promoter will drive the expression of HSV-TK, which converts pro-drug into active form and kill the cells. The tumor-killing efficiency of this system was enhanced not only by the improved promoter activity, but also bystander effects of HSV TK plus GCV treatment. We demonstrated that our system significantly suppressed the growth of human colon cancer cells in both tissue culture and nude mouse model, whereas the same regimen did not suppress growth of human hepatoma cells in the control experiment.

In order to test the hypothesis that colon cancer cells can be selectively killed by targeting β -catenin/TCF pathway with a responsive promoter, the activities of five sets of β -catenin/TCF-responsive promoters were compared in four cell lines. Two well-characterized colon cancer cell lines, SW480 and DLD-1, were selected for this study. In both of the cell lines, the APC gene is mutated and β -catenin levels are elevated. Chang liver and SK-HEP-1 cell lines were included in this study as controls. These two cell lines are derived from liver origins and exhibit very low level of β -catenin/Tcf transcription activity (data not shown). Fig 1A indicates the structures of the five sets of β -catenin/TCF responsive promoters. All of the β -catenin/TCF responsive promoters were constructed by fusing three copies of β -catenin/TCF binding sites (wild-type sequence in TOP and mutated one in FOP promoters) with minimal human or viral promoters. For instance, the minimal CMV promoter in the TOP-CMV construct contains only 90-bp core sequence of CMV promoter and is used to provide a basal level activity and the TOP

sequences are enhancers responsive to β -catenin/TCF interaction. On the contrary, the full-length CMV promoter of the CMV-Luc construct which contains 660-bp sequence is constitutively activated in most mammalian cells and usually represents the maximal promoter activity in the cells. The activities of the promoters were measured with luciferase assays and the results are indicated in Fig 1B. The constitutively active full-length CMV promoter served as positive control, and the activities of the tested promoter were expressed as the percent of CMV promoter activity. Except for TOP-hTERT, all β -catenin/TCF-responsive promoters were selectively activated in colon cancer cell lines, as shown by the fact that their TOP/FOP ratios were much higher in the β -catenin activated colon cancer cells (SW480 and DLD-1) than liver-derived cells in which β -catenin is not activated (Chang liver and SK-HEP-1). However, TOP-CMV exhibited much higher activity than any other β -catenin/TCF-responsive promoters in the two colon cancer cell lines. Because of its high specificity and activity for the colon cancer cell lines, TOP-CMV promoter was used in the rest of this study.

In the next step, an adenoviral vector was selected as the gene deliver system and the HSV- TK as the therapeutic gene. Four adenoviral vectors, AdCMV-luc, AdTOP-CMV-luc, AdCMV-TK, and AdTOP-CMV-TK were constructed. To test the activation of these adenoviral vectors by β -catenin/TCF signaling, stable transfectants of HEK 293 cells bearing hyperactive β -catenin mutant (293. β cat-10 and 293. β cat-12) or selection marker only (293.neo) were infected with AdCMV-luc and AdTOP-CMV-luc. As shown in the Fig. 2A, the activity of AdTOP-CMV-luc was much stronger in β -catenin-hyperactive cells than in cells with basal β -catenin activity in luciferase assay. This result indicated that the adenoviral vector AdTOP-CMV could still selectively target β -catenin-hyperactive cells. The ability of AdCMV-TK and AdTOP-CMV-TK adenoviral vectors to kill cells with different β -catenin levels was compared by an *in vitro* assay. The four cell lines were infected with adenoviruses and treated with GCV 24 hours after viral infection, then once daily for 7 days. Finally, the cell viability was measured by MTT assay. As shown in Fig. 2B, the color intensity in each well was proportional to the

number of survival cells. Fig. 2C showed the quantification of Fig. 2B. Cells with elevated β -catenin levels, such as SW480 and DLD-1, were killed efficiently by infection with either β -catenin/TCF-responsive AdTOP-CMV-TK adenovirus or constitutively active AdCMV-TK adenovirus, serving as positive control, plus GCV treatment. However, only the positive control virus AdCMV-TK, not AdTOP-CMV-TK, plus GCV treatment efficiently killed SK-HEP-1 and Chang liver cells, which were derived from liver origin. These results indicated that AdTOP-CMV-TK plus GCV treatment could be used in gene therapy to selectively kill colon cancer with little effect on liver.

To test the effectiveness of AdTOP-CMV-TK/GCV in suppressing tumor formation in animals, an *ex-vivo* strategy was carried out. DLD-1 and SK-HEP-1 cells were infected with adenoviruses *in vitro*, harvested after 24 hours, and then inoculated subcutaneously into nude mice. The animals received intraperitoneal GCV treatment daily for 10 days and the sizes of tumor were monitored twice per week. As shown in Fig. 3A, both AdCMV-TK and AdTOP-CMV-TK viruses dramatically suppressed tumor growth with GCV treatment in DLD cells. However, the AdTOP-CMV-TK did not suppress SK-HEP-1 tumor growth as efficiently as AdCMV-TK even in the combination of GCV treatment (Fig. 3B). These results, indicating that AdTOP-CMV-TK indeed selectively kills colon cancer, were consistent with the hypothesis that suicide gene expression driven by the TOP-CMV promoter can effectively suppress the growth of tumor with APC mutations and that the tumor suppression effect is diminished in liver cells in which the β -catenin pathway is inactivated.

In a recent report (Chen and McCormick, 2001), a similar gene therapy strategy targeting colon cancer by a β -catenin/TCF-responsive promoter was reported. In that study, the commonly used TOP-TK promoter was inserted into adenoviral vector AdWt-Fd to drive the expression of pro-apoptotic gene Fadd. The authors showed that TOP-TK promoter-containing AdWt-Fd could selectively kill colon cancer cells in tissue culture. Unlike their studies that have used HSV TK core promoter in the constructs, we combined minimal CMV promoter and β -catenin/TCF-responsive element as TOP-CMV

promoter in the construct. This simple manipulation significantly improved the activity of the β -catenin/TCF-responsive promoter in the β -catenin-hyperactive cell lines, while still kept the specificity (Fig 1B). Success of cancer gene therapy depends not only on the specificity, but also the expression level, of the therapeutic gene. Thus TOP-CMV promoter may be a better choice than TOP-TK.

In addition to the improvement in promoter activity, we adopted a different therapeutic gene, thymidine kinase (TK), as well as GCV treatment, to further enhance the expected efficiency of this gene therapy. In the cells expressed TK, GCV was converted into an active compound, which not only killed that cell but also neighboring ones by a bystander effect. As shown in Fig. 3, growth of colon cancers and hepatomas in the animal model was not influenced by infection of AdTOP-CMV-TK in the absence of GCV treatment. However, growth of the infected colon cancer cells, but not hepatoma cells, was significantly suppressed by GCV treatment.

Although mutations in APC gene are limited predominately to colon or rectal cancers, hyperactivity of β -catenin has been reported in other tumors like hepatocellular carcinomas, melanomas, pilomatricomas, breast cancer, etc. (de La Coste *et al*, 1998; Rubinfeld *et al.*, 1997; Chan *et al.*, 1999; Lin *et al*, 2000.). Since mutations in β -catenin gene also resulted in the activation of β -catenin/TCF-responsive promoters, the gene therapy system described here may also be applied to these tumors. In fact, the hepatocellular carcinoma cell line HepG2, in which β -catenin is mutated, was very sensitive to treatment with AdTOP-CMV-TK/GCV (data not shown).

In conclusion, we improved the activity of a β -catenin/TCF-responsive promoter and showed such promoter was selectively activated in colon cancer cells. We also showed that the combination of AdTOP-CMV-TK adenovirus and GCV treatment selectively killed β -catenin-hyperactive colon cancer cells, but not liver cells with low β -catenin activity, in both tissue culture and animal model. Thus, our work demonstrates this approach may have therapeutic potential for the treatment of metastatic colon cancer in the liver.

Acknowledgement

We thank Dr. Hans Clevers, (University Hospital, Utrecht, Netherlands) for generously providing TOP-fos-LUC (TOPFLASH), FOP-fos-LUC (FOPFLASH), TOPTK-LUC, and FOPTK-LUC plasmids. This work in part was supported by the Faculty Achievement Award (to M-C. H.) and the Breast Cancer Research Program of M. D. Anderson Cancer Center (to M-C. H.).

Figure Legend

Fig. 1. β -catenin-mediated promoter activities. **(a)** β -catenin-activated promoters containing TOP consensus sequence in the presence of the TCF/LEF-1 family transcription factors. AT to GC changes in the FOP sequence abolish Tcf/LEF-1 binding and render the promoters non-responsive to β -catenin. To construct β -catenin/TCF-responsive promoters, three copies of the TCF/LEF-1 binding oligomers (TOP) were fused with minimal promoters from viral origins (TOP-CMV, TOP-TK), human cellular genes (TOP-hTERT, TOP-fos), or a combination of human and viral promoter elements (TOP-E2F-CMV). A corresponding control plasmid was constructed for each promoter by replacing the TOP oligomers with the mutant TCF binding oligomers FOP. TOP and FOP elements were generated by digestion of TOP-fos-LUC (TOPFLASH), FOP-fos-LUC (FOPFLASH), TOPTK-LUC, or FOPTK-LUC plasmids. **(b)** 1.5 μ g of each plasmid was transfected into colorectal cancer cell lines DLD-1 and SW480 as well as liver cell lines Chang liver and SK-HEP-1. Transfection experiments were normalized by the Dual Luciferase system (Promega). 0.2 μ g of control plasmid RL-TK (Promega) was used for normalization. Luciferase activities, which represented promoter activities, were measured 24 to 36 hours after transfection according to the manufacturer's instruction. The TOP/FOP ratio represents the specificity of the promoters in β -catenin/Wnt-active cells. The activities of the tested promoter were expressed as the percent of constitutively active full-length CMV promoter activity.

Fig. 2. The AdTOP-CMV-TK virus preferentially targets colon cancer cell lines in vitro. The adenoviral vectors were constructed by the AdEasy system (He *et al.* 1998b). The transcription termination sequences from the pGL3-Basic (Promega) and pcDNA3 plasmids (Invitrogen, Carlsbad, CA) were inserted into pShuttle plasmid in a tail-to-tail orientation to construct pShuttleGB. The promoters and reporter genes were then cloned into pShuttleGB vectors. Genomic adenoviral plasmids pAdCMV-luc, pAdTOP-CMV-luc, pAdCMV-TK, and pAdTOP-CMV-TK were generated by homologous recombination in *E. coli* strain BJ5183 from the pShuttleGB vectors. Adenovirus production and purification were performed by following standard procedures. (a) HEK293 transfectant cell lines were infected with AdCMV-luc and AdTOP-CMV-luc viruses at various concentration (MOI, multiplicity of infection) and the luciferase activities were measured after 12 hours. 293. β cat-10 and 293. β cat-12 are two independent clones which expressed constitutively activated β -catenin mutant (S45Y), while 293.neo was vector transfectant. Luciferase activities were measured with Dual Luciferase system (Promega) 24 to 36 hours after infection (means \pm s.d.) according to the manufacturer's instruction. (b) Chang Liver (not shown in this picture), SK-HEP-1, DLD-1, and SW480 cells were infected with AdTOP-CMV-TK or AdCMV-TK viruses and treated with ganciclovir (GCV) once daily for 7 days. Twenty-four hours after adenoviral infection of cells in 96-well culture plates, culture medium was replaced by medium containing ganciclovir (GCV) (Roche, Basel, Switzerland) once daily for 7 days. Cell viability was measured by the MTT (Sigma, St. Louis, MO) assay at the end of the 7 days treatment. The number of viable cells is proportional to the color intensities. The numbers on the right indicate the viral particles per cell for infection. (c) Quantification of the MTT assays by measuring the absorbance at 570 nm. The data shown are the means of triplicate wells for each condition. This experiment has been repeated once and the result was consistent with data shown here.

Fig. 3. AdTOP-CMV-TK and GCV treatment preferentially suppressed growth of β -catenin- hyperactive tumors in nude mice. **(a)** Human DLD-1 colon cancer cells were infected with 25 MOI of adenoviral vectors in serum free medium. Six to twelve hours after adenoviral infection, equal volumes of medium supplemented with 10% FBS were added to the infected cells, which were then incubated at 37°C overnight. At 24 hours after adding the virus, the cells were trypsinized and inoculated subcutaneously into nude mice with 2×10^6 DLD-1 cells per mouse. One day after inoculation of cancer cells, the mice in treatment groups received daily intraperitoneal injection of 2 mg of GCV in 0.5 ml 0.9% saline (approximately 100 mg/kg body weight) for 10 consecutive days. In two independent experiments, DLD-1 tumors in control groups reached 2 cm in diameter after 4 weeks and were killed in accordance with institutional animal policy. The tumors were dissected and their weights measured. Results from the two experiments were pooled and are shown in the same diagram. **(b)** An independent experiment was performed with human SK-HEP-1 hepatoma cells. Each mouse was inoculated with 5×10^6 of SK-HEP-1 cells subcutaneously. Other steps were the same as in (a).

References

- Bienz M, Clevers H. (2000) *Cell*. **103**, 311-20.
- Chan, E.F., Gat, U., McNiff, J.M. & Fuchs, E. (1999). *Nat Genet*, **21**, 410-3.
- Chen, R.H., McCormick, F. (2001) *Cancer Res.*, **61**, 4445-9.
- Crawford, H.C., Fingleton, B.M., Rudolph-Owen, L.A., Goss, K.J., Rubinfeld, B., Polakis, P. & Matrisian, L.M. (1999). *Oncogene*, **18**, 2883-91.
- de La Coste, A., Romagnolo, B., Billuart, P., Renard, C.A., Buendia, M.A., Soubrane, O., Fabre, M., Chelly, J., Beldjord, C., Kahn, A. & Perret, C. (1998). *Proc Natl Acad Sci U S A*, **95**, 8847-51.
- Gao, X. & Huang, L. (1991). *Biochem Biophys Res Commun*, **179**, 280-5.
- Goss KH, Groden J. (2000). *J Clin Oncol*. **18**, 1967-79.
- He, T.C., Sparks, A.B., Rago, C., Hermeking, H., Zawel, L., da Costa, L.T., Morin, P.J., Vogelstein, B. & Kinzler, K.W. (1998a). *Science*, **281**, 1509-12.
- He, T.C., Zhou, S., da Costa, L.T., Yu, J., Kinzler, K.W. & Vogelstein, B. (1998b). *Proc Natl Acad Sci U S A*, **95**, 2509-14.
- Melton and Knox (ed). (1999). *Enzyme-Prodrug Strategies for Cancer Therapy*. KluwerAcademic/Plenum Publishers, New York., p216
- Landis, S.H., Murray, T., Bolden, S. & Wingo, P.A. (1998). *Ca: a Cancer Journal for Clinicians*, **48**, 6-29.
- Landis, S.H., Murray, T., Bolden, S. & Wingo, P.A. (1999). *Ca: a Cancer Journal for Clinicians*, **49**, 8-31, 1.

Lin, S.Y., Xia, W., Wang, J.C., Kwong, K.Y., Spohn, B., Wen, Y., Pestell, R.G. & Hung, M.C. (2000). *Proc Natl Acad Sci U S A*, **97**, 4262-6.

Morin, P.J., Sparks, A.B., Korinek, V., Barker, N., Clevers, H., Vogelstein, B. & Kinzler, K.W. (1997). *Science*, **275**, 1787-90.

Polakis, P. (2000). *Genes Dev*, **14**, 1837-51.

Rubinfeld, B., Robbins, P., El-Gamil, M., Albert, I., Porfiri, E. & Polakis, P. (1997). *Science*, **275**, 1790-2.

Shtutman, M., Zhurinsky, J., Simcha, I., Albanese, C., D'Amico, M., Pestell, R. & Ben-Ze'ev, A. (1999). *Proc Natl Acad Sci U S A*, **96**, 5522-7.

Tetsu, O. & McCormick, F. (1999). *Nature*, **398**, 422-6.

A

CCTTTGATC

**Wild type TCF binding
sequence (TOP)**

CCTTTGGCC

**Mutant TCF binding
sequence (FOP)**

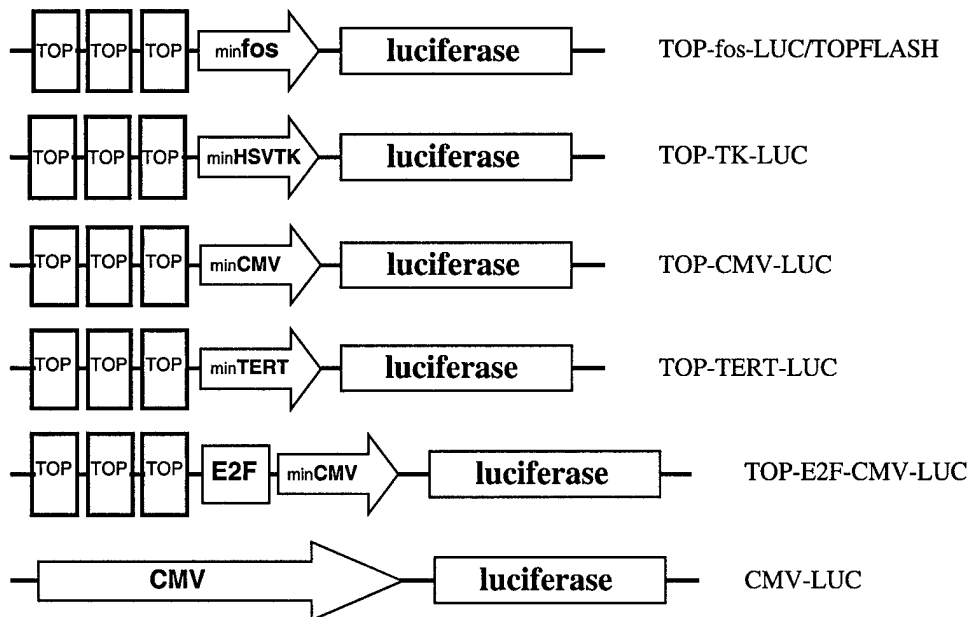


Fig 1 A

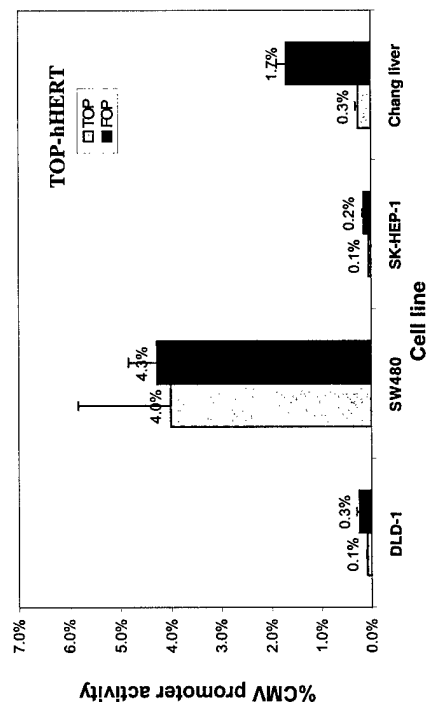
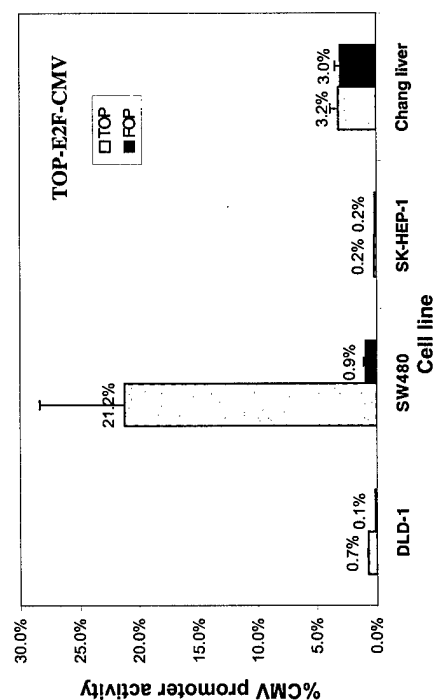
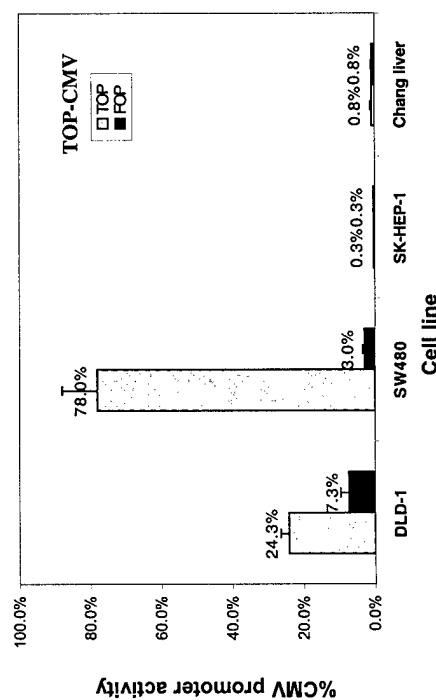
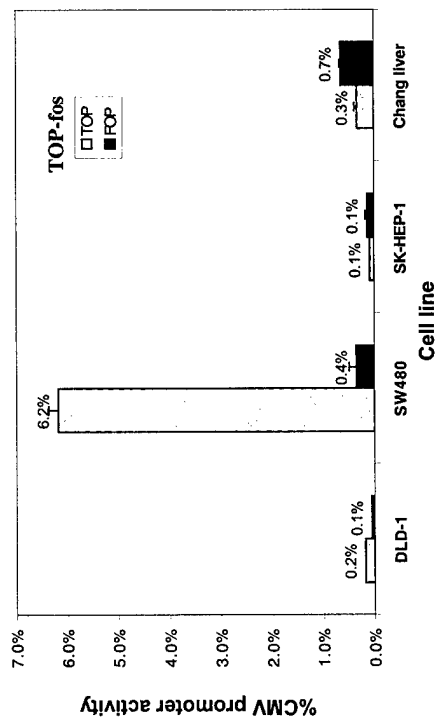
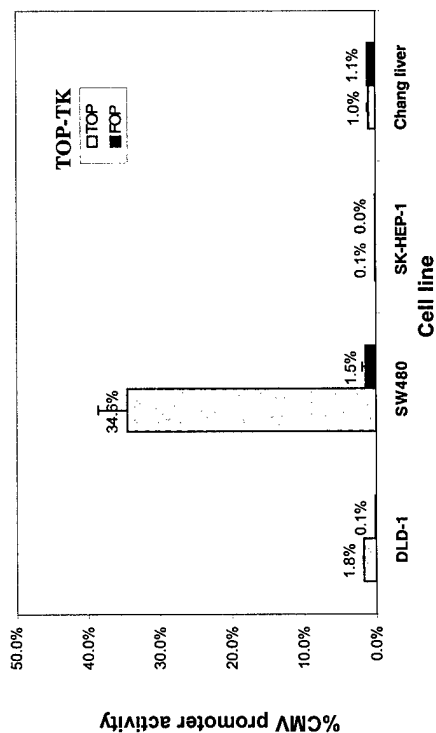


Fig 1B

A

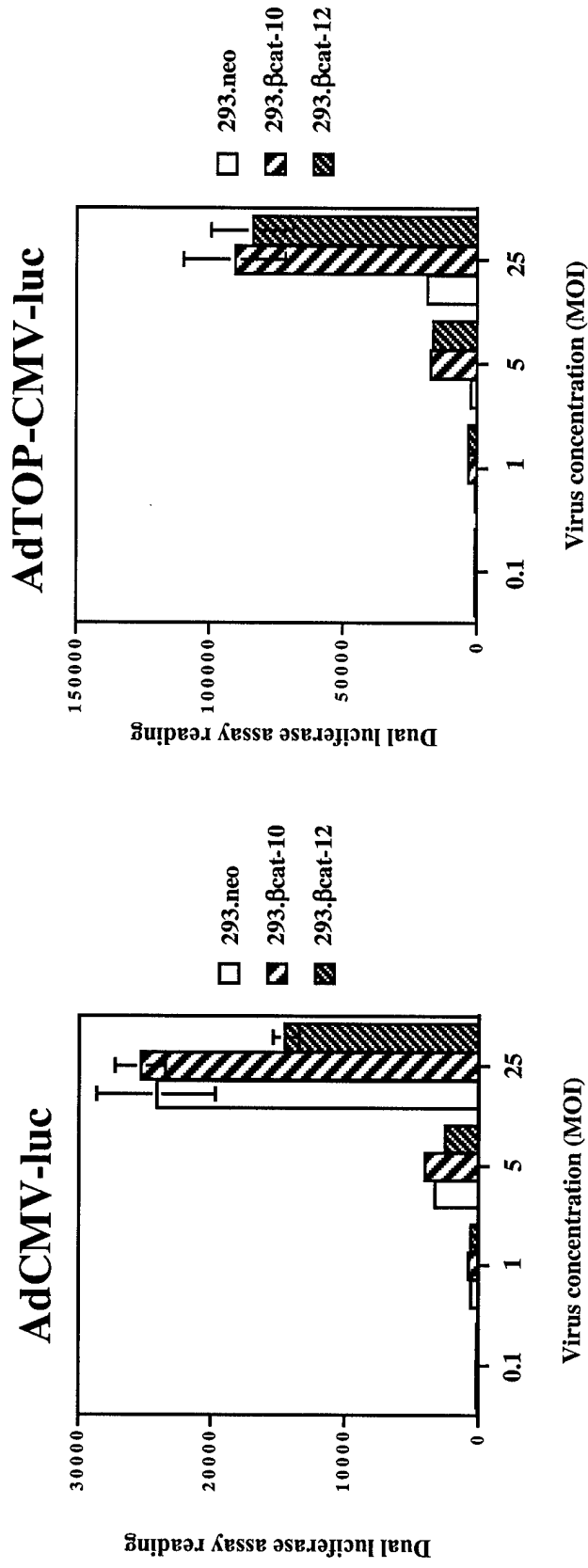


Fig 2A

B

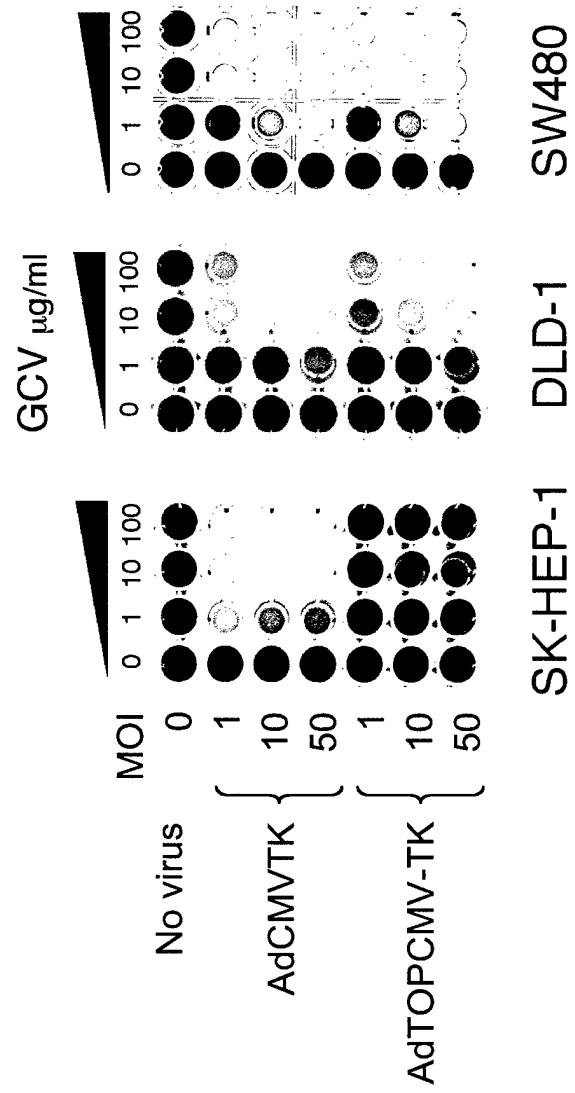
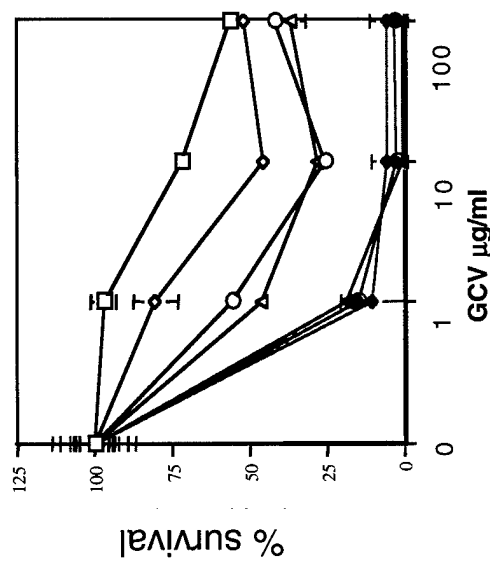


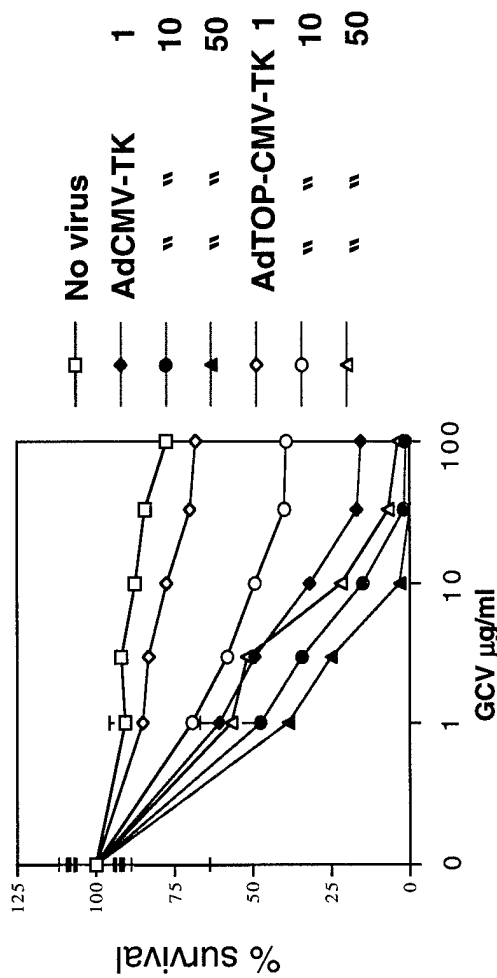
Fig 2B

C

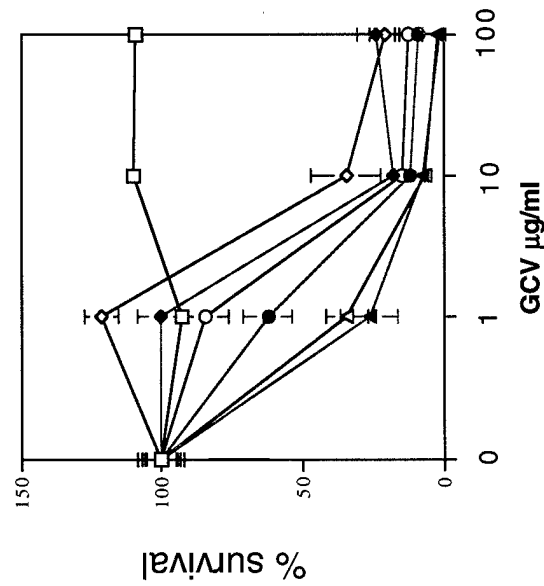
SK-HEP-1



Chang Liver



DLD-1



SW480

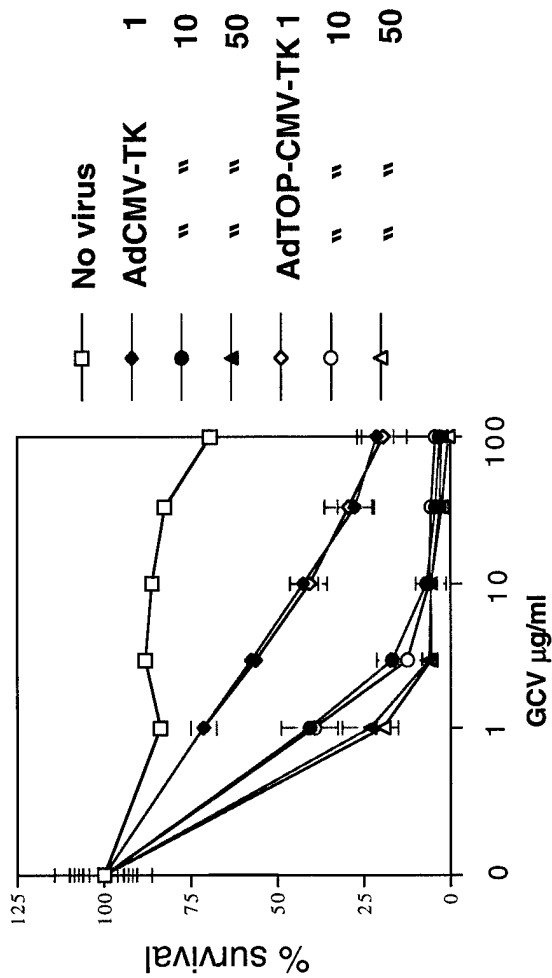


Fig 2C

DLD-1 tumors

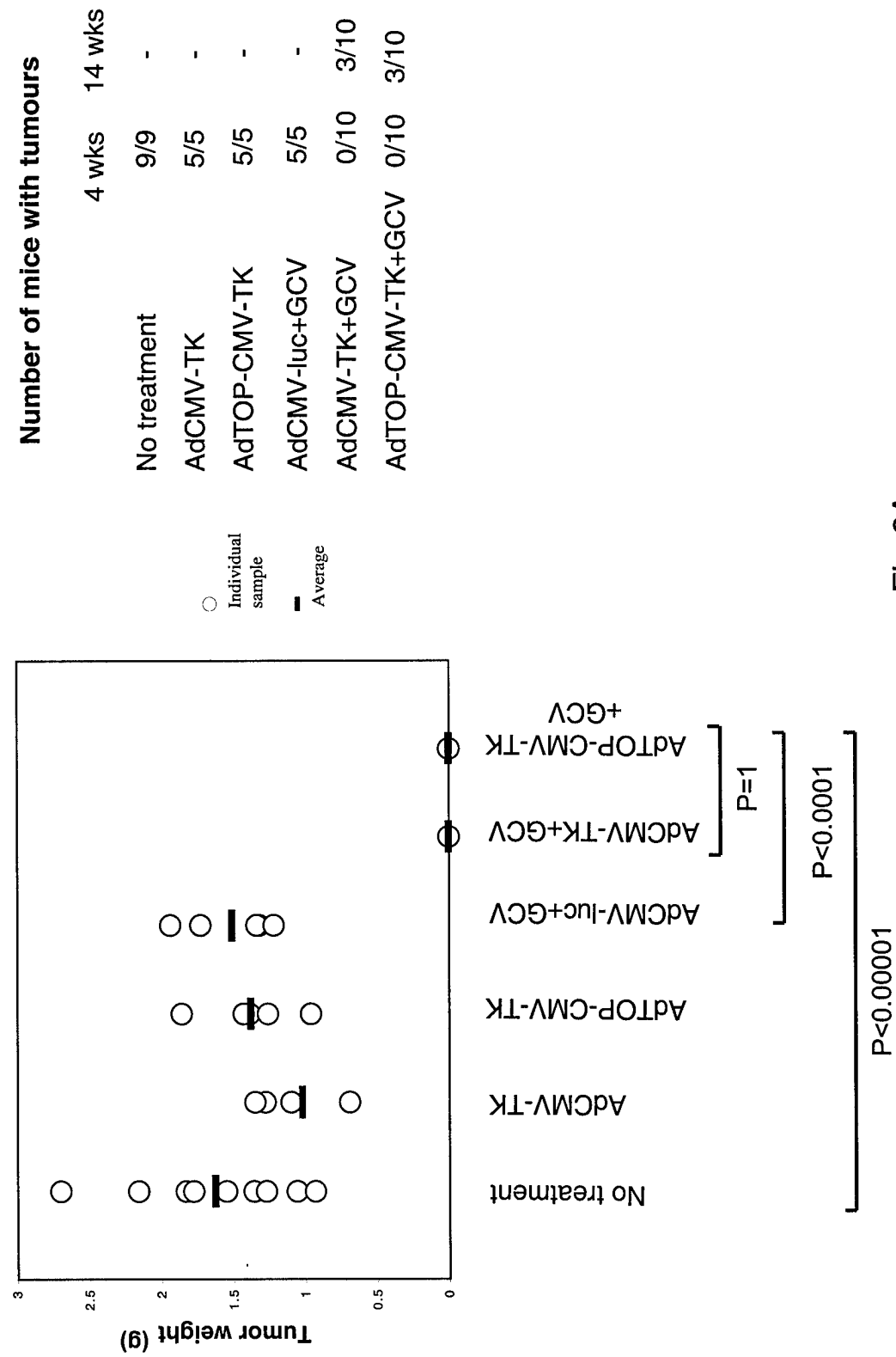


Fig 3A

B

SK-HEP-1 tumors (8 weeks)

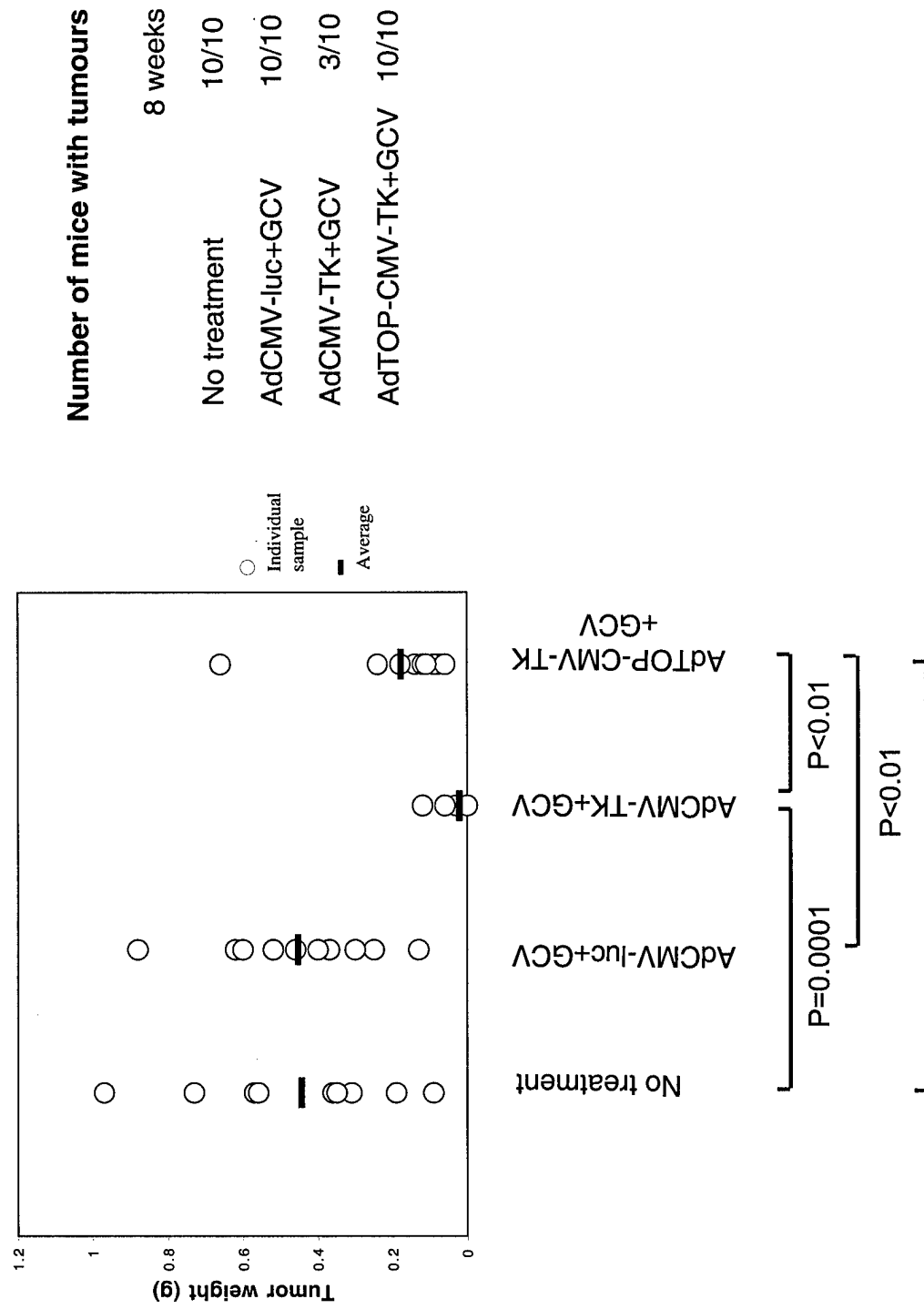


Fig 3B

Phosphorylation on Tyrosine-15 of p34^{Cdc2} by ErbB2 Inhibits p34^{Cdc2} Activation and Is Involved in Resistance to Taxol-Induced Apoptosis

Ming Tan,¹ Tong Jing,¹ Keng-Hsueh Lan,¹
Christopher L. Neal,¹ Ping Li,¹ Sangkyou Lee,¹
Dexing Fang,¹ Yoichi Nagata,¹ Jiaxin Liu,²
Ralph Arlinghaus,² Mien-Chie Hung,³ and Dihua Yu^{1,3,4}

¹Department of Surgical Oncology

²Department of Molecular Pathology

³Department of Molecular and Cellular Oncology
The University of Texas M.D. Anderson Cancer Center
Houston, Texas 77030

Summary

ErbB2 overexpression confers resistance to taxol-induced apoptosis by inhibiting p34^{Cdc2} activation. One mechanism is via ErbB2-mediated upregulation of p21^{Cip1}, which inhibits Cdc2. Here, we report that the inhibitory phosphorylation on Cdc2 tyrosine (Y)15 (Cdc2-Y15-p) is elevated in ErbB2-overexpressing breast cancer cells and primary tumors. ErbB2 binds to and colocalizes with cyclin B-Cdc2 complexes and phosphorylates Cdc2-Y15. The ErbB2 kinase domain is sufficient to directly phosphorylate Cdc2-Y15. Increased Cdc2-Y15-p in ErbB2-overexpressing cells corresponds with delayed M phase entry. Expressing a nonphosphorylatable mutant of Cdc2 renders cells more sensitive to taxol-induced apoptosis. Thus, ErbB2 membrane RTK can confer resistance to taxol-induced apoptosis by directly phosphorylating Cdc2.

Introduction

The p34^{Cdc2}-cyclin B complexes are known to catalyze chromosomal condensation and nuclear envelope breakdown during mitosis, thus having a central and rate-limiting function in the transition from G₂ into M phase (Norbury and Nurse, 1992). These complexes also play a role in the nuclear changes that accompany apoptosis (Gao and Zelenka, 1995), and, as we have demonstrated, Cdc2 activation is a prerequisite for taxol-induced apoptosis in MDA-MB-435 breast cancer cells (Yu et al., 1998). Activation of the cyclin-dependent kinase Cdc2 (Cdk1) at the G₂/M transition is precisely regulated through accumulation of Cdc2-associated cyclin B and phosphorylation of three sites on Cdc2 (Nurse, 1997). Phosphorylation at the threonine (Thr) 161 residue of Cdc2 by cyclin H-Cdk7 complexes is essential for Cdc2 catalytic activity (Harper and Elledge, 1998). The inhibitory phosphorylations on Cdc2 are by the Wee1 tyrosine kinase that induces phosphorylation of Cdc2 on Y15 (Cdc2-Y15-p) and by the Myt1 kinase that phosphorylates Cdc2 on Thr14 (Liu et al., 1997). Moreover, activation of Cdc2 is initiated at mitosis by increased activity of Cdc25C phosphatase that dephosphorylates Cdc2 on Y15 and Thr14 (Gautier et al., 1991). Additionally, the Cdk inhibitor p21^{Cip1} was shown to directly inhibit Cdc2 activity (Dulic et al., 1998; Niculescu

et al., 1998; Yu et al., 1998). Since activation of Cdc2 is the biochemical step required for mitosis, the regulation of Cdc2 activation is extremely critical and can be more complex than what is currently known. It is vitally important to unravel the possible existence of other regulators of Cdc2 activation that are involved in the control of the G₂/M transition.

The *erbB2* (HER2) gene encodes a 185 kDa transmembrane glycoprotein (ErbB2), which is a receptor tyrosine kinase (RTK) that belongs to the epidermal growth factor receptor (EGFR) subfamily (Yamamoto et al., 1986). ErbB2 overexpression is found in ~30% of human breast cancers (Slamon et al., 1987) and many other cancer types with poor clinical outcome (Yu and Hung, 2000). A detrimental consequence of ErbB2 overexpression in breast cancer is that it confers increased resistance to the chemotherapeutic agent paclitaxel (taxol) (Yu et al., 1996). This is supported by data from a phase III clinical trial showing that the taxol response rate was significantly improved in breast cancer patients when ErbB2 was downregulated by the humanized anti-ErbB2 antibody, Herceptin (Trastuzumab) (Slamon et al., 2001). One mechanism for ErbB2-mediated taxol resistance is that ErbB2 inhibits Cdc2 activation and apoptosis in taxol-treated breast cancer cells (Yu et al., 1998). Since Cdc2 activation is required for taxol-induced apoptosis, the mechanisms employed by ErbB2 to inhibit Cdc2 activation must be clearly elucidated in order to develop effective strategies to overcome taxol resistance. We have previously reported that ErbB2 overexpression inhibits Cdc2 activation by upregulation of p21^{Cip1} (Yu et al., 1998). Here we present findings for an additional mechanism of ErbB2 inhibition of Cdc2 activation that is involved in the control of the G₂/M transition and resistance to taxol-induced apoptosis.

Results

Increased Cdc2-Y15-p in ErbB2-Overexpressing Breast Cancer Cells and Primary Tumors

To study the inhibition of Cdc2 activation by ErbB2, we compared the inhibitory Cdc2-Y15-p in ErbB2-overexpressing 435.eB transfectants (Yu et al., 1996) with ErbB2 low-expressing control 435.neo cells, both derived from the MDA-MB-435 breast cancer cell line. Western blot analysis using the phosphospecific Cdc2-Y15 antibody detected a higher level of Cdc2-Y15-p in 435.eB transfectants compared with 435.neo cells, whereas Cdc2 protein levels are similar in these cells (Figure 1A). On the other hand, Cdc2-Y15-p in the 435eB.R spontaneous revertant, a 435.eB derivative that partially lost the transfected *erbB2* gene and expresses lower levels of ErbB2, was similar to that in 435.neo cells. Higher levels of Cdc2-Y15-p were also observed in the 435.tet-off ErbB2 cell line when ErbB2 expression was induced without doxycycline (–) compared with ErbB2 turned off with doxycycline (+) (Figure 1A). High levels of Cdc2-Y15-p were also detected in ErbB2-overexpressing BT474, and MDA-MB-361 cells (Figure 1A).

⁴Correspondence: dyu@notes.mdacc.tmc.edu

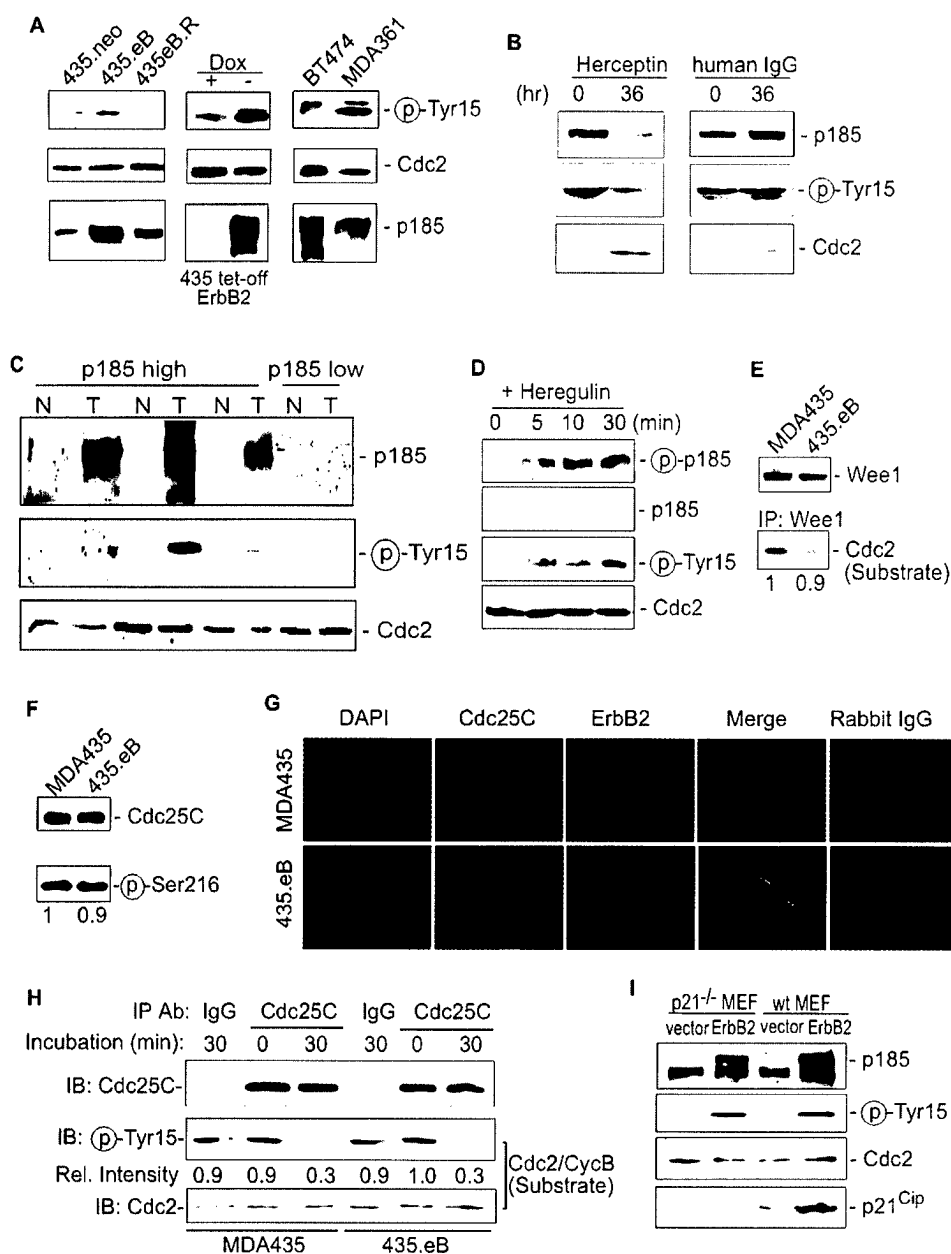


Figure 1. Higher Cdc2-Y15-p in Breast Cancer Cells and Tumors with Overexpressed or Activated ErbB2

(A) Increased Cdc2-Y15-p in ErbB2-overexpressing cells. The 435 tet-off ErbB2 cells were cultured in the presence (+) or absence (-) of doxycycline for 72 hr before collection. Cell lysates were immunoblotted for Cdc2-Y15-p, Cdc2, and ErbB2.

(B) Herceptin downregulates ErbB2 and reduces Cdc2-Y15-p in 435.eB cells. Cells were treated with 20 nM Herceptin or human IgG for 0 or 36 hr. Lysates were immunoblotted for ErbB2 (top), Cdc2-Y15-p (middle), and Cdc2 (bottom).

(C) Higher Cdc2-Y15-p in breast tumors with overexpressed ErbB2. Lysates from paired breast tumors (T) and normal tissues (N) (200 μ g) were immunoblotted for ErbB2, Cdc2-Y15-p, and Cdc2. Representative data are shown.

(D) Induction of Cdc2-Y15-p in MCF7 cells by heregulin. Serum-starved MCF7 cells were treated with heregulin (50 ng/ml), and lysates were immunoblotted for phosphorylated ErbB2 (top), ErbB2 (line 2), Cdc2-Y15-p (line 3), and Cdc2 (bottom).

(E) Wee1 protein levels and activities in MDA-MB-435 and 435.eB cells. Immunoblotting detected Wee1 proteins (top). Wee1 activities were assayed by IP of Wee1 followed by a kinase assay using Cdc2/cyclin B1 complexes as substrates (bottom).

(F) Cdc25C protein levels and Cdc25C-Ser216 phosphorylation in MDA-MB-435 and 435.eB cells. Cell lysates were immunoblotted for Cdc25C (top) and Cdc25C-Ser216 (bottom).

(G) Cdc25C subcellular localization in MDA-MB-435 and 435.eB cells. Indirect immunofluorescence staining was performed with Cdc25C and ErbB2 antibodies. Nuclei were stained with DAPI, and controls were stained with rabbit IgG.

(H) Cdc25C phosphatase activity is not altered by ErbB2 overexpression. MDA-MB-435 and 435.eB cell lysates were precipitated with anti-Cdc25C or IgG. IP efficiency was determined by anti-Cdc25C blotting (top). The precipitates were mixed with phosphorylated Cdc2/cyclin B1 complex and incubated at 25°C. Dephosphorylation of Y15 on Cdc2 was blotted with anti-Cdc2-Y15-p (middle). The blot was reprobed with anti-Cdc2 to show Cdc2 substrate used (bottom).

(I) ErbB2 overexpression increases Cdc2-Y15-p in both wt and p21 null MEF cells. WtMEF and p21^{-/-} MEF cells were transiently transfected with pcDNA3 or pcDNA3-erbB2. After 40 hr, cell lysates were immunoblotted for ErbB2 (top), Cdc2-Y15-p (line 2), Cdc2 (line 3), and p21 (bottom).

Furthermore, downregulation of ErbB2 in 435.eB cells by Herceptin (Shepard et al., 1991) led to reduced Cdc2-Y15-p (Figure 1B). These data indicate a positive relationship between ErbB2 and increased Cdc2-Y15-p.

To assess the relevance of our findings in breast cancer patients, 13 pairs of breast tumors and autologous normal tissues were collected from patients and assayed for ErbB2 expression and Cdc2-Y15-p and Cdc2 protein levels (Figure 1C). Three of the tumors were found to express higher levels of ErbB2 (p185 high) than their autologous normal tissue, and Cdc2-Y15-p was elevated in all three tumors. In contrast, Cdc2-Y15-p was hardly detectable in the ten tumors that expressed ErbB2 at levels similar to those of the paired normal tissues (p185 low). Thus, the molecular event discovered in cultured breast cancer cells is also identified in primary breast tumors.

To see if activation of ErbB2 RTK in ErbB2 low-expressing cells may also lead to elevated Cdc2-Y15-p, MCF7 breast cancer cells expressing low levels of ErbB2 were treated with heregulin, a ligand of the ErbB3 and ErbB4 receptors that activates ErbB2 by inducing heterodimerization of ErbB2 with ErbB3 or ErbB4 (Carraway, 1995). Compared with untreated MCF7 cells, heregulin increased the phosphorylation of ErbB2 receptors, indicating ErbB2 activation, and this ErbB2 activation corresponded with increased Cdc2-Y15-p (Figure 1D). Together, activation of ErbB2 RTK by overexpression (Figures 1A–1C) or by heregulin can lead to increased Cdc2-Y15-p.

Elevated Cdc2-Y15-p in ErbB2-Overexpressing Cells Is Independent of Wee1, Cdc25C, and p21^{Cip1}

Until now, Wee1 was the only known relevant tyrosine kinase to phosphorylate Cdc2-Y15, thus inhibiting Cdc2 activation (Parker and Piwnicka-Worms, 1992). However, Wee1 protein levels and Wee1 kinase activities were not increased in 435.eB cells compared with MDA-MB-435 cells (Figure 1E). Cdc25C phosphatase dephosphorylates Cdc2-Y15 and thus activates Cdc2 (Gautier et al., 1991). However, Cdc25C expression and Cdc25C-Ser216 phosphorylation, a negative indicator of Cdc25C phosphatase activity (Ogg et al., 1994), were similar in these cells (Figure 1F). Subcellular localizations of Cdc25C were also similar in asynchronous (Figure 1G) and taxol-treated MDA-MB-435 and 435.eB cells (data not shown). Finally, Cdc25C phosphatase activities for dephosphorylating Cdc2-Y15 are similar between MDA-MB-435 and 435.eB cells (Figure 1H). Thus, Wee1 and Cdc25C are unlikely mechanisms underlying increased Cdc2-Y15-p in ErbB2-overexpressing cells.

Cdc2 activity can be positively regulated by activated Cdc2 itself via a feedback mechanism (Coleman and Dunphy, 1994). Since increased expression of p21^{Cip1} in ErbB2-overexpressing cells inhibits Cdc2 activity (Yu et al., 1998), ErbB2-overexpressing cells may manifest increased Cdc2-Y15-p due to Cdc2 inhibition by p21^{Cip1}. To test this, we examined whether ErbB2 increases Cdc2-Y15-p in p21^{Cip1} null cells. ErbB2 expression vector or control vector was transiently transfected into mouse embryonic fibroblasts (MEF) from a wild-type (wtMEF) or a p21^{Cip1} knockout (p21^{-/-}MEF) mice. ErbB2 overexpression increased p21^{Cip1} expression in wtMEF but not

in p21^{-/-}MEF, whereas ErbB2 overexpression led to increased Cdc2-Y15-p in both wtMEF and p21^{-/-}MEF (Figure 1I). Thus, elevated Cdc2-Y15-p in ErbB2-overexpressing cells is independent of p21^{Cip1}.

ErbB2 Can Bind to and Colocalize with Cyclin B-Bound Cdc2

ErbB2 itself is a tyrosine kinase overexpressed in 435.eB cells. We investigated whether the ErbB2 RTK may phosphorylate Cdc2-Y15. ErbB2 association with Cdc2 was examined in lysates from different breast cancer cell lines expressing ErbB2 at various levels. ErbB2 proteins were detected in the anti-Cdc2 immunoprecipitates from ErbB2-overexpressing 435.eB, MDA-MB-361, and BT474 cells, but barely from ErbB2 low-expressing MDA-MB-231, MDA-MB-435, or 435.eB.R cells (Figure 2A). ErbB2 proteins were also detected in 435.eB cell immunoprecipitates using anti-cyclin B. Immunoprecipitation (IP) of 400 µg MDA-MB-361 cell lysates with 1.5 µg anti-Cdc2 brought down ~95% of Cdc2, which coprecipitated with ~15% of total ErbB2 (Figure 2B, left). Conversely, Cdc2 was detected in anti-ErbB2 immunoprecipitates (Figure 2B, right). ErbB2 colocalization with Cdc2 and cyclin B were detected in the cytoplasm and the nucleus of the ErbB2-overexpressing SKBr3 cells (Figure 2C). In contrast, EGFR, another member of the ErbB RTK family, did not bind Cdc2 in EGFR-overexpressing MDA-MB-468 cells (Figure 2D). Thus, overexpressed ErbB2, but not EGFR, specifically associated with cyclin B-Cdc2 complexes.

Cdc2-Y15-p by ErbB2 Complexes

Phosphorylation of Cdc2 by ErbB2 was examined by IP of ErbB2 from three different breast cancer cell lines followed by kinase reactions using GST-Cdc2N50 (amino acids 1–50 of Cdc2) or GST protein substrates. The anti-ErbB2 precipitates of 435.eB and BT474 cells contained kinase(s) that phosphorylated GST-Cdc2N50, which was undetectable in the ErbB2 low-expressing MDA-MB-435 cells (Figure 2E). To examine whether Y15 was phosphorylated, kinase reactions were repeated with BT474 cell lysates as in Figure 2E using cold ATP. Western blotting with the phosphospecific Cdc2-Y15 antibody detected Cdc2-Y15-p in ErbB2 precipitates but not in the IgG control (Figure 2F, top). Again, this Cdc2-Y15-p is independent of Wee1, because Wee1 was not detected in ErbB2 precipitates (Figure 2F, bottom). These data indicated that the kinase(s) brought down by anti-ErbB2 antibody phosphorylated Cdc2 on Y15.

Direct Phosphorylation of Cdc2 by ErbB2

To determine whether ErbB2 may directly associate with and phosphorylate Cdc2, various histidine-tagged domains of the ErbB2 protein were expressed in *E. coli*. These included a wild-type (wt) tyrosine kinase domain (His-ErbB2KD^K), a kinase-defective mutant of the kinase domain in which Lys753 is mutated to Met (His-ErbB2KD^M), and a wt extracellular domain (His-ErbB2ECD) (Figure 3A). Previous studies indicated that Cdc2 undergoes a conformational change upon cyclin B binding, resulting in the exposure of Y15 to kinase(s) that phosphorylates Cdc2 (Norbury and Nurse, 1992). Consistent with this, His-ErbB2KD^K did not bind to puri-

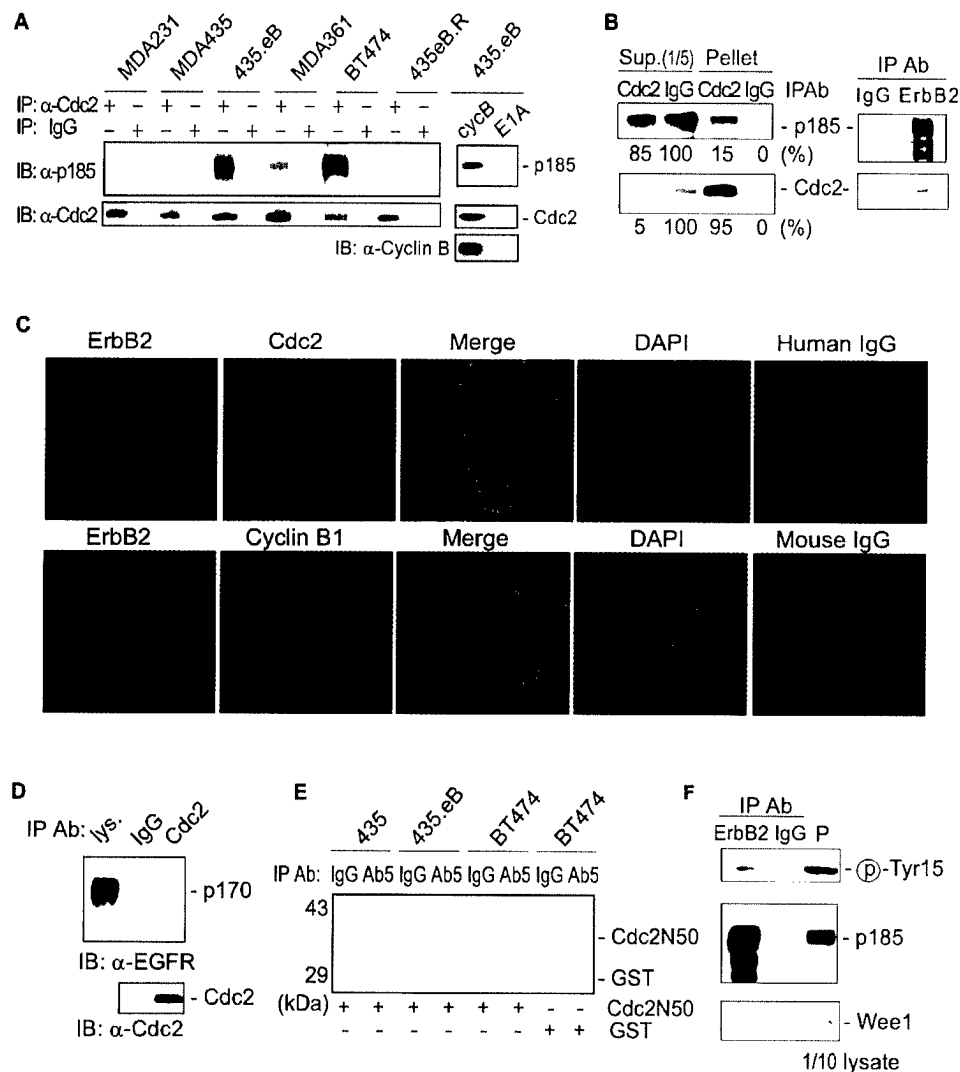


Figure 2. Association and Phosphorylation of Cdc2 by ErbB2

(A) Association of ErbB2 with Cdc2/cyclin B in vivo. Cell lysates were precipitated with anti-Cdc2, anti-cyclin B, IgG, or anti-E1A (isotype matching anti-Cdc2/anti-cyclin B) and then immunoblotted for ErbB2 (top), Cdc2, and cyclin B (bottom).

(B) Analyses of Cdc2/ErbB2 association. Left: MDA-MB-361 cell lysates were precipitated with Cdc2 antibody or normal IgG. Precipitates (Pellet) and 1/5 of the supernatants (Sup.) were resolved on SDS-PAGE. Cdc2 and ErbB2 were immunoblotted and quantitated. Right: BT474 cell lysates were precipitated using Herceptin or IgG, and then were immunoblotted for ErbB2 and Cdc2.

(C) Colocalization of ErbB2 and Cdc2/cyclin B in SKBr3 cells by 2D deconvolution immunofluorescent microscopy. Immunofluorescence staining with ErbB2, Cdc2, and cyclin B1 antibodies, nuclei staining with DAPI, and control staining with human and mouse IgG were performed as in the Experimental Procedures.

(D) EGFR does not associate with Cdc2. MDA-MB-468 cell lysates were precipitated with anti-Cdc2 or IgG, and then immunoblotted for EGFR and Cdc2 (lys., cell lysates).

(E) Phosphorylation of Cdc2N50 by the ErbB2 complex. Cell lysates were precipitated using antibodies against ErbB2 extracellular domain or IgG; immunocomplexes were subjected to kinase assay using Cdc2N50 or GST as the substrate.

(F) Cdc2-Y15-p by the ErbB2 complex. BT474 cell lysates were precipitated with ErbB2 antibody or mouse IgG. Top: half of the immunocomplexes were subjected to kinase assay with cold ATP using Cdc2N50 substrate. Reaction mixtures were separated on SDS-PAGE along with Y15-phosphorylated Cdc2 (P, positive control) and blotted with the Cdc2-Y15-p antibody. Middle and bottom: half of the immunocomplexes were separated on SDS-PAGE along with cell lysates and blotted for ErbB2 or Wee1.

fied Cdc2 in the absence of cyclin B (data not shown). Therefore, recombinant ErbB2 proteins were co-incubated with Cdc2-cyclin B complexes precipitated from 435.eB cells using Cdc2 antibodies. His-ErbB2KD^K and His-ErbB2KD^M, but not His-ErbB2ECD, bound to Cdc2-cyclin B complexes, and the binding of endogenous ErbB2 to Cdc2 was partially depleted by His-ErbB2KD^K (Figure 3B). Thus, the ErbB2 kinase domain is sufficient

for binding to the Cdc2-cyclin B complex. On the other hand, purified GST-Cdc2N50, containing the Cdc2 N-terminal 50 amino acids, is sufficient for binding to His-ErbB2KD^K (Figure 3C) and ErbB2 proteins precipitated from ErbB2-overexpressing cells (data not shown).

To determine whether ErbB2 directly phosphorylates Cdc2, His-ErbB2KD^K and His-ErbB2KD^M were incubated with GST-Cdc2N50 or GST in kinase buffer. The wt ki-

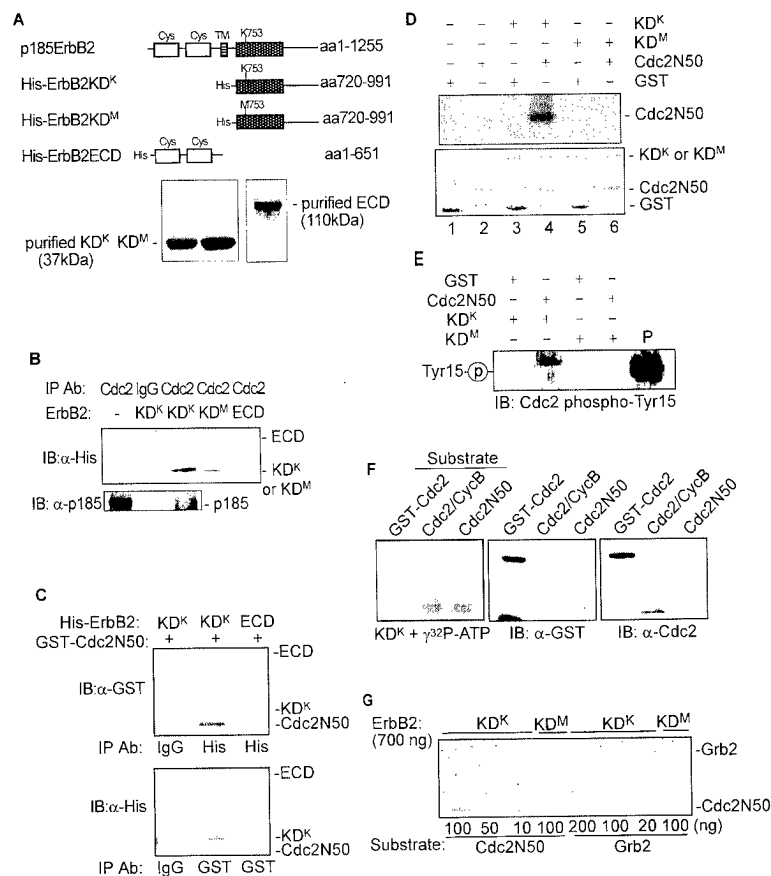


Figure 3. Direct Phosphorylation on Cdc2-Y15 by ErbB2

(A) Top: schematic diagrams of wild-type (wt) full-length ErbB2, His-tagged wt kinase domain (His-ErbB2KD^K), mutant kinase domain (His-ErbB2KD^M), and wt extracellular domain (His-ErbB2ECD) of ErbB2. Bottom: Coomassie blue staining of the recombinant proteins on SDS-PAGE.

(B) His-ErbB2KD^K and His-ErbB2KD^M, but not His-ErbB2ECD, bind to Cdc2. The 435.eB cell lysates were precipitated with Cdc2 antibody or IgG. The precipitates were incubated with His-ErbB2KD^K, His-ErbB2KD^M, or His-ErbB2ECD. Extensively washed immunocomplexes were immunoblotted using His-tag antibody for Cdc2-bound recombinant proteins and ErbB2 antibody for Cdc2-bound endogenous 185^ErbB2.

(C) Cdc2N50 binds to ErbB2KD^K. GST-Cdc2N50 and His-ErbB2KD^K or His-ErbB2ECD were mixed and precipitated with antibodies to His-tag, GST-tag, or IgG. The immunocomplexes were immunoblotted with anti-GST (top) or anti-His (bottom).

(D) Direct phosphorylation of Cdc2 by the ErbB2 kinase in vitro. His-ErbB2KD^K or His-ErbB2KD^M was incubated with GST-Cdc2N50 or GST in kinase buffer containing [γ -³²P]ATP. Samples were resolved on SDS-PAGE and stained by Coomassie blue (bottom) and then dried for autoradiography (top).

(E) Direct phosphorylation on Y15 of Cdc2N50 by ErbB2KD^K. The kinase reaction was carried out with cold ATP. The reaction mixture was separated on SDS-PAGE along with Y15-phosphorylated Cdc2 (P, positive control) and blotted using Cdc2-Y15-p antibody.

(F) Requirement of cyclin B1 for Cdc2-Y15-p by ErbB2KD^K. His-ErbB2KD^K (200 ng) was incubated (20 min) with 100 ng full-length Cdc2 (GST-Cdc2), 20 ng purified Cdc2/cyclin B complex (Cdc2/CycB), or 50 ng GST-Cdc2N50 (Cdc2N50), respectively, in kinase buffer containing [γ -³²P]ATP. Samples were resolved on SDS-PAGE and autoradiographed (left). The GST-Cdc2, Cdc2/cyclin B, and GST-Cdc2N50 proteins were immunoblotted by anti-GST (middle); the bottom band in GST-Cdc2 lane is GST) or anti-Cdc2 (right).

(G) Phosphorylation of Cdc2N50 and Grb2 by ErbB2KD^K or His-ErbB2KD^M. His-ErbB2KD^K or His-ErbB2KD^M was incubated with Cdc2N50 or Grb2 in kinase buffer containing [γ -³²P]ATP. Samples were resolved on SDS-PAGE and autoradiographed.

nase domain His-ErbB2KD^K, but not the kinase-dead His-ErbB2KD^M, phosphorylated GST-Cdc2N50 in vitro (Figure 3D). Furthermore, His-ErbB2KD^K phosphorylated Cdc2 on Y15, as demonstrated by repeating kinase assays with cold ATP followed by Western blotting using the phosphospecific Cdc2-Y15 antibody (Figure 3E). Thus, ErbB2 can function as a Wee1-like Cdc2 kinase to directly phosphorylate Cdc2 on Y15. His-ErbB2KD^K also phosphorylated purified cyclin B-Cdc2 but not the purified GST-Cdc2 without cyclin B (Figure 3F), indicating that cyclin B is required for Cdc2 phosphorylation by ErbB2. The C-terminal deletion mutant GST-Cdc2N50 without cyclin B was phosphorylated at a similar level as the cyclin B-bound full-length Cdc2 by His-ErbB2KD^K (Figure 3F). This suggested that the C terminus of Cdc2 could mask the Y15 phosphorylation site in the absence of cyclin B. Next, we compared ErbB2KD^K phosphorylation of Cdc2N50 with Grb2, a well-known in vivo substrate of ErbB2 tyrosine kinases (Li et al., 2001). ErbB2KD^K, but not ErbB2KD^M, directly phosphorylated Cdc2N50 with similar kinetics and efficiency as it phosphorylated Grb2 (Figure 3G), suggesting that Cdc2 is likely an in vivo substrate of ErbB2.

ErbB2 Specifically Phosphorylates Y15 of Cdc2

Y15 was believed to be a unique site of Cdc2 tyrosine phosphorylation in animals (Krek and Nigg, 1991), but multiple Y residues exist in Cdc2 that may be potential substrate sites for ErbB2. The Cdc2 N-terminal 20 amino acid sequence contains Y15 as well as a neighboring Y residue on each side (Y4 and Y19). If ErbB2 could nonspecifically phosphorylate Y residues other than Y15, the neighboring Y4 and Y19 that are in close proximity to Y15 would likely be phosphorylated. A panel of wt or mutated 20-mer peptides derived from the Cdc2 N-terminal sequence (Cdc2N20) was synthesized in which all three or two of the three Y residues were changed to phenylalanine (F) (Figure 4A). These Cdc2N20 peptides were used as substrates in ErbB2 kinase assays with [γ -³²P]ATP (Figure 4B). Only the mutant peptide that retained the Y15 (Y4/F19) was phosphorylated by ErbB2, as was the wt Cdc2N20 peptide, demonstrating that ErbB2 specifically phosphorylates Y15, but not the neighboring Y4 and Y19, of Cdc2N20. To assure that the phosphorylation occurs on Y, these Cdc2N20 peptides were first phosphorylated by ErbB2 with [γ -³²P]ATP and then subjected to phospho-amino acid

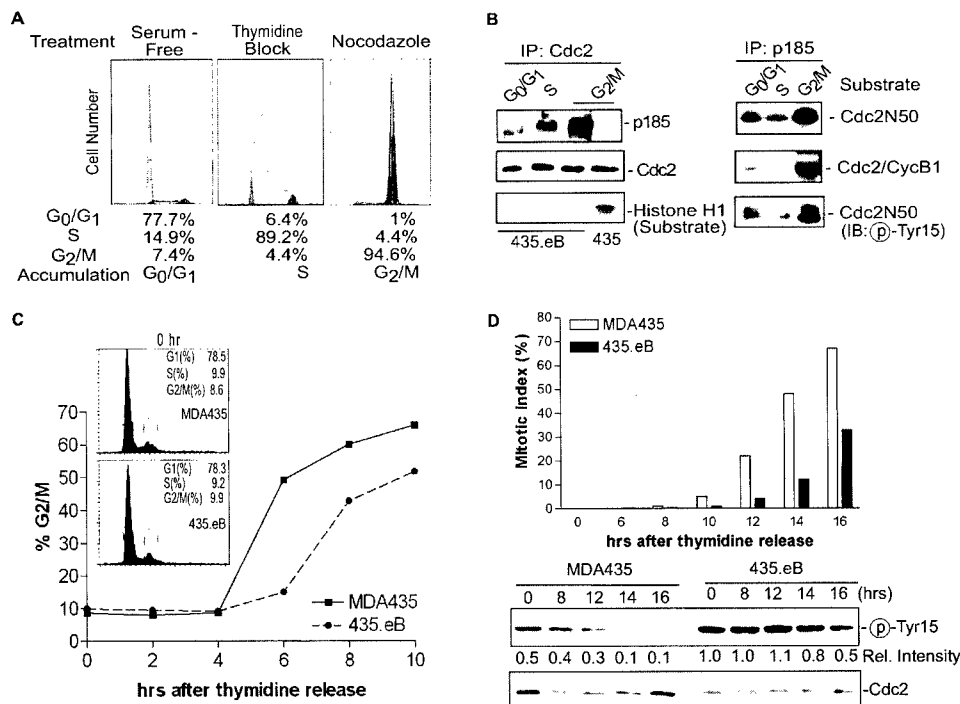


Figure 5. ErbB2 Phosphorylation of Cdc2 during the Cell Cycle and the Impact on M Phase Entry

(A) 435.eB cells enriched in G₀/G₁, S, or G₂/M phases. Cells were collected and stained with propidium iodide for flow cytometry analyses. (B) Left: association of ErbB2 with Cdc2 and Cdc2 kinase activities during the cell cycle. Cdc2 was precipitated from 435.eB or MDA-MB-435 cells at the indicated phase, immunoblotted for ErbB2 (top) and Cdc2 (middle), or assayed for Cdc2 kinase activity (bottom). Right: phosphorylation of Y15 on GST-Cdc2N50 or Cdc2/cyclin B1 complex by ErbB2 during the cell cycle. ErbB2 was precipitated from 435.eB cells followed by kinase assay using GST-Cdc2N50 (top) or purified Cdc2/cyclin B1 (middle) substrates. Kinase reactions were repeated with cold ATP and GST-Cdc2N50. Reaction mixtures were blotted using anti-Cdc2-Y15-p (bottom). (C) 435.eB cells had delayed G₂/M progression. MDA-MB-435 and 435.eB cells were synchronized in G₀/S by double thymidine block (insets). Cells were released and collected every 2 hr for flow cytometry analyses of the percentage of cells in G₂/M phase. (D) 435.eB cells have lower mitotic indices that correlate with higher levels of Cdc2-Y15-p. Top: MDA-MB-435 and 435.eB cells were synchronized at G₀/S by double thymidine block and treated with 0.02 μ M taxol for indicated times after release. At least 500 cells were counted for mitotic cells under light microscopy for each time point. Cell lysates were blotted for Cdc2-Y15-p (middle) and Cdc2 (bottom).

to a slightly higher level compared with wt ErbB2 (Figure 6D). Thus, ErbB2 tyrosine kinase activity is required for in vivo Cdc2 phosphorylation by ErbB2.

To estimate the fraction of phosphorylated Cdc2 from total Cdc2 in these ErbB2 mutant cells, the slow migrating phosphorylated Cdc2 was separated from the fast migrating unphosphorylated Cdc2 (Figure 6E). Thr14/Thr161 phosphorylation and Wee1-mediated Cdc2-Y15-p are present in both ErbB2 low- and overexpressing cells. Thus, the increase in the slow migrating Cdc2 fraction in 435.eB and V659E cells over that in the MDA-MB-435 or K753M cells is likely the fraction of Cdc2-Y15-p by ErbB2. The 435.eB and V659E cells had a 36%–45% increase of slow migrating Cdc2 compared with MDA-MB-435 or K753M cells (Figure 6E).

We previously reported that ErbB2 upregulates p21^{Cip1}, which inhibits Cdc2 (Yu et al., 1998); therefore, we examined whether Cdc2-Y15-p inhibited a different Cdc2 population from that inhibited by p21^{Cip1}. The 435.eB cell lysates were precipitated by anti-Cdc2-Y15-p to deplete Y15-phosphorylated Cdc2 (Figure 6F, top), and the supernatant was precipitated again by anti-p21^{Cip1} (Figure 6F, bottom). Following each IP, precipitates and one-fifth of the supernatant were analyzed by Western blotting of Cdc2-Y15-p, p21^{Cip1}, and Cdc2.

Under these conditions, the Y15-phosphorylated Cdc2 did not bind to p21^{Cip1}, which constituted ~35% of total Cdc2 (Figure 6F, top), and ~75% of cellular Cdc2 is either Y15-phosphorylated or p21^{Cip1} bound (Figure 6F). These data indicate that Cdc2-Y15-p plays very important roles in ErbB2-mediated Cdc2 inhibition, as does p21^{Cip1} upregulation.

ErbB2 overexpression inhibits Cdc2 activation and apoptosis in taxol-treated breast cancer cells (Yu et al., 1998). We next determined the contribution of Cdc2-Y15-p by ErbB2 to the inhibition of Cdc2 activation in ErbB2 mutant cells. Parental MDA-MB-435 cells, wt ErbB2, and mutant ErbB2 transfectants were treated with (+) or without (–) taxol, and Cdc2-Y15-p was detected using anti-phospho-Cdc2-Y15. Before taxol treatment, the 435.eB and V659E cells had higher Cdc2-Y15-p than the MDA-MB-435 and K753M cells (Figure 6G, top). Taxol led to reductions of Cdc2-Y15-p, which were more apparent in the MDA-MB-435 and K753M cells than in the 435.eB and V659E cells (Figure 6G, top). Cdc2 kinase was activated in MDA-MB-435 cells after taxol treatment, whereas Cdc2 activation was inhibited in 435.eB (wt ErbB2) and V659E cells (Figure 6G, middle). Interestingly, overexpression of the K753M mutant did not inhibit Cdc2 activation effectively (65% inhibition in

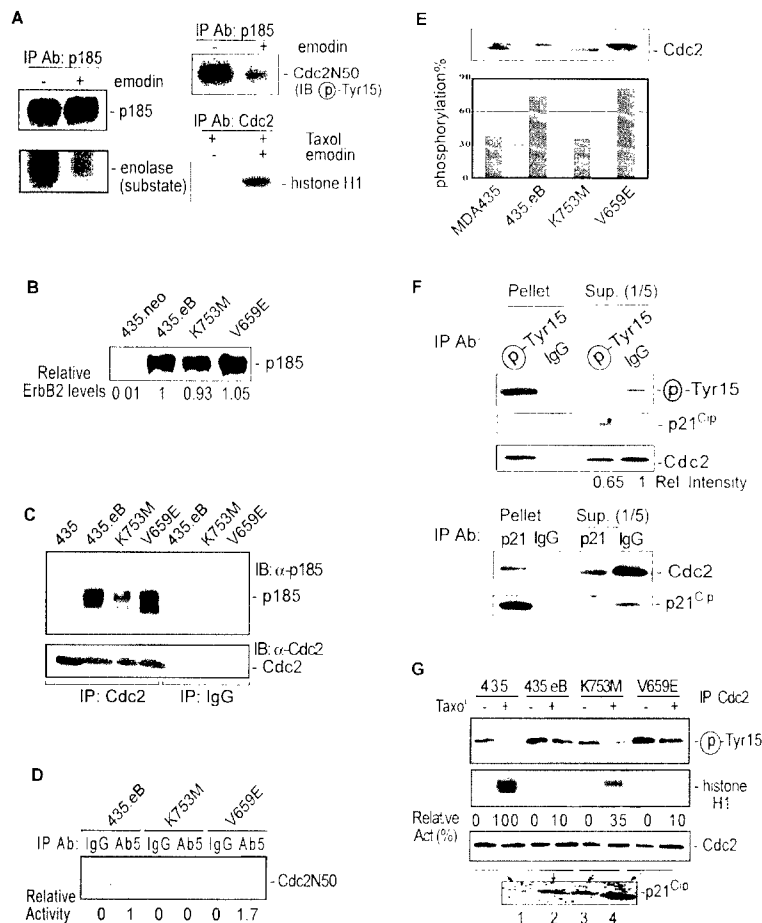


Figure 6. In Vivo Cdc2-Y15-p by ErbB2 Requires ErbB2 Tyrosine Kinase Activity and Contributes to Cdc2 Inhibition

(A) Emodin inhibited the kinase activity of ErbB2 and inhibited Cdc2-Y15-p, resulting in effective Cdc2 activation. BT474 cells were cultured in serum-free medium in the absence (–) or presence (+) of 20 μ M emodin for 24 hr. Top left: cell lysates were immunoblotted for ErbB2. Bottom left: ErbB2 was precipitated by Herceptin, followed by a kinase assay using enolase as the substrate. Top right: ErbB2 was precipitated, followed by a kinase assay using cold ATP and Cdc2N50 as substrates. The reaction mixture was immunoblotted with anti-Cdc2-Y15-p. Bottom right: cells cultured without (–) or with (+) emodin were treated without (–) or with (+) taxol for an additional 10 hr. Cdc2 was precipitated with anti-Cdc2, followed by a kinase assay on histone H1 substrate.

(B) ErbB2 protein levels in MDA-MB-435 cells and ErbB2 transfectants. Wild-type and mutant ErbB2 were immunoblotted from the lysates of the indicated transfectants.

(C) Association of mutant ErbB2 with Cdc2. IP-Western was performed as in Figure 2A using the indicated transfectants.

(D) Phosphorylation of GST-Cdc2N50 by wt and mutant ErbB2. ErbB2 immunocomplex kinase assay was performed as in Figure 2E. (E) The percentage of phosphorylated Cdc2 in MDA-MB-435 cells and ErbB2 transfectants. Lysates were analyzed by 15% SDS-PAGE and blotted with anti-Cdc2. The phosphorylation rates were calculated as the percentage of the phosphorylated Cdc2 (slow migrating bands) in total Cdc2 protein.

(F) Association of Y15 nonphosphorylated,

but not Y15 phosphorylated, Cdc2 with p21. Top: 435.eB lysate was precipitated by Cdc2-Y15-p antibody. Precipitates and 1/5 of the supernatant were immunoblotted for Cdc2-Y15-p, p21, and Cdc2. Bottom: following the above IP, the remaining 4/5 of the supernatant was reprecipitated with anti-p21. Precipitates and 1/5 of the supernatant were immunoblotted for Cdc2 and p21.

(G) Cdc2-Y15-p and Cdc2 activation in ErbB2 transfectants. MDA-MB-435 cells and ErbB2 transfectants were cultured in the absence (–) or presence (+) of taxol (0.02 μ M) for 8 hr. Cdc2-Y15-p was immunoblotted (top). Cdc2 was precipitated, followed by a kinase assay using a histone H1 substrate (line 2). Cdc2 and p21 protein levels were blotted using anti-Cdc2 (line 3) and anti-p21 (bottom). Lanes 1–4 (bottom) represent MDA-MB-435, 435.eB, K753M, and V659E cells.

K753M versus 90% in 435.eB and V659E). Wt ErbB2 upregulates p21^{Cip1} and phosphorylates Cdc2-Y15, and both can lead to Cdc2 inhibition (Figure 7E). The K753M mutant upregulates p21^{Cip1} similarly to wt ErbB2 (Figure 6G, bottom) but cannot phosphorylate Cdc2 (Figure 6D). Therefore, the inability of K753M to phosphorylate Cdc2-Y15 should account for its ineffective inhibition of Cdc2 activation (Figure 6G, middle).

Cdc2-Y15-p by ErbB2 Is Involved in Taxol Resistance

The role of Cdc2-Y15-p in the ErbB2 anti-taxol-induced apoptosis was explored by comparing the susceptibility to taxol-induced apoptosis in these ErbB2 transfectants. Apoptosis was readily detected by DNA fragmentation assays in K753M and MDA-MB-435 cells (Figure 7A); neither has elevated Cdc2-Y15-p. However, taxol-induced apoptosis was inhibited in the 435.eB and V659E cells (Figure 7A); both had increased Cdc2-Y15-p and inhibited Cdc2 activation (Figures 6D–6G). Double-label flow cytometry analyses simultaneously measuring DNA content and DNA strand breaks (Darzynkiewicz et

al., 1992) showed that the majority of untreated cell lines were in G₁ phase without significant DNA strand breaks (Figure 7B, top). After taxol treatment, 47.2% of the ErbB2 low-expressing 435.neo cells progressed to G₂/M phase and 28.9% of the cells had increased dUTP labeling, indicating apoptosis (Figure 7B, bottom). In contrast, for 435.eB cells, only 24.2% progressed to G₂/M phase and 0.1% had apoptosis. V659E cells were similar to 435.eB cells. Remarkably, 39.7% of K753M cells progressed to G₂/M phase and 18.8% of these cells died. Apoptosis in K753M cells is much less than in MDA-MB-435 cells, likely due to the upregulation of p21^{Cip1}. On the other hand, the K753M mutant failed to block taxol-induced apoptosis as effectively as the wt or V659E ErbB2, which is likely due to its defect in Cdc2-Y15-p. Thus, the ErbB2 kinase-dependent Cdc2-Y15-p is involved in resistance to taxol-induced apoptosis.

To further determine the role of Cdc2-Y15-p in resistance to taxol-induced apoptosis, we made a Y15 non-phosphorylatable Cdc2 mutant (Cdc2-Y15F) into a CMV-driven expression vector with a HA-tag. The 435.eB cells were transfected with the Cdc2-Y15F or the HA-control

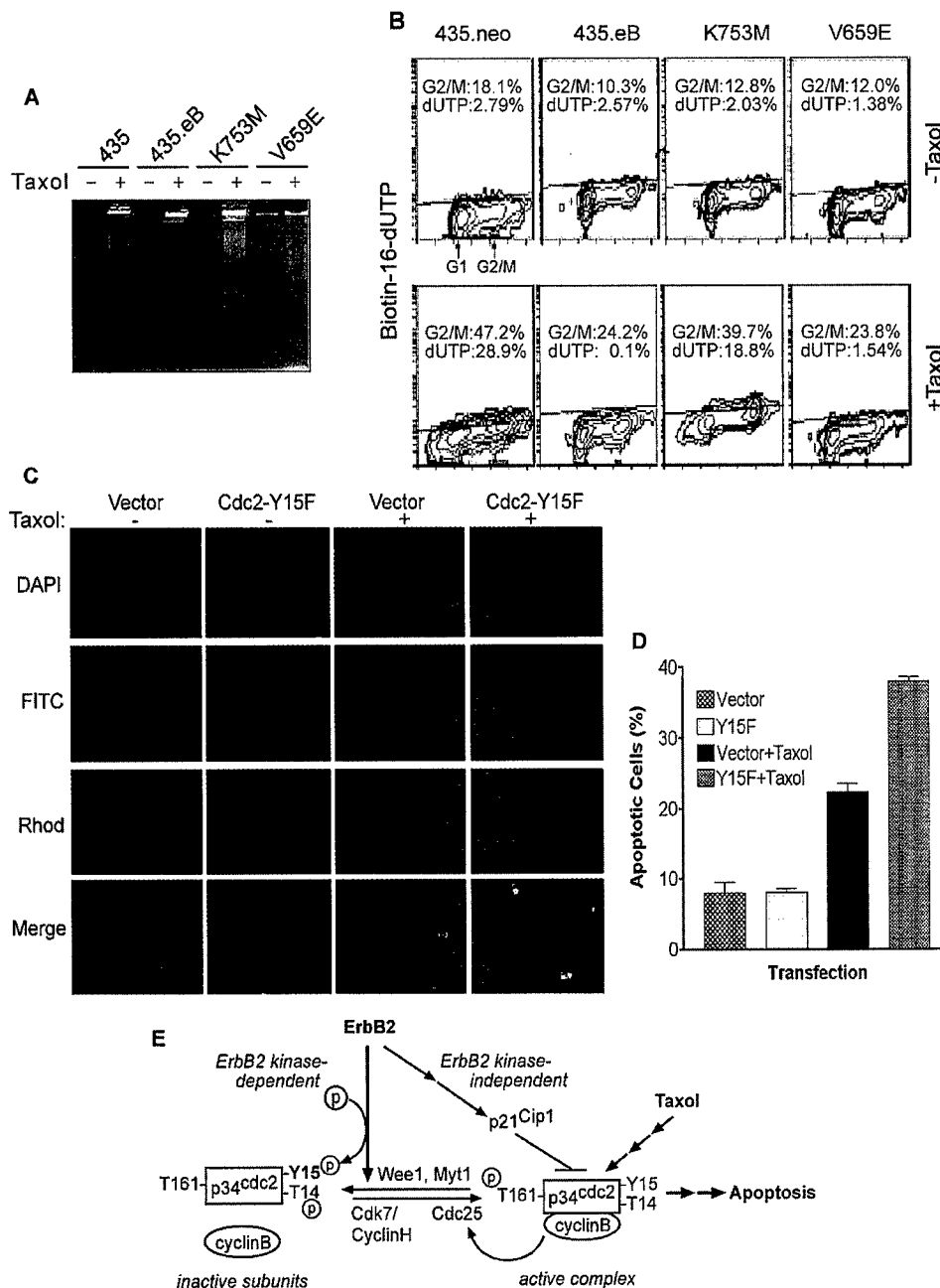


Figure 7. Cells Expressing the ErbB2 Kinase-Defective Mutant and the Cdc-Y15F Mutant Are Prone to Taxol-Induced Apoptosis

(A) Reduced resistance to taxol-induced apoptosis in K753M compared to the 435.eB and V659E cells. Low molecular weight DNAs were isolated from indicated cells cultured in the presence (+) or absence (-) of 0.02 μ M taxol for 21 hr and assayed for DNA fragmentation.

(B) Flow cytometry analyses of taxol-induced apoptosis in wt and mutant ErbB2 transfectants. Cells were cultured in the presence (+taxol) or absence (-taxol) of 0.02 μ M taxol for 21 hr and analyzed by double label flow cytometry. Apoptotic cells are shown to have a higher level of Biotin-16-dUTP labeling above the sloped lines. Percentages of cells in G₂/M and with strong dUTP labeling are indicated.

(C) 435.eB cells expressing HA-Cdc2-Y15F are more sensitive to taxol-induced apoptosis than 435.eB cells containing an HA-vector. The experiment was performed as in the Experimental Procedures. Cells expressing the HA-tag were labeled by FITC (green), apoptotic cells were stained by rhodamine-labeled anti-digoxigenin (red), and nuclei were stained by DAPI (blue).

(D) Quantitating apoptosis in the experiments of (C). To quantitate apoptosis, the transfected cells also exhibiting TUNEL staining (both FITC and rhodamine positive) were determined as a percentage of the total transfected cells (only FITC positive).

(E) Model of inhibition of Cdc2 activation and apoptosis by ErbB2 RTK. Cdc2 activity is regulated by cyclin B, Wee1, Myt1, Cdk7/cyclin H, and Cdc25C. Cdc2 activation is required for taxol-induced apoptosis. We have shown that ErbB2 overexpression can confer resistance to taxol-induced apoptosis by inhibiting Cdc2 activation through at least two mechanisms, ErbB2 kinase-dependent direct Cdc2-Y15-p and ErbB2 kinase-independent p21 upregulation (see text).

vector, then treated with or without taxol for 21 hr. The transfected HA (FITC)-positive cells were counted for apoptosis by TUNEL (rhodamine) positivity (Figures 7C and 7D). The Cdc2-Y15F-transfected 435.eB cells showed increased apoptosis after taxol treatment compared with control vector-transfected 435.eB cells. This clearly demonstrated that Cdc2-Y15-p by ErbB2 contributes to ErbB2-mediated resistance to taxol-induced apoptosis.

Discussion

Direct Phosphorylation on Cdc2-Y15 by ErbB2

Activation of Cdc2, the biochemical step required for mitosis (Nurse, 1990), is regulated by the accumulation and binding of cyclin B and by three phosphorylation sites on Cdc2 that are modulated by Cdk7-cyclin H, Cdc25C, Myt1, and Wee1 (Figure 7E). Our study has brought a new dimension to the regulation of Cdc2 activation by unraveling the role of ErbB2 as another regulator of Cdc2 activation. We demonstrated that the ErbB2 RTK, when overexpressed or activated in breast cancer cells, binds and colocalizes with Cdc2. Moreover, our data are most consistent with a model showing that ErbB2 directly phosphorylates Cdc2 specifically on Y15, the inhibitory phosphorylation site of Cdc2. To the best of our knowledge, that a membrane RTK may directly phosphorylate Cdc2-Y15 has not been previously reported.

ErbB2 colocalizes with the Cdc2/cyclin B complexes in both the cytoplasm and in the nucleus (Figure 2C). Although cytoplasmic Cdc2 is not employed in activating mitosis, it can translocate into the nucleus in late G₂ to activate mitosis (Heald et al., 1993). This may be analogous to the phosphorylation of cytoplasmic Cdc2 on Thr14 by Myt1 kinase, which inhibits Cdc2 activation (Liu et al., 1997). On the other hand, a fraction of overexpressed ErbB2 is localized in the nucleus (Xie and Hung, 1994), which may contribute to the nuclear interaction of ErbB2 and Cdc2 to inhibit Cdc2 activity. Thus, Cdc2-Y15-p by ErbB2 in both the cytoplasm and in the nucleus may contribute to the inhibition of Cdc2 activation.

Involvement of ErbB2 in the Mitotic Checkpoint in ErbB2-Overexpressing Cells

The unexpected Cdc2-Y15-p activity of ErbB2 establishes a direct link between the ErbB2 membrane RTK and Cdc2, a key player regulating mitosis in the cell cycle machinery. Cell cycle control involves multiple checkpoints, which may be viewed as signal transduction pathways whose effectors interact with Cdk-cyclin complexes to regulate the cell cycle (Nurse, 1997). Protein phosphorylation is important in cell cycle regulation, such as mitotic regulation (Maller and Smith, 1985). Our data indicated that overexpressed or activated ErbB2 in breast cancer cells perturbs the mitotic checkpoint by keeping the Cdc2-cyclin B complex inactive via Cdc2-Y15-p. This delays cell entry into M phase, which confers a survival advantage after taxol treatment (Figures 5 and 7). ErbB2 was also reported to promote G₁/S progression and tumor cell proliferation by reducing p27^{Kip1} stability and reducing the p27^{Kip1}-Cdk2 complex (Lane et al., 2000). Thus, ErbB2-mediated cell cycle de-

regulation results in detrimental consequences (e.g., apoptosis resistance and increased growth) in breast cancers.

Involvement of Cdc2-Y15-p in the ErbB2 Inhibition of Taxol-Induced Apoptosis

Our finding of Cdc2-Y15-p by ErbB2 provided an additional mechanism for ErbB2-mediated taxol resistance to p21^{Cip1} upregulation by ErbB2 (Yu et al., 1998). Thus, at least two mechanisms are involved in the ErbB2 inhibition of Cdc2 activation and taxol-induced apoptosis (Figure 7E). ErbB2 overexpression can inhibit Cdc2 activation and apoptosis in taxol-treated breast cancer cells by (1) upregulating p21^{Cip1} in an ErbB2 kinase-independent manner (Yu et al., 1998) and (2) by ErbB2 kinase-dependent Cdc2-Y15-p (the current study). The important contribution of Cdc2-Y15-p in ErbB2-mediated resistance to taxol-induced apoptosis is clearly demonstrated by data from K753M cells and by the finding that 435.eB cells with the Y15 nonphosphorylatable Cdc2-Y15F became sensitive to taxol-induced apoptosis (Figures 6 and 7). This is another example of an exquisite feature of cell biology that multiple mechanisms can be involved in an important cellular response.

Although other mechanisms may also contribute to the ErbB2 inhibition of taxol-induced apoptosis, increased Cdc2-Y15-p by ErbB2 may represent a clinically pertinent checkpoint defect in ErbB2-overexpressing breast cancers that is involved in taxol resistance. This is underscored by our finding that, of the 13 primary breast tumors examined, three overexpressed ErbB2 and had higher levels of Cdc2-Y15-p (Figure 1C), whereas none of the ErbB2 low-expressing tumors had increased Cdc2-Y15-p. Defects in checkpoint control can be novel therapeutic targets (Nurse, 2000). Thus, our findings may have promising implications for the future management of ErbB2-overexpressing breast cancers.

Experimental Procedures

Antibodies and Reagents

Antibodies and reagents were purchased from commercial sources: monoclonal Cdc2, polyclonal Cdc2, Wee1, cyclin B1, Cdc25C, EGFR, and mouse IgG antibodies from Santa Cruz Biotechnology (Santa Cruz, CA); polyclonal Cdc2, phospho-specific Cdc2-Y15 (Cdc2-Y15-p), and phospho-specific Cdc25C-ser216 antibodies from Cell Signaling Technology (Beverly, MA); E1A antibody from BD PharMingen (San Diego, CA); p21^{Cip1} (p21) polyclonal and ErbB2 monoclonal antibodies from Oncogene Science (Cambridge, MA); phospho-ErbB2 (Y1248) and recombinant GST-Grb2 from Upstate Biotechnology (Lake Placid, NY); and human IgG, enolase, and 4,6-diamidino-2-phenylindole (DAPI) from Sigma (St. Louis, MO). Texas Red-conjugated anti-human and fluorescein isothiocyanate (FITC)-conjugated anti-mouse and anti-rabbit antibodies were purchased from Jackson ImmunoResearch (West Grove, PA). Herceptin (Trastuzumab) anti-ErbB2 was from Genentech (South San Francisco, CA). Taxol was from Mead Johnson (Princeton, NJ); emodin was from Calbiochem (San Diego, CA); and purified Cdc2/cyclin B and Cdc2N50 were from New England BioLabs (Beverly, MA). The Cdc2N20 peptides were synthesized by the M.D. Anderson Cancer Center Peptide Core Facility. The EGF-like domain of heregulin was purified using Xpress System Protein Expression pRSET (Invitrogen, Carlsbad, CA).

Cell Lines

The tet-off ErbB2 transfectants were generated by transfecting into MDA-MB-435 cells the pTet-off plasmid (Clontech, Palo Alto, CA)

expressing the tet-operator transactivator (tTA). The stable transfectants (435.tTA) were transfected again with PBI-EGFP-erbB2 vectors. ErbB2 was under the control of the tetracycline (tet)-inducible promoter that can be switched off in the presence of doxycycline. Stable transfectants (435.tet-off ErbB2) were selected by FACS sorting for EGFP-positive cells. Other cell lines used have been described (Yu et al., 1998).

IP, Immunoblotting, and Immunocomplex Kinase Assay

These were performed as described (Yu et al., 1998). Nonradioactive signals were quantitated by Alpha Imager 2000 (Alpha Innotech, San Leandro, CA). Radioactive signals were quantitated by PhosphorImager (Molecular Dynamics, Sunnyvale, CA).

Double Immunofluorescence Staining

Cells were fixed in 3% paraformaldehyde in PBS for 20 min at RT, washed with PBS, and blocked in PBS with 1 M glycine (pH 8.5) for 5 min. Samples were permeabilized with 0.3% Triton-X100/PBS for 10 min at RT and incubated with primary antibodies overnight at 4°C. Cells were washed and incubated with fluorophore-labeled secondary antibodies. Cell nuclei were stained with DAPI. Slides were examined with a Nikon ECLIPSE E400 microscope and photographed ($\times 1000$) with a Sensys digital camera (Photometrics Ltd.). The haze of the images was removed using the 2D deconvolution function in the MetaMorph Imaging System (Universal Imaging, PA).

Cdc25C Tyrosine Phosphatase Assay

Cell lysates (300 μ g) were precipitated with 1 μ g anti-Cdc25C antibody or IgG. Precipitates were mixed with 120 ng phosphorylated Cdc2/cyclin B1 complex in 50 μ l reaction buffer (20 mM Tris-HCl [pH 7.5], 5 mM MgCl₂, 1 mM ATP, 10 mM EDTA, and 10 mM DTT). The mixture was incubated for 0 or 30 min at 25°C and stopped by boiling in SDS sample buffer. Dephosphorylation of Cdc2-Y15 was analyzed by Western blotting with Cdc2-Y15-p antibody.

In Vitro Binding Assay

His-ErbB2KD^K, His-ErbB2KD^M, and His-ErbB2ECD constructs were generated by inserting the DNA sequence corresponding to the kinase domain (wt or K753M) or extracellular domain of ErbB2 into the pRESTc containing a His-tag (Invitrogen). Proteins expressed in *E. coli* were purified by affinity chromatography using Ni-NTA agarose (Qiagen, Valencia, CA). Cells were lysed with IP buffer, and cell lysates were incubated at 4°C with Cdc2 antibody or IgG and protein A agarose. The precipitates were washed and incubated with His-ErbB2KD^K, His-ErbB2KD^M, or His-ErbB2ECD. Following three washes, immunocomplexes were analyzed by immunoblotting. Alternatively, GST-Cdc2N50 and His-ErbB2KD^K or His-ErbB2ECD were mixed and precipitated with antibodies against GST-tag, His-tag, or IgG. Protein G agarose was added to the mixture and incubated for 2 hr. The precipitates were washed and immunoblotted with antibodies against GST-tag and His-tag.

In Vitro Kinase Assays

His-ErbB2KD^K or His-ErbB2KD^M proteins (30 ng to 1 μ g) were mixed with GST-Cdc2N50, GST-Cdc2, purified Cdc2/cyclin B1 complexes, GST-Grb2, or GST substrates. The kinase assay was performed as described (Yu et al., 1998).

Phosphoamino Acid Analysis

These were performed as described (Liu et al., 1996).

Synchronization Procedures

Cells were arrested in G₀/G₁ by serum starvation for 48 hr. For synchronization at the G₁/S, cells were incubated with 4 mM thymidine for 20 hr and washed with medium. MDA-MB-435 cells were released from the thymidine block with 10% FBS medium for 12 hr. 435.eB cells were released for 17 hr. Thymidine was added to the culture for an additional 20 hr. To synchronize in M phase, cells were grown in culture medium containing 0.4 μ g/ml nocodazole (Sigma) for 10 hr. Cells with rounded mitotic morphology were detached and collected by centrifugation.

Mitotic Index Measurement

Asynchronous or synchronized cells were treated with taxol (0.02 μ M), collected at different times, stained with Giemsa, and the number of cells in metaphase was counted under a microscope.

DNA Fragmentation Assays and Flow Cytometry Analyses

These were performed as described (Yu et al., 1998).

In Situ Apoptosis Detection

HA-tagged Cdc2-Y15F mutant was cloned into a pcDNA3 vector (Invitrogen). The 435.eB cells were transiently transfected with p-CGN-HA or Cdc2-Y15F-HA vectors. After 24 hr, cells were treated with or without 0.05 μ M taxol for another 21 hr. Cells were fixed in 1% paraformaldehyde in PBS, dried on a slide, and apoptosis was detected using Apoptag in situ cell death detection kit (Intergen, Purchase, NY). Slides were examined with a Nikon ECLIPSE E400 and photographed ($\times 400$) with a Sensys digital camera.

Breast Tumor and Normal Tissue Specimens

Breast tumors and adjacent normal breast tissues were obtained from patients who had undergone mastectomies at M.D. Anderson Cancer Center. Tumor and normal tissue were confirmed by pathologists, and samples were immediately frozen until use.

Acknowledgments

We thank J.W. Harper, D.-H. Yan, J. Yao, S. Sellappan, W. Hittelman, W. Klein, and K. Klos for reagents, suggestions, computer artworks, and manuscript reading. The research was supported by NIH grants P30-CA16672 (MDACC) and NIH 2R01-CA60488, USAMRMC DAMD17-99-1-9271, DAMD17-01-1-0361, and the M.D. Anderson BCRP Fund (D.Y.).

Received: February 22, 2000

Revised: March 8, 2002

References

- Akiyama, T., Matsuda, S., Namba, Y., Saito, T., Toyoshima, K., and Yamamoto, T. (1991). The transforming potential of the c-erbB-2 protein is regulated by its autophosphorylation at the carboxyl-terminal domain. *Mol. Cell. Biol.* 11, 833-842.
- Carraway, K.L., III, Soltoff, S.P., Diamonti, A.J., and Cantley, L.C. (1995). Heregulin stimulates mitogenesis and phosphatidylinositol 3-kinase in mouse fibroblasts transfected with erbB2/neu and erbB3. *J. Biol. Chem.* 270, 7111-7116.
- Coleman, T.R., and Dunphy, W.G. (1994). Cdc2 regulatory factors. *Curr. Opin. Cell Biol.* 6, 877-882.
- Darzynkiewicz, Z., Bruno, S., Del Bino, G., Gorczyca, W., Hotz, M.A., Lassota, P., and Traganos, F. (1992). Features of apoptotic cells measured by flow cytometry. *Cytometry* 13, 795-808.
- Dulic, V., Stein, G.H., Far, D.F., and Reed, S.I. (1998). Nuclear accumulation of p21^{cip1} at the onset of mitosis: a role at the G2/M-phase transition. *Mol. Cell. Biol.* 18, 546-557.
- Gao, C.Y., and Zelenka, P.S. (1995). Induction of cyclin B and H1 kinase activity in apoptotic PC12 cells. *Exp. Cell Res.* 219, 612-618.
- Gautier, J., Solomon, M.J., Booher, R.N., Bazan, J.F., and Kirschner, M.W. (1991). Cdc25 is a specific tyrosine phosphatase that directly activates p34^{cdc2}. *Cell* 67, 197-211.
- Harper, J.W., and Elledge, S.J. (1998). The role of Cdk7 in CAK function, a retro-retrospective. *Genes Dev.* 12, 285-289.
- Heald, R., McLoughlin, M., and McKeon, F. (1993). Human wee1 maintains mitotic timing by protecting the nucleus from cytoplasmically activated cdc2 kinase. *Cell* 74, 463-474.
- Krek, W., and Nigg, E.A. (1991). Differential phosphorylation of vertebrate p34^{cdc2} kinase at the G1/S and G2/M transitions of the cell cycle: identification of major phosphorylation sites. *EMBO J.* 10, 305-316.
- Lane, H.A., Beuvink, I., Motoyama, A.B., Daly, J.M., Neve, R.M., and Hynes, N.E. (2000). ErbB2 potentiates breast tumor proliferation through modulation of p27^{Kip1}-Cdk2 complex formation. Receptor

overexpression does not determine growth dependency. *Mol. Cell. Biol.* 20, 3210–3223.

Li, S., Couvillion, A.D., Brasher, B.B., and Van Etten, R.A. (2001). Tyrosine phosphorylation of Grb2 by Bcr/Abl and epidermal growth factor receptor: a novel regulatory mechanism for tyrosine kinase signaling. *EMBO J.* 20, 6793–6804.

Liu, J., Wu, Y., Ma, G.Z., Lu, D., Haataja, L., Heisterkamp, N., Groffen, J., and Arlinghaus, R.B. (1996). Inhibition of Bcr serine kinase by tyrosine phosphorylation. *Mol. Cell. Biol.* 16, 998–1005.

Liu, F., Stanton, J.J., Wu, Z., and Piwnica-Worms, H. (1997). The human Myt1 kinase preferentially phosphorylates Cdc2 on threonine 14 and localizes to the endoplasmic reticulum and Golgi complex. *Mol. Cell. Biol.* 17, 571–583.

Maller, J.L., and Smith, D.S. (1985). Two-dimensional polyacrylamide gel analysis of changes in protein phosphorylation during maturation of *Xenopus* oocytes. *Dev. Biol.* 109, 150–156.

Niculescu, A.B.I., Chen, X., Smeets, M., Hengst, L., Prives, C., and Reed, S.I. (1998). Effects of p21^{Cip1/Waf1} at both the G₁/S and the G₂/M cell cycle transitions: pRb is a critical determinant in blocking DNA replication and in preventing endoreduplication. *Mol. Cell. Biol.* 18, 629–643.

Norbury, C., and Nurse, P. (1992). Animal cell cycles and their control. *Annu. Rev. Biochem.* 61, 441–470.

Nurse, P. (1990). Universal control mechanism regulating onset of M-phase. *Nature* 344, 503–508.

Nurse, P. (1997). Checkpoint pathways come of age. *Cell* 91, 865–867.

Nurse, P. (2000). A long Twentieth Century of the cell cycle and beyond. *Cell* 100, 71–78.

Ogg, S., Gabrielli, B., and Piwnica-Worms, H. (1994). Purification of a serine kinase that associates with and phosphorylates human cdc25C on serine 216. *J. Biol. Chem.* 269, 30461–30469.

Parker, L.L., and Piwnica-Worms, H. (1992). Inactivation of the p34^{cdc2}-cyclin B complex by the human Wee1 tyrosine kinase. *Science* 257, 1955–1957.

Shepard, H.M., Lewis, G.D., Sarup, J.C., Fendly, B.M., Maneval, D., Mordenti, J., Figari, I., Kotts, C.E., Palladino, M.A., Jr., Ullrich, A., et al. (1991). Monoclonal antibody therapy of human cancer: taking the HER2 protooncogene to the clinic. *J. Clin. Immunol.* 11, 117–127.

Slamon, D.J., Clark, G.M., Wong, S.G., Levin, W.J., Ullrich, A., and McGuire, W.L. (1987). Human breast cancer: correlation of relapse and survival with amplification of the HER-2/*neu* oncogene. *Science* 235, 177–182.

Slamon, D.J., Leyland-Jones, B., Shak, S., Fuchs, H., Paton, V., Bajamonde, A., Fleming, T., Eiermann, W., Wolter, J., Pegram, M., et al. (2001). Use of chemotherapy plus a monoclonal antibody against HER2 for metastatic breast cancer that overexpresses HER2. *N. Engl. J. Med.* 344, 783–792.

Xie, Y., and Hung, M.-C. (1994). Nuclear localization of p185^{neu} tyrosine kinase and its association with transcriptional transactivation. *Biochem. Biophys. Res. Commun.* 203, 1589–1598.

Yamamoto, T., Ikawa, S., Akiyama, T., Semba, K., Nomura, N., Miyajima, N., Saito, T., and Toyoshima, K. (1986). Similarity of protein encoded by the human *c-erbB-2* gene to epidermal growth factor. *Nature* 319, 230–234.

Yu, D., and Hung, M.-C. (2000). Overexpression of ErbB2 in cancer and ErbB2 targeting strategies. *Oncogene* 19, 6115–6121.

Yu, D., Liu, B., Tan, M., Li, J., Wang, S.-S., and Hung, M.-C. (1996). Overexpression of *c-erbB-2/neu* in breast cancer cells confers increased resistance to Taxol via *mdr-1*-independent mechanisms. *Oncogene* 13, 1359–1365.

Yu, D., Jing, T., Liu, B., Yao, J., Tan, M., McDonnell, T.J., and Hung, M.-C. (1998). Overexpression of ErbB2 blocks Taxol-induced apoptosis by upregulation of p21^{Cip1}, which inhibits p34^{cdc2} kinase. *Mol. Cell* 2, 581–591.

Zhang, L., Chang, C.J., Bacus, S.S., and Hung, M.-C. (1995). Suppressed transformation and induced differentiation of HER-2/*neu*-overexpressing breast cancer cells by emodin. *Cancer Res.* 55, 3890–3896.

β -catenin interacts with and inhibits NF- κ B in human colon and breast cancers

Jiong Deng², Stephanie A. Miller², Hong-Ying Wang, Weiya Xia, Yong Wen, Binhua P. Zhou, Yan Li, Shiaw-Yih Lin, and Mien-Chie Hung¹

Department of Molecular and Cellular Oncology, The University of Texas M. D. Anderson Cancer Center, Houston, Texas 77030 USA.

¹Correspondence: mhung@mdanderson.org

²The first two authors contributed equally to this work.

SIGNIFICANCE

β -catenin is known to play two important functions, as an E-cadherin-associated protein in cell-cell adhesion, and as a transcriptional activator, through its interaction with TCF, in Wnt signaling. In this study, we identified a novel role of β -catenin, as an inhibitor of NF- κ B. β -catenin exerts this function through physical interaction, which is independent of TCF mediated transcription. Importantly, β -catenin can repress expression of NF- κ B target gene Fas. As deregulated β -catenin and downregulation of Fas play a critical role in tumor progression, the function identified in this study reveals a new direction for understanding the oncogenic roles of β -catenin.

Summary

β -catenin plays an important role in development and homeostasis. Deregulated β -catenin is involved in oncogenesis. In this study, we found that β -catenin can physically complex with NF- κ B resulting in a reduction of NF- κ B DNA-binding, transactivation activity, and target gene expression. Repressed NF- κ B activity is found in human colon cancer cells in which β -catenin is activated. Importantly, activated β -catenin was found to inhibit the expression of NF- κ B target genes including Fas and TRAF1. Furthermore a strong inverse correlation was identified between the expression levels of β -catenin and Fas in colon and breast tumor tissues, suggesting that β -catenin regulates NF- κ B and its targets *in vivo*.

Thus β -catenin may play an important role in oncogenesis through the cross regulation of NF- κ B.

Introduction

β -catenin plays two important roles in cells, as a protein associated with E-cadherin in cell-cell adhesion (Ben-Ze'ev and Geiger, 1998) and as a transcriptional activator in Wnt signaling (Willert and Nusse, 1998). Wnt signaling via β -catenin plays a central role in development and homeostasis (Polakis, 2000). A critical control of this pathway is the level of cytosolic β -catenin, which determines the activation of Wnt responsive genes. Without stimulation, β -catenin is degraded by the ubiquitin proteasome pathway, which depends upon β -catenin phosphorylation (Orford et al., 1997). The phosphorylation of β -catenin occurs in a multiprotein complex composed of tumor suppressor proteins adenomatous polyposis coli (APC), Axin, and glycogen synthase kinase-3 (GSK-3). In this complex, GSK-3 phosphorylates the N-terminal region of β -catenin, marking β -catenin for ubiquitination-dependent proteolysis (Kikuchi, 1999). Wnt signaling inhibits β -catenin phosphorylation, thus inducing the accumulation of cytosolic β -catenin, which then associates with the TCF/LEF family of transcription factors to activate Wnt/ β -catenin-responsive genes (Behrens et al., 1998). Thus, β -catenin phosphorylation controls β -catenin protein level and Wnt signaling.

Defects in Wnt signaling play a major role in human cancers (Korinek et al., 1997; Morin et al., 1997). Inactive mutations of the APC tumor suppressor gene, which is

the predominant mechanism leading to β -catenin deregulation, has been reported in approximately 70-80% of colorectal cancers and a fraction of other types of cancers (Kinzler and Vogelstein, 1996). Mutations in the β -catenin (CTNNB1) gene sequences encoding the crucial GSK-3 β phosphorylation sites in β -catenin's N-terminal domain have been found in about 10% colorectal cancer as well as many other different cancer types (Polakis, 2000). The fact that APC mutations and oncogenic β -catenin mutations are mutually exclusive in colon cancer suggests that the major critical consequence of these mutations is the elevation of β -catenin levels in the cytoplasm and nucleus. Deregulation of β -catenin leads to constitutive formation of the β -catenin/TCF complex and altered expression of TCF target genes. Wnt/TCF target genes in cancer cells, which likely cooperate in effecting neoplastic transformation, include c-Myc (He et al., 1998), cyclin D1 (Tetsu and McCormick, 1999), and MMP-7 (matrix metalloproteinase 7/matrilysin) (Crawford et al., 1999).

The transcriptional factor NF- κ B is another important signal transduction pathway that participates in the induction of a wide variety of cellular genes involved in immunity, inflammation, and regulation of apoptosis (Bours et al., 2000; Ghosh et al., 1998; Gilmore et al., 1996; Wang et al., 1999). The active complex of NF- κ B is composed of two subunits, p65 and p50. Binding sites for NF- κ B are present in the promoter region of many genes such as those encoding cell adhesion molecules, cytokines and growth factors. NF- κ B exists in the cytosol of resting cells bound to inhibitory I κ B- α proteins (Baeuerle and Baltimore, 1988). Stimulation with specific inducers, such as TNF or LPS, activates the I κ B kinase (IKK) complex that phosphorylates I κ B- α , triggering its degradation by the proteasome and allowing free

NF- κ B to translocate to the nucleus and activate gene expression (Gumbiner, 1995).

High levels of NF- κ B activity have been shown in diverse solid tumor-derived cell lines, which is associated with increased resistance to apoptosis induced by TNF and a variety of anti-cancer reagents (Bours et al., 2000). However, NF- κ B plays a dual role in regulation of apoptosis (Bours et al., 2000). NF- κ B has been also shown to be essential for Fas expression, a pro-apoptotic molecule (Chan et al., 1999; Zheng et al., 2001), and to be required for p53 mediated apoptosis under some circumstances (Ryan et al., 2000).

Fas (CD95/APO-1) is a cell surface “death receptor” belonging to the tumor necrosis factor receptor (TNFR) family. Fas is constitutively expressed in normal colon epithelial cells which are sensitive to Fas-mediated apoptosis. Fas is downregulated in the majority of colon carcinomas, representing a mechanism for cancer cells to escape lymphocyte-mediated immune surveillance (O'Connell et al., 2000). NF- κ B RelA (p65) has been shown to be essential for induction of Fas expression although strong induction of Fas expression requires combination of multiple cytokines or mitogens (Ouaaz et al., 1999). Thus, in response to TNF- α induced apoptosis, NF- κ B functions as an anti-apoptotic molecule. However, NF- κ B is required for Fas expression and therefore has a positive role in Fas induced apoptosis. This represents a dual role of NF- κ B in regulation of normal tissue homeostasis.

Recently, GSK-3 β has been shown to be required for NF- κ B activation (Hoeflich et al., 2000). As β -catenin is a major substrate of GSK-3 β , it raises an interesting possibility that β -catenin might serve as a mediator for the cross-regulation between these two pathways. In this study, we found that β -catenin can physically interact with NF- κ B

and inhibit its activity. Additionally, suppressed NF- κ B activity and NF- κ B target gene expression can be found in β -catenin-high expressing cancer cells. Importantly, β -catenin was found to inhibit Fas expression through repression of NF- κ B. Furthermore, there is a strong inverse correlation of β -catenin and Fas expression in human breast and colon tumor tissues. Thus, this study provides a mechanistic linkage between two important pathways critical for oncogenesis, and also provides a novel mechanism for β -catenin-mediated tumor progression.

Results

β -catenin inhibits NF- κ B activity

To investigate the potential effect of β -catenin on NF- κ B activity, we first examined the effects of β -catenin on a NF- κ B-driven luciferase reporter that can be activated by either p65 or TNF. Co-transfection of human epithelial kidney (HEK) 293 cells with a fixed dose of p65 and increasing doses of either wild type β -catenin or active mutant β -cateninS37A (Orford et al., 1997) results in a dose dependent suppression of luciferase activity (Fig. 1A), suggesting that β -catenin inhibits p65 transcriptional activity. β -Catenin also inhibited the basal level κ B-luciferase (in the absence of exogenous p65) to a lesser extent, probably due to suppression of endogenous p65 activity (data not shown). Likewise, TNF-induced NF- κ B activity was also suppressed in 293- β -catenin A cells (Fig. 1B), 293 cells stably transfected with β -cateninS45Y (another

active mutant) (Lin et al., 2000). These observations indicate that β -catenin can inhibit NF- κ B transcriptional activity.

To determine whether the suppression of NF- κ B transactivation is due to an effect on NF- κ B DNA-binding, we performed an electrophoretic mobility shift assay (EMSA). We noticed that both the basal level (Fig. 1C, Lanes 1 and 8) and the TNF-induced level of DNA-binding (Fig. 1C, lanes 2-3 and 9-10) were significantly reduced in the 293- β -catenin A cells as compared to the parental cells. Quantification of the bands shows about 3-5-fold suppression (data not shown). Similar effects were observed with another stable transfectant, 293- β -catenin B cells (data not shown). The inhibition of NF- κ B by β -catenin is specific since the DNA-binding of Oct-1, another transcription factor used as an internal control, was not inhibited (Fig. 1C, bottom). Thus β -catenin has an inhibitory effect on NF- κ B DNA-binding activity.

NF- κ B is known to inhibit TNF-induced apoptosis. To determine the effect of β -catenin on this function of NF- κ B, we examined its effect in Saos-2 cells, which are sensitive to TNF-induced apoptosis (Ryan et al., 2000). We transfected Saos-2 cells with β -catenin and/or β -catenin plus p65, and then examined the survival cells after TNF treatment. We found that β -catenin enhanced TNF-induced cell death (Fig. 1D, lane 3 compared to lane 2). Furthermore, the p65-mediated repression of TNF induced cell death (Fig. 1D, lane 4 compared to lane 2) was derepressed by β -catenin (Fig. 1D lane 5 compared to lane 4) or β -catenin-mediated sensitivity to TNF was reduced by p65 (Fig. 1D, lane 5 compared to lane 3), suggesting β -catenin-mediated effect is through the NF- κ B pathway. Thus, β -catenin is able to exert inhibitory effect on NF- κ B.

β -catenin is known to function as a co-transcription factor for TCF4-directed transcription (Korinek et al., 1997). To determine whether TCF4 signaling is involved, we examined the effect of a dominant negative mutant TCF4 (dnTCF4) (Morin et al., 1997) on β -catenin-mediated inhibition of NF- κ B. Using a co-transfection assay, we found that although dnTCF4 abrogated β -catenin-mediated activation of TOP, a reporter known to be activated by the β -catenin/TCF4 pathway (Korinek et al., 1997) (Fig. 1E right), it did not affect either β -catenin-mediated inhibition on NF- κ B-driven reporter (Fig. 1E, left) or p65-stimulated NF- κ B reporter (data not shown). Similarly, dnTCF4 was not able to block β -catenin mediated-sensitivity in Saos-2 cells (data not shown). This indicates that β -catenin-mediated inhibition of NF- κ B does not go through the β -catenin/TCF4 signaling pathway.

I κ B- α is a major regulator of NF- κ B. To determine whether I κ B- α is involved in this regulation, we examined the effect of β -catenin on I κ B- α regulation by immunoblot. We found that overexpression of β -catenin did not effect I κ B- α regulation since there was no difference in either the phosphorylation or the degradation of I κ B- α between the 293 cells and the 293- β -catenin cells following TNF treatment (Fig. 1F). Therefore the inhibition of NF- κ B activity by β -catenin occurs in an I κ B- α and TCF4-independent manner.

β -Catenin complexes with NF- κ B

To examine the possibility that β -catenin may inhibit NF- κ B through physical interaction, we tested whether β -catenin and NF- κ B can form a complex. By a co-immunoprecipitation (IP) assay we found that both p65 and p50 were able to form a complex with β -catenin, either endogenous β -catenin in the 293 vector cells, or stably expressed β -catenin in the 293- β -catenin A and B cells (Fig. 2A). This interaction is independent of I κ B- α as it occurred regardless of TNF treatment, which reduced the binding of I κ B- α to NF- κ B due to I κ B- α degradation (Baeuerle and Baltimore, 1988) (Fig. 2A). Expression of β -catenin does not change the protein levels of p65, p50 (Fig. 2A) or I κ B- α (Fig. 1F). The interaction was also observed in MCF-7 cells, a breast cancer cell line, suggesting the interaction as a general phenomenon (data not shown). To determine whether β -catenin and NF- κ B can directly form a complex, we translated p65 and p50 *in vitro*, and mixed them with GST- β -catenin protein. By pulling down the GST- β -catenin-interacting proteins using glutathione-agarose, we found that GST- β -catenin does not interact with p65 or p50 alone (Fig. 2B). However, in presence of cell lysate, both *in vitro* translated, exogenous p65 and p50 were able to bind β -catenin (Fig. 2C-D). This interaction did not occur when the endogenous p65- or p50-depleted cell lysate were used (Fig 2C-D, insert), suggesting that additional factors that associate with endogenous p65 or p50 are required for the exogenous p65 and p50 to interact with β -catenin. The *in vitro* translated p65 and p50 are in natural form as a p65 antibody can bring down both exogenous p65 and p50 (Fig. 2C). The GST- β -catenin is also in natural form since it can bring down TCF4 protein (Fig. 2D). Thus, β -catenin is indeed able to complex with p65 and p50 although additional cellular factors are required.

Since β -catenin physically associates with NF- κ B components, we also asked whether β -catenin is directly involved in the NF- κ B-DNA complex. However, a supershift assay by EMSA does not support this notion, as the β -catenin antibody does not effect the migration of the NF- κ B-DNA complex (Fig. 1C, lanes 7 and 13). Another molecule, p300, known to form complex with both NF- κ B (Gerritsen et al., 1997; Perkins et al., 1997) and β -catenin (Hecht et al., 2000; Miyagishi et al., 2000; Sun et al., 2000) also does not seem to be involved in as there is no effect in the DNA-binding with p300 antibody (Fig. 1D lanes 6 and 12). Thus, β -catenin may interact with NF- κ B and disrupt the ability of NF- κ B to bind to the DNA.

NF- κ B is suppressed in colon cancer cells

β -catenin is frequently activated in colon cancer cells (Korinek et al., 1997; Morin et al., 1997). As β -catenin inhibits NF- κ B, we asked whether NF- κ B activity could also be reduced in colon cancer cells in which β -catenin is activated. We examined four colon cancer cell lines, three of which have a high level of β -catenin, HCT116, DLD-1, and SW480, while one has a low level of β -catenin, RKO (Fig. 3A). We found that TNF-induced NF- κ B DNA-binding activity was dramatically lower in high β -catenin expressing cells (Fig. 3B, top, lanes 3-8), compared with that in low β -catenin expressing cells (Fig. 3B, top, lanes 1-2). The suppression is specific since there was no significant difference in the control, Oct-1, DNA-binding (Fig. 3B, bottom). Similarly, NF- κ B transcriptional activity in response to TNF, as measured by a NF- κ B-driven luciferase assay, was also lower in the high β -catenin expressing colon cancer cells (Fig. 3C). The reduced NF- κ B activity appears to correlate well with the increased β -catenin expression

since the other NF- κ B family proteins (p65, p50, and I κ B- α) protein levels are similar among these cells (Fig. 3A). To determine whether the downstream targets of NF- κ B were also affected, we also examined the expression of TRAF1, a downstream target gene of NF- κ B (Wang et al., 1998), in response to TNF. Consistent with DNA-binding activity and NF- κ B driven reporter, TNF treatment induced a significant amount of TRAF1 expression in RKO cells in a dose (data not shown) and time dependent manner (Fig 3D). Contrarily, TNF treatment failed to induce TRAF1 expression in HCT116 cells (Fig. 3D), and failed to further enhance TRAF1 expression in DLD-1 and SW480 cells although there was a basal level of TRAF1 expression in these two cells lines (data not shown). To determine whether the effect was indeed due to β -catenin, we further characterized the role of β -catenin on NF- κ B in RKO and HCT116 cells by both overexpression and depletion systems. First, we established RKO- β -cateninS37A stable transfectant cells and then examined TNF-induced TRAF1 expression. We found TRAF1 expression was greatly inhibited in these stable transfectant cells (Fig. 3E). Moreover, TNF induced NF- κ B driven reporter (Fig. 3F), NF- κ B DNA-binding (data not shown) were also greatly inhibited. Thus, overexpression of β -catenin is able to inhibit NF- κ B activity and its downstream target gene expression.

Next we asked whether β -catenin is required for NF- κ B activity. To this end, we characterized the effects of depletion of β -catenin in β -catenin-overexpressing cells, HCT116, which exhibits a high level of β -catenin and suppressed NF- κ B activity (Fig. 3). HCT116 cells were sensitive to TNF-induced cell death as TNF treatment dramatically reduced survival cells (Fig 4A). Introduction of GFP-p65, but not GFP as

expected (Schmid et al., 2000), inhibited TNF-induced cell death, (Fig. 4A). Introduction of GFP-p65 also induced κ B-driven reporter (Fig. 4B) and TRAF1 expression (Fig. 4C). Thus p65 is able to activate its downstream target gene and induce resistance to TNF-mediated apoptosis, in HCT116 cells, which overexpress β -catenin. We then used RNA interference to deplete β -catenin in HCT116 cells and examined its effect on NF- κ B activities. We transfected small interfering RNA targeting β -catenin mRNA (siRNA- β -cat.) or non-specific siRNA (siRNA-NS) into HCT116 cells, and then examined the effect on NF- κ B activity and its downstream target gene expression. We found that treatment of HCT116 cells with siRNA- β -cat. but not siRNA-NS resulted in a reduced level of β -catenin, indicating depletion of β -catenin by siRNA method was effective (Fig. 4D). Importantly, TNF stimulation was able to induce the NF- κ B target gene TRAF1 expression in cells treated with siRNA- β -cat., but not in those treated with siRNA-NS (Fig. 4D). This result indicates that depletion of β -catenin by siRNA restored NF- κ B activation in response to TNF stimulation in the β -catenin overexpressing HCT116 cells, suggesting that suppressed NF- κ B is a result of β -catenin overexpression. This conclusion was further supported by EMSA analysis, in which NF- κ B DNA-binding activity was increased in the cells treated with siRNA- β -cat. as compared to cells treated with siRNA-NS after stimulation with TNF or TNF plus IFN- γ (Fig. 4E). The effect of siRNA- β -cat. on NF- κ B was specific since it did not affect the DNA binding activity of another transcription factor Oct-1 (Fig. 4E bottom). These results indicate that depletion of β -catenin in β -catenin high-expressing colon cancer cells can release the suppression on NF- κ B activity, and restore the inducible expression of NF- κ B target genes. Taken

together, the above observations indicate that β -catenin is able to exhibit an inhibitory effect on NF- κ B activity and its downstream target gene expression.

β -catenin inhibits Fas expression

To investigate the physiological relevance of this cross-regulation, we examined the relationship of β -catenin with another important NF- κ B-regulated gene Fas (CD95). Fas is a member of TNF receptor family and expressed at high level in normal colonic epithelial cells. In colon cancer cells and breast cancer cells, Fas was frequently found downregulated, which may contribute to resistance to Fas-mediated apoptosis (von Reyher et al., 1998) and was proposed to allow cancer cells to escape from lymphocyte-mediated immune surveillance (O'Connell et al., 2000). However, the mechanism of Fas downregulation is unclear. The p65 (RelA) subunit of NF- κ B is known to be required for Fas expression (Ouaaz et al., 1999). Since activation of β -catenin is also frequently found in colon and breast cancers (Morin et al., 1997; Lin et al., 2000), and β -catenin can inhibit NF- κ B activity, it raises an interesting possibility that β -catenin may inhibit NF- κ B activity and results in the downregulation of Fas in cancer cells, thus allowing cancer cells to escape Fas ligand-induced cell death by lymphocyte. To investigate this possibility, we wanted to confirm that NF- κ B is required for Fas expression by comparing Fas express level between MEF wild type and MEF p65^{-/-} cells. Fas expression level is much lower in p65 knockout MEF cells than in wild type MEF cells (Fig. 5A), indicating that the RelA subunit is indeed required for Fas expression. We then

compared the expression levels of β -catenin and Fas in a panel of human breast cancer cell lines by immunoblot. We found that there is an inverse relationship between the expression of β -catenin and that of Fas as well as TRAF1 (Fig. 5B). In HBL-100 and MDA-MB-231 cells in which β -catenin expression is low, the levels of Fas and TRAF1 expression are high (Fig 5B); whereas in BT474, 468 and MCF7 cells in which β -catenin expression level is relatively high, the levels of Fas and TRAF1 are low (Fig. 5B). This result implies that high-expression of β -catenin may be involved in downregulation of Fas as well as TRAF1 expression. To determine the regulatory relationship of β -catenin on Fas expression, we then examined the Fas expression in RKO and RKO- β -cat. cells. We found that the Fas expression level was much lower in RKO- β -cat. than in parental RKO cells (Fig. 5C, left). Moreover, with treatment of cells with anti-Fas antibody to stimulate Fas-mediated cell death, we found that RKO- β -cat. cells were more resistant to Fas antibody induced cell death than parental RKO cells (Fig. 5C, right), supporting the observation that Fas expression was downregulated in these cells (Fig. 5C, left). As the increased level of β -catenin in RKO- β -cat. cells can suppress NF- κ B activity (Fig. 3), we asked if the repressed Fas expression was due to suppression of NF- κ B in these cells. To this end, we transfected RKO- β -cat. cells with GFP-p65 or GFP, and measured the Fas expression on the GFP-positive cells using PE-labeled anti-Fas antibody by FACS analysis. We found that introduction of GFP-p65 increased Fas expression in the RKO- β -cat. cells (Fig. 5D), indicating that p65 derepresses β -catenin mediated Fas repression. This result also suggests that the repressed Fas expression in β -catenin stable transfectants is due to suppression of NF- κ B (Fig. 3E-F). Thus, β -catenin-mediated repression of Fas expression was at least partially due to an inhibitory effect on NF- κ B

pathway. Taken together, overexpression of β -catenin is able to downregulate Fas expression by inactivation of NF- κ B.

To further characterize the regulatory role of β -catenin on Fas expression, we then examined the effects of depletion of β -catenin on Fas expression in β -catenin-high expressing cancer cells. Transfection of HCT116 cells with siRNA- β -cat., which resulted in decreased β -catenin (Fig. 5E, left, top insert), was found to increase Fas expression, suggesting that β -catenin may suppress Fas expression in HCT116 cells (Fig. 5E, left bottom). The effect is specific since it was not observed in the cells transfected with siRNA-NS (Fig. 5E, left). To determine the biological consequence of this effect, we then examined Fas-mediated apoptosis in these cells. We treated siRNA- β -cat. or siRNA-NS transfected cells with anti-Fas antibody and measured Fas-mediated apoptosis by FACS analysis. Consistent with the result from Fas expression, anti-Fas antibody induced an increased apoptosis in cells transfected with siRNA- β -cat. as compared to the cells treated with siRNA-NS (Fig. 5E, right). This observation suggests that depletion of β -catenin in β -catenin high-expressing colon cancer cells restores the expression of Fas and increases the sensitivity of cells to Fas antibody-mediated apoptosis. As depletion of β -catenin resulted in both increased NF- κ B activity (Fig. 4D, E) and Fas expression in HCT116 cells (Fig 5E, left), we asked if repression of Fas expression by β -catenin overexpression is through NF- κ B pathway. We then introduced GFP-p65 into HCT116 cells and measured Fas expression in GFP-positive cells. We found that GFP-p65, but not GFP increased Fas expression in HCT116 cells (Fig. 5F), suggesting that repressed Fas expression is resulted from suppressed NF- κ B in these cells. Thus, inhibition of NF-

κ B by β -catenin was at least partially responsible for the suppressed Fas expression.

Taken together, depletion of β -catenin in high β -catenin expressing colon cancer cells can restore NF- κ B activity (Fig. 4D, E) and Fas expression (Fig 5E), and increase the sensitivity of Fas-mediated apoptosis (Fig. 5F).

Downregulation of Fas in primary cancer tissues

Activation of β -catenin has been reported in a number of cancers, such as colon cancer, and breast cancer (Polakis, 1999). To further investigate the potential cross-regulation of β -catenin on Fas expression *in vivo*, we then examined the relationship in primary cancer tissues. By immunohistochemical staining, we found a strong inverse correlation between the active β -catenin expression and the reduction of Fas expression (Fig. 6 and Table 1). In the tumor tissues, in which β -catenin expression is low and inactive (membrane), Fas expression is high (case 1 in Fig. 6); whereas in tumor tissues in which β -catenin expression is high and active (cytoplasmic and nuclear), Fas expression is low (case 2 in Fig. 6). It should be mentioned that the two images (top left and right, or bottom left and right) show adjacent spots of the same tumor tissue with antibodies against either Fas or β -catenin by immunohistochemical staining. This indicates that the activation of β -catenin correlates very well with suppression of Fas in the same tumor tissue area, which strongly suggests that activation of β -catenin is involved in the downregulation of Fas expression *in vivo*. Taken together, an inverse relationship was found between aberrant activation of β -catenin in colon cancers and downregulation of Fas expression *in vivo*, which suggests that downregulation of Fas might be involved in β -catenin-mediated tumor progression.

Discussion

In this study, we have shown that β -catenin can physically interact with NF- κ B (Fig. 2), and inhibit its activity (Fig. 1, 3, 4). Importantly, we have also shown that activation of β -catenin is involved in downregulation of Fas (Fig. 5), a NF- κ B-regulated gene product, suggesting a novel mechanism for β -catenin-mediated oncogenesis, namely, β -catenin inhibits NF- κ B activity, downregulating Fas expression, which may allows cancer cells to escape immune surveillance.

β -catenin inhibits NF- κ B through physical interaction, which is independent of regulation of the I κ B- α (Fig. 1F and 2A) and TCF4 signaling pathways (Fig.1E). Thus, in addition to acting as a transcriptional activator for TCF4 and androgen receptor (Yang et al., 2002), β -catenin is also able to act as an inhibitor participating in regulation of other signal transduction pathways. The *in vitro* protein interaction analysis indicates that the physical interaction between β -catenin and NF- κ B is indirect and an additional cellular protein is required (Fig. 2B-D). This implies that the interaction between β -catenin and NF- κ B may be subject to another level of regulation. Thus, identification of the interactive domain in β -catenin and the intermediate protein for this interaction, which requires further investigation, would be important for understanding the detailed mechanism of the cross-regulation by β -catenin on the NF- κ B pathway.

Inhibition of NF- κ B by β -catenin may provide a plausible mechanism for the observation from the GSK-3 β knockout study in which the GSK-3 β pathway has been shown to be required for NF- κ B activation (Hoeftlich et al., 2000). As β -catenin is a major downstream target of GSK-3 β , depletion of GSK-3 β may lead to an elevated β -catenin expression and suppressed NF- κ B activity. However, in the original study, there

was no evidence of β -catenin accumulation in GSK-3 β (-/-) cells. Although severe cell death was detected in the hepatocyte of the GSK-3 β (-/-) mice, it is not clear whether β -catenin might contribute to the hepatocyte apoptosis or it could be caused by other mechanisms in GSK-3 β (-/-) mice. In our study, we found that β -catenin can inhibit NF- κ B. In addition, inhibition of GSK-3 β with GSK-3 β inhibitors in human colon and breast cancer cell lines increased β -catenin and suppressed both basal and TNF-induced NF- κ B activity, suggesting that β -catenin can serve a mediator for inhibition of NF- κ B (data not shown). Taken together, our study strongly suggests that β -catenin is a major mediator for the cross-regulation of NF- κ B by the GSK-3 β pathway, although other mechanisms are not excluded.

β -catenin has been shown to be proapoptotic, which was independent of TCF4- and the transcriptional function of β -catenin (Kim et al., 2000). However the mechanism of this observation is not clear. Similarly, the proapoptotic activity of β -catenin has also been observed *in vivo*. It was shown that overexpression of an activated form of β -catenin in transgenic mice results in a 3-4 fold increase of apoptotic cells in the intestinal villi of transgenic mice (Romagnolo et al., 1999; Wong et al., 1998). The results of our study may provide a plausible mechanism for these observations. β -catenin is also implicated to be anti-apoptotic in a different system. A recent report demonstrates that Wnt-1, which inhibits GSK-3 β and increases β -catenin, can inhibit cellular sensitivity to two anti-cancer agents vincristine (VCR)- and vinblastine (VBL)-induced apoptosis

(Chen et al., 2001). However, this activity requires β -catenin/TCF-mediated transcription, suggesting a different pathway is involved.

NF- κ B has been shown to mediate inhibition of TNF- and other anti-cancer drug-induced apoptosis (Liu et al., 1996; Wang et al., 1996). Aberrant activation of NF- κ B has also been found in various types of cancers, which associates with malignant and apoptosis-resistant properties (Bours et al., 2000). In this study, we found that β -catenin inhibits NF- κ B. However, as NF- κ B exhibits a dual role in regulation of apoptosis and oncogenesis, the phenotypic effects or biological consequences of β -catenin activation may be dependent on the cellular context and/or combined with the activation of particular signaling pathways. For example, it has been recently shown that depletion of NF- κ B in the *rela* (NF- κ B) knockout mice results in a malignantly transformed phenotype of embryonic fibroblast cells regardless of increased sensitivity to TNF (Gapuzan et al., 2002). It should be mentioned that many proto-oncogenes, such as *ras* (Cheng and Meinkoth, 2001; Trent et al., 1996), *c-myc* (Eischen et al., 2001; Hsu et al., 1995) and *E2F-1* (Hunt et al., 1997; Macleod, 1999) have all been shown to have a proapoptotic activity when activated and/or over-expressed. As these genes also play a regulatory function in normal cells, association of a proliferative activity with proapoptotic activity may be normal for host to keep homeostasis. Thus, the association of proapoptotic and oncogenic activities by β -catenin may not be a surprise.

Fas is expressed in normal epithelial cells in colon and breast tissue, which are sensitive to Fas-induced apoptosis (von Reyher et al., 1998). This mechanism is important in maintaining the homeostasis of these tissues. However, Fas is

downregulated or lost in the majority of colon carcinomas, which usually lead to resistance to Fas-mediated apoptosis. Downregulation of Fas is suggested to be an important mechanism for cancer cells, especially in colon cancer, to escape Fas ligand-mediated immune surveillance (Butler et al., 1998). The mechanisms of Fas downregulation in different cancers is unclear. The promoter of the Fas gene contains two NF- κ B binding sites which are required for NF- κ B-mediated activation. However, NF- κ B activation may be required but not sufficient for Fas expression, as a concert of cytokines is required for strong induction of Fas expression (Chan et al., 1999; Ouaz et al., 1999). In this study, we demonstrated that β -catenin can inhibit NF- κ B which may limit Fas expression. This observation was demonstrated *in vitro* and strongly supported by analysis *in vivo*. By both overexpression and depletion systems, we have shown that β -catenin limits the expression of NF- κ B target Fas. Moreover, the expression level of Fas was found to inversely correlate with that of β -catenin in human breast cancer cell lines, and more importantly in primary tumor tissues. Thus, β -catenin may also be able to contribute to tumorigenicity through downregulation of Fas and/or prevention of Fas-mediated apoptosis, a novel mechanism for β -catenin-involved tumor progression. NF- κ B RelA (p65) has been shown to be essential but not sufficient for Fas expression in MEF cells. Other members of NF- κ B family, such as p50 and c-Rel, are also involved in the regulation of Fas expression (Zheng et al., 2001). Thus, a primary function of NF- κ B may be to promote Fas-induced cell death through the enhancement of Fas expression, rather than inhibit cell death through expression of survival genes (Zheng et al., 2001). It should be noted that RelA is required for Fas expression in MEF cells, although it is dispensable for Fas expression in T lymphocytes (Zheng et al., 2001), suggesting a cell type difference. Thus, the detailed mechanism remains to be investigated of how β -catenin affects Fas expression in human colon and/or breast cancers and the role of this function in β -catenin-mediated oncogenesis.

NF- κ B plays a dual role in regulating apoptosis. For example, NF- κ B has been shown to be required for p53-induced apoptosis and for induction of resistance to TNF-induced apoptosis (Ryan et al., 2000). It is likely that NF- κ B is required for induction of a subset of survival genes against TNFR-mediated apoptosis, as well as a subset of the genes essential for p53-induced apoptosis. In this study, we showed that β -catenin plays a dual role in regulating Fas- and TNFR-mediated apoptosis. Moreover, we have shown that this function may go through the NF- κ B pathway. The results of this study suggest that NF- κ B is at least partially required for β -catenin-mediated dual regulation of both Fas- and TNFR-mediated apoptosis. In fact, depletion of β -catenin in high β -catenin expressing colon cancer HCT116 cells did increase Fas expression and Fas-mediated apoptosis (Fig. 5E), whereas overexpression of β -catenin increased the sensitivity of Saos-2 cells to TNF-induced apoptosis (Fig. 1D). Because of the dual role in the regulation of apoptosis, disruption of Fas-mediated apoptosis may thus particularly be important for β -catenin-mediated oncogenesis in tissues, such as colon, in which the Fas pathway plays a major role in maintaining homeostasis. This possibility was strongly supported by the analysis *in vivo*, as an inverse relationship was identified between β -catenin and Fas expression in both human colon cancers and breast cancers. Because of the dual regulatory role on the outcome in cells, it is likely that the oncogenic role of β -catenin also requires the cooperation of specific oncogenic alterations during tumor progression. For example, deregulated β -catenin was found to cooperate with ras in cell transformation when ARF and p53 are inactively mutated (Damalas et al., 2001). Thus, the biological outcome of the dual role of β -catenin on cell biology, which goes through NF- κ B, may be dependent on cellular context, and tissue environment.

In summary, we have shown that β -catenin can inhibit NF- κ B in an I κ B-independent and TCF-4-independent manner. β -catenin forms a complex with NF- κ B components (p65 and p50). β -catenin can inhibit NF- κ B transactivation, DNA binding

activity, and target gene expression. Importantly, activation of β -catenin inhibits expression of Fas, a NF- κ B target gene. Moreover, an inverse correlation between β -catenin and Fas expression was identified in both human colon and breast tumor tissues. Thus, the results of this study provide a novel mechanism for the role of β -catenin on tumor progression.

Experimental procedures

Cell Culture and Transfection assays

All cell lines were grown in Dulbecco's modified Eagle's medium/F12 (Life Technologies, Inc) supplemented with 10% fetal bovine serum. HEK 293 cells, human colon cancer cell lines SW480, DLD-1, HCT116, and RKO (Morin et al., 1997; Sasaki et al., 2000), breast cancer cell lines MDA-MB-231 and MCF-7, BT474, 468, and the immortalized breast cell line HBL100 were used. Transient transfections were performed with NF- κ B-driven-luciferase plasmid (κ B-luc.) as reporter, and p65, β -catenin, or active mutant β -cateninS37A (β -catS37A), APC or mutant APC as effectors. The ratio of effectors and reporter was as indicated. 293 β -cateninS45Y stable transfectants (293- β -cat A and B) were as described (Lin et al., 2000). The transfection agents LPD1 or SN liposomes were incubated with DNA in serum free media for 30 minutes before adding to cells and incubating for 3 hours. RKO stable transfectants were established by transfection with β -cateninS37A plasmid. Cell lysates for luciferase activity were collected 48 hours after transfection; cells were treated with TNF (10 ng/ml) 8 hours

before harvesting unless otherwise indicated. In all the experiments, the total DNA is kept constant by addition of the empty vector. Plasmid pRL-tk (Promega) was used as internal control in all transfection assays. Similar results were obtained when repeated with β -galactosidase as an internal control (data not shown). Cell viability was determined either by number of blue cells stained by β -gal or through trypan blue exclusion as indicated in figure legend. Error bars are the mean \pm standard error. Apoptosis induction via Fas pathway was performed by using anti-Fas antibody (CH11, Upstate) at 50 ng/ml for 24 hours.

Immunoprecipitation (IP) and Immunoblot

IP was performed with 2 μ g of antibodies against p65 or p50 (normal IgG as a negative control) in 1.0 mg whole lysate protein (TNF treatment was 30 minutes, at 10ng/ml). Samples were first pre-cleared with a non-specific IgG antibody. Pre-cleared lysates were then incubated with antibody either to p65 or p50 for 1 1/2 hours, then incubated overnight with protein G agarose. Samples were washed 4 times with phosphate buffered solution with 0.1% tween and then subjected to immunoblot as indicated. Cell lysates were separated by SDS/PAGE in a 10% acrylamide gel and transferred onto nitrocellulose membrane for immunoblot. Antibodies to p65 (A), p50 (C-19), I κ B- α (C-21), and TRAF1 (G-20, H132), GFP (FL) and Fas (c-20) were from Santa Cruz. Antibody to β -catenin was from BD Transduction Laboratories.

***In vitro* Translation and GST-pull down**

³⁵S-Met labeled p65 was *in vitro* translated from pBS-p65 (T7) using TNT T7 quick-coupled translation/transcription system (Promega). ³⁵S-Met labeled p50 proteins were *in vitro* translated from pBS-p105 (T3) using TNT T3 coupled reticulocyte lysate system (Promega). pBS-p105 plasmid was first digested with Best EII, which cut at site 1572 before use. Translation from this digested plasmid resulted in a protein product close to p50. *In vitro* translated proteins were mixed either with GST- β -catenin or GST (10 μ g) in presence or absence of whole or p65- or p50-depleted (by 3 times IP with excess antibody to p65 or p50) RKO cell lysate (100 μ g), for 2 hours at 4°C, then pulled down by glutathione-agarose, subjected to SDS-PAGE (10%), and autoradiography.

Electrophoresis mobility shift assay (EMSA)

Nuclear extracts from normal or TNF treated cells were used in EMSA with an oligonucleotide probe containing the NF- κ B-binding site as described (Zhou et al., 2000) or with the Oct-1-binding site as described (Hoeflich et al., 2000). Eighty-fold of cold wild type or mutant NF- κ B oligonucleotides were used for competition in the nuclear extracts of control or TNF-treated (15 min) 293 cells, doses are as indicated. Antibodies used for supershifting the complex were as indicated. Antibodies to p65 (A), p50 (C-19), p300 (C-20) and Oct-1 (C-21) for supershift were from Santa Cruz.

Flow Cytometry

Cells were harvested, washed once with PBS, and stained with PE-conjugated mouse anti-Fas (CD95) antibody (DX2) or normal IgG1 (Pharmigen) for 30 min at room temperature. Cells were then washed once with PBS, fixed in 2% paraformaldehyde, and

analyzed using Becton Dickinson flow cytometer. For cells transfected with GFP or GFP-p65, GFP positive cells were analyzed for PE intensity. The mean values of PE intensity minus the background (PE-labeled normal mouse IgG) were used as relative Fas protein expression level.

Immunohistochemical Staining

Tissue samples were deparrifinized and then subjected to a gradient of alcohol and washed five times. They were trypsinized in 0.05% trypsin in PBS and treated with 0.3% H₂O₂ in methanol. Then they were treated with 10% horse serum for 30 minutes. Sections were incubated with primary antibodies overnight, either β -catenin mAb (1:50 dilution), or Fas (Transduction Laboratoris, 1:100). Secondary antibodies Bio-Anti mouse and rabbit IgG (1:200 dilution) for 1 hour and then incubated with avidin biotin-peroxidase complex diluted in PBS and visualized with amino-ethyl carbazole chromogen stock solution. The Fisher exact test was used for statistical analysis with $p < 0.05$ as statistical significance for Fas expression.

Small interfering RNA transfection

Small interfering RNA (siRNA) duplex oligo (Dharmacon) targeting β -catenin mRNA (5' AAG UCC UGU AUG AGU GGG AAC 3') or a non specific duplex oligo as a negative control (5' AAC AGU CGC GUU UGC GAC UGG 3') (1.6 μ g / 35mm plate or 12.8 μ g/100mm plate) were transfected using Lipofectamine (Invitrogen) at a ratio of 1 μ g RNA to 3 μ l Lipofectamine. Experiments were performed on day 1 after transfection.

Acknowledgements:

This work was supported by NIH grants CA58880 and Ovarian SPORE grant P50 CA83639 (to M-C Hung), by a pre-doctoral fellowship from the US Army Breast Cancer Research Training Grant Program, Grant No. DAMD17-99-1-9264 (to Y. Wen), and Grant No. DAMD 17-02-1-0454 (to Y. Li). We would like to thank Dr. S.W. Byers for the wild type β -catenin and β -cateninS37A plasmids and Dr. H. Clevers for the dominant negative TCF4 (pcDNA3- Δ NTCF4), TOP and FOP plasmids, Dr. L.K Su for the APC expression plasmid. We would also like to thank Dr. A. G. de Herreros for the GST- β -catenin, Dr. P. J. Chiao for the pBS-p65 and pBS-p105 and MEF rela $-/-$ cells, and Dr. J. Schmid for the GFP-p65 plasmid.

References:

- Baeuerle, P. A., and Baltimore, D. (1988). I kappa B: a specific inhibitor of the NF-kappa B transcription factor, *Science* 242, 540-6.
- Behrens, J., Jerchow, B. A., Wurtele, M., Grimm, J., Asbrand, C., Wirtz, R., Kuhl, M., Wedlich, D., and Birchmeier, W. (1998). Functional interaction of an axin homolog, conductin, with beta- catenin, APC, and GSK3beta, *Science* 280, 596-9.

Ben-Ze'ev, A., and Geiger, B. (1998). Differential molecular interactions of beta-catenin and plakoglobin in adhesion, signaling and cancer, *Curr Opin Cell Biol* 10, 629-39.

Bours, V., Bentires-Alj, M., Hellin, A. C., Viatour, P., Robe, P., Delhalle, S., Benoit, V., and Merville, M. P. (2000). Nuclear factor-kappa B, cancer, and apoptosis, *Biochem Pharmacol* 60, 1085-9.

Butler, L. M., Hewett, P. J., Butler, W. J., and Cowled, P. A. (1998). Down-regulation of Fas gene expression in colon cancer is not a result of allelic loss or gene rearrangement, *Br J Cancer* 77, 1454-9.

Chan, H., Bartos, D. P., and Owen-Schaub, L. B. (1999). Activation-dependent transcriptional regulation of the human Fas promoter requires NF-kappaB p50-p65 recruitment, *Mol Cell Biol* 19, 2098-108.

Chen, S., Guttridge, D. C., You, Z., Zhang, Z., Fribley, A., Mayo, M. W., Kitajewski, J., and Wang, C. Y. (2001). Wnt-1 signaling inhibits apoptosis by activating beta-catenin/T cell factor-mediated transcription, *J Cell Biol* 152, 87-96.

Cheng, G., and Meinkoth, J. L. (2001). Enhanced sensitivity to apoptosis in Ras-transformed thyroid cells, *Oncogene* 20, 7334-41.

Crawford, H. C., Fingleton, B. M., Rudolph-Owen, L. A., Goss, K. J., Rubinfeld, B., Polakis, P., and Matrisian, L. M. (1999). The metalloproteinase matrilysin is a target of beta-catenin transactivation in intestinal tumors, *Oncogene* 18, 2883-91.

- Damalas, A., Kahan, S., Shtutman, M., Ben-Ze'ev, A., and Oren, M. (2001).
Deregulated beta-catenin induces a p53- and ARF-dependent growth arrest and
cooperates with Ras in transformation, *Embo J* 20, 4912-22.
- Eischen, C. M., Roussel, M. F., Korsmeyer, S. J., and Cleveland, J. L. (2001).
Bax loss impairs Myc-induced apoptosis and circumvents the selection of p53
mutations during Myc-mediated lymphomagenesis, *Mol Cell Biol* 21, 7653-62.
- Gapuzan, M. E., Yufit, P. V., and Gilmore, T. D. (2002). Immortalized embryonic
mouse fibroblasts lacking the RelA subunit of transcription factor NF-kappaB
have a malignantly transformed phenotype, *Oncogene* 21, 2484-92.
- Gerritsen, M. E., Williams, A. J., Neish, A. S., Moore, S., Shi, Y., and Collins, T.
(1997). CREB-binding protein/p300 are transcriptional coactivators of p65, *Proc
Natl Acad Sci U S A* 94, 2927-32.
- Ghosh, S., May, M. J., and Kopp, E. B. (1998). NF-kappa B and Rel proteins:
evolutionarily conserved mediators of immune responses, *Annu Rev Immunol* 16,
225-60.
- Gilmore, T. D., Koedood, M., Piffat, K. A., and White, D. W. (1996). Rel/NF-
kappaB/IkappaB proteins and cancer, *Oncogene* 13, 1367-78.
- Gumbiner, B. M. (1995). Signal transduction of beta-catenin, *Curr Opin Cell Biol*
7, 634-40.

He, T. C., Sparks, A. B., Rago, C., Hermeking, H., Zawel, L., da Costa, L. T., Morin, P. J., Vogelstein, B., and Kinzler, K. W. (1998). Identification of c-MYC as a target of the APC pathway, *Science* 281, 1509-12.

Hecht, A., Vleminckx, K., Stemmler, M. P., van Roy, F., and Kemler, R. (2000). The p300/CBP acetyltransferases function as transcriptional coactivators of beta-catenin in vertebrates, *Embo J* 19, 1839-50.

Hoeflich, K. P., Luo, J., Rubie, E. A., Tsao, M. S., Jin, O., and Woodgett, J. R. (2000). Requirement for glycogen synthase kinase-3beta in cell survival and NF-kappaB activation [see comments], *Nature* 406, 86-90.

Hsu, B., Marin, M. C., el-Naggar, A. K., Stephens, L. C., Brisbay, S., and McDonnell, T. J. (1995). Evidence that c-myc mediated apoptosis does not require wild-type p53 during lymphomagenesis, *Oncogene* 11, 175-9.

Hunt, K. K., Deng, J., Liu, T. J., Wilson-Heiner, M., Swisher, S. G., Clayman, G., and Hung, M. C. (1997). Adenovirus-mediated overexpression of the transcription factor E2F-1 induces apoptosis in human breast and ovarian carcinoma cell lines and does not require p53, *Cancer Res* 57, 4722-6.

Kikuchi, A. (1999). Roles of Axin in the Wnt signalling pathway, *Cell Signal* 11, 777-88.

Kim, K., Pang, K. M., Evans, M., and Hay, E. D. (2000). Overexpression of beta-catenin induces apoptosis independent of its transactivation function with LEF-1 or the involvement of major G1 cell cycle regulators, *Mol Biol Cell* 11, 3509-23.

Kinzler, K. W., and Vogelstein, B. (1996). Lessons from hereditary colorectal cancer, *Cell* 87, 159-70.

Korinek, V., Barker, N., Morin, P. J., van Wichen, D., de Weger, R., Kinzler, K. W., Vogelstein, B., and Clevers, H. (1997). Constitutive transcriptional activation by a beta-catenin-Tcf complex in APC^{-/-} colon carcinoma, *Science* 275, 1784-7.

Lin, S. Y., Xia, W., Wang, J. C., Kwong, K. Y., Spohn, B., Wen, Y., Pestell, R. G., and Hung, M. C. (2000). Beta-catenin, a novel prognostic marker for breast cancer: its roles in cyclin D1 expression and cancer progression, *Proc Natl Acad Sci U S A* 97, 4262-6.

Liu, Z. G., Hsu, H., Goeddel, D. V., and Karin, M. (1996). Dissection of TNF receptor 1 effector functions: JNK activation is not linked to apoptosis while NF-kappaB activation prevents cell death, *Cell* 87, 565-76.

Macleod, K. (1999). pRb and E2f-1 in mouse development and tumorigenesis, *Curr Opin Genet Dev* 9, 31-9.

Miyagishi, M., Fujii, R., Hatta, M., Yoshida, E., Araya, N., Nagafuchi, A., Ishihara, S., Nakajima, T., and Fukamizu, A. (2000). Regulation of Lef-mediated

transcription and p53-dependent pathway by associating beta-catenin with CBP/p300, *J Biol Chem* 275, 35170-5.

Morin, P. J., Sparks, A. B., Korinek, V., Barker, N., Clevers, H., Vogelstein, B., and Kinzler, K. W. (1997). Activation of beta-catenin-Tcf signaling in colon cancer by mutations in beta-catenin or APC, *Science* 275, 1787-90.

O'Connell, J., Bennett, M. W., Nally, K., Houston, A., O'Sullivan, G. C., and Shanahan, F. (2000). Altered mechanisms of apoptosis in colon cancer: Fas resistance and counterattack in the tumor-immune conflict, *Ann N Y Acad Sci* 910, 178-92; discussion 193-5.

Orford, K., Crockett, C., Jensen, J. P., Weissman, A. M., and Byers, S. W. (1997). Serine phosphorylation-regulated ubiquitination and degradation of beta-catenin, *J Biol Chem* 272, 24735-8.

Ouaaz, F., Li, M., and Beg, A. A. (1999). A critical role for the RelA subunit of nuclear factor kappaB in regulation of multiple immune-response genes and in Fas-induced cell death, *J Exp Med* 189, 999-1004.

Perkins, N. D., Felzien, L. K., Betts, J. C., Leung, K., Beach, D. H., and Nabel, G. J. (1997). Regulation of NF-kappaB by cyclin-dependent kinases associated with the p300 coactivator, *Science* 275, 523-7.

Polakis, P. (1999). The oncogenic activation of beta-catenin, *Curr Opin Genet Dev* 9, 15-21.

Polakis, P. (2000). Wnt signaling and cancer, *Genes Dev* 14, 1837-51.

Romagnolo, B., Berrebi, D., Saadi-Keddoucci, S., Porteu, A., Pichard, A. L., Peuchmaur, M., Vandewalle, A., Kahn, A., and Perret, C. (1999). Intestinal dysplasia and adenoma in transgenic mice after overexpression of an activated beta-catenin, *Cancer Res* 59, 3875-9.

Ryan, K. M., Ernst, M. K., Rice, N. R., and Vousden, K. H. (2000). Role of NF-kappaB in p53-mediated programmed cell death, *Nature* 404, 892-7.

Sasaki, T., Irie-Sasaki, J., Horie, Y., Bachmaier, K., Fata, J. E., Li, M., Suzuki, A., Bouchard, D., Ho, A., Redston, M., *et al.* (2000). Colorectal carcinomas in mice lacking the catalytic subunit of PI(3)Kgamma, *Nature* 406, 897-902.

Schmid, J. A., Birbach, A., Hofer-Warbinek, R., Pengg, M., Burner, U., Furtmuller, P. G., Binder, B. R., and de Martin, R. (2000). Dynamics of NF kappa B and Ikappa Balpha studied with green fluorescent protein (GFP) fusion proteins. Investigation of GFP-p65 binding to DNA by fluorescence resonance energy transfer, *J Biol Chem* 275, 17035-42.

Sun, Y., Kolligs, F. T., Hottiger, M. O., Mosavin, R., Fearon, E. R., and Nabel, G. J. (2000). Regulation of beta -catenin transformation by the p300 transcriptional coactivator, *Proc Natl Acad Sci U S A* 97, 12613-8.

Tetsu, O., and McCormick, F. (1999). Beta-catenin regulates expression of cyclin D1 in colon carcinoma cells, *Nature* 398, 422-6.

Trent, J. C., 2nd, McConkey, D. J., Loughlin, S. M., Harbison, M. T., Fernandez, A., and Ananthaswamy, H. N. (1996). Ras signaling in tumor necrosis factor-induced apoptosis, *Embo J* 15, 4497-505.

von Reyher, U., Strater, J., Kittstein, W., Gschwendt, M., Krammer, P. H., and Moller, P. (1998). Colon carcinoma cells use different mechanisms to escape CD95-mediated apoptosis, *Cancer Res* 58, 526-34.

Wang, C. Y., Mayo, M. W., and Baldwin, A. S., Jr. (1996). TNF- and cancer therapy-induced apoptosis: potentiation by inhibition of NF-kappaB, *Science* 274, 784-7.

Wang, C. Y., Mayo, M. W., Korneluk, R. G., Goeddel, D. V., and Baldwin, A. S., Jr. (1998). NF-kappaB antiapoptosis: induction of TRAF1 and TRAF2 and c-IAP1 and c-IAP2 to suppress caspase-8 activation, *Science* 281, 1680-3.

Wang, W., Abbruzzese, J. L., Evans, D. B., Larry, L., Cleary, K. R., and Chiao, P. J. (1999). The nuclear factor-kappa B RelA transcription factor is constitutively activated in human pancreatic adenocarcinoma cells, *Clin Cancer Res* 5, 119-27.

Willert, K., and Nusse, R. (1998). Beta-catenin: a key mediator of Wnt signaling, *Curr Opin Genet Dev* 8, 95-102.

Wong, M. H., Rubinfeld, B., and Gordon, J. I. (1998). Effects of forced expression of an NH2-terminal truncated beta-Catenin on mouse intestinal epithelial homeostasis, *J Cell Biol* 141, 765-77.

Yang, F., Li, X., Sharma, M., Sasaki, C. Y., Longo, D. L., Lim, B., and Sun, Z. (2002). Linking beta-catenin to androgen-signaling pathway, *J Biol Chem* 277, 11336-44.

Zheng, Y., Ouaaz, F., Bruzzo, P., Singh, V., Gerondakis, S., and Beg, A. A. (2001). NF-kappa B RelA (p65) is essential for TNF-alpha-induced fas expression but dispensable for both TCR-induced expression and activation-induced cell death, *J Immunol* 166, 4949-57.

Zhou, B. P., Hu, M. C., Miller, S. A., Yu, Z., Xia, W., Lin, S. Y., and Hung, M. C. (2000). HER-2/neu blocks tumor necrosis factor-induced apoptosis via the Akt/NF- kappaB pathway, *J Biol Chem* 275, 8027-31.

Figure Legends

Figure 1 β -catenin inhibits NF- κ B transcriptional and DNA-binding activities. **A:** 293 cells were transfected with κ B-luc. (0.1 μ g), p65 (0.2 μ g), β -catenin, or active mutant β -cateninS37A (β -cat.S37A) (0.6, 1.2, 1.8 μ g). **B:** 293 and 293 β -cateninS45Y stable transfectants (293- β -cat A) were transfected with κ B-luc (0.1 μ g), with or without treatment of TNF, basal levels was normalized to 100%. Insert shows β -catenin level by immunoblot. **C:** NF- κ B DNA-binding activity was measured by EMSA. Antibodies against p65, p50, p300 and β -catenin were used for supershifting the complex. Oct-1 DNA-binding activity by EMSA used as an internal control. **D:** Saos-2 cells were transfected with pcmv- β -gal (0.1 μ g), p65 (0.6 μ g) I κ B- α (0.6 μ g), β -catenin (0.6 μ g) or p65 plus β -catenin (0.6 μ g and 1.2 μ g) and then treated with TNF (10 ng/ml) for 24 hours. Percent Cell death was calculated from number of viable cells as compared to untreated. **E:** 293 cells were transfected with κ B-luc. (0.1 μ g, left) or TOP (0.1 μ g, right), p65 (0.2 μ g), β -catenin (0.6 μ g), and dnTCF4 (1.2 μ g). There was no effect by β -catenin or dnTCF4 on the mutant reporter FOP (data not shown). **F:** I κ B- α level by immunoblot with or without TNF (10 ng/ml) treatment. In all transfection experiments the total amount of DNA was kept constant with transfection of the empty vector.

Figure 2 β -catenin physically interacts with NF- κ B (p65 and p50). **A:** Immunoprecipitation (IP) was performed with antibodies against p65 or p50

(normal IgG as a negative control). The complexes were then subjected to immunoblot as indicated. **B:** *In vitro* translated p65 and p50 (³⁵S-Met labeled) were mixed with GST- β -catenin or GST alone, pulled down by glutathione-agarose, and subjected to SDS-PAGE. **C:** and **D:** *in vitro* translated p65 and p50 proteins were mixed with GST- β -catenin or GST in the presence of whole, or p65- or p50-depleted (by repeated IP) cell lysates (RKO), and analyzed as in (B), inserts show loaded protein.

Figure 3 Reduced NF- κ B activity in human colon cancer cells that express high level of β -catenin. **A:** Protein levels of β -catenin, p65, p50, and I κ B- α in colon cancer cell lines by immunoblot. **B:** Top, EMSA analysis of NF- κ B DNA-binding activity. TNF treatment was at 10 ng/ml for 15 minutes. Bottom, EMSA of Oct-1 used as an internal control. Lanes are the same as in NF- κ B gel shifting unless specified by antibody used as indicated. **C:** Colon cancer cell lines were transfected with κ B-luc. (1.0 μ g) and then treated with TNF (1 ng/ml, 9 h). **D:** and **E:** Immunoblot analysis of NF- κ B target gene TRAF1 (TNF concentration for E was 1 ng/ml). **F.** RKO and RKO- β -cat. cells were transfected with κ B-luc (0.3 μ g) and treated with TNF as above.

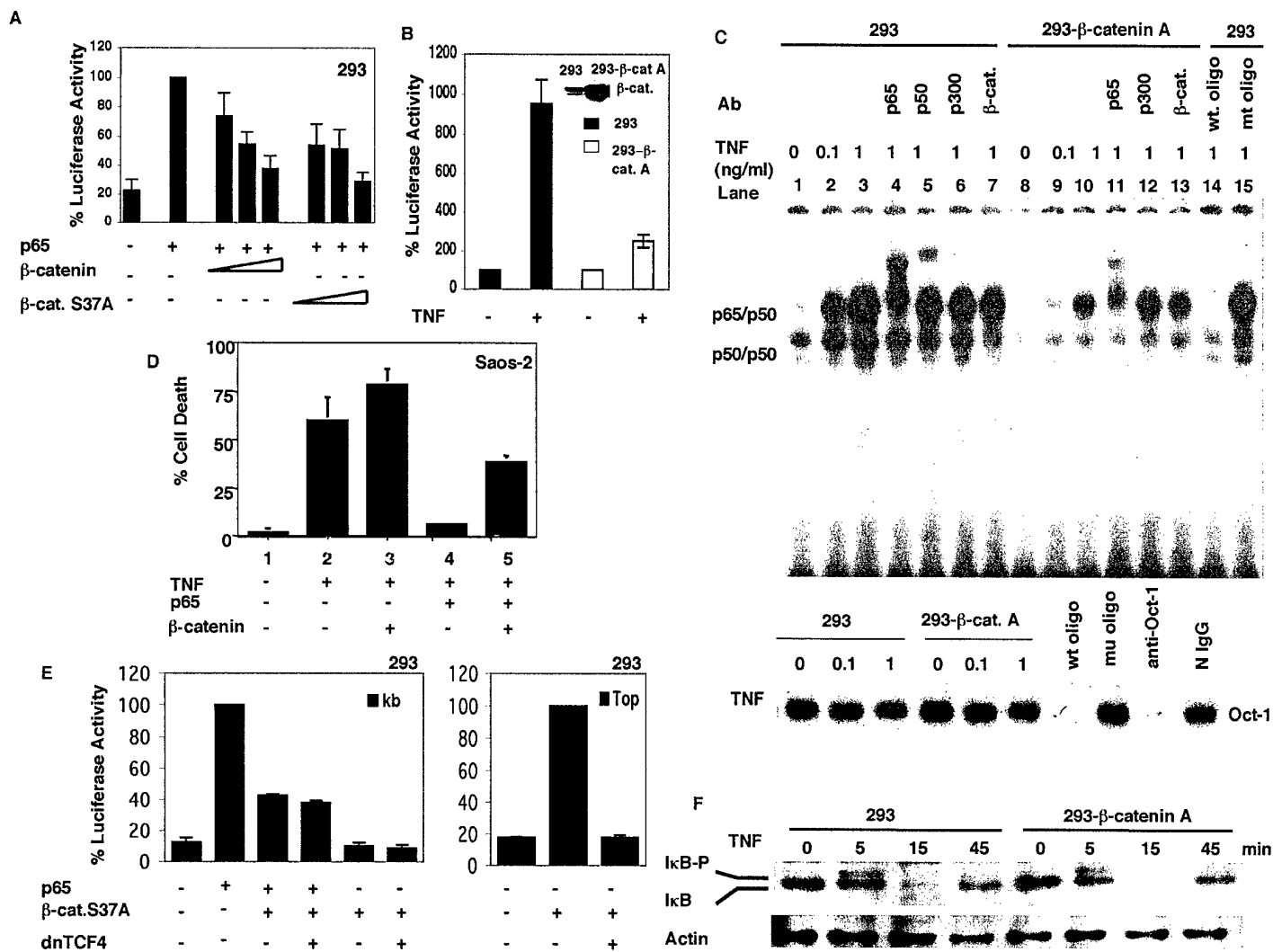
Figure 4 Depletion of β -catenin restores NF- κ B activity. **A:** HCT116 cells were transfected with β -Gal (0.2 μ g) and GFP-p65 or GFP (1.6 μ g). Two days later, cells were treated with TNF for 24 hours. Percentage of β -Gal-positive cells was counted as surviving cells (viability). **B:** HCT116 cells were transfected with κ B-luc. reporter (0.2 μ g) with vector, pGFP-p65 and pGFP (1.6 μ g). **C:** Immunoblot

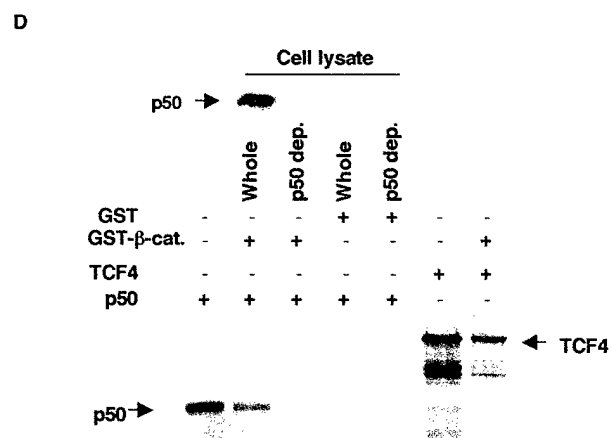
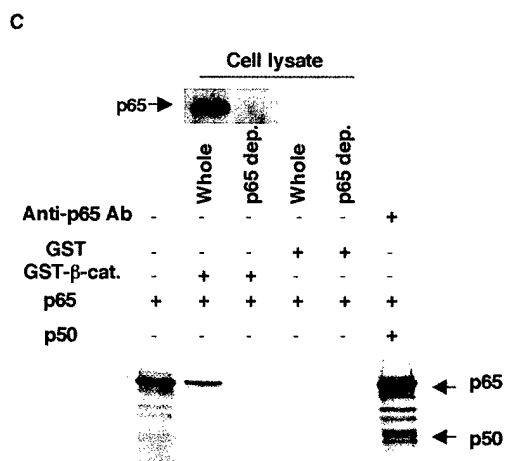
of cell lysates from HCT116 cells transfected with GFP-p65 or GFP (1.6 μ g) or none. Antibodies used in the assay were as indicated. **D:** Immunoblot of cell lysates of cells transfected with siRNA- β -cat. (1.6 μ g) or siRNA-NS (1.6 μ g) for 1 or 2 days as indicated (see experimental procedures). Before harvesting, cells were treated with TNF (10 ng/ml) for 9 hours. **E:** EMSA analysis of NF- κ B (top) and Oct-1 (bottom) DNA-binding activity. Nuclear extracts from cells transfected with siRNA- β -cat. or siRNA-NS for 2 days, then TNF treatment (10 ng/ml) or TNF plus INF- γ (10 ng/ml) for 15 min.

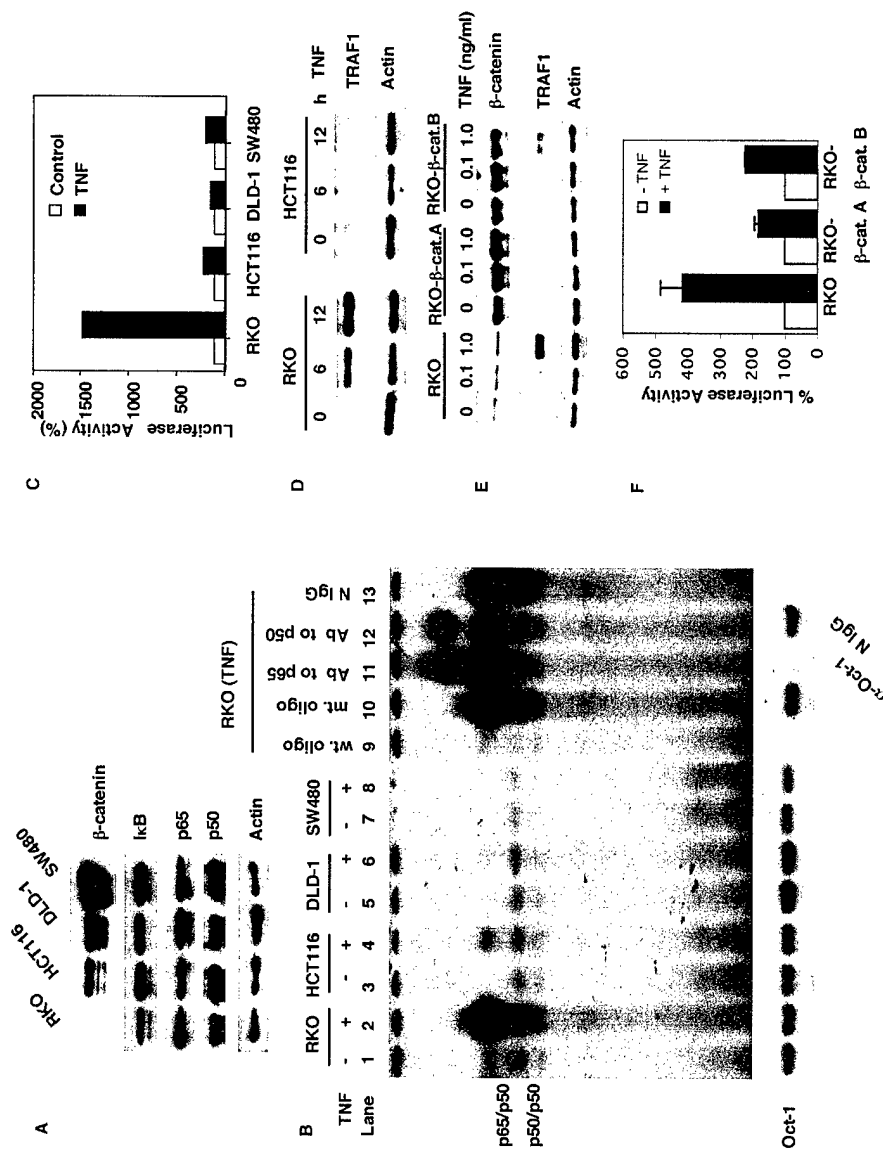
Figure 5 β -catenin inhibits Fas expression. **A:** Immunoblot of cell lysates from MEF wt or *rela*^{-/-} cells. **B:** Immunoblot of cell lysates from human breast cancer cells with antibodies as indicated. **C:** Left, Immunoblot of cell lysates from RKO and RKO- β -cat. A cells. Right, Cells were treated with cytokines, IFN- γ (10 ng/ml) plus TNF (10 ng/ml) as indicated for 24 hours and then treated with antibody to Fas (CH11) (0.5 μ g/ml) or normal mouse IgG (in presence of actinomycin D 5 ng/ml) for another 24 hours. Viable cells were harvested and counted by Trypan Blue exclusion. Bars indicate the percent of surviving cells divided by the untreated control. **D:** RKO- β -cat. cells were transfected with GFP-p65 or GFP. Two days later cells were harvested, and measured for Fas-expression intensity on GFP-positive cells by FACS analysis. **E:** Left, HCT116 cells were transfected with siRNA- β -cat. or siRNA-NS for 2 days, then harvested for Fas expression analysis by FACS. Bars show the intensity of Fas expression in each group in comparison with that of control. Right, HCT116 cells were transfected with siRNA- β -cat. or siRNA-SN for two days, then treated with anti-Fas antibody

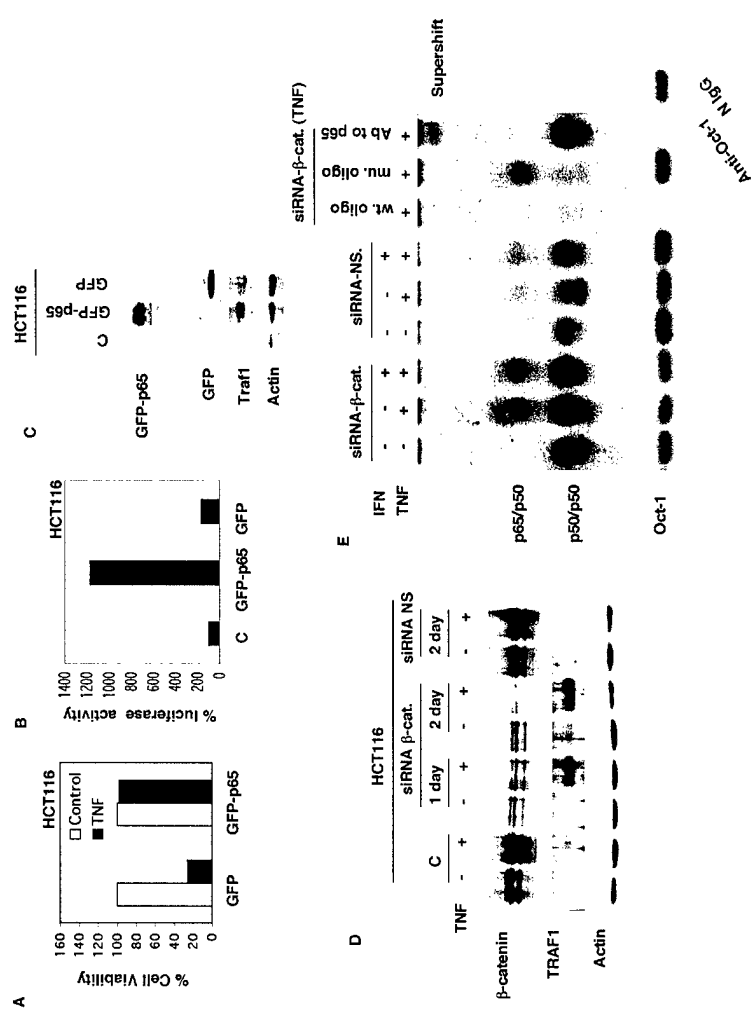
(CH11) at 0.5 $\mu\text{g/ml}$ for 24 hour. The percentages of apoptotic cells were derived from analyzing the subG1 population labeled with PI by FACS. **F:** HCT116 cells were transfected with GFP-p65 and GFP for two days. Cells were then harvested and assayed for Fas expression as in D.

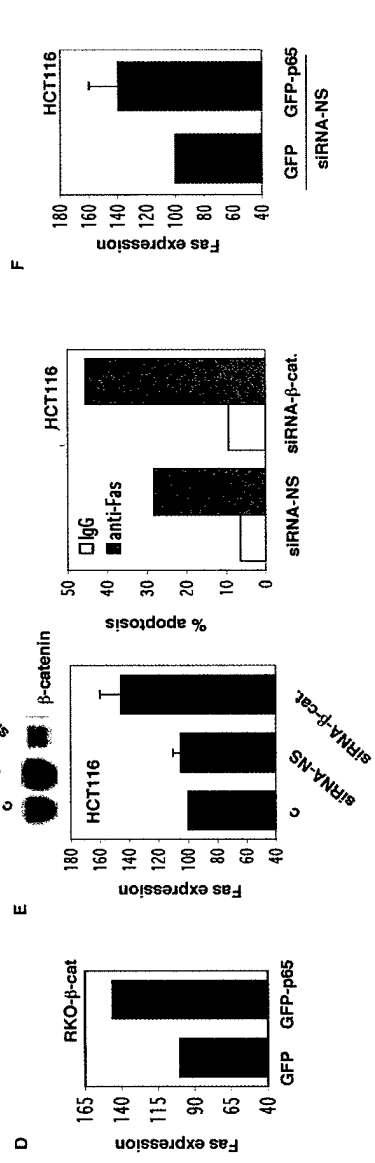
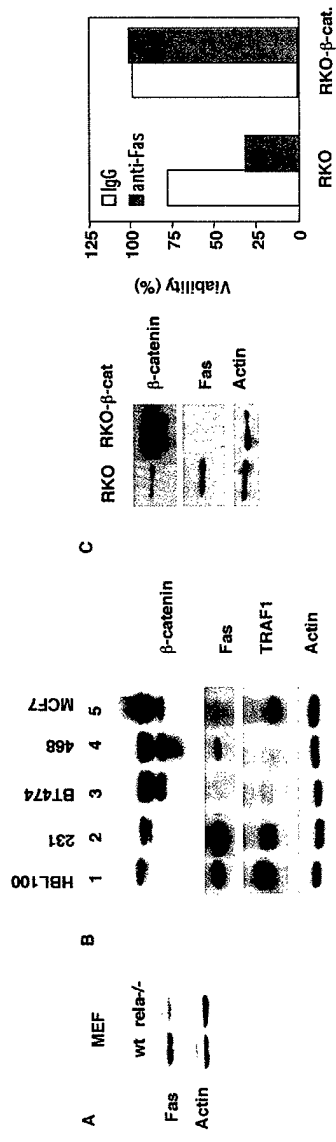
Figure 6 β -catenin inversely correlates with Fas expression in colon cancer. **A:** Representative human colon primary tumor tissues samples by immunohistochemistry staining. Case 1, when β -catenin is inactive (primarily in the membrane (top left), Fas expression is high (top right)(two stainings from adjacent areas). Case 2, when β -catenin is active (in the cytoplasm and the nucleus)(bottom left), Fas expression level is low (bottom right).



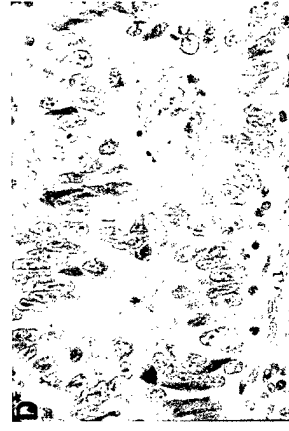








Fas



β -catenin



Case 1

Case 2

Table 1 Summary of Primary Tumor Tissue

Table 1A Summary of Colon Cancer Primary Tissue

		p-catenin		
		-	+	total
Fas	-	2 (10.5%)	15 (78.9%)	17 (89.5%)
	+	2 (10.5%)	0 (0%)	2 (10.5%)
	total	4 (21%)	15 (78.9%)	19 (100%)

p=0.0051

Table 1B Summary of Breast Cancer Primary Tissue

		p-catenin		
		-	+	total
Fas	-	0 (0%)	5 (33%)	5 (33%)
	+	7 (46.7%)	3 (20%)	10 (66%)
	total	7 (46.7%)	8 (53%)	15 (100%)

p=0.0256

carcinogen, namely 2-amino-1-methyl-6-phenylimidazo[4,5-b]pyridine (PhIP), 4-aminobiphenyl (ABP), and benzo[a]pyrene (BP), in epithelial cell DNA isolated from human breast milk. Milk was collected from healthy, non-smoking mothers. The isolated DNA was digested to 3'-nucleotides and subjected to ^{32}P -postlabelling. Adduct enrichment was achieved using Oasis Sep-Paks and the analyses were conducted by HPLC using radiometric detection. Critical to the analysis was the syntheses of bis(phosphate) standards for the C8-dG adducts of PhIP and ABP, and N²-dG adduct of BP, which were added to each reaction as UV markers. Of the 64 samples analyzed, adducts were found in 31 samples. Thirty samples contained detectable levels of PhIP adducts, with a mean value of 4.7 adducts/10⁷ nucleotides; 18 were positive for ABP adducts with a mean value of 4.7 adducts/10⁷ nucleotides; and 13 were found to contain BP adducts with a mean level of 1.9 adducts/10⁷ nucleotides. The effect of metabolic genotype and other host factors on adduct levels were also investigated. Samples were genotyped for NAT1, NAT2, SULT1A1, GSTA1, GSTA2, CYP1A1, GSTM1, and GSTT1. Of these, higher PhIP and ABP adducts appeared to be associated with the rapid NAT2 and rapid NAT1 genotypes. Interestingly, the presence of ABP adducts was highly associated with the use of hair coloring products. These data indicate that women are exposed to several classes of dietary and environmental carcinogens and that metabolic genotype can be a susceptibility factor.

#5044 Detection of 2-amino-1-methyl-6-phenylimidazo [4,5-b] pyridine (PhIP)-DNA adducts in normal breast tissues by immunohistochemistry and risk of breast cancer. Jijiang Zhu, Ping Chang, Melissa Bondy, Aysegül Sahin, Eva Singletary, Satoru Takahashi, Tomoyuki Shirai, and Donghui Li. *University of Texas MD Anderson Cancer Center, Houston, TX, and Nagoya City University Medical School, Nagoya, Japan.*

Environmental carcinogens have been suspected to play a role in human breast cancer but no specific agent has been definitely implicated except radiation. 2-amino-1-methyl-6-phenylimidazo [4,5-b] pyridine (PhIP), the most abundant heterocyclic amines (HCAs) in cooked food, is known to induce mammary and prostate tumors in female and male rats, respectively. Consumption of well-done meat and PhIP intake has been associated with an increased risk of breast cancer. PhIP and PhIP metabolites have been detected in human milk and urine samples, but PhIP-DNA adducts have not been analyzed in breast tissues from women with unknown exposure to HCAs due to technical difficulties. By using a polyclonal antibody against PhIP-DNA adducts, this study has examined normal breast tissues from women with newly diagnosed breast cancer in comparison with those from women undergoing reduction mammoplasty. The specificity and sensitivity of the antibody was first tested in MCF-7 breast cancer cell line treated with different doses of N-hydroxy PhIP, an intermediate PhIP metabolite. A significant dose-response relationship was detected and the levels of PhIP-DNA adducts detected by ^{32}P -postlabeling and immunohistochemistry (IHC) was highly correlated ($r = 0.98$). We then measured PhIP-DNA adducts in normal breast tissue sections from 105 cases and 49 non-cancer controls using the IHC and image analysis method. PhIP-DNA adduct was detected in 83% (87/105) of the cases and 71% (35/49) of the controls by IHC. An average of 801 ± 252 nuclei of breast epithelial cells was analyzed on each positive tissue section by image analysis. The mean \pm SD absorbency was 0.36 ± 0.10 and 0.30 ± 0.09 for cases and controls, respectively ($P = 0.02$). Using the mean value in the controls as a cut off point, 62% of the cases and 31% of the controls were distributed in the higher range ($\chi^2 = 13.1$, $P < 0.0001$). Logistic regression analysis demonstrated an odds ratio of 3.75 (95% confidence interval: 1.7 - 8.3) after adjusting for age and ethnicity ($P = 0.001$). Further analysis found the level of PhIP-DNA adducts was not associated with smoking status or polymorphisms of CYP1A1, GSTM1, and NAT2 genes. These data strongly support the hypothesis that PhIP exposure contributes to human breast cancer. The association between the level of PhIP-DNA adducts and dietary intake of HCAs as well as the role of genetic susceptibility to PhIP exposure is under current investigation (Supported by NIH grant CA70264).

#5045 Polymorphisms in the DNA repair enzyme XPD are associated with levels of PAH-DNA adducts and breast cancer risk in a case-control study. Deliang Fang, Stan Cho, Andrew Rundie, Senqing Chen, David Phillips, Jingzi Zhou, Freya Schnabel, Alison Estabrook, and Frederica Perera. *Columbia University, New York, NY, Institute of Cancer Research, Sutton, UK, and St. Luke's Hospital, New York, NY.*

We present findings on the associations between DNA damage from polycyclic aromatic hydrocarbons (PAH), risk of breast cancer, and genetic susceptibility due to inherited polymorphisms of the DNA repair enzyme XPD. Prior to surgery, breast cancer cases and benign breast disease (BBD) controls were enrolled into the study, took part in an interview and donated a blood sample. A second control group of healthy women recruited from the GYN practices were also enrolled, took part in an interview and donated blood samples. PAH-DNA adduct levels were measured by immunohistochemistry in breast tissue samples retrieved from pathology blocks, and by aromatic-DNA adducts were measured in mononuclear white blood cells (MWBC) by ^{32}P postlabelling. XPD genotype at codons 312 and 751 was determined by PCR and RFLP analysis using white blood cell DNA. The XPD analysis included 103 cases, 94 benign breast disease (BBD) controls, and 121 healthy controls. Neither of the polymorphisms were associated with case-control status. However, XPD polymorphisms at codons 312 and 751 were associated with higher levels of PAH-DNA in tumor tissue from breast cancer

cases. Subjects with an AG or AA polymorphic genotype in codon 312 of XPD had elevated levels of PAH-DNA adducts compared to subjects with the GG genotype. PAH-DNA adducts were significantly associated with increasing copy number of the C allele for the codon 751 polymorphism (p for trend, <0.01). Among subjects who had the polymorphic XPD genotypes, adduct levels in tumor tissue were significantly higher than in tissue from BBD controls. For both the codon 312 and 751 polymorphisms, the associations between the polymorphism and adduct levels was significantly different in tumor tissue from benign tissue. Our results show XPD polymorphisms are associated with increased levels of DNA damage in tumor tissue, suggesting a possible basis for genetic susceptibility to tumor progression.

#5046 Functional significance of XRCC1 genotype in DNA repair capacity and prostate carcinogenesis. Kristin L. Lockett, M. Craig Hall, Larry Grossman, Mahmood Hedyati, Kurt Lohman, and Jennifer J. Hu. *Wake Forest University School of Medicine, Winston-Salem, NC, and Johns Hopkins School of Hygiene and Public Health, Baltimore, MD.*

Prostate cancer is the second leading cause of cancer death in men. While human cancer genetics are advancing at a rapid pace, the etiology of prostate cancer is not fully understood. To understand the etiology of prostate cancer and to provide an effective etiology-based preventive strategy, we investigated the importance of DNA repair in human prostate carcinogenesis. In a prostate cancer case-control study, we evaluated the functional significance of four amino acid substitution variants of DNA repair genes (XRCC1, 194 Arg/Trp and 399 Arg/Gln; XRCC3 241 Thr/Met; XPD 751 Lys/Gln) in DNA repair capacity and prostate cancer susceptibility. PCR-RFLP assays were used for genotyping and a plasmid-based assay was used to determine DNA repair capacity. Our data show that controls with the XRCC1 399Gln/Gln genotype has significantly lower DNA repair capacity ($p = 0.03$, ANOVA); the mean \pm SE of DNA repair capacity in controls with the Arg/Arg, Arg/Gln, and Gln/Gln genotype was 9.69 ± 0.98 ($n = 31$), 8.99 ± 1.02 ($n = 29$), and $3.8 - 2.45$ ($n = 5$), respectively. There was a significant association between below-median DNA repair capacity and prostate cancer risk (odds ratio [OR] = 4.45; 95% confidence interval [CI] = 1.65-11.96) in the younger age group (<60). The association was weaker in the older age group ($60+$) (OR = 1.21; 95%CI = 0.68-2.16). The XRCC1 399Gln/Gln genotype is also associated with prostate cancer risk (OR = 3.22; 95%CI = 1.01-10.28). These results suggest that amino acid substitution variant of XRCC1 may contribute to deficient DNA repair and prostate carcinogenesis. Supported by ACS grant CNE-10111

#5047 Expression profiles of DNA repair genes in resting and proliferating human peripheral blood lymphocytes. Peter Schmezer, Claudia Mayer, Odilia Popanda, Marie-Charlotte von Brevem, Alfred Bach, and Helmut Bartsch. *German Cancer Research Center, Heidelberg, Germany, and BASF-LYNX Bioscience AG, Heidelberg, Germany.*

DNA repair plays an important role in maintaining genomic integrity, and functional deficiencies are linked to cancer development. Several molecular epidemiology studies have explored the individual capacity to repair DNA damage in peripheral blood lymphocytes (PBLs) as a cancer risk marker, using both phytohemagglutinin (PHA)-stimulated (i.e. dividing) and resting PBLs. The cell's ability to remove DNA damage may however be correlated with its proliferative activity, and there is evidence that cell cycle dependent regulation of DNA repair enzymes leads to their enhanced expression. We therefore investigated the effect of cell proliferation on the expression of 70 different human DNA repair genes. Their transcriptional profiles were analysed using a custom-made cDNA array. Hybridisation experiments were performed with mRNA isolated from both unstimulated PBLs and cells with PHA-stimulation for 24, 48 and 72h. Signal intensities for 46 out of 70 DNA repair genes were sufficient for quantitative analysis. We identified 12 genes that responded 72 h after PHA treatment with an over 2fold increase of transcripts to the mitogenic stimulus, the highest induction levels being up to 18fold. Most of these upregulated repair enzymes are known to play also a role in DNA replication. In contrast, 34 out of 46 (74%) genes evaluated showed no increased expression levels and were within a 2fold range as compared to unstimulated cells. As an independent technique for mRNA quantification, we verified the array results for 8 genes (5 with increased and 3 with constant expression levels; by real-time RT-PCR. For 6 of these 8 genes, the obtained results by the two methods were quantitatively and/or qualitatively similar. We conclude that there is no overall upregulation of DNA repair genes upon mitogenic stimulation of human PBLs. This is in agreement with our previous observation where no difference in DNA repair capacity between PHA-stimulated and resting PBLs was found, when the alkaline comet assay was used for measuring DNA repair capacity of γ -irradiation induced DNA damage. Thus, our results do not support a general recommendation for the obligatory use of stimulated PBLs in molecular epidemiological studies when measuring individual DNA repair capacity.

#5048 Polymorphic variants of DNA repair and cell cycle genes associated with acute myeloid leukemia identified by genotyping DNA pools. Sara Rollinson, James M. Allan, Graham R. Law, Philippa L. Roddam, Alexandra G. Smith, Russell Higuchi, Soren Germer, Eva Roman, Martyn T. Smith, and Gareth J. Morgan. *Academic Unit of Oncology and Hematology, Leeds, UK, Leukemia Research Fund Centre for Clinical Epidemiology, 30 Hyde Terrace, Leeds, UK, Roche Molecular Systems, Alameda, CA, and Division of Environmental Health Sciences, School of Public Health, University of California, Berkeley, CA.*

REGULATION OF BRCA1 DEPENDS ON P53 STATUS FOLLOWING TREATMENT WITH CISPLATIN

Chenyi Zhou and Jinsong Liu

*Department of Pathology, The University of Texas M. D. Anderson Cancer Center, 1515
Holcombe Boulevard, Houston, TX 77030-4095*

e-mail address: Chenzhou@mail.mdanderson.org

Germline mutation in *BRCA1* is responsible for approximately half of all cases of hereditary breast cancer and for almost all combined hereditary breast and ovarian cancers cases. Recent studies suggest that *BRCA1* plays an important role in maintenance of genomic stability through DNA repair. Cisplatin is a DNA damaging reagent that crosslinks with DNA. Because different DNA-damaging agents can be involved in different DNA repair pathways, we hypothesize that the DNA-crosslinking reagent cisplatin may involve a different DNA repair pathway than that of ionizing irradiation. To test this hypothesis, we used three cancer cell lines: SNU251 containing both p53 and *BRCA1* mutations, SKOV3 carrying only a p53 mutation but containing wild-type *BRCA1*, and OVCA433 bearing both wild-type p53 and wild-type *BRCA1*. All three cell lines were treated with cisplatin or γ -radiation. Our results demonstrated that *BRCA1* expression levels were upregulated in the p53 mutation cell lines SKOV3 and SNU251 but is downregulated in the wild-type p53 cell line OVCA433 following cisplatin treatment. On the other hand, only minimal changes in *BRCA1* expression levels were detected in all three cell lines following γ -radiation. These results provided experimental evidence that cisplatin regulated the expression of *BRCA1*. Such regulation may depend on the status of p53 mutation. Our data also showed that after cisplatin treatment, wild-type *BRCA1* was phosphorylated in SKOV3 cells, which are cisplatin resistant. Further study is in progress to reveal the underlying mechanism of the role of *BRCA1* in cisplatin-resistant cancer cells.

This work is supported by a U.S. Army Breast Cancer Research Training Grant. Grant number: DAMD17-99-1-9264

2. AACR abstract p304, #1511, 93rd Annual Meeting.

Inhibition of the Catalytic Subunit of Human Telomerase Expression by BRCA1 in Human Ovarian Cancer Cell Lines

Chenyi Zhou and Jinsong Liu

Department of Pathology, The University of Texas M. D. Anderson Cancer Center, 1515 Holcombe Boulevard, Houston, TX 77030-4095

The catalytic subunit of human telomerase (hTERT) is responsible for the synthesis and maintenance of the telomeric repeats at the distal ends of human chromosomes. Multiple studies have demonstrated that telomerase expression is repressed in normal human cells, but is activated in immortal cells and during tumorigenesis. The mechanism by which telomerase expression is regulated is not fully understood. Previous studies identified two Myc binding sites (E-box) on the hTERT promoter. Myc can stimulate transcription from the hTERT promoter. BRCA1 is a tumor suppressor gene responsible for approximately half of hereditary breast and ovarian cancers, and part of its function is to maintain genomic stability through DNA repair. It has been reported that BRCA1 forms a functional protein complex with Myc in vivo (Wang et al., *Oncogene*, 17: 1939-1948, 1998). We hypothesize that BRCA1 may interact with Myc to regulate the expression of telomerase in vivo. To test this hypothesis, we examined the effect of BRCA1 on the expression of wild-type and mutant hTERT promoters by transient transfection assay in ovarian cancer cells. Myc activated the hTERT expression by 4 fold and BRCA1 abrogated this activation. A mutation in the Myc binding site (E-box) of the hTERT promoter resulted in loss of Myc activation and inhibition by BRCA1. Deletion of the Myc binding domain in BRCA1 resulted in loss of inhibition of BRCA1. BRCA1 inhibited hTERT most dramatically in SKOV3 and SNU-251 cells but not in 293T cells. Our data indicate that BRCA1 interacts with Myc to negatively regulate hTERT expression. Our results suggest that BRCA1 inhibits tumor growth at least in part through the inhibition of hTERT expression. We are in the process of extending this study to other cancer cell types including breast cancer.

PI3/Akt Enhance HIF pathway to Activate Vascular Endothelial Growth Factor Expression in Her2/neu overexpressing cells

Yan Li and Mien-Chie Hung

Department of Molecular and Cellular Oncology, University of Texas M. D. Anderson Cancer Center, Houston, TX 77030

HER-2/neu amplification or overexpression in cancer cell is associated with increased tumor angiogenesis and metastasis, chemotherapy resistance and poor clinical outcome. HER-2/neu phosphorylates many downstream molecules that in turn activate a variety of signaling cascades, including the phosphatidylinositol-3-OH kinase (PI-3K)/Akt, which seem to be particularly important in mediating cell survival, cell-cycle progression and angiogenesis. Vascular endothelial growth factor (VEGF) plays a major role in tumor angiogenesis, which can be induced by exposure to hypoxia or growth factors due to increased transcription mediated by hypoxia-inducible factor 1 (HIF-1). HIF-1 is a transcriptional activator composed of HIF-1 α and HIF-1 β subunits. Increased (PI-3K)/Akt or decreased PTEN can increase the rate of HIF-1 α synthesis in nonhypoxic cells via PI3K-AKT- FRAP pathway. The mechanism of HIF activation by the PI3-Akt pathway under hypoxic condition still remains unclear. In this study, we found Akt can enhance HIF-1 α expression in HER-2/neu overexpressing cells; HIF-1 α expression can be dramatically inhibited by either dominant -negative Akt or PI-3K inhibitors. Akt may block the protein degradation of HIF-1 α in hypoxic condition. We also found Akt can bind HIF-1 β in vivo. Inside the HLH-PAS domain of HIF-1 β , there is a consense Akt phosphorylation motif that conserve among many species. Phosphorylation of HIF-1 β may enhance HIF-1 DNA binding affinity and further stabilize HIF-1 α , which may constitute a major mechanism for HIF-1 activation by the PI3-Akt pathway.

Vaccination Against HER2/*neu* Using Alphavirus-Based Vectors

Xiaoyan (Sunny) Wang, MD, Jianping Wang, MD, Ph.D., Lawrence B. Lachman, Ph.D.,
Department of Bioimmunotherapy, University of Texas M.D. Anderson Cancer Center,
Houston, TX 77030

Overexpression of Her-2/*neu*, a member of the epidermal growth factor receptor family with tyrosine kinase activity, is associated with aggressive disease and poor prognosis in breast cancer. Her-2/*neu*'s low-level expression in normal adult tissues, high-level expression in malignancies, its cell surface localization and its native immunogenicity in humans have made it an attractive target for immunotherapeutic intervention. Gene vaccines have demonstrated that antitumor immunity can be developed by immunizing with bacterial expression plasmids that encode the DNA sequence for tumor antigens such as HER2/*neu*. Gene vaccines have been shown to induce strong, lasting immunity that includes the generation of cytotoxic T lymphocytes (CTL), the main mechanism for immunological control of tumor growth. The most recent findings for gene vaccines indicate that maximum effectiveness is achieved using a Prime-Boost strategy in which a plasmid containing the gene of interest is used as the priming vaccine and a crippled virus, also containing the gene, is used for the boosting vaccination. We have shown that vaccination of mice with an Alphavirus-based plasmid, called ELVIS (created by Chiron Technologies, San Diego, CA), which expresses the cDNA sequence for Her2/*neu*, protected mice from challenge with a HER2/*neu*-expressing murine breast tumor cell line. The mice were protected from challenge with tumor cells injected directly into the mammary fat tissue and intravenous injection, a model of experimental tumor metastasis. The vaccination also prolongs the life of *neu*⁺-transgenic mice and induces antigen-specific T cells as demonstrated by tetramer analysis and interferon- γ induction. ELVIS is the first step of a two-stage vaccination protocol that uses Viral Replicon Particles (VRP) as the second step. The non-pathogenic VRP are similar to attenuated viruses known to induce long-lasting immunity when used for childhood diseases. We have found VRP-*neu* to be more effective than ELVIS-*neu* in the assays described above and we anticipate that a strategy of primary vaccination with ELVIS-*neu* followed by boosting with VRP-*neu* will be maximally effective in controlling tumor growth and metastasis. We hope to perform a phase 1b clinical trial in breast and ovarian cancer patients using either ELVIS-*neu* or VPR-*neu* in the near future.